

**SYNTHESIS AND CHARACTERIZATION OF FERROCENYL STANNANES AND
POLYFERROCENYL STANNANES**

by

Jonathan Ward

Bachelor of Science, Ryerson University, Toronto, Ontario, Canada, 2010

A thesis

presented to Ryerson University

in partial fulfillment of the

requirements for the degree of

Masters of Science

in the program of

Molecular Science

Toronto, Ontario, Canada, 2013

©(Jonathan Ward) 2013

Author's Declaration

I hereby declare that I am the sole author of this thesis. I authorize Ryerson University to lend this thesis to other institutions or individuals for the purpose of scholarly research.

Name: _____ Signature: _____

I further authorize Ryerson University to reproduce this thesis by photocopying or by other means, in total or in part, at the request of other institutions or individuals for the purpose of scholarly research.

Name: _____ Signature: _____

SYNTHESIS AND CHARACTERIZATION OF FERROCENYL STANNANES AND POLYFERROCENYL STANNANES

Jonathan Ward

Masters of Science, Molecular Science, Ryerson University 2013

Abstract

A novel polymer polybis(dimethyl stannyl)ferrocene was synthesized through both metal catalyzed intermolecular dehydrogenative condensation and ring-opening polymerization. This polymer was the first evidence of a dibridged polyferrocenyl stannane, and was found to be of low to moderate molecular weight by gel permeation chromatography and ^1H NMR spectroscopy. This polymer displayed extensive electronic communication observed previously synthesized monobridged ferrocenyl stannane polymers. The first tristanna-bridged [3.3]ferrocenophane was discovered through an amine coupling of a tin amine, and 1,1'-bis(dimethyl stannyl) ferrocene. The [3.3]ferrocenophane displayed a strong interaction between connected ferrocenes despite the large distance, (8.49 Å) between Fe centers. Finally, a new and improved synthesis of 1,1,2,2-tetramethyldistanna-[2]ferrocenophane was found. This metal catalyzed intramolecular dehydrogenative coupling employs $\text{Pd}_2(\text{dba})_3$ as a catalyst and yields 90% product. All products were characterized where possible ^1H , ^{13}C , and ^{119}Sn NMR and UV-Visible spectroscopy, as well as through cyclic voltammetry and DFT modeling.

Acknowledgements

Firstly, I would like to thank Dr. Daniel Foucher. His teaching and guidance for the past three years has been invaluable. It has been a pleasure being a part, and eventually a leader in his research group. As well, thank you to my committee members Dr Robert Gossage and Dr. Russell Viirre for their input throughout my research.

Next I would like to thank all the members of the Foucher research group, both past and present. Working with everyone has been challenging at times, although I have many fond memories of both working with, and distracting each other. Special thanks must be made to Damion Miles who helped train me, and Aman Khan who has been an excellent member of our group. I have worked with Aman for almost 5 years and have appreciated him as both a co-worker and a friend.

Thanks must be made to all the undergraduate researchers that have helped in small parts to the ongoing project that I have been working on. Thanks to Patricia, Tamara, Katie and Shane. It has been a pleasure working with all of you, and I have found working with all of you both fun and entertaining.

Both Matthew Forbes and Timothy Burrow from the University of Toronto deserve both acknowledgement and thanks for their help with mass spectrometry and NMR spectroscopy. Thanks also to Dr. Brian Koivisto and Saif Al-Alul for the use of and support with cyclic voltammetry, as well as Shawn McFadden for this assistance with the equipment in the RUAC. Thank as well Dr. Russell Viirre for the continued upkeep and support of the NMR.

I must also thank all of my friends both in the research labs and abroad for their continued support and guidance throughout my graduate thesis. I would like to specially thank Robert Denning and Rama Sriharsha who have been friends through this ordeal.

Finally, thanks to the continued support of my parents, Martin and Gail Ward, my siblings, Bronwen and Matthew Ward. Thanks also to the three additions to our family, Alaura, my brother's beautiful wife, as well as Isabella and Skylynn, who were born during the making of this thesis.

Dedication

**This is dedicated to my parents Martin
and Gail Ward, for their moral,
emotional and (most importantly)
financial support**

Table of Contents

1.0 Introduction.....	1
1.1 Polystannanes.....	1
1.1.1 Synthesis.....	2
1.1.2 Properties.....	7
1.1.3 Stability.....	11
1.2 Ferrocenophanes.....	12
1.3 Polyferrocenylenes.....	15
1.3.1 Synthesis.....	16
1.3.2 Properties.....	23
1.4 Ferrocenyl stannanes.....	28
1.5 Polyferrocenyl stannanes.....	33
1.5.1 Synthesis.....	33
1.5.2 Properties.....	37
1.6 Research objectives.....	39
2.0 Polymerisation of Novel Polyferrocenyl Dimethyl Stannyl Polymers.....	40
2.1 Introduction:.....	40
2.2 Results and discussion.....	41
2.2.1 Synthesis of monomers.....	41

2.2.2	Condensation polymerization.....	44
2.2.3	Ring-opening polymerization.....	47
2.2.4	Characterization by ^1H , ^{13}C , and ^{119}Sn NMR.....	48
2.2.5	Molecular weight determination by GPC.....	52
2.2.6	Electrochemistry.....	54
2.2.7	UV-Visible spectroscopy and DFT studies.....	56
2.3	Conclusion	59
3.0	Synthesis and Spectral Electrochemical Properties of a Symmetrical Tristanna-Bridged [3.3]Ferrocenophane	60
3.1	Introduction.....	60
3.2	Results and discussion	62
3.2.1	Sn NMR and NMR simulation.....	65
3.2.2	Electrochemistry.....	67
3.2.3	DFT modelling and UV-Vis spectroscopy.....	70
3.2.4	Mass spectrometry.....	72
3.3	Conclusion	76
4.0	Experimental.....	77
4.1	Equipment and procedures.....	77
4.1.2	Nuclear magnetic resonance.....	77
4.1.3	^{119}Sn NMR simulator	78

4.1.4 Cyclic voltammetry	78
4.1.5 Density functional theory calculations	79
4.1.6 UV-Visible spectroscopy	79
4.1.7 Gel permeation chromatography	79
4.1.8 Mass spectrometry.....	79
4.2 Preparation of 1,1'-bis(trimethyl stannyl) ferrocene 1a.....	80
4.3 Preparation of 1,1'-bis(dimethyl stannyl) ferrocene 3a	80
4.4 Preparation of 1,1'-bis(tributyl stannyl) ferrocene 1b.....	81
4.5 Attempted preparation of 1,1'-bis(chlorodi(<i>n</i> -butyl) stannyl) ferrocene 2b through route 1.....	82
4.6 Attempted preparation of 1,1'-bis(chlorodi(<i>n</i> -butyl) stannyl) ferrocene 2b through route 2.....	82
4.7 Preparation of polybis(dimethyl stannyl) ferrocene 4 route 1	83
4.8 Preparation of polybis(dimethyl stannyl)ferrocene 4 route 2	83
4.9 Ring-opening polymerization of 5a to form polybis(dimethyl stannyl) ferrocene 4 ..	84
4.10 Preparation of 1,1,2,2-tetramethyl-distannanediyl-[2]ferrocenophane 5a from the reaction of 3 with Pd ₂ (dba) ₃	84
4.11 Attempted preparation of 5a with Pt(acac) ₂	85
4.12 Attempted preparation of 5a with ClRh(PPh ₃) ₃	85
4.13 Preparation of 1,1,14,14-tetra- <i>n</i> -butyl-2,2,13,13,15,15,26,26-octamethyl-1,2,13,14,15,26-hexastanna-[3.3]ferrocenophane 11 (low dilution).....	85

4.14	Preparation of 1,1,14,14-tetra-n-butyl-2,2,13,13,15,15,26,26-octamethyl-1,2,13,14,15,26-hexastanna-[3.3]ferrocenophane 11 (high dilution).....	87
5.0	Conclusion	88
	Appendix.....	89
	References.....	206
	Glossary	Error! Bookmark not defined.

List of Tables

1.1	UV-Vis of selected poly(diaryl)stannanes	4
1.2	UV-Vis of selected poly(diaryl)stannanes	8
1.3	Thermal transitions of alkyl Polystannanes	10
1.4	Charge mobility of Group 14 polymers	11
1.5	Structure, size and electrochemical data for bridged ferrocenylenes synthesised through ROP.....	22
1.6	Glass transition temperature, λ_{\max} , and CV of various polyferrocenylenes.	24
1.7	Refractive indices for various polyferrocenylenes.....	26
1.8	Electronic properties of ferrocenyl stannanes	38
2.1	Cyclic voltammetry of polyferrocenyl stannanes.....	55
3.1	Comparison of catalytic activity for main group and transition metalcatalysts in the ring-closing formation of 4a from 6	62
3.2	Half-potentials for bridged bisferrocenes and selected ferrocene polymers	68
3.3	DART-TOF-MS relative abundance of mass fragments @200°C and 300°C	75

List of Figures

1.1	Three reaction routes for the synthesis of polystannanes.....	2
1.2	Tilley's catalysts evaluated for the dehydrogenative coupling of $(n\text{-Bu})_2\text{SnH}_2$	5
1.3	Dehydrogenative coupling reactions.....	6
1.4	Basic structures of ferrocenophanes.....	12
1.5	Examples of the four routes to [n]ferrocenophanes	13
1.6	Diagram of the ring strain of ferrocenophanes.....	14
1.7	Reaction to synthesized [5.5]ferrocenophane	15
1.8	Proposed mechanism dehydrosilylation of 1,1'-bis-(dimethylsilyl)ferrocene	17
1.9	Structure of polyferrocenylenes, polyferrocenyl siloxanes, and polyferrocenyl disulphides.....	19
1.10	ROP of Group 14 [1]- and [2]ferrocenophanes.....	20
1.11	General ROP of ferrocenylenes from ferrocenophanes	22
1.12	Methods of preparation of ferrocenyl stannanes	28
1.13	Routes to various 1,1'-bis(chlorostannyl)ferrocenes and 1,1'-bis(stannyl)-ferrocenes	29
1.14	Synthesis of monolithioferrocene or monoiodoferrocene	30
1.15	Preparation of stanna-[n]ferrocenophanes	32
1.16	Synthesis of [1]ferrocenyl stannanes and ROP to form polyferrocenylstannane..	34
1.17	Route to synthesis of alternating FcSnFcSi oligomers.....	35

1.18	The synthesis of trocicenophane monomer and associated ring opening polymerization.....	36
2.1	Synthesis of 3a from 1a	42
2.2	Metal catalyzed dehydrogenative coupling to form polyferrocenyl stannane 4 ...	44
2.3	Coordination of DMF to a Sn center.....	45
2.4	Dehydrogenative coupling reaction mechanism for 3a to form 4	46
2.5	¹ H NMR (C ₆ D ₆) spectra for compound 4	49
2.6	¹¹⁹ Sn NMR spectrum of polymer 4	50
2.7	The GPC for polymer 4	52
2.8	GPC chromatograph of oligomers of compound 4	53
2.9	Cyclic voltammetry of compound 4 at scan rates	54
2.10	UV-Visible spectra for 4	56
2.11	Calculated HOMO and LUMO of 4a	58
2.12	Calculated HOMO and LUMO of 4b	58
3.1	Previously made ferrocenyl stannanes and stannyl ferrocenophanes	61
3.2	Reactions to synthesize 5a and 11	63
3.3	¹ H NMR (C ₆ D ₆) of compound 11 with inset of Cp region.....	64
3.4	The design of the matrices used in ¹¹⁹ Sn modeling program	66
3.5	Calculated and Experimental ¹¹⁷ Sn and ¹¹⁹ Sn NMR spectra.....	67
3.6	Cyclic voltammetry of 11 at 100 mV/s	69

3.7	Structure of compound 12a-d , 13 , 14 , and 15	69
3.8	Molecular Orbital Diagrams of compound 11	70
3.9	Comparison of calculated UV-Visible spectra for compounds 9b and 11 with experimental spectra.....	72
3.10	DART-TOF MS spectrum of 11 at 300°C.....	74

List of Appendices

Appendix 1 ^1H , ^{13}C , ^{117}Sn , and ^{119}Sn NMR	89
Appendix 2: Mass spectrometry.....	126
Appendix 3: Cyclic voltammetry	133
Appendix 4: Sn NMR simulator program for calculating isotopic intensities.....	134
Appendix 5: DFT .mol2 files for optimized structures	164

List of Abbreviations

15-crown-5	1,4,7,10,13-Pentaoxacyclopentadecane
acac	acetylacetonate
Cp	Cyclopentadiene
CV	Cyclic voltammetry
DART	Direct analysis in real time
DCM	Dichloromethane
dba	Debenzylideneacetone
DFT	Density functional theory
DMA	Dynamic mechanical analysis
DMF	<i>N,N</i> -Dimethyl formamide
<i>n</i> -Dod	Normal dodecyl
DP	Intrinsic viscosity
DSC	Differential scanning calorimetry
Et ₂ O	Diethyl ether
GPC	Gel permeation chromatography
HMO	Sandorf/Huckel molecular orbital approximation
LDF	First principles local density functional method
Lineweaver-Burk	Correlation reacted to the linear reciprocal of the energy against the length
LSDA	Local spin density approximation
MeCN	Acetonitrile
MeOH	Methanol
M _n	Number average molecular weight
MS	Mass spectrometry
M _w	Weight average molecular weight
NMR	Nuclear magnetic resonance

OTf	Trifluoromethanesulfonate
PDI	Polydispersity index
PiPP	Triisopropylphenyl
PMDTA	<i>N,N,N',N',N''</i> -pentamethyldiethylenetriamine
RALS	Right angle light scattering
RI	Refractive index
ROP	Ring-opening polymerization
SDD	Dunning/Huzinaga full double zeta up to Ar, Stuttgart/Dresden electron core potential
T _g	Glass transition temperature
TD-DFT	Time dependent density functional theory
THF	Tetrahydrofuran
TLC	Thin layer chromatography
TMEDA	<i>N,N,N',N'</i> -Tetramethylethylenediamine
TOF	Time of flight
UV-Vis	Ultra violet-visible spectroscopy
ZPE	Zero point energy

1.0 Introduction

Polymers are everywhere and are connected to every facet of our modern world. From commodity plastics and rubbers to speciality elastomers and films for use in corrective optics, electronics and engineered materials, polymers are highly visible in everyday life. Within the modern study of polymers, the inorganic and organometallic polymer subset continues to be the basis of important research due to their unusual structural, optical, thermal, and electronic properties. The field of inorganic polymers is so prevalent in materials chemistry today that more than one thousand* review articles and at least one book¹ have been published on this topic. These polymers have been prepared through a variety of polymerization methods, some of which will be described in the following sections.

1.1 Polystannanes

Tin, as far as we know, is the only metal that has the ability to form covalently bonded oligo- and polymeric structures. The unique structural features and unusual electronic properties of polystannanes distinguish them from other Group 14 polymers. There have been at least 2 review articles in the past 12 years on the topic of polystannanes,^{2,3} however due to their relative lack of stability, there has been considerably less recent research into these systems compared to other more stable inorganic polymeric systems.

Polystannanes were likely first discovered in the mid-19th century and have been synthesized via a variety of routes throughout the last 150 years.³ The modern era of polystannanes began in the 1980s with the discovery by Zou *et al.*⁴ of the Wurtz coupling of

* A search of the Scopus database found 1046 review articles on the topic of inorganic polymers. Similarly, a search of the ISI Web Of Knowledge database found 711 inorganic polymer review articles.

dichlorostannanes. Polystannanes have also been successfully prepared by the groups of Price,⁵ Okano,^{6,7} Tilley,⁸⁻¹¹ Sita,¹² Caseri,¹³⁻¹⁶ and Foucher.¹⁷ The methods used by these groups will be discussed in detail in Section 1.1.1.

1.1.1 Synthesis

There are three major routes to the preparation of polystannanes (Figure 1.1); Wurtz coupling, electrochemical coupling, and dehydrogenative coupling. In most of these methods, there is often an impurity of 5- and 6-membered cyclic oligomers formed. These impurities are readily identified through ¹¹⁹Sn NMR spectroscopy as the polymer will, in most cases, have a lower field signal than the corresponding cyclic oligomers.*

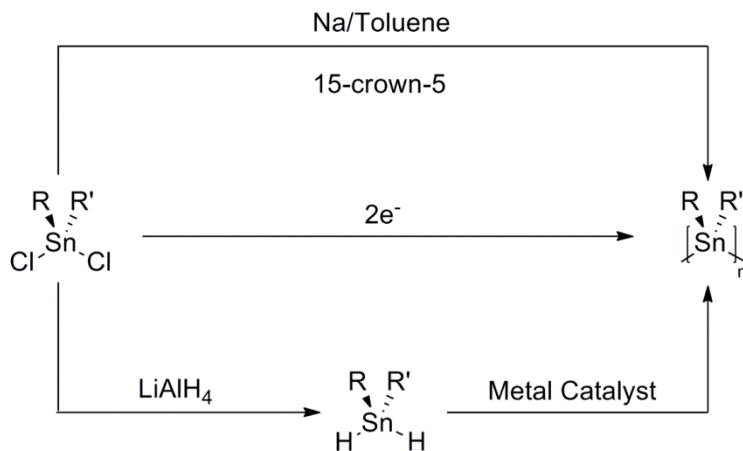


Figure 1.1: Three reaction routes for the synthesis of polystannanes from dichlorostannanes a) Wurtz coupling, b) electrochemical coupling c) reduction of dichlorostannane to form tin dihydrides followed by dehydrogenative coupling.

The preparation of suitable tin-containing monomers for polymerization by either Wurtz or electrochemical coupling (tin dichlorides) or dehydrogenative coupling (tin dihydrides) is well established (Figure 1.1). There are several known syntheses for the preparation of tin chlorides

* [Bu₂Sn]_n shows a ¹¹⁹Sn NMR peak at -190 ppm whereas the cyclic (Bu₂Sn)₅ species shows a ¹¹⁹Sn NMR signal at -202 ppm.

including the controlled thermal redistribution of R_4Sn ($R = \text{alkyl, aryl}$) and $SnCl_4$. These reactions are carried out in the absence of solvent and at relatively low temperatures ($<120^\circ\text{C}$) to form monochlorides (R_3SnCl), or at higher temperatures ($>120^\circ\text{C}$) where the formation of dichlorides (R_2SnCl_2) becomes more prevalent. These tin dichlorides can then be used for polymerization by Wurtz or electrochemical coupling or further reacted with reducing agents, such as $LiAlH_4$, to form mono- or di- tin hydrides, (R_3SnH or R_2SnH_2), the latter of which can be used as a monomer for dehydrogenative polymerization. Tin dialkyl and diaryl dibromides have also been prepared using Br_2 as a brominating agent with R_4Sn . Tin dibromides can then be reduced to form tin dihydrides suitable for polymerization.¹⁸

Wurtz coupling is a reductive process by which a radical is formed from a halogenated species, which goes on to react with a second halogenated species through a method of radical chain growth. Originally carried out in the presence of molten sodium, *Zou et al.*⁴ modified the Wurtz coupling of dichlorostannanes to employ considerably less harsh conditions. The reaction that Zou performed using toluene as the solvent is carried out first via dispersion of Na metal at reflux with the help of 15-crown-5. The reaction is then brought down to a temperature of 60°C and the tin dichloride monomer slowly added in additional toluene over several hours. The method was further improved by *Price et al.*⁵ who showed that shorter reaction times are a key factor in increasing the size and lowering the dispersity of the polymers formed as well as reducing the percent impurity of cyclic oligomers. An optimal reaction period of 4 h was found to yield the highest molecular weight polystannanes* with the lowest amount of cyclic oligomers formed (Table 1.1). Wurtz type coupling has also been used to produce co-polymers containing both silicon and tin within the backbone.^{19,20}

* Examples from the of Wurtz coupling prepared $[R_2Sn]_n$ where $R = n\text{-Bu}$ or Ph .

Table 1.1: Wurtz Coupling of $(n\text{-Bu})_2\text{SnCl}_2$ in toluene at 60°C as a function of time.⁵

Time (h)	$M_n(\times 10^6)$ (Da)	M_n/M_w	R^a
1	1.15	1.3	0.25
2	1.17	1.3	0.33
4.2	1.09	1.4	0.80
5.5	0.91	1.3	0.10

^a Ratio of high molecular weight polymer to cyclic oligomers at 1000 Da

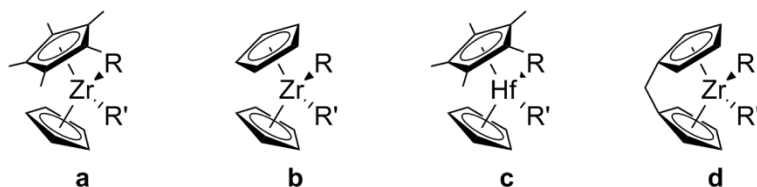
Wurtz coupling of polystannanes was also carried out by Caseri *et al.*¹³ in a solution of liquid ammonia at -78°C . Wurtz coupling was achieved by a one (all monomer added in one aliquot) or two (monomer separated into two aliquots and added in steps) step methods. Using these processes, Caseri was able to prepare both polymers and copolymers of butyl and phenyl tin systems, with molecular weights $\approx 1 \times 10^4$ Da and PDIs of between 2.2 and 3.8.*

A more recently discovered route to the preparation of polystannanes was via electrolysis. This was accomplished by Okano *et al.*⁶ in 1998 who electrochemically reduced $R_2\text{SnCl}_2$ ($R = n\text{-Bu}, n\text{-Oct}$) to form the associated polymers. This was achieved in a one compartment cell fitted with a syringe port, a Pt anode and an Ag cathode with tetra-*n*-butylammonium perchlorate as the supporting electrolyte in 1,2-dimethoxyethane. Molecular weights of the polydi(*n*-butyl)stannanes, $[(n\text{-Bu})_2\text{Sn}]_n$, were found to be between 6×10^3 - 1.2×10^4 Da with PDIs ranging from 1.3-2.6 respectively, depending on the current efficiency. These reactions were also performed with RSnCl_3 ($R = \text{Me}, n\text{-Bu}, n\text{-Oct}, \text{Ph}$) that showed the formation of ladder polystannanes.⁷ These polymers were of the chemical formula $[\text{RSnCl}_x]_n$ where x is between 0 and 2. Polystannanes formed this way were not fully characterized,

* PDI dependent on substituent and backbone structure.

however they display a UV-visible spectra tailing well into the visible range (850 nm) with no identifiable peak, indicative of an amorphous network.

Dehydrogenative coupling is the more common method for the synthesis of polystannanes. This involves building Sn-Sn σ -bonds by the elimination of hydrogen gas. First demonstrated by Tilley *et al.*,⁸ dehydrogenative coupling was successfully achieved using neat $(n\text{-Bu})_2\text{SnH}_2$ or Ph_2SnH_2 dihydrides with a zirconocene based catalyst, $[\text{Zr}(\eta^5\text{-C}_5\text{H}_5)(\eta^5\text{-C}_5\text{Me}_5)(\text{Si}(\text{SiMe}_3)_3\text{Me})]$, in the absence of light. After 5 h, the resulting polymer was precipitated in dry methanol yielding a linear polystannane.



1) R = Si(SiMe₃)₃, R' = Me 2) R = Si(SiMe₃)₃, R' = Cl 3) R = Me, R' = Me

Figure 1.2: Tilley's catalysts evaluated for the dehydrogenative coupling of $(n\text{-Bu})_2\text{SnH}_2$. **1(a,b,d)**, **2(a,b,c)**, **3(a,b,c)** under various test conditions.

Tilley⁹ used a defined protocol of adding the neat tin monomer to catalyst (2 mol %) under nitrogen and screened a series of zirconocene based catalysts (Figure 1.2) over different reaction times. These catalysts include various derivatives used in a prior study,⁹ as well as a cationic catalyst, and a catalyst loading with a small amount of solvent. The best polymerization result from this screening was with ansa-2-zirconocene (Figure 1.2, **1d**) with $M_w = 6.7 \times 10^4$ Da after 11 h. This catalyst showed a high degree of depolymerisation after 24 h. Tilley was also able to polymerize a series of diaryl tin dihydrides to produce polymers of varying structures and molecular weights (Table 1.2).¹⁰

The zirconocene system (a d^0 metal) was further studied mechanistically using a hafnium metallocene analogue due to the inability of the zirconocene system to trap intermediate species.¹¹ This system showed an α -H elimination, forming a free stannylene. This was immediately followed by insertion of the stannylene between the SnH bond.

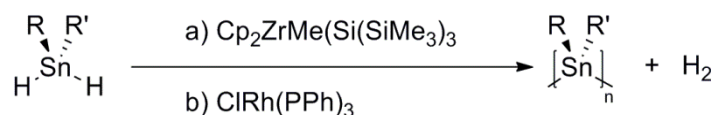


Figure 1.3: Dehydrogenative coupling reactions by a) Tilley⁹ and b) Caseri^{14,15} to synthesize $[\text{R}_2\text{Sn}]_n$.

Sita¹² and Caseri^{14,15} were also able to synthesis polystannanes through a dehydrogenative coupling reaction involving secondary tin hydrides and rhodium catalysts, $\text{CORh}^{\text{I}}(\text{PPh}_3)_3\text{H}$ and $\text{ClRh}^{\text{I}}(\text{PPh}_3)_3$ (Figure 1.3). Sita, using the same reaction protocol as Tilley was able to make highly branched systems that contained cyclic oligomers within the reaction mixture. Caseri was able to demonstrate good molecular weight control by adding the dialkyl tin monomer drop wise to the Wilkinson's catalyst in DCM, driving the reaction to completion without the production of cyclic oligomers and forming high molecular weight linear $[(n\text{-Bu})_2\text{Sn}]_n$. The polymer was then isolated from solution by cooling the DCM reaction solution. Caseri,¹⁶ using the same conditions, prepared a series of dialkylstannyl hydrides (Et, *n*-Pr, *n*-Bu, *n*-Pe, *n*-Hex, *n*-Oct, *n*-Dod) that readily formed poly(dialkyl)stannanes using Wilkinson's catalyst. These polymers had $M_w \approx 10^4$ Da and PDIs ranging from 1.5-2.7.

There has been some evidence in the literature indicating that dehydrogenative coupling occurs with other catalytic systems including platinum complexes,^{21,22} Group 4 metallocenes, Group 6 carbonyl complexes,^{23,24} and lanthanide species.²⁵ The majority of these systems produced only dimers or small oligomers. The notable exception to this is the platinum complex

$[(\kappa^2\text{-P,N})\text{-Ph}_2\text{PC}_2\text{H}_4\text{NMe}_2]\text{PtMe}_2$ from Schubert *et al.*^{21,22} Using ^{119}Sn NMR spectroscopy they were able to demonstrate that they could synthesize $[(n\text{-Bu})_2\text{Sn}]_n$ with no cyclic oligomers. However, no further research of this system was completed beyond the initial NMR studies.

Foucher *et al.*¹⁷ demonstrated the catalyst free thermally driven dehydrogenative coupling of $(n\text{-Bu})_2\text{SnH}_2$ to form $[(n\text{-Bu})_2\text{Sn}]_n$. These solvent and catalyst free reactions were carried out under reduced pressure for a period of 6 h. Modest molecular weights (1.8×10^4 Da) and broad polydispersities (PDI = 6.9) were observed through GPC. There was a significant fraction (20%) of low molecular weight cyclic oligomers also formed.

1.1.2 Properties

Polystannanes are covalently bonded main group metal polymers with interesting properties. Optically, poly(dialkyl)stannanes range from yellow to orange semi-solids. The λ_{max} of $[(n\text{-Bu})_2\text{Sn}]_n$ is at 382 nm with the λ_{max} values of 360-400 nm for other alkyl polymers ranging from Et to *n*-Dod substituents. Oligostannanes of diethyl tin ($[\text{Et}_2\text{Sn}]_{2-6}$), show a trend towards redshifting from 232 nm to 325 nm (UV to visible) as the chains become increasingly longer.²⁶ Similarly, $[\text{Ph}_2\text{Sn}]_n$ (low M_w in THF*) is slightly redshifted ($\lambda_{\text{max}} = 402$ nm) compared to dialkyl species.⁹ The addition of different aryl substituents was able to further decrease the band gap of these polystannanes and redshift the λ_{max} of these materials from red to green.¹⁰ These polymers show λ_{max} values of 432-506 nm as seen in Table 1.2.

* high molecular weight poly(diphenyl)stannane is insoluble.

Table 1.2: UV-Vis of selected $[R_2Sn]_n$.

Substituent ^a	Color	λ_{\max} (nm) ^b
C_6H_5	Yellow	402
<i>p</i> -(<i>t</i> -Bu)- C_6H_4	Orange	432
<i>p</i> -(<i>n</i> -Hex)- C_6H_4	Yellow-orange	436
<i>o</i> -Et- C_6H_4	Red-orange	468 ^c
<i>p</i> -(<i>n</i> -BuO)- C_6H_4	Orange	448
<i>o</i> -Et- <i>p</i> -(<i>n</i> -Bu)O- C_6H_4	Dark red	506
<i>p</i> -(Me ₃ Si) ₂ N- C_6H_4	Green	450

^a All compounds have the structure $[R_2Sn]$ where R = the substituent. ^b Extinction coefficients where not reported for these polymers ^c Insoluble therefore the λ_{\max} of film was reported instead.

The electronics of polystannanes have been modelled via Sandorfy HMO²⁷ and LDF²⁸ level calculations. When the calculated band gap energies of polystannanes are compared to those of polysilanes (PSi = 3.89 eV) and polygermanes (PGe = 3.31 eV), polystannanes are considerably lower (PSn = 2.80 eV) based on an all ‘trans-planar’ (TP) geometry. * Calculations using a ‘gauche-helix’ (GH) geometry** lead to larger band gaps following the same trend as the TP geometry (PSi = 5.94 eV, PGe = 5.13 eV, PSn = 4.65 eV). A correlation between the length of the system and the band gap was observed showing a rapid increase slowing towards a horizontal asymptote following a Lineweaver-Burk plot.²⁹

In these calculations, the molecular orbitals that were associated with the HOVB (Highest Occupied Valence Band) and the LUCB (Lowest Unoccupied Conduction Band) were found.

* Trans-planar geometry is a zigzag confirmation with a Sn-Sn-Sn-Sn torsion angle equal to zero.

** Gauche-helix geometry is a coil confirmation with a Sn-Sn-Sn-Sn torsion angle larger than zero.

The HOVB structurally exhibits a $p\sigma$ characteristic between $5p_x$ orbitals of neighbouring tins. The LUCB shows σ^* characteristic of the $5p_y$ and $5s$ orbitals.

Bond lengths and angles of polystannanes are heavily dependent on the nature of the side chain substituent. Sn-Sn bond lengths are generally longer with larger substituents, such as $(\text{Me}_3\text{Si})_2\text{HC}$ or *t*-Bu. Larger substituents also distort the tetrahedral nature of the Sn center by increasing bond angles. The changes in bond lengths and bond angles directly correlates to observable and electronic properties such as UV-Vis (band gap), IR/Raman (resonance), NMR chemical shifts, as well as the Sn-Sn coupling in the ^{119}Sn NMR spectroscopy. This was first studied with model compounds by Dräger *et al.*³⁰ who explored the electronic and structural properties of tin dimers, trimers, and tetramers. Generally, band gaps were found to decrease with longer Sn-Sn bonds and larger Sn-Sn-Sn angles resulting in a red-shifting of the UV-Vis spectra.

^{119}Sn NMR signals are closely related to the nature and type of substituents at the tin center. Methyl systems display a larger shielding than *n*-butyl, while *t*-butyl substituents result in even greater deshielding. Dräger also found that the experimental ^{119}Sn NMR Sn-Sn 1J coupling also correlated to bond length while the 2J coupling correlated to bond angle.³⁰

Differential Scanning Calorimetry (DSC) of $[(n\text{-Bu})_2\text{Sn}]_n$ show a phase change between crystalline and liquid-crystalline (LC) mesophase structures at approximately* -25°C and the reverse at 0°C . Alkyl polymers with side chains shorter than *n*-butyl showed only one phase transition. Alkyl polymers with longer side chains showed two reversible phase transitions (see Table 1.3).¹⁶ Upon further examination of these polymers through microscopy and X-ray

* Cycling through heating cooling showed variation of a few degrees, most likely due to size of crystals formed.

diffraction, it was observed that all polymers were birefringent below the first transition. Polystannanes bearing Et, *n*-Pr, *n*-Bu, and *n*-Pe substituents showed no change in birefringence up to 100°C.* In contrast, *n*-Hex and *n*-Dod polymers showed a decrease in the birefringence above the first transition with *n*-Oct showing no birefringence** above the first transition. Finally, polystannanes with *n*-Hex, *n*-Dod and *n*-Oct substituents lost all birefringence above the second transition.

Table 1.3: Thermal transitions of $[R_2Sn]_n$.¹⁶

Compound		First Transition (°C)	Second Transition (°C)
$[Et_2Sn]_n$	heating	15	-
	cooling	6	-
$[(n-Pr)_2Sn]_n$	heating	93	-
	cooling	63	-
$[(n-Bu)_2Sn]_n$	heating	1	-
	cooling	-26	-
$[(n-Pe)_2Sn]_n$	heating	6	57
	cooling	-16	42
$[(n-Hex)_2Sn]_n$	heating	34	68
	cooling	21	43
$[(n-Oct)_2Sn]_n$	heating	29	74
	cooling	13	58
$[(n-Doc)_2Sn]_n$	heating	55	91
	cooling	39	80

The charge mobility of $[(n-Bu)_2Sn]_n$ has been studied via Pulse-Radiolysis Time Resolved Microwave Conductivity (PR-TRMC).³¹ Charge mobilities were found to be from 0.097 and 0.027 $cm^2V^{-1}s^{-1}$ for crystalline and LC mesophase respectively. This is comparable to

* Observations were only made to 100°C due to stability issues.

** Properties of materials where refraction is dependent on the polarization and propagation direction of light

charge mobilities previously observed for dialkyl silicon and germanium based polymers as shown in Table 1.4.

Table 1.4: Charge mobility of Group 14 polymers.

Compound	Transition Temperature ^a		$\Sigma\mu_{1D}$		λ_{max} (nm)	$d(X-X)$ (Å)
	°C		(cm ² V ⁻¹ s ⁻¹)			
	K→M	M→K	K	M		
[(<i>n</i> -Bu) ₂ Si] _n	38	74	0.021	0.108	315	2.35
[(<i>n</i> -Hex) ₂ Ge] _n	23	36	0.021	0.078	324	2.50
[(<i>n</i> -Bu) ₂ Sn] _n	-25	0	0.027	0.097	382	2.85

^a K = crystalline, M = liquid-crystal mesophase.

1.1.3 Stability

Polystannanes show a remarkable thermal stability up to 200°C. However, polystannanes display inherent light and moisture sensitivity. All known polystannanes suffer from stability issues and therefore must be handled in an inert atmosphere void of light. This makes the synthesis, characterization and processing of polystannanes challenging and reduces their value as materials.

Polystannanes have been shown to be air sensitive.⁶ However, when polystannanes are exposed to pure O₂, there is no observed depolymerisation. This indicates that the stability issues are due to moisture and not O₂.¹⁹ The usual method for the evaluation of the stability of polystannanes is to follow the degradation of the UV-Vis λ_{max} signal. When exposed to small amounts of moisture (water) the UV-Vis signal decreases rapidly over time. This decomposition is accelerated by the addition of a wet solvent.

The light sensitivity of polystannanes has been well studied using both NMR and UV-Vis spectroscopies. It was established that solid state polystannanes are considerably more stable

than dissolved polymers and solvents has a great overall effect on the stability of polystannanes. When dissolved in aromatic or aliphatic solvents such as benzene, toluene or short chain alkenes, stability was very poor, with THF showing only slightly higher stability. When polystannanes are dissolved in chlorinated solvents or solvents such as styrene, a higher stability is observed. The stability of polystannanes can be increased by the addition of radical scavengers or dyes.³²

The ^{119}Sn NMR chemical shifts for the breakdown products after light exposure range in from +150 to -200 ppm and have not fully been identified. However, the breakdown to smaller molecular mass 5- and 6-membered cyclic oligomers was observed with little to no further degradation noted. The likely mechanism of degradation is an unzipping of the chains and not random chain cleavage.

1.2 Ferrocenophanes



Figure 1.4: The basic structure of from left to right [1]ferrocenophane, [2]ferrocenophane and [1.1]ferrocenophane

Metallophenanes are macrocyclic structures that contain at least one, and possibly multiple, metallocenes within their cyclic structure. Ferrocenophanes (Figure 1.4) are of particular interest due to the oxidative and light stability of the ferrocene unit. [1]ferrocenophanes (and to a lesser extent [2]- and [3]ferrocenophanes) have been used as monomers for ROP to form polyferrocenylenes (see Section 1.3). Ferrocenophanes where the cyclopentadiene rings of one ferrocene are attached via a bridging unit (also known as ansaferrocenes) are named [n]ferrocenophanes where n denotes the size of the bridging chain.

When multiple ferrocenes are involved, a decimal is placed between the lengths of each bridging unit. Therefore a [1.1]ferrocenophane has two ferrocenes that are attached via two bridges with a length of one atom.

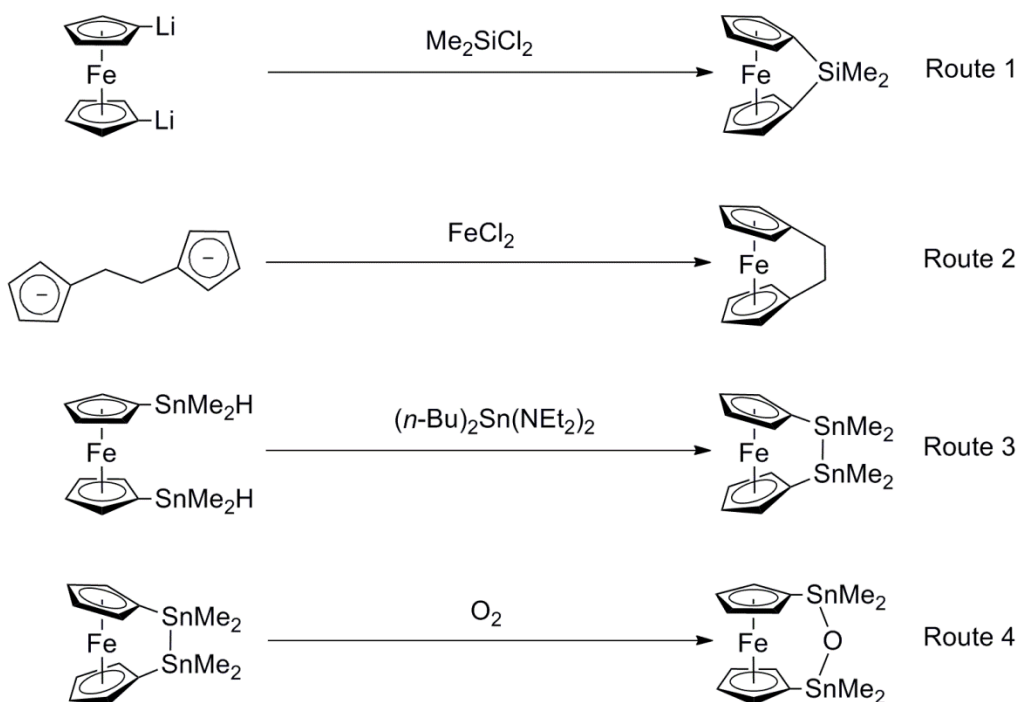


Figure 1.5: Examples of the four routes to [n]ferrocenophanes

The synthesis of [1]ferrocenophanes is generally carried out through a salt elimination between $\text{Fe}(\eta^5\text{-C}_5\text{H}_4\text{Li})_2 \cdot \text{TMEDA}$ (1,1'-dilithioferrocene • *N,N,N',N'*-tetramethylethylenediamine) and a dichloride (ECl_2) related to the desired bridging unit (Route 1). This was first described by Osborne, who in 1975³³ synthesized diphenylsilyl-[1]ferrocenophane. Previous to this, several other larger [n]ferrocenophanes had been prepared via three different methods (Figure 1.5). The routes of preparation of [n]ferrocenophanes include building the [n]ferrocenophane from a reaction between a linked bi-cyclopentadiene dianion and FeCl_2 (Route 2); ring-closing the cyclophane with substituted ferrocenes (Route 3); and finally ring expansion of an existing

[n]ferrocenophane (Route 4).³⁴ These four routes (Figure 1.5) are the main methods of synthesis of many of the ferrocenophanes known today.

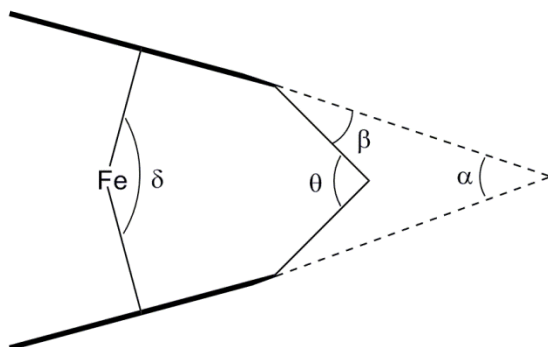


Figure 1.6: Diagram of the ring strain of ferrocenophanes.

The salt elimination method (Route 1) used by Osborne has been used to prepare [1]ferrocenophanes of Group 13 (B, Al, Ga),^{35,36} 14 (Si, Ge, Sn)^{33,37,38} or 15 (P, As)^{37,39} as well as Group 4 (Ti, Zr, and Hf).⁴⁰ These [1]ferrocenophanes have considerable ring strain (α between in Figure 1.5) which makes them prime candidates for ring-opening polymerizations. [2]ferrocenophanes that contain mixed Group 14 elements (Ge-C and Sn-C bridged) were synthesized via a similar salt elimination of dilithiated methyl ferrocene ($\eta^5\text{-C}_5\text{H}_4\text{CH}_2\text{Li}$) $\text{Fe}(\eta^5\text{-C}_5\text{H}_4\text{Li})$ with either dialkyl germanium or tin dichlorides. The tetramethylgermyl-[2]ferrocenophane was also prepared through a reaction between $\text{Fe}(\eta^5\text{-C}_5\text{H}_4\text{Li})_2$ and 1,2-dichloro-1,1,2,2-tetramethyldigermane. Other [2]ferrocenophanes can be prepared via the formation of the ferrocene with the bridge already in place (Route 2), eg. ethylene bridged [2]ferrocenophane; or through a ring closing reaction of a 1,1'-substituted ferrocene, like in the case of 1,1,2,2-tetramethylstannyl-[2]ferrocenophane (see Section 1.4). Several [n]ferrocenophanes where n is greater than two have been isolated including elements in Group 13, 14,⁴¹ 15 and 16,⁴² usually through expansion reactions (Route 4 in Figure 1.5).

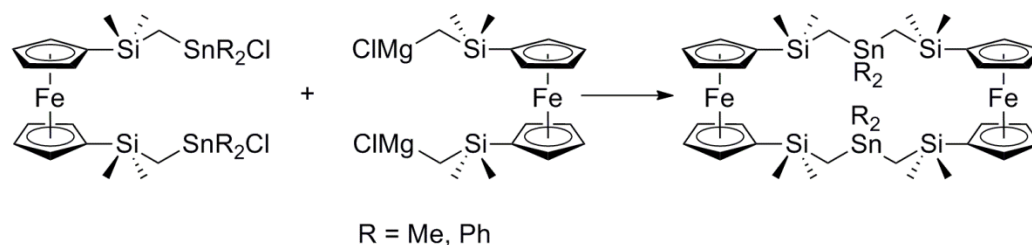


Figure 1.7: Reaction to prepare a [5.5] ferrocenophane.

Larger homogeneous* [n.m]ferrocenophanes have been of interest to organometallic chemists, however there has been relatively little synthetic, commercial, or industrial use of these materials. [1.1]ferrocenophanes containing Group 12 (Hg),⁴³ 13 (B, Ga, In),⁴⁴⁻⁴⁶ 14 (C, Si, Sn)⁴⁷⁻⁵⁰ or 15 (P, As)^{51,52} have been synthesized through a variety of different methods. The majority of these products have been isolated as a by-product from the synthesis of [1]ferrocenophanes or from the ROP of [1]ferrocenophanes to form polyferrocenylenes, and the yields of these products are typically low. A few larger [2.2]ferrocenophanes containing mainly first row elements have also been synthesized,⁵³ however there has been little research into their material properties. Jurkschat *et al.* prepared a [5.5]ferrocenophane through a Grignard reaction of two 1,1'-disubstituted ferrocenes (Figure 1.7).^{54,55}

1.3 Polyferrocenylenes

Considerable research effort has been focused on the synthesis of inorganic polymers with specific tunable properties that may be useful in optic and electronic technologies. One such polymeric system under consideration is polymers that contain ferrocene, both as a substituent or as a part of the backbone of the polymer. There has been several review articles published on the

* Only one element is present in the main chain of the bridge of homogeneous [n.m]ferrocenophanes.

topic of polyferrocenes.⁵⁶⁻⁵⁸ A very brief history of the synthesis of ferrocene-containing polymers and their some of their key properties will be discussed in this section.

1.3.1 Synthesis

Since its discovery in the middle of the 20th century, ferrocene has been utilized in a variety of chemical and biochemical sensing systems. This is largely due to its interesting optoelectric properties, its excellent structural stability, and unique bonding structure. Within a few years of ferrocene's discovery, polymers containing ferrocene as a pendant group were prepared by Arimoto and Haven.⁵⁹ These polymers were synthesized through both radical and acid catalyzed polymerization of vinylferrocene. Homopolymers and copolymers with methyl methacrylate, styrene and 2-chloro-1,3-butadiene were also synthesized forming ferrocene containing materials with various physical properties.

Polymers containing ferrocene and optionally another bridging group within the backbone of the polymer, or polyferrocenylenes, have been largely synthesized through two methods; condensation or ring-opening polymerization (ROP). Of these two routes, condensation is a more established method, but often leads to low molecular weight polymers or oligomers. By contrast, ROP of [1]ferrocenophanes affords high molecular weight polymers as well as demonstrating a living nature, offering greater control over the polymers synthesized. For the most part, ROP of [1]ferrocenophanes is the preferred method of synthesis of high molecular weight ferrocene-based polymers.

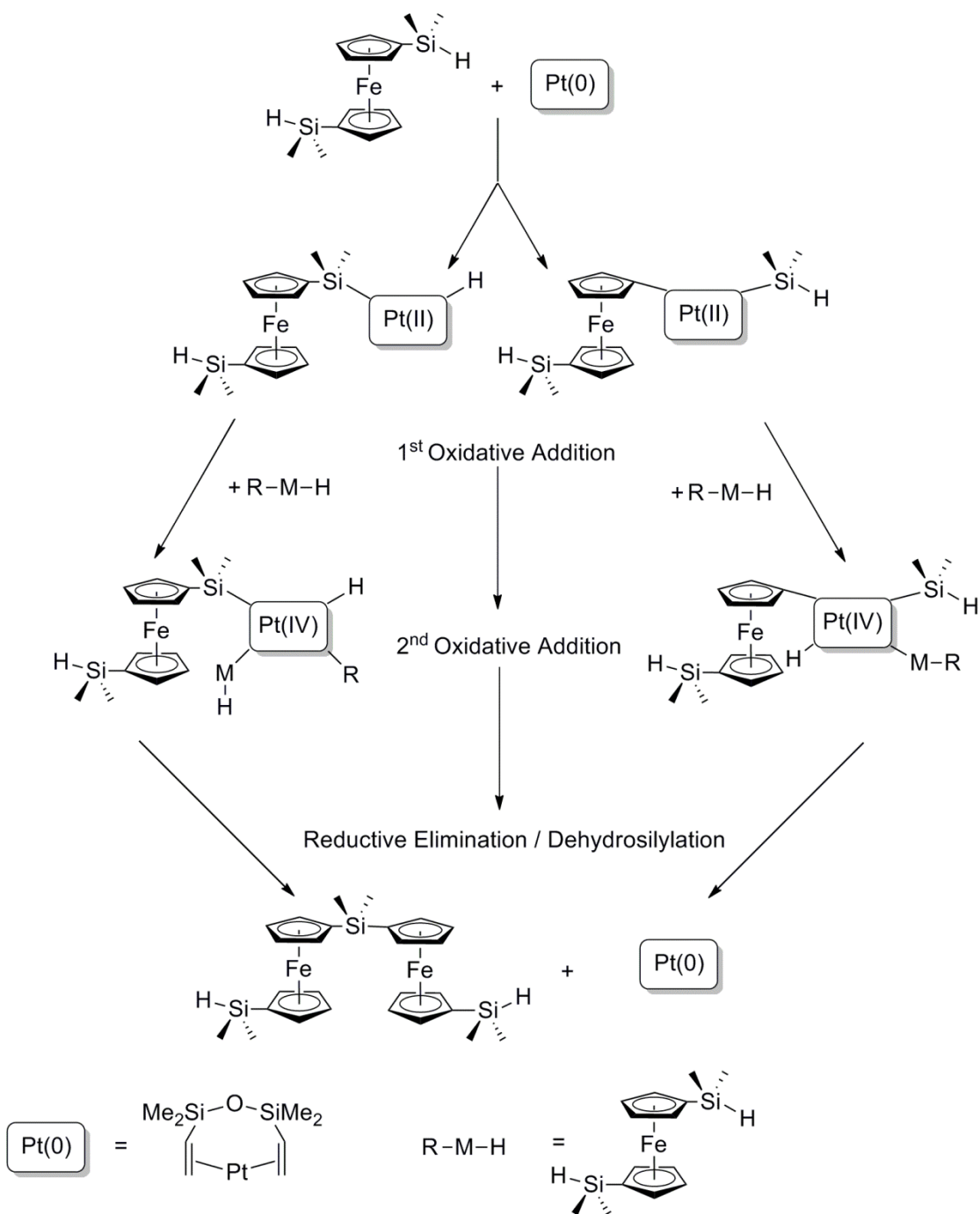


Figure 1.8: Proposed mechanism dehydrosilylation of $\text{Fe}(\eta^5\text{-C}_5\text{H}_4\text{SiMe}_2\text{H})_2$.⁶⁰

The first macromolecular structures with ferrocene as part of the backbone were prepared by Korshak⁶¹ through radical recombination.* Later, Neuse described the radical recombination reaction of *t*-butyl hydrogen peroxide with ferrocene at high temperatures to form insoluble homopolymers of ferrocene (polyferrocenylene).⁶² Around the same time, low molecular weight a poly(mercuri)-ferrocenylene was prepared though the reaction of 1.1'-dichloromercuriferrocene with either ethanolic sodium iodide or aqueous sodium thiosulfate.⁶³ Poly(mercuri)ferrocenylene was further reacted in molten ferrocene to form low molecular weight ($M_n = 3.5 \times 10^3$ Da) polyferrocenylene. Neuse reacted equal parts $\text{Fe}(\eta^5\text{-C}_5\text{H}_4\text{Li})_2 \cdot \text{TMEDA}$ and $\text{Fe}(\eta^5\text{-C}_5\text{H}_4\text{I})_2$ and was able to prepare a slightly larger ($M_n = 6.2 \times 10^3$ Da) polyferrocenylene $[\text{Fe}(\eta^5\text{-C}_5\text{H}_4)_2]_n$.⁶⁴ These materials were not, however, well characterized. Polyferrocenylene was also prepared by Yamamoto *et al.*⁶⁵ via a condensation of ferrocenyl dihalides in the presence of Mg to form mainly insoluble oligomers with an $M_n \approx 3 \times 10^3$ Da.** When Nishihara *et al.*⁶⁶ reacted $[\text{Na}][(\eta^5\text{-C}_5\text{H}_4(n\text{-Hex}))]$ with iodide and *n*-BuLi, the bicyclopentadiene dianion, $[\text{Na}]_2[(\text{C}_5\text{H}_3(n\text{-Hex}))_2]$, was formed. The product was further reacted with $\text{FeCl}_2 \cdot \text{THF}_2$ to form $[(\eta^5\text{-C}_5\text{H}_4(n\text{-Hex}))_2\text{Fe}]_n$ of $M_n = 5 \times 10^3$ Da and a PDI of 1.2.*** Rausch *et al.*⁶⁷ performed an Ullman coupling reaction to synthesize oligoferrocenylene in the melt through a copper catalyzed reaction. Ullman coupling of $\text{Fe}(\eta^5\text{-C}_5\text{H}_4\text{I})_2$ catalyzed by copper was later used by Foucher *et al.*⁶⁸ to prepare modest molecular weight polyferrocenylene of $M_w = 5.2 \times 10^3$ (PDI = 3.1). Ullman coupling to produce soluble polyferrocenylenes was also carried out using $\text{Fe}(\eta^5\text{-C}_5\text{H}_3(\text{Me})\text{I})_2$ ($M_w = 2.0\text{-}3.4 \times 10^3$ Da, PDI = 1.21-1.35) and as well as the $\text{Fe}(\eta^5\text{-C}_5\text{H}_3(\text{SiMe}_3)\text{I})_2$ ($M_w = 3.6\text{-}8.6 \times 10^3$ Da, PDI = 1.60-3.01).

* Radical recombination was originally carried out by Korshak however was not fully described until Neuse investigated it in 1966.

** Calculated by Elemental Analysis assuming end group of halide.

*** Polymer was separated via GPC from smaller oligomeric species.

Condensation reactions to form oligomeric and low to medium molecular weight polymeric species that contain both ferrocene and a spacer molecule in the backbone have been also been carried out. Rosenberg was able to prepare polyferrocenylsilanes (both dimethyl and diphenyl) of low molecular weights (methyl $M_w = 1 \times 10^3$ Da and phenyl $M_w = 7 \times 10^3$ Da) through a condensation of $\text{Fe}(\eta^5\text{-C}_5\text{H}_4\text{Li})_2 \cdot \text{TMEDA}$ with dihalosilanes.⁵⁸ Foucher *et al.*⁶⁰ using the Karstedt's catalyst was able to synthesis oligomeric $[\text{Fe}(\eta^5\text{-C}_5\text{H}_4)_2\text{SiMe}_2]_n$ through a dihydrosilylation of $\text{Fe}(\eta^5\text{-C}_5\text{H}_4\text{SiMe}_2\text{H})_2$ in DCM (Figure 1.8). When this reaction was carried out in DMF the reaction formed a polyferrocenyl disiloxane through an oxygen insertion, forming polymers of molecular weight of 1×10^5 Da and a PDI of 1.12.⁶⁹ A similar oxygen insertion was earlier performed by Nakazawa *et al.*⁷⁰ using the iron based catalyst $(\eta^5\text{-C}_5\text{H}_5)(\text{CO})_2\text{Fe}(\text{Me})$ to produce the same polyferrocenyl disiloxane.*

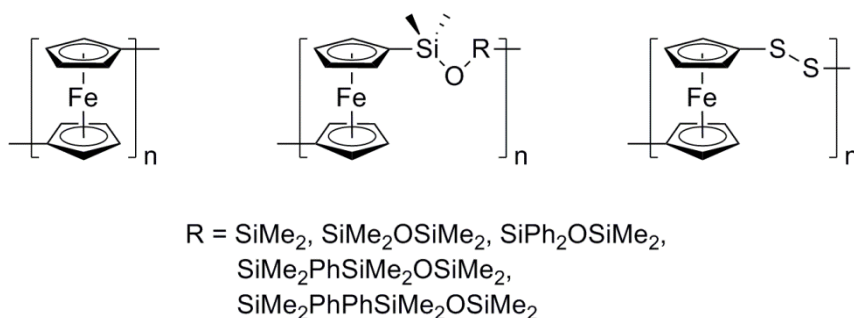


Figure 1.9: Structure of polyferrocenylenes, polyferrocenyl siloxanes, and polyferrocenyl disulphides.

Well characterized polyferrocenyl disiloxanes were formed through a reaction between a 1,1'-bis-silylamide ferrocene and a disilanol by Pittman *et al.*^{71,72} to form polymers $[\text{Fe}(\eta^5\text{C}_5\text{H}_4)_2\text{SiMe}_2\text{-O-R-O-SiMe}_2]_n$ where R is SiMe₂, SiPh₂, (SiMe₂)Ph(SiMe₂), and (SiMe₂)Ph-Ph(SiMe₂). These polymers were found to have molecular weights ranging from 7×10^3 to

* The publication originally reported the formation of polyferrocenylbis(dimethyl silane) and were forced to issue a correction due to elemental analysis data being wrong.

5.1×10^4 Da with PDI's in the range of 2.01 to 2.72. Condensation reactions have been carried out as well to form an azo-bridged polyferrocene. This was performed through a high pressure reaction with $\text{Fe}(\eta^5\text{-C}_5\text{H}_4\text{Li})_2 \cdot \text{TMEDA}$ and N_2O gas. The resulting polymer had a molecular weight of 8.7×10^4 Da and a PDI of 6.69.

Rauchfuss *et al.*,⁷³ through a novel ring-opening abstraction, was able to synthesize a disulfide bridged polyferrocene utilizing a Lewis base, $(n\text{-Bu})_3\text{P}$, initiated polymerization of a trithia-[3]ferrocenophane. The resulting disulfide polymer was insoluble and difficult to characterize. The issue of solubility was resolved by the substitution of one of the cyclopentadiene rings with an *n*-butyl group allowing for processing and characterization. The isolated soluble polymer had a molecular weight ranging from 7×10^3 - 1.5×10^5 Da. These polymers were yellow orange oils and showed thermal stability up to 230°C .

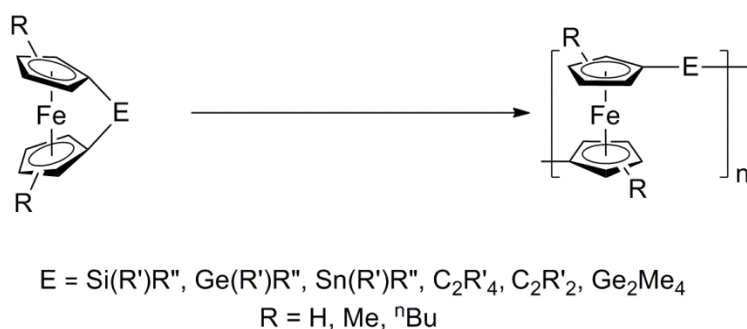


Figure 1.10: ROP of Group 14 [1]- and [2]ferrocenophanes.

As noted previously the preferred method of synthesis of ferrocene polymers is via ring-opening polymerization. This was first carried out by Manners *et al.*⁷⁴ who reported the synthesis of polydimethyl-silylferrocene through a thermal ROP of $\text{Fe}(\eta^5\text{-C}_5\text{H}_4)_2\text{SiMe}_2$. The thermal ROP reaction was performed at 150°C resulting in polymers that had a M_w of 5.2×10^5 Da and a PDI of ≈ 1.5 . In addition to the methyl substituted polymer, the phenyl analogue was also synthesised

through a similar route. The thermal ROP of $\text{Fe}(\eta^5\text{-C}_5\text{H}_4)_2\text{SiPh}_2$ was performed at 210°C. The polymeric material formed from this reaction was insoluble and therefore not fully characterized.

There have been several experimental conditions used to prepare polyferrocenylsilanes through ROP. These include the use of transition metal catalysts,^{75,76} anionic initiators,⁷⁷ and finally initiation through the use of UV radiation.⁷⁸⁻⁸¹ Both anionic and UV initiated polymerizations were found to be living polymerizations. A considerable amount of control over the molecular weights and polydispersities of this class of polymer has been achieved. ROP has been successfully expended to the preparation a variety single bridged ferrocene based polymers. These include Group 13 (B,⁸² Al,⁸³ Ga^{83,84}), 14 (Si,⁷⁴ Ge,^{85,86} Sn*), 15 (P⁸⁶), and 16 (S,^{73,87} Se⁸⁷). Polyferrocenyl-silanes have been synthesized with a variety of substituents including carbon based substituents (alkyl,^{86,88} alkyne,⁸⁰ and aryl groups⁸⁸) chlorides,⁸⁹ and ferrocene.⁹⁰ Finally there have been several polymetallocenes prepared via ROP with different metals including ruthenium⁸³ and vanadium.⁹¹

The living ROP methods of synthesis of $[\text{Fe}(\eta^5\text{-C}_5\text{H}_4)\text{SiMe}_2]_n$ have been used to produce block copolymers. These copolymers include polystyrene, polydimethylsiloxane, and polyferrocenyl silanes of differing functionality. Additionally, the preparation of di-, tri- and even penta- block copolymers can be accessed through these methods. These polymeric materials have shown great potential in nanomaterial and preceramics, due to their optoelectric properties and ability to self-assemble.⁵⁷

* See section 1.5 for more information on polyferrocenyl stannanes.



Figure 1.11: General ROP of ferrocenylenes from ferrocenophanes.

Table 1.5: Structure and molecular weight data for ferrocenylenes synthesised through ROP.

ROP ^a	E ^b	R ^b	M _w (Da)	PDI
Thermal	Me ₂ Si ⁸⁶	H	5.2×10 ⁵	1.53
	Et ₂ Si ⁸⁶	H	7.4×10 ⁵	1.54
	ⁿ Bu ₂ Si ⁸⁶	H	8.9×10 ⁵	2.6
	ⁿ Hex ₂ Si ⁸⁶	H	1.2×10 ⁵	1.58
	Ph ₂ Si	H	5.1×10 ⁴	1.6
	Me ₂ Ge ⁸⁶	H	2.3×10 ⁵	4.42
	H ₂ C-CH ₂ ⁸⁶	Me	8.1×10 ⁴	1.23
	PhP ⁸⁶	ⁿ Bu	^d	^d
	PhP	Me ₃ Si	6.6×10 ⁵	1.98
	S ⁸⁷	Me	1.15×10 ⁴	1.95
	R'Ga ^e	H	4.8×10 ⁵	3.3
MC	HC=CH ^{c,92}	H	2.1×10 ⁴	1.91
	Me ₂ Si	H	1.3×10 ⁵	1.08
A	Me ₂ Si ⁷⁷	H	9.4×10 ⁵	1.09
UV	Me ₂ Si ⁸¹	H	7.8×10 ⁵	1.12

^a Type of ROP, MC = metal catalyst, A = anionic, ^b see figure 1.11 for further structural detail ^c value for norbornene copolymer ^d adsorbed to GPC column ^e R' = 2-(3,5-di-*t*-butylphenyl)-*N,N*-dimethylmethanamine

Ring opening polymerization has also been used to synthesize polyferrocenes with two Group 14 atoms in the bridge. This includes CH₂CH₂,⁹³ HC=CH⁹² and GeMe₂GeMe₂.⁹⁴ The only evidence of a dibridge later Group 14 containing ferrocene polymer was prepared by Mochida *et al.*⁹⁴ who carried out ROP of tetramethyl-digermanyl-[2]-ferrocenophane with a few select Pd

and Pt catalysts. The resulting polyferrocenyl bis(dimethylgermane) had molecular weights of 2×10^4 - 5×10^5 Da, and PDI's ranging from 1.7-2.6.

1.3.2 Properties

One of the more interesting properties of polyferrocenylenes is their electrochemical behaviour. First described for biferrocene, cyclic voltammetry presented two defined redox waves (${}^1E_{1/2} = 0.31\text{V}$ and ${}^2E_{1/2} = 0.64\text{V}$ relative to ferrocene). This is due to strong Fe-Fe interactions between connecting ferrocenes. Tri- and quater-ferrocenes presented one redox event separated by approximately $\Delta E_{1/2} \approx 0.2\text{V}$ for every Fe center contained in the molecule. Oligomeric dimethylsilyl bridged ferrocene* species showed similar cyclic voltammetry to that of the unbridged oligoferrocenes with the presence of multiple peaks based on the length of the oligomers. All oligomeric systems with an odd number of iron centers showed only two redox waves (${}^{1-3}\Delta E_{1/2} \approx 0.22\text{V}$), the lowest of them being broader and having a larger integration. These uneven redox waves are due to two separate undefined oxidations within the first redox event. The systems with an even number of ferrocenes (other than the dimer) showed three redox waves (${}^{1-2}\Delta E_{1/2} \approx 0.15\text{V}$, ${}^{1-3}\Delta E_{1/2} \approx 0.22\text{V}$) however the integration of the central event decreased with an increase in the size of oligomers. A study carried out by Pannell *et al.*⁹⁵ using ferrocene dimers separated by a small dimethylsilane chain ($n = 0,1,2,3,6$) as model compounds showed a decrease in the $\Delta E_{1/2}$ with an increase in the chain length of the spacer between adjacent ferrocenes. In these model systems interactions between ferrocenes with three spacers showed little peak resolution while six spacers were completely insulating.

* Oligomeric species, although they do not show the exact same properties as polymeric materials are good model compounds for electrochemical interactions.

Table 1.6: Glass transition temperature, colour, and CV of $[\text{Fe}(\eta^5\text{-C}_5\text{H}_4)\text{E}]_n$.

Structure of Bridge (E)	T_g ($^{\circ}\text{C}$)	Colour	${}^1E_{1/2}$ (V)	${}^2E_{1/2}$ (V)	ΔE (V)
$\text{Me}_2\text{Si}^{88}$	$33^a/25^b$	Yellow	-0.04	0.17	0.21
$\text{Et}_2\text{Si}^{88}$	22^a	Yellow	-0.04	0.23	0.27
$(n\text{-Bu})_2\text{Si}^{88}$	3^a	Yellow	0.00	0.29	0.29
$(n\text{-Hex})_2\text{Si}^{88}$	$-26^a/-27^b$	Amber	0.02	0.31	0.29
$\text{Me}_2\text{Ge}^{86}$	nd^d	Yellow	-0.01	0.19	0.20
$\text{H}_2\text{C-CH}_2^{86}$	nd^d	Gold yellow	-0.27	-	0
PhP^{86}	nd^d	Red	-0.04	0.15	0.19
HC=CH^{c92}	nd^d	Orange	nd^d	nd^d	0.25
R^cGa	205^b	Orange	-0.047	-	-

^a Measured by DMA, ^b Measured by DSC, ^c R = 2-(3,5-di-*t*-butylphenyl)-*N,N*-dimethylmethanamine, ^d not reported.

The cyclic voltammetry of bridged polyferrocenyldialkylsilanes displayed two redox waves with $\Delta E_{1/2}$ values ranging from 0.21-0.29V indicating significant interaction between the Fe centers. When ferrocene based oligomers are bridged with an insulating methylene carbon, there is a notable decrease in the interaction between the Fe centers resulting in a smaller $\Delta E_{1/2}$ (0.1V). The insertion of an ethylene group between adjacent ferrocenes reduces the Fe-Fe interaction to 0V,⁸⁶ however if the ethylene group is replaced with a vinyl group then the system regains its conductivity with a $\Delta E = 0.25\text{V}$. Similarly, GeMe_2 bridged polyferrocenes showed a slightly decreased ability to communicate with adjacent Fe centers ($\Delta E = 0.20\text{V}$) while a PPh bridge decreased interactions even further ($\Delta E = 0.19\text{V}$). This is likely due to the increased distance between the Fe centers. When GaR was introduced into the backbone, it showed a similar insulating effect to that of a single C bridge displaying two undefined oxidation events and one broad reduction event.

The thermal properties of polyferrocenylenes are largely dependent on the composition of the bridge. Smaller substituents on the bridge allow for a tighter packing space and less free volume within the molecular structure of the polymer. As a result, the T_g (glass transition temperature) of polyferrocenylenes decrease with length of the linear side chain (Me>Et>*n*-Bu>*n*-Hex).⁸⁸ However the insertion of ferrocene within the polymer backbone raises the T_g significantly. For example $[\text{Fe } \eta^5\text{-C}_5\text{H}_4)_2\text{Si}(n\text{-Bu})_2]_n$ has a $T_g = 3^\circ\text{C}$, while the T_g for $[(n\text{-Bu})_2\text{Sn}]_n$ is found at -40°C .^{*} In general, symmetrically bridged polyferrocenylenes have lower glass transition temperatures than unsymmetrical ones. This can be seen through polyferrocenylysilylchlorides ($\text{Si}(\text{Cl})\text{Me}$ or SiCl_2) which have glass transition temperatures of 29°C (SiCl_2) and 59°C ($\text{Si}(\text{Cl})\text{Me}$) respectively.⁸⁹

The optical nature of polymers that include metallocenes in the backbone is primarily based on the type of metallocene involved. This is due to the nature of the metallocene electronic structure. As a result, polyferrocenylenes are yellow to red in color. Polyferrocenylysilanes with dialkyl chains show a slight increase in their λ_{max} as chain length increases (430-450 nm).⁸⁸ These polydi(alkyl)ferrocenylysilanes are yellow in color with the exception of $[\text{Fe}(\eta^5\text{-C}_5\text{H}_4)_2\text{Si}(n\text{-Hex})_2]_n$ which is amber. Silylchloride bridged polyferrocenylenes are orange in color, as are the germanium and vinyl bridge polyferrocenylenes,⁸⁹ while phosphorus-bridged polymers are red in color.

^{*} The T_g of *n*-Hex polysilane ($T_g = -52.5^\circ\text{C}$) is much lower than that of the ferrocene analogue ($T_g \approx 26^\circ\text{C}$) as well.

Table 1.7: Refractive indices for various polyferrocenylenes.

Structure of Bridge	R	RI (598 nm)	Std Dev RI's
Si(R)R'	R=Me, R'=CH ₂ CH ₂ CF ₃	1.599	0.007
	R=Me, R'=Et	1.663	0.004
	R=Me, R'=Me	1.678	0.003
	R=Me, R'=Ph	1.681	0.004
	R=Me, R'=p-C ₆ H ₄ Br	1.682	0.003
	R=Me, R'=ferrocenyl	1.696	0.001
	F=Me, R'=thienyl	1.691	0.000
Ge(R)R'	R=Me, R'=Me	1.689	0.002
PR	R=p-C ₆ H ₄ - ^t Bu	1.663	0.004
	R=Ph	1.737	0.003
P(S)R	R=p-C ₆ H ₄ - ^t Bu	1.668	0.006
	R=Ph	1.723	0.006
P(Se)R	R=p-C ₆ H ₄ - ^t Bu	1.713	0.007
	R=Ph	1.747	0.004

The tuneable refractive indices (RI) of these polymers and optical dispersion of these materials show promise in optics and optical electronics. Refractive indices were measured with a spectroscopic ellipsometer at 589 nm, as well as several different wavelengths to determine optical dispersion. Polyferrocenylsilanes, [Fe(η^5 -C₅H₄)₂Si(R)R']_n, have a range of RIs from 1.599 (R = Me, R' = CH₂CH₂CF₃) to 1.696 (R = Me, R' = thienyl). For [Fe(η^5 -C₅H₄)GeMe₂]_n, the RI was found to be slightly higher (1.689) than its silyl analogue (1.678). Polyferrocenyl stannanes were also measured and will be discussed in Section 1.5.2. Polyferrocenylphosphines,

$[\text{Fe}(\eta^5\text{C}_5\text{H}_4)_2\text{PR}]_n$ and phosphine sulfides and phosphine selenides $[\text{Fe}(\eta^5\text{-C}_5\text{H}_4)_2\text{P}(\text{E}^*)\text{R}]_n$ show refractive indices larger any known Group 14 polyferrocenylenes ranging from 1.669-1.737 for phosphines and 1.668-1.747 for phosphine sulfides and selenides.

Using the experimental refractive indices seen in Table 1.7, the molar refractions (R_m) for the backbone of each polymer can be calculated. The molar refraction is a measure of the effect that one portion of a molecular has on the refractive index of the bulk material and is directly proportional to the change in refractive index. To calculate the molar refraction eqn. 1 is used where n is the refractive index, V_m is the molar volume and R_i is the molar refraction for different parts of the molecule (ie. the backbone of the polymer, or the substituents).

$$\frac{n^2-1}{n^2+1}V_m = R_m = \sum_i R_i \quad (1)$$

Since the molar refraction of a given substance is equal to the sum of the molar refractions of individual parts (Eqn. 1) then the molar refraction of the backbone repeat units of the polymer can be calculated. The series of molar refractions for the polyferrocenylenes is Si (57.2) < Ge (58.9) < P (63.2).** The molar refractions can be used to calculate hypothetical refractive indices for polymers that have not yet been synthesized allowing for molecular tailoring to produce desired optical properties.⁹⁶

Materials that possess high refractive indices can already be produced through conjugation of organic polymers, and through suspension of metal atoms throughout polymeric materials. However, the importance of polyferrocenylenes in this regard is their ability to retain a low amount of optical dispersion with higher refractive indices. This is not true for either

* E = S or Se

** For polyferrocenyl stannanes see section 1.5.2

conjugated organics or the suspension of metal atoms. This is based on the calculation of Abbe's number* which is inversely proportional to the optical dispersion.⁹⁷

1.4 Ferrocenyl stannanes

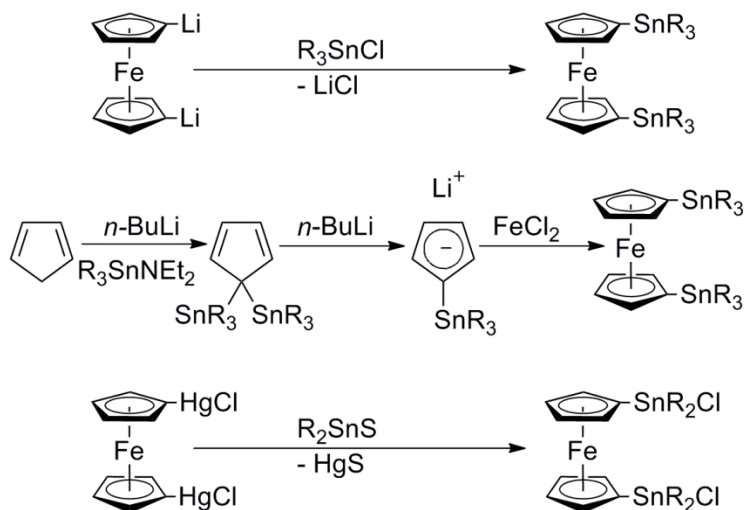


Figure 1.12: Methods of preparation of ferrocenyl stannanes.

Almost immediately after the discovery of ferrocene in 1951, ferrocenyl silanes^{98,99} were reported, and within a decade the first example of ferrocenyl germanes.¹⁰⁰ Beyond a few US patents,^{101,102} another decade passed before the synthesis of ferrocenyl stannanes was carried out. Dodo *et al.*¹⁰³ were able to produce a series (Et, *n*-Pr, *n*-Bu) of $(\eta^5-C_5H_4SnR_2H)_2Fe$ through the reaction of $Fe(\eta^5-C_5H_4Li)_2 \cdot TMEDA$ with trialkylstannyl halides. Ferrocenyl stannanes have also been prepared by first substituting the cyclopentadiene anion with Me_3SnNEt_2 (Figure 1.12). The resulting $C_5H_4(SnMe_3)_2$ reacted with *n*-BuLi to remove one trimethylstannyl group and resulting in the formation of the lithium salt $[Li][C_5H_4SnMe_3]$. The salt was then added to $FeCl_2$ to form the disubstituted tin ferrocene through a salt elimination of $LiCl$.¹⁰⁴

* Abbe's number is a ratio of the refractive indices at different wavelengths.

Dinh *et al.*¹⁰⁵ prepared the first chlorostannyl ferrocene in the literature. Both $\text{Fe}(\eta^5\text{-C}_5\text{H}_4\text{SnR}_2\text{H})_2$ and $\text{Fe}(\eta^5\text{-C}_5\text{H}_4\text{SnR}_2\text{Cl})_2$ ($\text{R} = \text{alkyl}$) were prepared via an exchange reaction with $\text{Fe}(\eta^5\text{-C}_5\text{H}_4\text{SnHgCl})_2$ with R_2SnS . The monosubstituted ferrocenyl stannanes have been synthesized through the same method. Dinh was also able to synthesis the phenyl analogue through the same route.

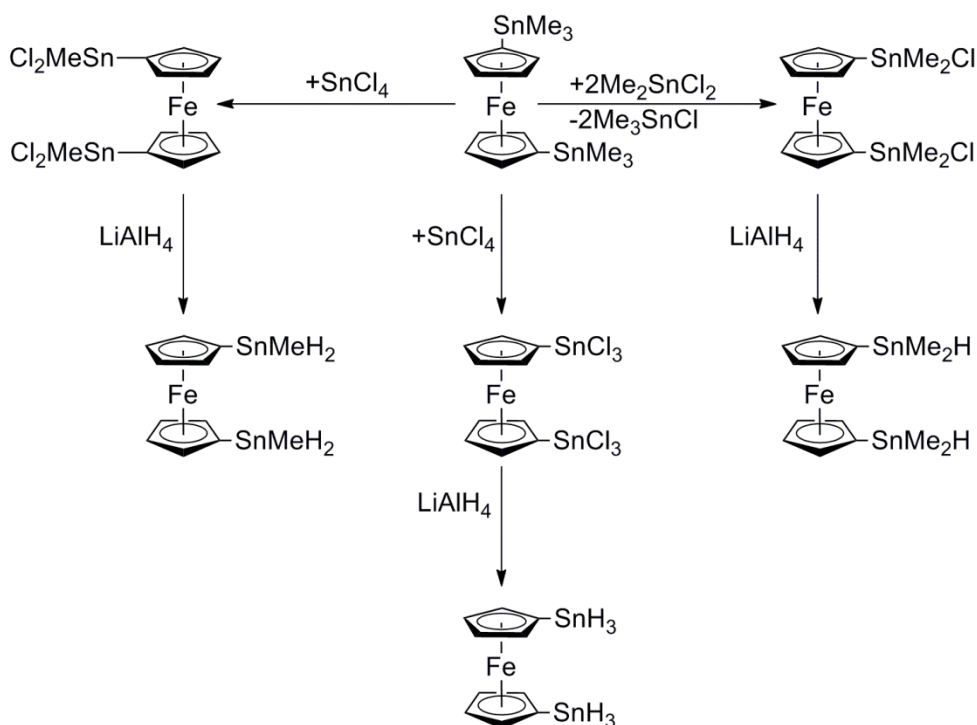


Figure 1.13: Routes to various 1,1'-bis(chlorostannyl)ferrocenes and 1,1'-bis(stannyl)ferrocenes.

Herberhold and Wrackmeyer were able to synthesize the $\text{Fe}(\eta^5\text{-C}_5\text{H}_4\text{SnMe}_2\text{Cl})_2$ through a redistribution reaction between $\text{Fe}(\eta^5\text{-C}_5\text{H}_4\text{SnMe}_3)_2$ and two equivalents of Me_2SnCl_2 at 140°C . This route was an improvement over the Dinh method as there was no use of mercury as either a reagent or a by-product; however this was only performed with methyltins. Herberhold and Wrackmeyer were also the first to prepare the corresponding ferrocenyl tin hydride through a reduction of the $\text{Fe}(\eta^5\text{-C}_5\text{H}_4\text{SnMe}_2\text{Cl})_2$.⁴¹ This involved reacting $\text{Fe}(\eta^5\text{-C}_5\text{H}_4\text{SnMe}_2\text{Cl})_2$ with

LiAlH₄ at 0°C under inert atmosphere. Further studies of the reactivity of the Fe(η⁵-C₅H₄SnMe₃)₂ system lead to production of a series of disubstituted mono-, di- and tri-chlorides, as well as the corresponding hydrides (Figure 1.13).¹⁰⁶

A variety of interesting structural ferrocenyl stannanes have produced through the systems described. Lenze *et al.* was able to prepare a series of multi-substituted methylstannylferrocenes through reactions with mono- and dilithioferrocene as well as through the initial formation of substituted cyclopentadiene rings that were then further reacted with FeCl₂ to form the corresponding ferrocene analogue.¹⁰⁷ Wu *et al.*¹⁰⁸ employed a mercury exchange with alkyl tin to form a 6-coordinate tin involving two ferrocenes, two chlorines and two aryl imines. Using (η⁵-C₅H₄SnCl₃)Fe(η⁵-C₅H₅) synthesized through a modified method Herberhold and Wrackmeyer used to prepare Fe(η⁵-C₅H₄SnCl₃)₂,¹⁰⁶ Dehnen *et al.* carried out a reaction with dry Na₂S to form a sulfur stannylferrocene cage.¹⁰⁹

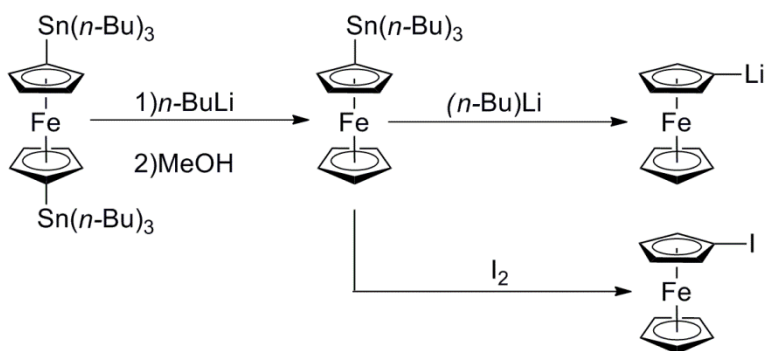


Figure 1.14: Synthesis of monolithio- or monoiodoferrocene.

In general the primary use of ferrocenyl stannanes is for the synthesis of monolithioferrocene and monoiodoferrocene. This can be achieved via a synthesis of (η⁵-C₅H₄Sn(n-Bu)₃)₂Fe by Dodo's method. The substituted ferrocene is then reacted with one

equivalent of *n*-BuLi producing a monolithiated (tri(*n*-butyl)stannyl)ferrocene. This product can either be reacted with another suitable halide to produce an unsymmetrical ferrocene¹¹⁰ or quenched with MeOH to form $(\eta^5\text{-C}_5\text{H}_4\text{Sn}(n\text{-Bu})_3)\text{Fe}(\eta^5\text{-C}_5\text{H}_5)$ ferrocene,¹¹¹ which then can be reacted with a further equivalent of *n*-BuLi to form $(\eta^5\text{-C}_5\text{H}_4\text{Li})\text{Fe}(\eta^5\text{-C}_5\text{H}_5)$, or the stannyl group can be exchanged via a reaction with I₂ to form $(\eta^5\text{-C}_5\text{H}_4\text{I})\text{Fe}(\eta^5\text{-C}_5\text{H}_5)$ and $(n\text{-Bu})_3\text{SnI}$ (Figure 1.14).^{112,113} The unsymmetrical ferrocene species have been used to form interesting small molecules,¹¹⁴ or undergone further manipulation to form polymers.¹¹⁵

Seyferth *et al.*⁵⁰ was the first to synthesize a homogenous bridged stannyl-[*n*]ferrocenophane in a very small yield ($\approx 3\%$). During a failed attempt to prepare $\text{Fe}(\eta^5\text{-C}_5\text{H}_4)_2\text{Sn}(n\text{-Bu})_2$, Seyferth was able to isolate, along with considerable polymeric material, the corresponding [1.1]ferrocenophane. Manners later discovered the route to stannyl-[1]ferrocenophanes involves the use of sterically bulky substituents.^{38,116} They synthesized both the $\text{Fe}(\eta^5\text{-C}_5\text{H}_4)_2\text{Sn}(t\text{-Bu})_2$ and the $(\eta^5\text{-C}_5\text{H}_4)_2\text{SnMes}_2$ through a reaction of $\text{Fe}(\eta^5\text{-C}_5\text{H}_4\text{Li})_2$ with R_2SnCl_2 (R = *t*-Bu and Mes).

The preparation of [2]- and [3]ferrocenophanes with di- or trisnanna bridging units was carried out by Herberhold and Wrackmeyer (Figure 1.15).⁴¹ They were able to perform an intramolecular dehydrogenative coupling of $\text{Fe}(\eta^5\text{-C}_5\text{H}_4\text{SnMe}_2\text{H})_2$ in the presence of $\text{R}_2\text{Sn}(\text{NEt}_2)_2$ when R = Et, *i*-Pr, and *n*-Bu to prepare 1,1',2,2'-tetramethyldistanna-[2]ferrocenophane $\text{Fe}(\eta^5\text{-C}_5\text{H}_4)_2(\text{SnMe}_2)_2$. When the same reaction was carried out with $\text{Me}_2\text{Sn}(\text{NEt}_2)_2$ a deamination coupling reaction occurred to form 1,1',2,2',3,3'-hexamethyltristanna-[3]ferrocenophane $\text{Fe}(\eta^5\text{-C}_5\text{H}_4)_2(\text{SnMe}_2)_3$ in a 43% yield.⁴¹

$\text{Fe}(\eta^5\text{-C}_5\text{H}_4)_2(\text{SnMe}_2)_2$ have been reacted with a series of Group 15 (P)¹¹⁷ and 16 (O, S, Se, Te)¹¹⁸ reactants allowing for insertion between the Sn-Sn bond to form heterogeneous 1,3-distanna-[3]ferrocenophanes. Pt metal complexes were also shown to insert between the Sn-Sn bond of a $\text{Fe}(\eta^5\text{-C}_5\text{H}_4)_2(\text{SnMe}_2)_2$.¹¹⁹ When elemental S, Se, or Te were reacted $\text{Fe}(\eta^5\text{-C}_5\text{H}_4)_2(\text{SnMe}_2)_3$ the central Sn was replaced with the corresponding chalcogen. When reacted with I_2 , the central Sn of the [3]ferrocenophane was removed as Me_2SnI_2 to form $\text{Fe}(\eta^5\text{-C}_5\text{H}_4\text{SnMe}_2)_2$.¹²⁰

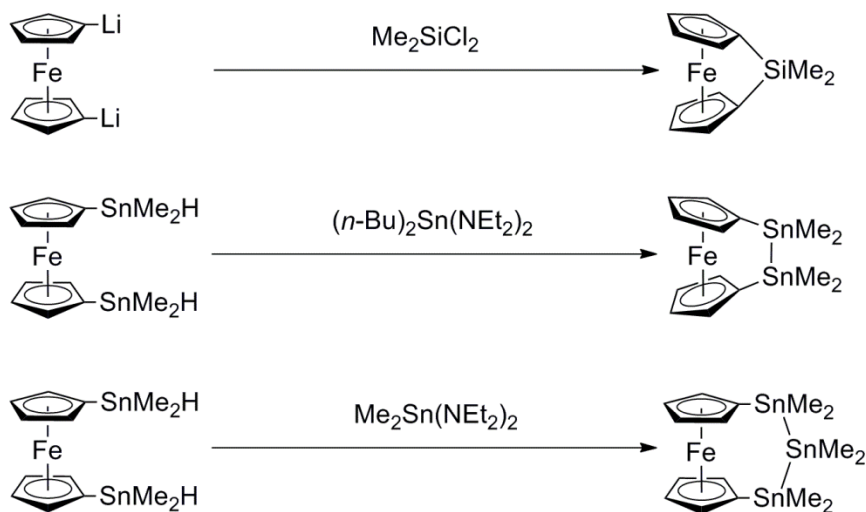


Figure 1.15: Preparation of stanna-[n]ferrocenophanes.

There has been some reports of the insertion of metal carbonyl groups into the Sn-C bond of [1]ferrocenophanes. When the insertion is performed with iron, $\text{Fe}(\text{CO})_4$ inserts to form the corresponding [2]ferrocenophane. However when $\text{Co}_2(\text{CO})_8$ is reacted with di(*t*-butyl)stannyl-[1]ferrocenophane, a ketone bridged biferrocene is formed with $\text{SnMe}_2\text{Co}(\text{CO})_4$ attached to the free cyclopentadiene ring of each ferrocene.¹²¹

1.5 Polyferrocenyl stannanes

Currently there are only a few known polyferrocenyl stannanes^{38,116,122} present in the literature, as well as one polyruthenocenyl stannane¹²³ and one polytroticenyl stannane*.¹²⁴ Due to limited methods of preparation and the small sampling of stannyl-[1]ferrocenophanes requiring sterically large substituents, the study of polyferrocenylstannanes has been limited. Attempts to synthesize less sterically bulky stannyl-[1]ferrocenophanes leads instead largely to the production of [1.1]ferrocenophanes and polymer.

1.5.1 Synthesis

In 1996 Manners *et al.*^{38,116} was able to ring open [1]ferrocenophanes $\text{Fe}(\eta^5\text{-C}_5\text{H}_4)_2\text{SnR}_2$ where R was either *t*-butyl or mesityl, to form high molecular weight polyferrocenylstannanes. When $[\text{Fe}(\eta^5\text{-C}_5\text{H}_4)_2\text{Sn}(t\text{-Bu})_2]_n$ was left in ambient temperatures for several days ROP spontaneously occurred to form $[\text{Fe}(\eta^5\text{-C}_5\text{H}_4)_2\text{Sn}(t\text{-Bu})_2]_n$, that was found to have a bimodal distribution of molecular weights at 2.3×10^5 Da and 1.5×10^4 Da with PDIs of 1.8 and 3.0 respectively. Thermal ROP of the *t*-butyl [1]ferrocenophane at 150°C produced polymer with a M_w of 1.5×10^5 Da and a PDI of 1.6 (Figure 1.16). When $\text{Fe}(\eta^5\text{-C}_5\text{H}_4)_2\text{Sn}(t\text{-Bu})_2$ was dissolved in toluene, non-catalyzed ROP occurred in only 6 h. The resulting high molecular weight polymer had an M_w of 9.0×10^6 Da and a PDI of 1.6. After 1 h, a low conversion (20%) with a molecular weight of 6.3×10^5 Da (PDI of 1.3) providing evidence that the polymerization is chain growth in nature. In the presence of chlorinated solvents such as CHCl_3 , lower molecular weight polymer ($M_w = 1 \times 10^4$ Da, PDI = 2.2), as well as the [1.1]ferrocenophane $[\text{Fe}(\eta^5\text{-C}_5\text{H}_4)_2\text{Sn}(t\text{-Bu})_2]_2$ formed within 6 h.

* troticene is the metallocene $(\eta^5\text{-C}_5\text{H}_5)\text{Ti}(\eta^7\text{-C}_7\text{H}_7)$

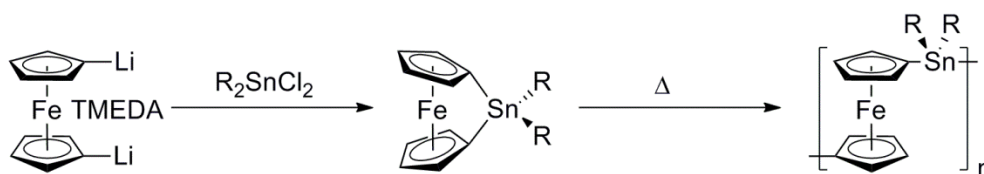


Figure 1.16: Synthesis of [1]ferrocenyl stannanes and ROP to form polyferrocenylstannane. When M = Fe R = (*t*-Bu), Mes, and PiPP, when M = Ru R = Mes.

Compared to the $\text{Fe}(\eta^5\text{-C}_5\text{H}_4)_2\text{Sn}(t\text{-Bu})_2$, the mesityl substituted monomer showed a reduced ability to undergo ROP. Mesityl monomers required heating for 6 h at 180°C (compared to 30 min at 150°C for the *t*-butyl monomer) before polymerization was completed. Completely stable when solvent free in ambient temperatures, these tin [1]ferrocenophanes took up to 30 d in solvents to ring open. Polymers formed via thermal ROP had molecular weight of around 1.5×10^5 Da with the largest polymers synthesized in solution (C_6D_6) at ambient temperatures for 15 d with molecular weight of 1.35×10^6 Da, PDI of 1.3 and a conversion of 50%.

Attempts to synthesize less sterically bulky tin containing [1]ferrocenophanes was less successful and produced only low to moderate molecular weight oligomeric species as well as cyclic [1.1]ferrocenophanes. These materials had molecular weights of $M_w = 1.4 \times 10^3$ Da. The only reported polydispersity index was that of the $[\text{Fe}(\eta^5\text{-C}_5\text{H}_4)_2\text{Sn}(t\text{-Bu})_2]_n$ ⁸⁶ with a PDI of 2.3.

The ROP of stannyl-[1]ferrocenophane to form polyferrocenylstannanes was initially believed to proceed through a radical mechanism, however there is no evidence for radicals* within ambient temperature reactions.¹²⁵ Furthermore, the addition of neutral nucleophiles dramatically increased the rate of reaction. When reacted with excess pyridine (0.1M in C_6H_6), the $\text{Fe}(\eta^5\text{-C}_5\text{H}_4)_2\text{SnMes}_2$ polymerization reached 95% conversion in 24 h compared to the

* negative radical trap and ineffective radical initiator of AIBN and Bu_3SnH at 60°C

control <3% conversion in 24 h at ambient temperatures. Due to the fact that pyridine did not add to the polymer, it was rationalized that the mechanism involved an attack of the Sn-C bond of one monomer by another. Similar results were discovered with the addition of a cationic species such as ROTf (R = H or (*n*-Bu)₃Sn).¹²⁶

Pannell *et al.*¹²² was also able to prepare and ring open the bulky Fe(η^5 -C₅H₄)₂SnPiPP₂ via a similar method. Thermal ROP was performed at 180°C for 2h to form polymeric material which, after precipitation in hexanes, was insoluble in organic solvents.*

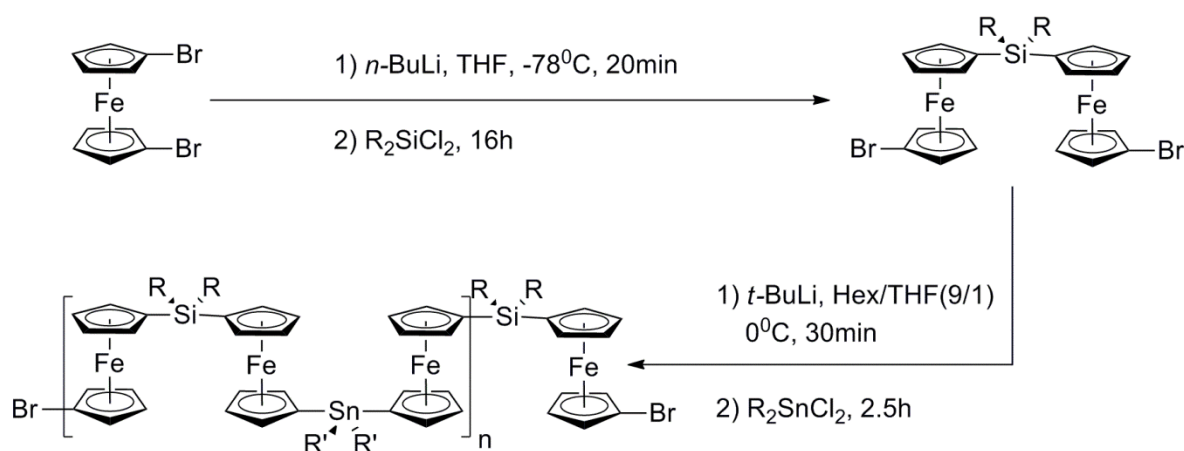


Figure 1.17: Route to synthesis of alternating FcSnFcSi oligomers. R = Me, Et; R' = Me, *n*-Bu, *t*-Bu

Muller *et al.*¹²⁷ in an attempt to synthesis [1.1]ferrocenophanes with alternating bridges of silicon and tin, was able to prepare oligomers of up to 10 repeating units of linear alternating ferrocenyl silanes and ferrocenyl stannanes [(η^5 -C₅H₄)Fe(η^5 -C₅H₄)-(SiR₂)-(η^5 -C₅H₄)Fe(η^5 -C₅H₄)-(SnR'₂)]^{**} (R = Me and Et, R' = Me, *n*-Bu, and *t*-Bu) as well as cyclic species of alternating ferrocenyl silanes and ferrocenyl stannanes of up to 11 repeating units. This was accomplished

* this is not surprising and follows with previously synthesised diarylsilyl and diarylgermyl ferrocene based polymers.

** this is the formula for the dimer, and the repeating unit that will always end with a ferrocenyl silane.

first by preparing a ferrocenyl silane dimer with two brominated cyclopentadiene rings, which was further reacted with *n*-BuLi, and finally with R'₂SnCl₂ (see Figure 1.17) to form linear and cyclic oligomeric species. Molecular weights of these oligomers ranged from 2.1-2.9×10³ Da with PDI's around 1.4 with two exceptions. Both oligomers (Me and Et silane) containing (*n*-Bu)₂Sn showed larger molecular weights of 6.3×10³ (Me) and 5.9×10³ (Et) Da with PDI's of 2.52 and 2.26 respectively.

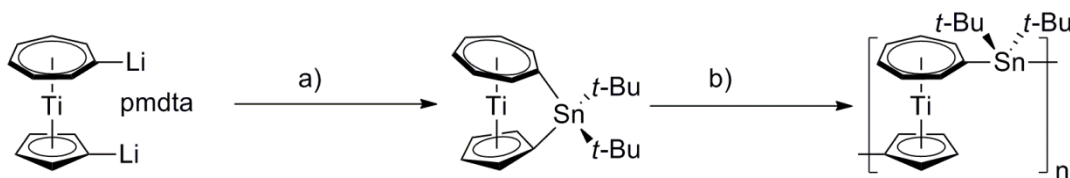


Figure 1.18: The synthesis of trocicenophane monomer and associated ring opening polymerization a) (*t*-Bu)₂SnCl₂ at -78°C in hexane b) 240°C solvent free or 2% *n*-BuLi in THF at room temperature.

Other polymetalloacenyl stannanes have been synthesised. The first was a thermal ROP of (dimesityl)stannyl-[1]ruthenocenophane to form a polyruthenocene dimesitylstannane, [Ru(η⁵-C₅H₄)₂Sn(Mes)₂]_n.¹²³ Through DSC, the thermal ROP of Ru(η⁵-C₅H₄)₂Sn(Mes)₂ commences at 181°C. When ROP was carried out at 200°C for 4.5 h a yield of 45% of the polymer was obtained, with a molecular weight of 6.2×10⁵ Da and a PDI of 2.28. Recently, an oligomeric trocicenylstannane was synthesized through a thermal ROP (onset of polymerization occurred at 233°C, DSC) of di-*t*-butylstanna-[1]trocicenophane at 240°C.¹²⁴ When *n*-BuLi was added to the same monomer in THF, polytrocicenylstannane was formed through an anionic initiated ROP. Polymers recovered had a molecular weight of 1.7×10³ Da for the thermal ROP and 1.4×10⁴ Da for the anionic ROP with PDI's of 1.4 and 1.9 respectively (Figure 1.18).

1.5.2 Properties

Polyferrocenyl stannanes display interesting optical, electronic, thermal, and structural properties. They are for the most part air and light stable which is typical of tetra alkyl or aryl tin compounds (R_4Sn where R = alkyl or aryl).

Thermally, polyferrocenyl stannanes show diverse properties that can be related to the rigidity of the tin bridge.* The $[Fe(\eta^5-C_5H_4)_2Sn(t-Bu)_2]_n$ prepared by Manners had a T_g of $124^\circ C$ and a thermal decomposition at $210^\circ C$ breaking down to a red/gold ceramic. This thermal stability is much lower than that of polyferrocenylsilanes,¹²⁸ in contrast to the much more rigid $[Fe(\eta^5-C_5H_4)_2SnMes_2]_n$ which showed a glass transition at $208^\circ C$ with thermal decomposition beginning at $320^\circ C$ forming a gold ceramic. With a T_g of $221^\circ C$ and thermal decomposition occurring at $270^\circ C$, the $[Ru(\eta^5-C_5H_4)_2SnMes_2]_n$ had similar thermal properties to its ferrocenyl analogue. The $[Fe(\eta^5-C_5H_4)_2SnPiPP_2]_n$ also shows a thermal decomposition between $300^\circ C$ and $400^\circ C$, although no glass transition was reported.

Metallocene based polymers have optical properties determined by the metallocene within their structure. Ferrocene based polymers are usually yellow to red in color. The polyferrocenyl stannanes are no exception, with the λ_{max} of the *t*-butyl and mesityl polymer 452 nm (with a shoulder at 340 nm) and 445 nm respectively. The ruthenocenyl stannanes polymer synthesised formed a white powder, while the zirconocenyl polymer was green in color.

Refractive indexes for polymers synthesized by Manners *et al.* have been studied extensively.^{96,97} The ferrocenyl stannane based polymers show refractive indexes of 1.64 (*t*-Bu) and 1.66 (Mes) measured at 589 nm. From the refractive index, the molar refraction of the

* The rigidity of the tin bridge is based on among other things the steric bulk of the substituents attached to the tin.

backbone was calculated to be $63.2^* \text{ cm}^3 \cdot \text{mol}^{-1}$ which was larger than those of Si and Ge. A theoretical calculation can be performed using the molar refraction values to predict the refractive index of unknown polyferrocenylstannanes substituted by methyl or naphthyl at 1.73 (methyl) and 1.80 (naphthyl). These values were higher than those measured for polyferrocenylsilanes, polyferrocenylgermanes, and polyferrocenylphosphines. The RI of the $[\text{Ru}(\eta^5\text{-C}_5\text{H}_4)_2\text{SnMes}_2]_n$ was found to be 1.66, the same as the $[\text{Fe}(\eta^5\text{-C}_5\text{H}_4)_2\text{SnMes}_2]_n$. The optical dispersion of these polymers was also calculated. The optical dispersion of polyferrocenyl stannanes was larger than that of polyruthenocenyl stannanes but still lower than organic and metal dispersed polymer of the same refractive indices.**

Table 1.8: Electronic properties of ferrocenyl stannanes.

E^{a}	${}^1\text{E}_{1/2} \text{ (V)}^{\text{b}}$	${}^1\text{E}_{1/2} \text{ (V)}^{\text{b}}$	$\Delta\text{E}_{1/2} \text{ (V)}$
$(n\text{-Bu})_2\text{Si}^{86}$	0.00	0.29	0.29
$(n\text{-Bu})_2\text{Sn}^{86}$	-0.06	0.18	0.24
$(t\text{-Bu})_2\text{Sn}^{116}$	0.00	0.24	0.24
$\text{Mes}_2\text{Sn}^{116}$	-0.07	0.14	0.21

^a where E is the bridging unit polymers with the molecular formula $[\text{FcE}]$ ^b all values are referenced to ferrocene/ferrocenium redox event.

Electronically, polyferrocenyl stannanes have the same effect that is observed by ferrocenyl silanes and germanes, specifically two redox events observed in cyclic voltammetry (CV). The observed $\text{E}_{1/2}$ values for that of polyferrocenyl stannanes are seen in Table 1.8.

* See section 1.3.2 for details of calculation.

** Based on calculation of Abbe's number, which is inversely proportional to optical dispersion.

1.6 Research objectives

The wide scale preparation of novel tin bridged ferrocene based polymers has to date met limited success due to the small number of monomers available for polymerization. The main objectives of this research to address this issue by synthesizing tin polymers by the synthesis of ferrocene based polymers via dehydrogenative of reactive monomers which avoids the need to prepare a large number of [1]ferrocenophanes. A further goal is to identify find a simple method of producing stannyl-[2]ferrocenophanes, as monomers for ROP. Finally the ROP of stannyl-[2]ferrocenophanes to prepare dibridged polyferrocenyl distannanes will be investigated.

2.0 Polymerisation of Novel Polyferrocenyl Dimethyl Stannyl Polymers

2.1 Introduction:

Since its discovery, ferrocene has been used in the modification of molecular structure. This is due, in part, to its structural stability and interesting optoelectric properties. The first examples of oligo- and low molecular weight polyferrocenyl silanes, $[\text{Fe}(\eta^5\text{-C}_5\text{H}_4)_2\text{SiR}_2]_n$ were prepared through the condensation of $\text{Fe}(\eta^5\text{-C}_5\text{H}_4\text{Li})_2$ with chlorosilanes.⁵⁸

The first well characterized high molecular weight polyferrocenylene was prepared in 1992 by Rauchfuss *et al.*⁷³ who was able to ring open, by a novel ring abstraction, trithia-[3]ferrocenophane through the use of a Lewis base, $(n\text{-Bu})_3\text{P}$, initiated reaction to form polyferrocenylene persulfide. In that same year Manners *et al.* synthesized high molecular weight $[\text{Fe}(\eta^5\text{-C}_5\text{H}_4)_2\text{SiMe}_2]_n$ through a thermal ring opening polymerization of a strained $\text{Fe}(\eta^5\text{-C}_5\text{H}_4)_2\text{SiMe}_2$.⁷⁴ Manners *et al.* were also able to perform ROP of these monomers to form $[\text{Fe}(\eta^5\text{-C}_5\text{H}_4)_2\text{SiR}_2]_n$ using transition metal catalysts,^{75,76} anionic initiators,⁷⁷ and UV radiation.⁷⁸⁻⁸¹ Since then, the synthesis, production, and characterization of different polyferrocenes have been of great interest to materials science. Ferrocene polymers that include bridging elements containing Groups 13-16⁸³⁻⁸⁷ have been synthesized through ROP of the corresponding [1]ferrocenophanes in high molecular weights and low PDI's.

Ferrocene based polymers containing a Group 14 element have been extensively studied. The Manners group has developed a large variety of these polyferrocenylenes containing C, Si, and Ge by ROP methods.^{85,86,92-94} Previous work in the Foucher group^{60,69} has described the preparation of $[\text{Fe}(\eta^5\text{-C}_5\text{H}_4)_2\text{SiMe}_2]_n$ through a desilylative coupling in DCM as well as a unique

polyferrocenyl disiloxane through the oxygen insertion reaction in DMF of $\text{Fe}(\eta^5\text{-C}_5\text{H}_4\text{SiMe}_2\text{H})_2$ using Karstedt's catalyst. Similar reactions to produce polyferrocenyl disiloxanes were also carried out by Nakazawa *et al.*⁷⁰ using an iron based catalyst ($(\eta^5\text{-C}_5\text{H}_5)(\text{CO}_2)\text{FeMe}$). Mochida *et al.*⁹⁴ was able to synthesize the only known dibridged ferrocene based polymer containing a later Group 14 element. A dibridged ferrocenyl germane polymer was prepared via a ROP of 1,1,2,2-tetramethyldigermyl-[2]ferrocenophane using both $\text{Pt}(\text{acac})_2$ and $\text{Pd}_2(\text{dba})_3$ as transition metal catalysts.

There are four examples of polyferrocenyl stannanes in the literature to date. Due to the nature of tin, bulky R groups must be used to stabilize stannyl [1]ferrocenophanes, which undergo thermal ROP. Manners was able to synthesize lower molecular weight *n*-Bu polymers through a condensation reaction of $\text{Fe}(\eta^5\text{-C}_5\text{H}_4\text{Li})_2$ and $(n\text{-Bu})_2\text{SnCl}_2$;⁸⁶ whereas the *t*-butyl and mesityl polymers were prepared through the thermal^{38,116} and nucleophilic¹²⁶ ROP* of the *t*-Bu and Mes stannyl-[1]ferrocenophane. Pannell¹²² also successfully synthesized and thermally ring-opened the diisopropylphenyl stannyl [1]ferrocenophane. Manners¹²³ was also able to ROP a tin-bridged [1]ruthenocenophane thermally to form the only known polyruthenocenylstannane.

2.2 Results and discussion

2.2.1 Synthesis of monomers

The preparation of monomers for condensation polymerization was carried out through a similar method to that reported by Herberhold and Wrackmeyer.⁴¹ Firstly, $(\eta^5\text{-C}_5\text{H}_4\text{Li})_2\text{Fe}\cdot\text{TMEDA}$ was prepared through a lithiation of ferrocene in the presence of TMEDA.

* The *n*-butyl polymer was attempt to synthesize the *n*-butyl [1]-ferrocenophane.

The $\text{Fe}(\eta^5\text{-C}_5\text{H}_4\text{Li})_2\cdot\text{TMEDA}$ was separated as an orange powder and stored under inert atmosphere conditions at room temperature.

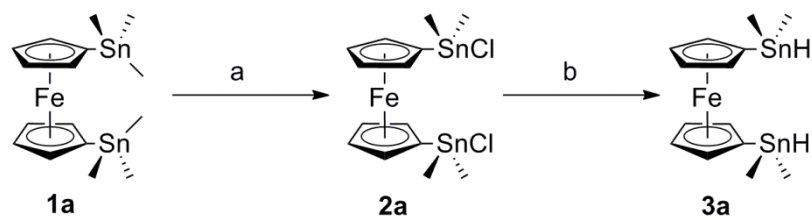


Figure 2.1: Synthesis of **3a** from **1a** via reactions a) Me_2SnCl_2 at 140°C in static vacuum for 3 h and b) LiAlH_4 in Et_2O at 0°C in inert atmosphere for 5 h.

The preparation of $\text{Fe}(\eta^5\text{-C}_5\text{H}_4\text{SnMe}_3)_2$, **1a** was carried out via a salt elimination reaction between the $\text{Fe}(\eta^5\text{-C}_5\text{H}_4\text{Li})_2\cdot\text{TMEDA}$ and Me_3SnCl . The resulting orange oil was moisture, light, and thermally stable up to 200°C . By-products of this reaction include a small amount mono-substituted trimethylstannyl ferrocene (5-10%) as well as unreacted ferrocene (1-2%). By-products were *in vacuo* at 180°C and purified product was recovered in a 95% yield. Through a redistribution reaction involving Me_2SnCl_2 and **1a** carried out at 140°C , forming $\text{Fe}(\eta^5\text{-C}_5\text{H}_4\text{SnMe}_2\text{Cl})_2$, **2a** (Figure 2.1) and Me_3SnCl . Compound **2a** (dark orange-green oil), was not fully purified, however it was placed *in vacuo* to remove some of the Me_3SnCl by-product and its purity monitored by ^{119}Sn NMR spectroscopy. Compound **2a** was immediately reduced with excess* LiAlH_4 , yielding the dihydride $\text{Fe}(\eta^5\text{-C}_5\text{H}_4\text{SnMe}_2\text{H})_2$ **3a**, recovered as a dark orange oil in 82% yield. The mono-substituted dimethylstannyl ferrocene, **3a'** was sometimes present as a by-product, however this was removed *in vacuo* at 90°C . **3a** is stable under N_2 in ambient temperatures and in light for a few weeks. When left for an extended period of time under inert

* excess LiAlH_4 allowed any remaining Me_3SnCl to be reduced to Me_3SnH . Me_3SnH is more volatile than its chlorinated counterpart and therefore can be removed completely *in vacuo* with little effort.

conditions, spontaneous dehydrogenative coupling occurs to form oligomeric di-bridged ferrocenyl stannane **4** (Figure 2.2).

An attempt was made to synthesize $\text{Fe}(\eta^5\text{-C}_5\text{H}_4\text{Sn}(n\text{-Bu})_2\text{H})_2$, **3b** through two different routes. Firstly, through a salt elimination reaction, **1b** was prepared in a 85% yield and purified at 230°C *in vacuo*. When a redistribution reaction was performed on compound **1b**, the result was a mixture of chlorinated species of $\text{Fe}(\eta^5\text{-C}_5\text{H}_4\text{Sn}(n\text{-Bu})_2\text{Cl})_2$ (**2b**), $\text{Fe}(\eta^5\text{-C}_5\text{H}_4\text{Sn}(n\text{-Bu})\text{Cl}_2)_2$, and $\text{Fe}(\eta^5\text{-C}_5\text{H}_4\text{SnCl}_3)_2$. The redistribution of **1b** did not proceed in the same fashion as **1a** due to the difference in boiling points of Me and *n*-Bu tin chlorides. Me_3SnCl boils at a lower temperature than Me_2SnCl_2 ; whereas the boiling point of $(n\text{-Bu})_3\text{SnCl}$ is higher than $(n\text{-Bu})_2\text{SnCl}_2$. In the redistribution of **1a**, the reaction is driven forward by the removal of Me_3SnCl ; however in the redistribution of **1b**, $(n\text{-Bu})_3\text{SnCl}$ remain in the reaction and is allowed to react further. Attempts to purify **2b** were unsuccessful, due to its reactivity with silica, and the ability for **2b** to undergo redistribution at temperatures needed for distillation.

A second unsuccessful route to the synthesis of **3b**, was to first synthesize di(*n*-butyl)-(diethylamine)tin chloride, $((n\text{-Bu})_2\text{SnCl}(\text{NEt}_2))$ through a salt elimination of lithium diethylamide (LiNEt_2) with one equivalent to $(n\text{-Bu})_2\text{SnCl}_2$. Due to the nature of Sn-N bonds the resulting compound was impure and reactive in moisture, on silica, or when heated *in vacuo*. When the reaction with $\text{Fe}(\eta^5\text{-C}_5\text{H}_4\text{Li})_2 \cdot \text{TMEDA}$ was carried out, a viscous oil was recovered displaying the presence of at least 3 distinct, inseparable species. No further efforts to obtain this species were attempted.

2.2.2 Condensation polymerization

Attempts to polymerize **3a** were initially carried out thermally at 120°C and 150°C. Observations by ^{119}Sn -NMR spectroscopy revealed that both the 1,1,2,2-tetramethyldistanna-[2]ferrocenophane **5a**, as well as polymer **4** were formed via a thermally driven dehydrogenative coupling reaction. Unfortunately, up to 50% of the reaction mixture was found to be an insoluble solid, which is likely cross-linked polyferrocenyl stannane.

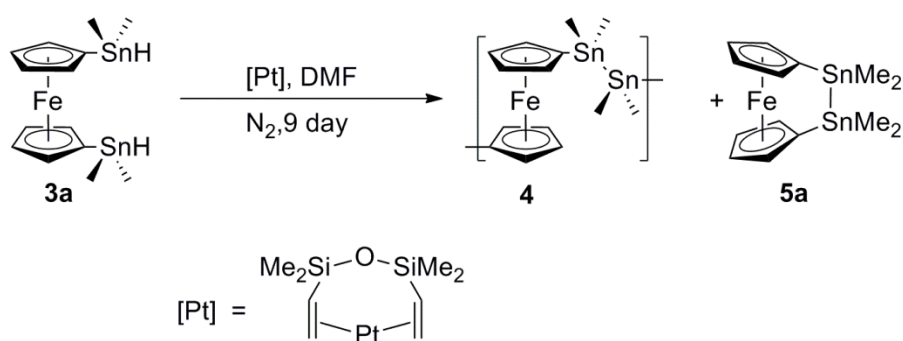


Figure 2.2: Metal catalyzed dehydrogenative coupling to form **4**.

Polymerization of **3a** via a Pt catalyzed condensation was performed in *N,N*-dimethyl formamide (DMF) at room temperature in inert atmosphere (Figure 1.8). By ^1H NMR spectroscopy the resulting polymer was determined to be the polyferrocenyl bis(dimethyl)stannane, **4**. This was a surprising result based on earlier research that was carried out by this group involving $\text{Fe}(\eta^5\text{-C}_5\text{H}_4\text{SiMe}_2\text{H})_2$. When the reaction to Figure 1.8 was performed on $\text{Fe}(\eta^5\text{-C}_5\text{H}_4\text{SiMe}_2\text{H})_2$ at 90°C in inert atmosphere, oxygen insertion to form a Si-O-Si bond was observed lead to the formation of $[\text{Fe}(\eta^5\text{-C}_5\text{H}_4\text{SiMe}_2)_2\text{O}]_n$.⁶⁹ The oxygen source was attributed to the Pt catalyzed reduction of DMF to form NMe_3 and subsequent release of oxygen. When a condensation reaction using $\text{Fe}(\eta^5\text{-C}_5\text{H}_4\text{SiMe}_2\text{H})_2$ with the Karstedt's catalyst was

carried out in DCM, a desilylative reaction to form the mono-bridged polymer $[\text{Fe}(\eta^5\text{-C}_5\text{H}_4)_2\text{SiMe}_2]_n$ occurred.

When dehydrogenative coupling was performed on **3a** in the absence of light, the reaction did not proceed at the same rate. Additionally, only the synthesis of smaller oligomeric species were detected by GPC. When the polymerization of **3a** was carried out in DMF at higher temperatures ($> 40^\circ\text{C}$) or highly concentrated ($> 20\% \text{ w/w}$)* 40% of the product recovered was insoluble polymer. This was at first surprising given the fact that the monomer was heated to 90°C *in vacuo* and showed no dehydrogenative coupling through this process. The insoluble solid is likely associated with a cross-linked polyferrocenyl stannane, however there is little definitive evidence based on the lack of solubility of this compound. The cross-linked polymers likely form due to a lowering of the stability of the Sn-Me bond because of coordination of DMF to the Sn center of **3a**.

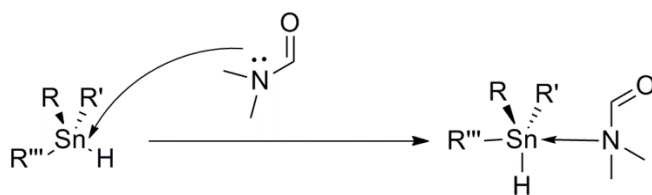


Figure 2.3: Coordination of DMF to a Sn center change the shape form tetrahedral to trigonal bipyramidal.

Evidence in the literature¹²⁵ suggests that amides are good coordinating agents with organo tin compounds. The coordination of N to Sn causes Sn-C bonds to expand due to the larger amount of electron density on the Sn center, decreasing the already low stability of these bonds. The Sn center will shift from tetrahedral to trigonal bipyramidal geometry (Figure 2.3). When heat is added to $\text{N}\rightarrow\text{Sn-C}$ systems, C-Sn bonds become more susceptible to breaking and

* Concentration of reactions is measured in w/w due to the ease of weighing solvent in the inert atmosphere system.

thus a site for crosslinking is formed. This hyper coordination is also a possible reason why this reaction occurs at such low temperatures. In this instance, the coordination of DMF to the Sn center of **3a** causes elongation of the Sn-H bond, destabilizing it, and making it more reactive to coupling reactions.

Condensation polymerization of **3a** in the presence of Karstedt's catalyst was performed in DMF over a period of 3 d. After the reaction was quenched with MeOH, analysis of the crude material by ^{119}Sn NMR spectroscopy displayed only the shifts for compounds **4** and **5a**.

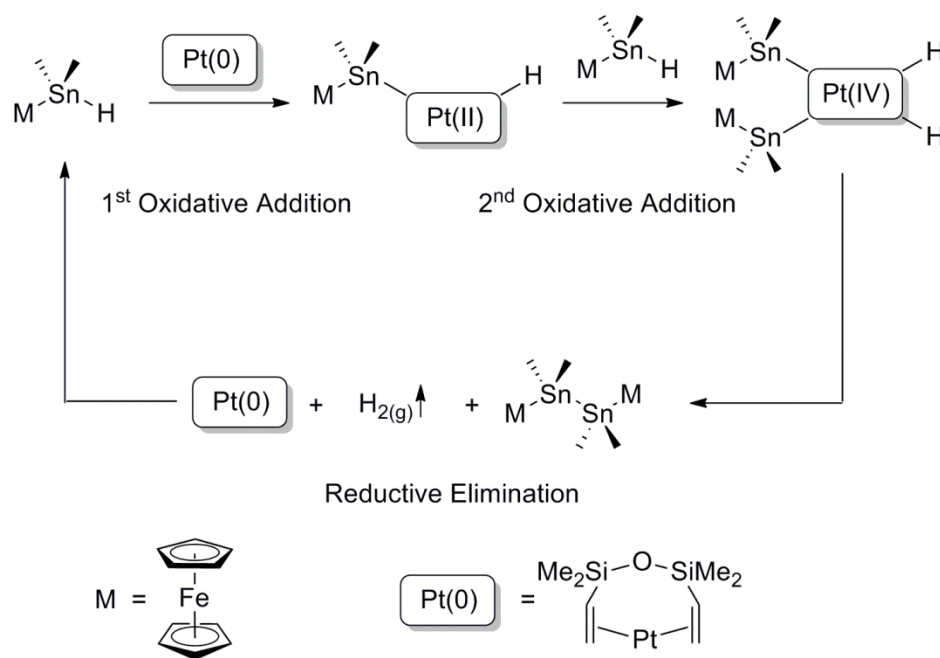


Figure 2.4: Dehydrogenative coupling reaction mechanism for **3a** to form **4**.

Dehydrogenative coupling of **3a** was also performed for several days in C_6H_6 , using a [Pt] catalyst. Using C_6H_6 as a solvent required higher temperatures and longer reaction times to drive the reaction forward (70°C , 3 d). The longer reaction time as well as the higher temperature of reaction is most likely due to the inability of C_6H_6 to coordinate to the Sn center.

A proposed mechanism for the dehydrogenative coupling of **3a** to form **4** follows a similar pathway as the proposed mechanism for the dehydrogenative coupling of $(\eta^5\text{-C}_5\text{H}_4\text{SiMe}_2\text{H})_2\text{Fe}$ by Foucher *et al.*⁶⁰ The reaction begins (Figure 2.4) with an oxidative addition of Pt(0) into the Sn-H bond to form a Pt(II) complex. Unlike the analogous reaction with the Si-H (Figure 1.8), there is no preference for insertion into the Sn-C bond. Instead, a second oxidative addition occurs as the Pt(II) complex inserts into a second unit of **3a** to form a Pt(IV) complex. Finally there is a reductive elimination to reform Pt(0) and create a Sn-Sn bond with concomitant the release $\text{H}_2(g)$ as a by-product.

2.2.3 Ring-opening polymerization

The synthesis of **5a** as a polymerizable monomer for the ring-opening polymerization was attempted through the same method originally used by as Herberhold and Wrackmeyer.⁴¹ Attempts to prepare **5a** in this way resulted in the formation of a previously unreported larger ferrocenophane, as well as minimal amount of the desired product (5%). An improved method utilizing $\text{Pd}_2(\text{dba})_3$ to facilitate the intramolecular dehydrogenative coupling of **3a** to form **5a** was discovered and all monomer was prepared via this new method. The novel reaction to synthesize **5a** and the characterization and structural determination of the novel ferrocenophane will be discussed in detail in Section 3.0.

An attempt was made to synthesize polyferrocenyl distannanes through a metal catalyzed ROP of **5a**. This was carried out based on previous work by Mochida *et al.* who performed the ROP of 1,1,2,2-tetramethyldigermyl-[2]ferrocenophane.⁹⁴ Several metal catalysts were employed, and these reactions were monitored by ^{119}Sn NMR spectroscopy.

All ROPs were carried out in C₆H₆ with Pt(acac)₂, Pd₂(dba)₃, and Pd(PPh₃)₄ catalysts at low concentrations. Reaction temperatures varied from RT to 60°C. All reactions proceeded slowly, with a trace of oligomeric material evident in analysis by ¹¹⁹Sn NMR spectroscopy and were not further purified. The only reaction that showed any substantial polymer formation was when the Pd(PPh₃)₄ catalyst was utilized.

The Pd(PPh₃)₄ catalyzed reaction was carried out at 60°C for 3 d in the dark. The resulting polymer was precipitated from minimal amount of THF into MeOH. Two ¹¹⁹Sn NMR signals were detected at -11.63 ppm and at 104.72 ppm, the latter of which is now identified as the chemical shift for the distanna bridged polymer **4**. The resonance detected at -11.63 has not been identified, however this could be an end group, or a Pd inserted complex of compound **5a** that is not soluble in MeOH.

2.2.4 Characterization by ¹H, ¹³C, and ¹¹⁹Sn NMR

All compounds were identified by ¹¹⁹Sn NMR spectroscopy and in almost all cases contained only one unique Sn environment. Compounds **1a**, **3a**, **4**, **5a** were studied by ¹H, ¹³C and ¹¹⁹Sn NMR spectroscopy. After redistribution reaction of **1a** with Me₂SnCl₂ compound **2a** was confirmed by ¹¹⁹Sn NMR spectroscopy. Compound **5a** was identified as a by-product in several dehydrogenative coupling reactions by its distinct ¹¹⁹Sn NMR signal at -43 ppm. Compound **4** was prepared in two different solvents (DMF and C₆H₆), extensive NMR evaluations were only carried out on polymer prepared in DMF.

Compounds **1a** and **3a** were readily identified by their ¹¹⁹Sn NMR shifts at -5.6 and -101.3 ppm respectively. With the addition of chlorine to the Sn center, the ¹¹⁹Sn chemical resonances moved down field to 126.8 ppm, similar to values reported by Herberhold.¹⁰⁶ Both **1a** and **3a**

were shifted down field from their mono-substituted analogues, with ^{119}Sn NMR shifts at -4.86 and -101.91 ppm respectively. ^1H NMR spectra for **1a** and **3a** displayed two cyclopentadiene protons that were split into pseudo triplets ranging between 3.9-4.6 ppm. The methyl protons of **1a** are present as a singlet at 0.28 ppm (CDCl_3) with one set of Sn satellites ($^1J_{\text{Sn-H}} = 54.3$ Hz). With the introduction of a hydride, the methyl chemical shift was split into a doublet ($^2J = 2.3$ Hz) and two sets of satellites ($^1J_{\text{Sn-H}} = 59.0$ Hz). The tin hydride chemical shift was split into a septet at 5.47 ppm ($^2J = 2.3$ Hz).

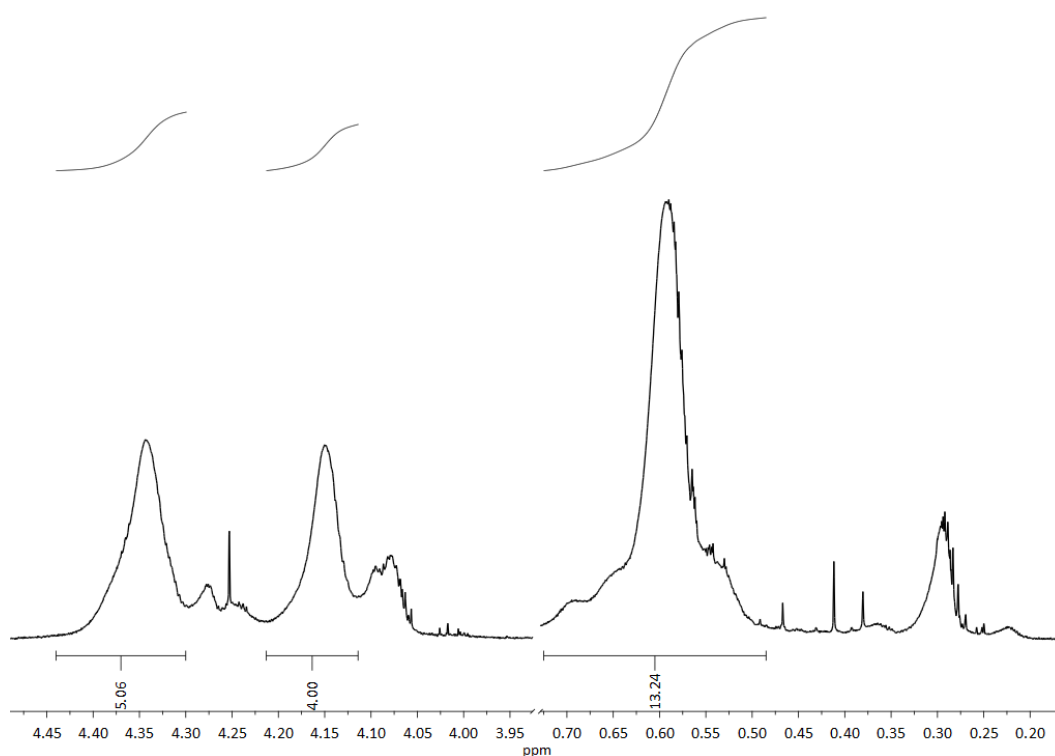


Figure 2.5: ^1H NMR (C_6D_6) spectra for compound **4**.

The ^1H NMR (Figure 2.5) spectra of polymer **4** displayed broad shifts associated with two cyclopentadiene proton environments at 4.35 and 4.15 ppm, and one methyl environment of

0.60 ppm integrating for approximately 4, 4, 12 protons respectively. The methyl shift at 0.60 ppm has one set of broad satellites ($^1J_{\text{Sn-H}} = 236.6$ Hz). Also visible in the ^1H NMR spectra were broad end groups with chemical shifts of 4.27 and 4.08 ppm for the cyclopentadiene region, and 1.24 for the methyl shift respectively. Based on the integration of the spectra, the structure was believed to be the dibridged polymer **4** instead of the mono-bridged analogue. Due to the apparent instability of this material, obtaining providing a clean ^1H NMR has been a challenge.

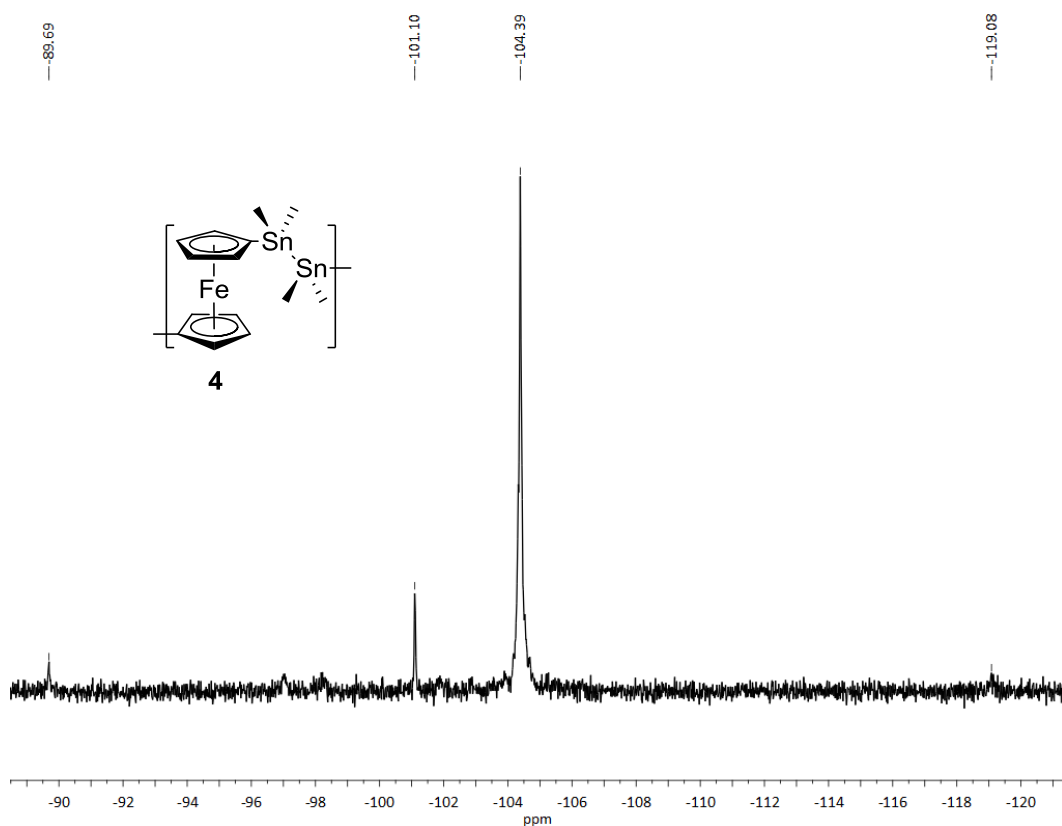


Figure 2.6: ^{119}Sn NMR spectrum of polymer **4** that contains the main polymer peak (-104.4 ppm) the $^{119}\text{Sn}/^{117}\text{Sn}$ coupling pattern (-89.7 ppm and -119.1 ppm) and the end group (-101.1 ppm).

The crude ^{119}Sn NMR (Figure 2.6) spectra confirmed the presence of compound **5a** as the by-product of condensation polymerization. Compound **5a** is present in most reactions where **3a**

is a reactant. The ^{119}Sn NMR shift of **5a** is easily identified at -43 ppm with a large set of $^{119}\text{Sn}/^{117}\text{Sn}$ satellites ($^1J = 5261.5$ Hz). When the sample is purified through precipitation in anhydrous MeOH, three chemical shifts are visible. A large shift at -104.4 ppm was identified as polymer **4** and displayed one set of $^{119}\text{Sn}/^{117}\text{Sn}$ satellites ($^1J = 4381.2$ Hz). The coupling constant is within reason for that of a $^{119}\text{Sn}/^{117}\text{Sn}$ 1J coupling constant between adjacent tins. This is hard evidence for a Sn-Sn bond within the structure of the polymer. Present in the precipitated polymer **4** was a small shift at -5.70 ppm (Appendix 1.5). The nature of this chemical environment is still unknown, however it must either be associated with polymer **4** (in the form of a stannoxane end group or impurity) or a separate polymer (possibly the mono-bridged ferrocenyl dimethyl stannane). Other than the main ^{119}Sn chemical shift for compound **4**, only a small end group resonance at -101.10 and a chemical shift for **5a** at -43 ppm was observed.

Polymer **4** was also characterized by ^{13}C NMR spectroscopy. Three broad chemical shifts were detected for the main chain of the polymer, as well as two smaller end group chemical shifts. These chemical shifts were identified as the cyclopentadiene shifts at 74.62, 71.23 and 69.32 (for the ipso-C) ppm and a methyl shift at -8.68 ppm. There was no observed $^{119}\text{Sn}/^{13}\text{C}$ coupling, however that was not surprising due to the broad nature of the chemical shifts and the low natural abundance of ^{13}C and ^{119}Sn or ^{117}Sn isotopes. The two small resonances that were associated with end groups were observed at 74.82 and 71.41 ppm, slightly down field from main chain polymer peaks.

The presence of end group resonances in the NMR spectra (^1H , ^{13}C , ^{119}Sn), of **4** more accurately describe a low molecular weight polymer. When the methyl end group was integrated by ^1H NMR spectroscopy and compared to the main methyl polymer, the end group shift is

approximately 12.9% of the signal intensity of the main chain polymer. This suggests that there are approximately 8 (SnMe₂)₂ bridges in the backbone of this polymer, with a M_n ≈ 4300 Da.

2.2.5 Molecular weight determination by GPC

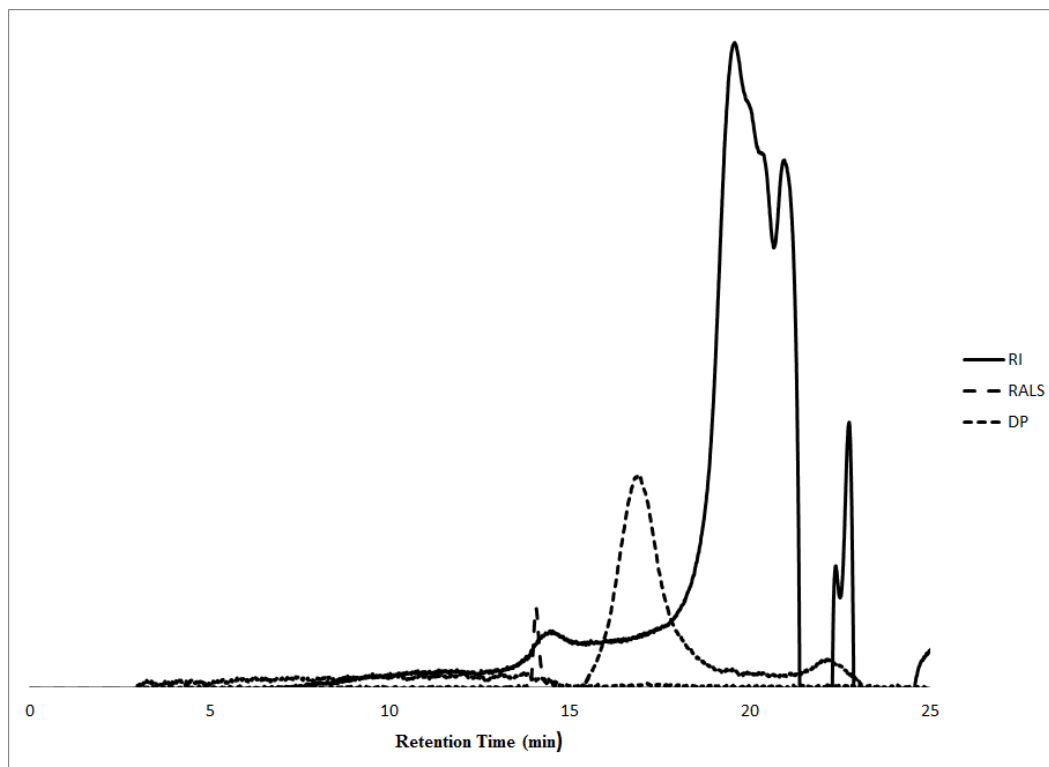


Figure 2.7: The GPC chromatogram for polymer **4** prepared in THF.

Gel permeation chromatography (GPC), along with ¹H NMR spectroscopy, was used to determine the molecular weight of polymer **4** prepared by dehydrogenative coupling of **3a**. For these largely oligomeric species the use of GPC was found to be problematic for the determination of molecular weights. A high concentration of polymer (>10 mg/mL) was needed to obtain a small amount of signal, and the RI detector had an extremely low response for the polymeric signal. However, from the right angle light scattering (RALS) and the intrinsic viscosity (DP) the size of compound **4** estimated (from the reaction of **3a** in C₆H₆) was approximately at 5 × 10⁴ Da. A large response in the RI was visible later in the chromatograph,

and is most likely due to the presence of oligomeric species in the sample even after precipitation in anhydrous methanol.

When polymer **4** was prepared in the absence of light in DMF (Figure 2.8), the GPC chromatograph displayed no evidence of high molecular weight polymer. The resulting GPC chromatograph displayed three distinct peaks at about 20 min retention time. These peaks were most likely oligomeric species based on the large retention times. Accurate an molecular weight calculation could not be performed due to a lack of light scattering of oligomeric species.

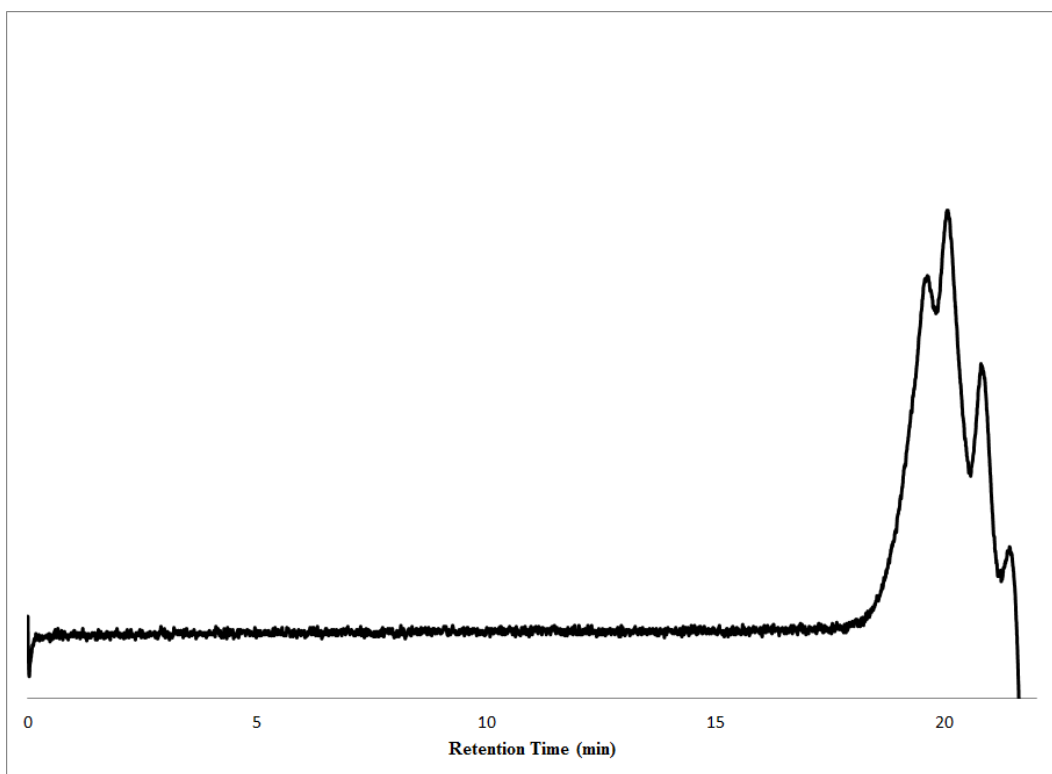


Figure 2.8: The GPC chromatograph of oligomers of **4** in THF.

2.2.6 Electrochemistry

Electrochemical studies were used to probe the electronic nature of **4**. Through cyclic voltammetry, the conductive nature of these materials can be understood fully. The relative communication between the iron centers is generally reduced when the distance between them is increased (Section 1.3.2).

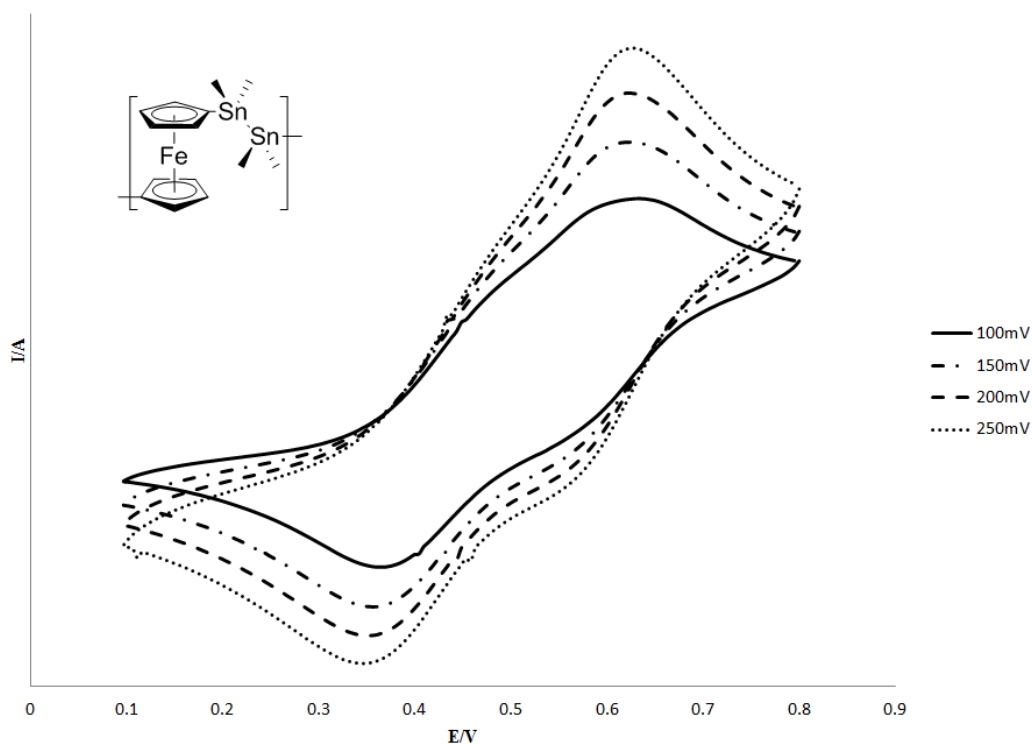


Figure 2.9: Cyclic voltammetry of compound **4** at various scan rates.

For compound **4**, there were two identifiable redox waves present in the CV (Figure 2.9) with $^1E_{1/2}$ and $^2E_{1/2}$ of -0.16V and 0.02V respectively ($\Delta E_{1/2} = 0.18V$). When this is compared with known monobridged polyferrocenyl stannanes (Table 2.1) a loss of interaction was observed. Pannell's model ferrocenyl silane dimers⁹⁵ also display a loss of communication with expansion of the bridge from 1 to 2 units. Pannell's dimers showed a $\approx 27\%$ of communication

between ferrocenes ($\Delta E_{1/2} = 0.15$ V for monobridged and 0.11 V for dibridged ferrocenyl silane dimers) when switching between the mono and dibridged dimers. The degree of electronic communication between known monobridged polyferrocenyl stannanes and polymer **4** is comparable.

Table 2.1: Cyclic voltammetry of $[\text{Fe}(\eta^5\text{-C}_5\text{H}_4)_2\text{E}]_n$.

Bridge Structure (E)	$^1E_{1/2}$ (V)	$^2E_{1/2}$ (V)	$\Delta E_{1/2}$ (V)
(<i>n</i>-Bu)₂Sn	-0.06	0.18	0.24
(<i>t</i>-Bu)₂Sn	0.00	0.24	0.24
(Mes)₂Sn	-0.07	0.14	0.21
Me₂SnMe₂Sn	-0.02	0.16	0.18

This loss of interaction can be attributed to several different factors. Firstly, redox waves are broad in the CV, obfuscating the signal which will affect the measurement of the $E_{1/2}$ locations. Secondly, the loss of interaction between iron centers may be associated with a loss of through space interaction.* Finally, when smaller, less bulky substituents are attached to Sn, a loss of interaction between Fe centers is often observed. Although not a direct correlation, the monobridged ferrocenyl silane polymers show a voltage drop of $\approx 28\%$ ($\Delta E_{1/2}$ for $[\text{Fe}(\eta^5\text{-C}_5\text{H}_4)_2\text{SiMe}_2]_n$ is 0.21 V vs $\Delta E_{1/2}$ of 0.29 V for $[\text{Fe}(\eta^5\text{-C}_5\text{H}_4)_2\text{Si}(n\text{-Bu})_2]_n$) *n*-butyl is exchanged with a methyl substituent.⁸⁶ This, in combination with the first two effects, explains why the loss of signal is as large as in the case of Pannell's model ferrocenyl silane dimers.

* The loss of through space interaction has cited behind the loss of communication between Fe centers of other bridged polyferrocenylenes.

2.2.7 UV-Visible spectroscopy and DFT studies

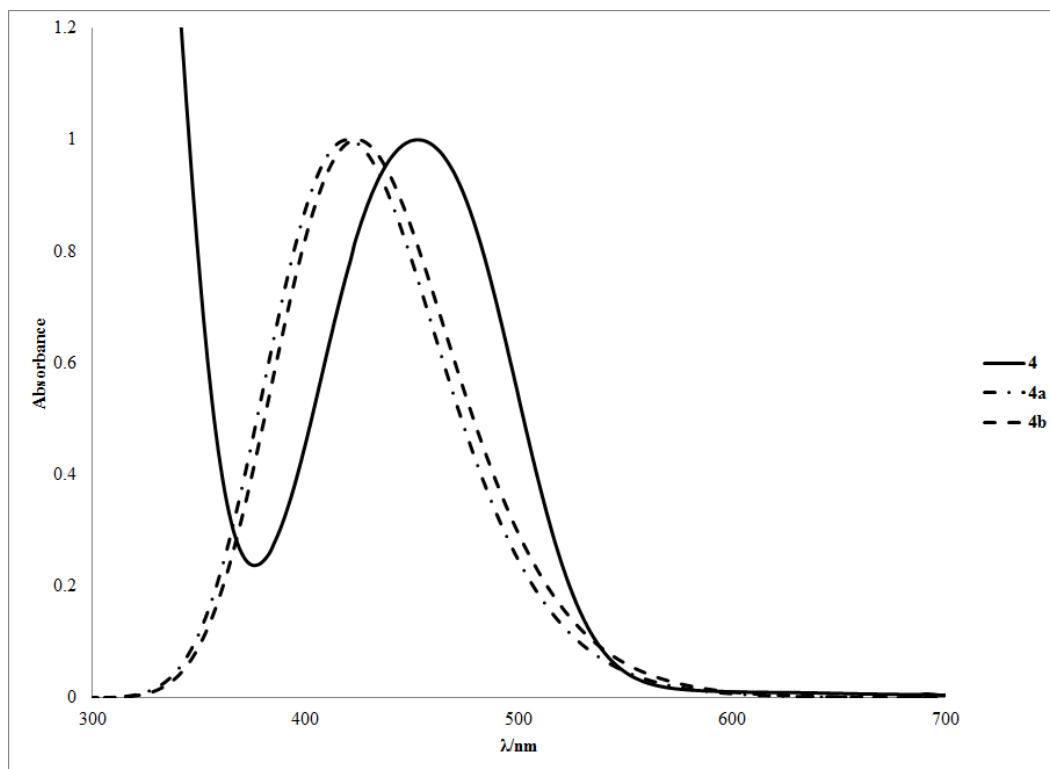


Figure 2.10: UV-Visible spectra in C_6H_6 for **4** and the TD-DFT calculated spectra for **4a** and **4b**.

The UV-Visible spectrum of compound **4** was carried out in C_6H_6 . The λ_{max} of this polymer was found to be 452 nm ($\epsilon = 115.98 \text{ L}\cdot\text{mol}^{-1}\cdot\text{cm}^{-1}$) similar to other polyferrocenylenes which generally have a $\lambda_{max} \approx 450$ nm. A series of UV-Visible spectra were collected for oligomers of **4** that were prepared in absence of light in DMF. After 100 spectra were collected at 30 s intervals (Figure 2.10), no degradation of the λ_{max} absorbance was observed. It was later determined by GPC that the sample used was largely oligomeric, rather than polymeric in nature and therefore could theoretically possess higher light stability. Polymer **4** displays a certain degree of light stability as it can be processed under atmospheric conditions with limited degradation. However, if left under atmospheric conditions for extended periods, polymer **4** degraded into an insoluble material.

To better understand the electronic structure of compound **4**, Density Functional Theory (DFT) studies were carried out on the dimeric and trimeric model system of this polymer, **4a** and **4b** respectively. The computational software Gaussian 09 revision C01 was utilized for these DFT studies, which were performed using the Local Spin Density Approximation (LSDA) method and the SDD* basis set. The effectiveness of this method/basis set was determined, along with several other method/basis sets, in a calculation of a basic ferrocene unit. LSDA/SDD was found to be the best at approximating the systems in the lowest amount of calculation time.

When the molecular orbitals of **4a** were calculated, the nature of the electronic transition was apparent (Figure 2.11). The HOMO of **4a** shows a bonding orbital that communicates between the two bridging Sn atoms. As well, there is electron density within the $\pi d(z^2)$ system of both ferrocene moieties. This is also true of **4b** (Figure 2.12), where the σ -conjugation is clearly present within both bridges of the molecule. The electronic structure of the LUMO orbitals shows conjugation through the π system of the ipso C on both ferrocenes for **4a** and the central ferrocene in **4b** as well as empty anti-bonding orbitals of the connected Sn. The HOMO-LUMO energy gap was calculated for both the **4a**, and **4b** and was found to be 2.86 eV and 2.81 eV respectively.

The TD-DFT was performed on **4a** to estimate the UV-Visible spectrum. A calculated λ_{\max} at 422 nm is 0.18 eV (7%) higher in energy than the experimental value. Polymers typically generally have a lower gap energy than oligomeric or model systems.

* SDD basis set uses the Dunning/Huzinaga full double zeta (D95) basis set for atoms up to Ar and the Stuttgart/Dresden electron core potential (ECP) for the remainder of the periodic table.

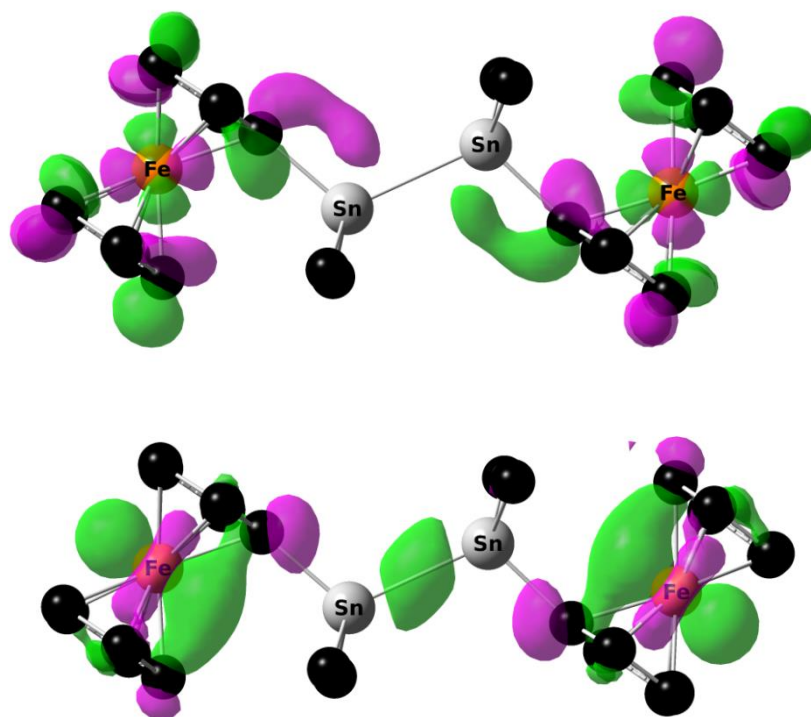


Figure 2.11: Calculated HOMO (below) and LUMO (above) of **4a**.

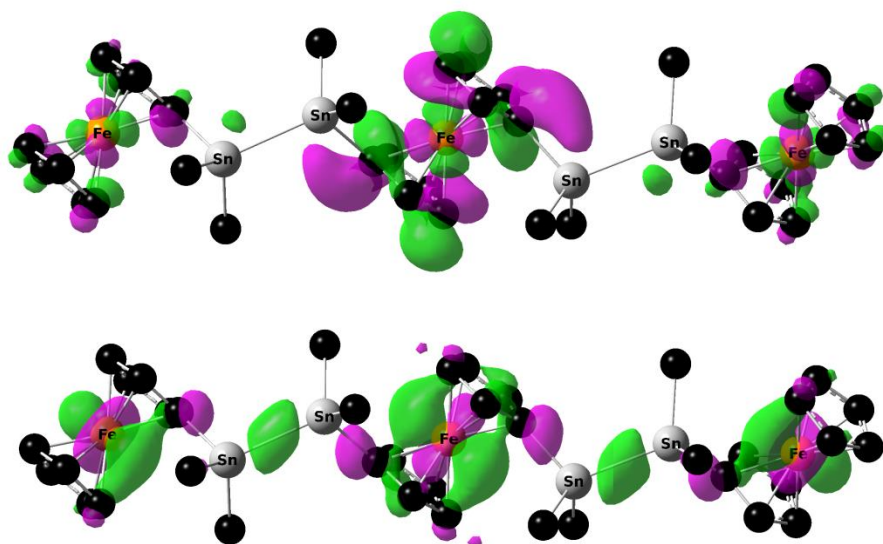


Figure 2.12: Calculated HOMO (below) and LUMO (above) of **4b**.

2.3 Conclusion

The first dibridged tin containing polyferrocenylene, $[\text{Fe}(\eta^5\text{-C}_5\text{H}_4\text{SnMe}_2)_2]_n$, **4** was synthesized through a metal catalyzed polymerization of **3a**. Polymer **4** was successfully prepared through a condensation reaction in both DMF and C_6H_6 using the Karstedt's catalyst. Evidence for polymer **4** was also detected in the ROP of **5a** using $\text{Pd}(\text{PPh}_3)_4$. Strong evidence that **4** is a low to moderate molecular weight polymer was confirmed by the integration of the proton resonances in the ^1H NMR spectra in addition to presence of $^{119}\text{Sn}/^{117}\text{Sn}$ coupling which is characteristic of a Sn-Sn bond.

Cyclic voltammetry was also used to explore the electronic interaction between two adjacent Fe centers where a significant interaction was observed between adjacent Fe centers despite an increased Fe-Fe distance. TD-DFT was used in combination with UV-Visible spectroscopy of polymer **4** to further delve into the nature of the electronic interaction of these distannyl ferrocene polymers. In these studies, electron density was located in a σ bond between the distannane bridge of a model system at the HOMO energy level.

3.0 Synthesis and Spectral Electrochemical Properties of a Symmetrical Tristanna-Bridged [3.3]Ferrocenophane

3.1 Introduction

[n.n]Ferrocenophanes are macrocyclic organometallic ring systems that contain two ferrocene moieties linked to each other through their cyclopentadienyl rings. Several examples of symmetrical [1.1]ferrocenophanes containing Group 12 (Hg),⁴³ 13 (B, Ga, In),⁴⁴⁻⁴⁶ 14 (C, Si, Sn)⁴⁷⁻⁵⁰ or 15 (P, As)^{51,52} linking moieties have been described since the late 1960s. Very recently, several new [1.1]ferrocenophanes containing Al, Ga, or Si bridging elements containing intramolecularly coordinating ligands have been synthesised by the Müller group.¹²⁹ Larger symmetrical macrocyclic [1.1]ferrocenophanes were also reported by Manners *et al.* for species with either five or six alternating linked ferrocenes and dimethylsilyl groups.¹³⁰ Such [n.n]ferrocenes with one or two heteroatom spacer atom(s) usually display strong electronic communication between the ferrocenyl centers as evidenced by cyclic voltammetry, with sequential, well separated, multi-step oxidation potentials as a result of the intimate structural connectivity of the metal centers.

The first tin-containing [1.1]ferrocenophane (**6a**, R = *n*-Bu) was reported by Seyferth⁵⁰ who isolated, in very low yield (3%), a crystalline product in the attempted preparation of the strained di-*n*-butylstanna[1]ferrocenophane (**7a**, R = *n*-Bu). The groups of Manners¹¹⁶ and Pannell¹²² successfully prepared and polymerized examples of ring-strained stanna[1]ferrocenophanes (**7b-d**) in to polyferrocenylstannanes (**8b-d**). Also isolated from the solution polymerizations of monomers (**7b**, **7c**) were tin-containing [1.1]ferrocenophanes (**6b**, **6c**) in modest yields (20-30%). Concurrently, Herberhold and co-workers⁴¹ described the

synthesis of the closely related [2]- and [3]ferrocenophanes with tetramethyldistannanediyl **5a** and hexamethyltristannyl **9a** bridges via the reductive coupling reactions of 1,1'-bis-(dimethylstannyl)ferrocene **3a** with dialkylstannyldiamines (**10a** = $(n\text{-Bu})_2\text{Sn}(\text{NEt}_2)_2$, **10b** = $\text{Me}_2\text{Sn}(\text{NEt}_2)_2$). A more sterically hindered distanna[2]ferrocenophane **5b** was recently prepared by Braunschweig via salt elimination of dilithioferrocene•tmeda (tmeda = *N, N, N', N'*-tetramethylethylenediamine) with the bulky dichlorodistannane, $t\text{-Bu}_4\text{Sn}_2\text{Cl}_2$, in good yield.¹³¹

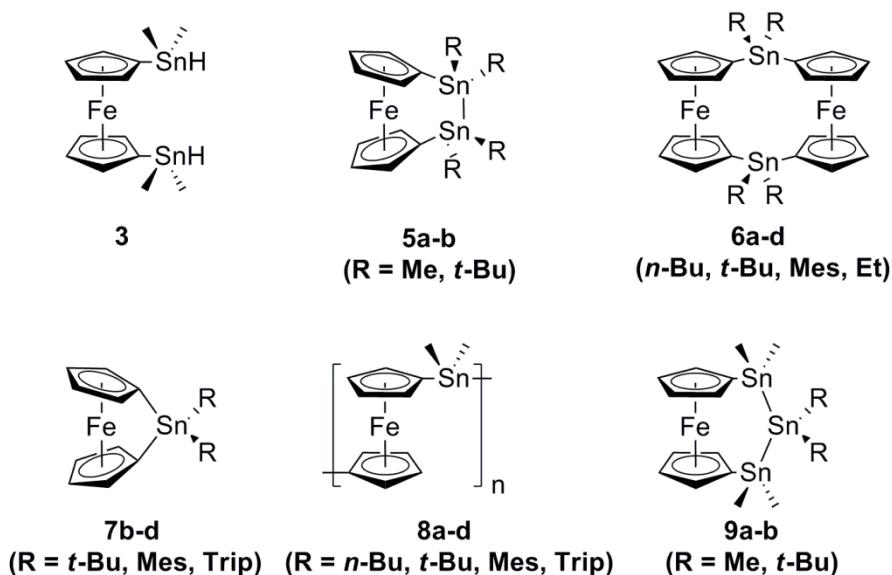


Figure 3.1: previously made ferrocenyl stannanes and stannyl ferrocenophanes.

There have been a few examples of larger [n.n]ferrocenophanes in the literature^{54,55,132} including a tin-containing [5.5]ferrocenophane with two $(\text{Me}_2\text{SiCH}_2)_2\text{SnMe}_2$ bridges isolated by Jurkschat and coworkers⁵⁴ in a 60% yield. We report herein, the isolation, in modest yield, the first example of a symmetrical tin-containing [3.3]ferrocenophane, its characterization by NMR spectroscopy and identification by mass spectrometry, and detail the electronic properties investigated by UV-Vis spectroscopy and cyclic voltammetry.

3.2 Results and discussion

Our interest in Group 14 metallocenes has been focused on the preparation of oligo- and polymetallocenes with at least two bridging atoms between ferrocene units. In particular, dehydrogenative coupling reactions of suitable Group 14 hydrides such as **3a**, and metal-catalyzed ring-opening polymerization of novel monomers like the [2]ferrocenophane **5a**, have been targeted. Following procedures outlined by Herberhold and Wrackmeyer,⁴¹ we readily prepared **3a** in comparable yields and purity. Room temperature dehydrogenative coupling of **3a** to yield **5a** was then attempted with a few Group 9 and 10 metal catalysts. These results are listed in Table 1.

Table 3.1. Comparison of catalytic activity for main group and transition metal catalysts in the ring-closing formation of **4a** from **6**.

Catalyst	Mol ratio Cat. to 3	% Yield of 5a	Reference
Pt(acac)₂	0.13:1	No reaction	This work
ClRh(PPh₃)₃	0.007:1	No reaction	This work
Pd₂(dba)₃	0.043:1	90	This work
(n-Bu)₂Sn(NEt₂)₂	1:1	5	This work
(n-Bu)₂Sn(NEt₂)₂	1:1	52	41
Hg(SiMe₃)₂	1.3:1	29	41

Of the three catalyst examined, an efficient intramolecular dehydrogenative coupling of **3a** to form **5a** was only observed with catalytic amounts of Pd₂(dba)₃ (tris(dibenzylideneacetone)dipalladium(0)). This proceeded with an isolated product yield of 90%. By contrast, compound **5a** previously synthesized by Herberhold *et al.*,⁴¹ used a stoichiometric quantity of **10a** at higher dilution resulting in only a 52% yield.

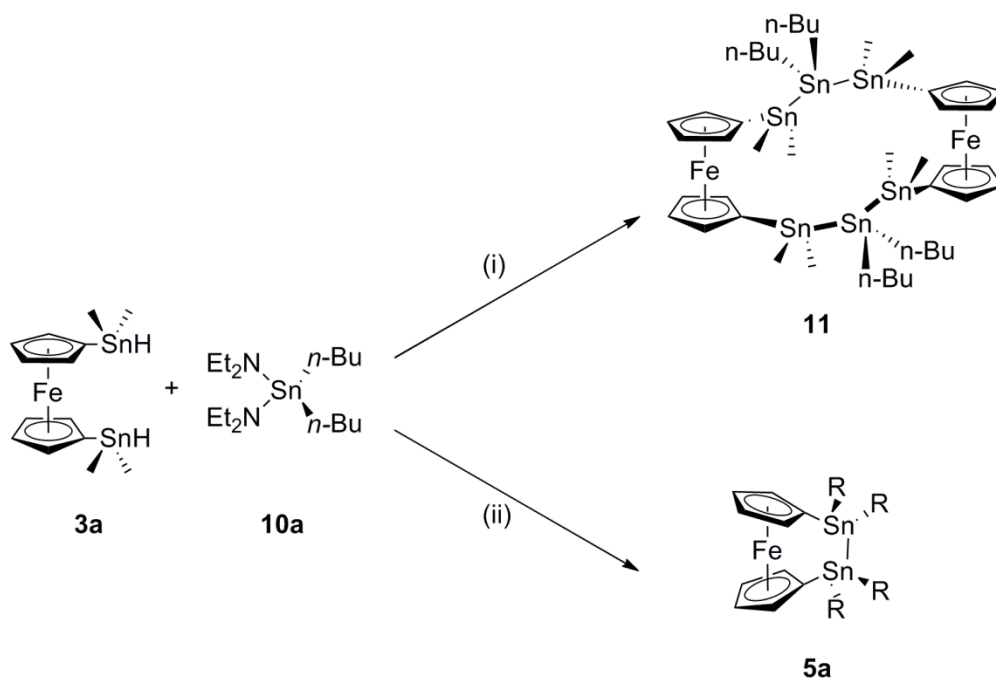


Figure 3.2: (i) Et₂O ([**3a**], [**10a**] = 0.1 M), 0° C 1hr, reflux 3hr, hexanes/silica col. (82% yield of **11**), (ii) Et₂O ([**3a**], [**10a**] 0.02 M) 0°C 1hr , reflux 2hr, 3:2 DCM/hexanes/silica col. (52% yield of **5a**).

Under an inert atmosphere, the reaction of **3a** (Scheme 1) with a stoichiometric equivalent of **10a** in Et₂O solution was initially carried out at 0°C, followed by heating this mixture to reflux temperature (3 hr) to ensure ring-closing, to give **5a**. When this process was performed by Herberhold, purification by a silica gel column using a DCM/hexanes (3:2) in an inert atmosphere (N₂(g)) resulted in a 52% recovery of **5a**. In our hands, the reactants were used independently at both the same and at a higher concentration (5 ×) than Herberhold and TLC

performed using an identical DCM/hexanes mixture. Unfortunately, this resulted in a considerable “streaking” being observed on the TLC plate. Conversely, development in neat hexanes (also under N₂(g)) yielded two distinct spots by TLC. The crude sample was purified by silica gel chromatography eluting with neat hexanes, with two distinct fractions being collected. This accounted for approximately 87% of the product mass (**11** and **9a**); the remainder of the reaction material remained on the column and could not be recovered.

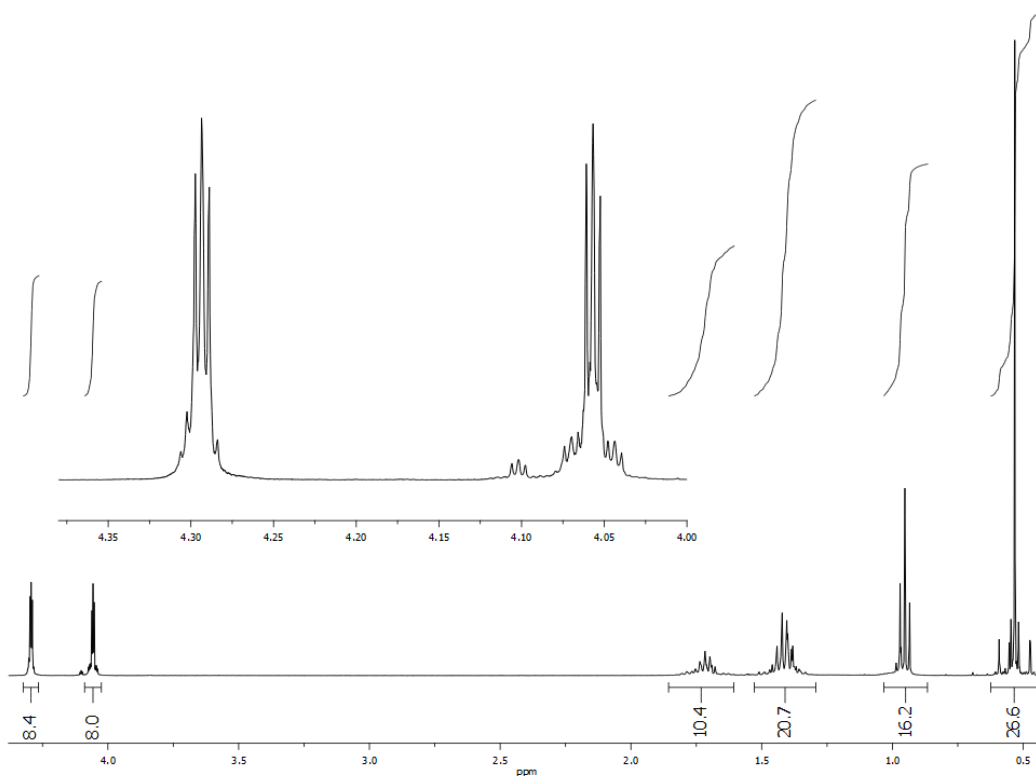


Figure 3.3. ¹H NMR (C₆D₆) of compound **11** with inset of Cp region.

Surprisingly, analysis by NMR (¹¹⁹Sn; C₆D₆) confirmed the smaller second fraction (5% of the recovered materials) was **5a** displaying a resonance at -43 ppm. By contrast, the first fraction, recovered as a bright, orange oil (stable for short periods in air), was isolated in an 82% yield. Initial attempts to carry out the NMR analysis of both the 1st and 2nd fractions in CDCl₃

resulted in broad, unresolved resonances in the Cp and *n*-butyl regions, indicative of immediate decomposition in this solvent. When the NMR (^1H , Figure 1) of the first fraction was analysed in C_6D_6 , a highly symmetrically substituted [n.n]ferrocenophane, with a detectable trace of another 1,1'-ferrocene or ferrocenophane containing compound (<1% by ^1H NMR) along with ferrocene, were revealed. Both trace contaminants were subsequently removed via column chromatography; however attempts to crystallize compound **11** were unsuccessful.

3.2.1 Sn NMR and NMR simulation

The ^{119}Sn NMR (C_6D_6 ; Figure 3.4) spectrum of this first fraction proved less straightforward with the two largest resonances assigned to the (SnMe_2) substituent at -100.4 and the ($\text{Sn}(n\text{-Bu})_2$) group at -211.8 ppm respectively, with a chemical shift difference ($\Delta\delta$) of ≈ 112 ppm. Multiple isotopic couplings were also identified at each resonance cluster. A simulation of the ^{117}Sn and ^{119}Sn NMR spectra was then conducted to elucidate whether the symmetrical ferrocenophane contained one (**9b**) or two (**11**) ferrocene units and to accurately predict the expected $^{117}\text{Sn}/^{119}\text{Sn}$ isotopic coupling patterns.

$$P_{\text{Pattern}} = \sum I \times \left(\frac{\prod P_{\text{Sn}}}{100^{(X \times Y)}} \right) \quad (2)$$

At present, there are no readily available NMR modelling tools to accurately predict $^{117}\text{Sn}/^{119}\text{Sn}$ coupling patterns, particularly for compounds that possess multiple Sn-Sn bonds. The data generated from our in-house ^{117}Sn and ^{119}Sn NMR simulator (see appendix S5 for program data) for the signal intensities is within reasonable agreement with the patterns of coupling observed experimentally, although direct integration of these peak intensities is obviously not possible. This is due to a few factors, including the nature of ^{117}Sn [^1H] or ^{119}Sn [^1H] experiments where small intensity deviations are likely due to the low intensity of Sn-Sn

couplings based on natural abundance. The system was calculated based on equation (2) where P_{Pattern} is the total probability of each pattern occurring, I is equal to the number of identical systems, P_{Sn} is the probability that a tin atom will be one of the NMR active nuclei and X and Y are the number of bridging tins and the number of ferrocenes in the structure respectively. Equation 2 is based on a matrix derived from the structure of the [3.3]ferrocenophane as seen in Figure 3.4.

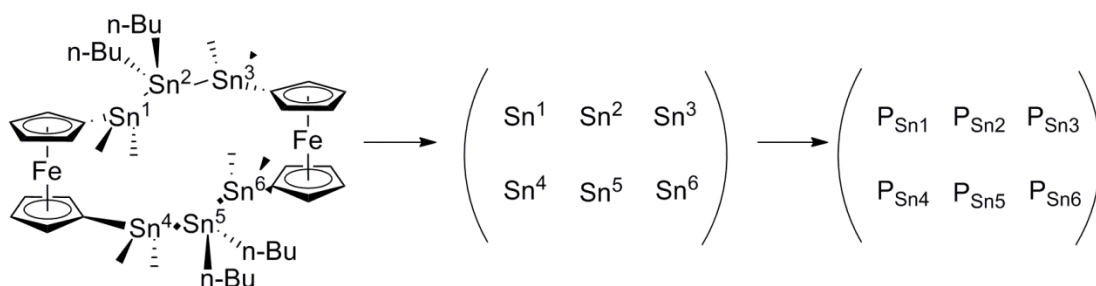


Figure 3.4: The design of the matrices used in ^{119}Sn modeling program.

In the simulated and experimental ^{119}Sn spectrum (Figure 2a, b) of **11**, the two largest calculated intensities were experimentally fixed at -100.5 (SnMe_2) and at -211.8 ($\text{Sn}(n\text{-Bu})_2$) ppm respectively. Calculated resonance satellites were located based on experimental coupling constants. Using a statistical model (eqn 2), $^{117}\text{Sn}/^{119}\text{Sn}$ and $^{119}\text{Sn}/^{119}\text{Sn}$ satellite intensities were calculated with intensities above 1% of the largest signal, identifying 12 (2 singlets and 5 doublet) resonances, which was two less than observed experimentally.

There were several additional predicted peaks of low calculated intensities that are not observed. It should be noted, that while both compounds (**9b** and **11**) would be expected to have the same coupling patterns on a statistical basis, chemical shifts for the different tin environments should be distinct. The two smaller resonances at -90.8 and -221.2 ppm ($\Delta \delta = 130.4$ ppm) were tentatively assigned as **9b** based on the assignment of the ^{119}Sn resonances by

Herberhold for the hexamethyltristannane bridged [3]ferrocenophane, **9a**, (-102.5, -249.3 ppm; $\Delta\delta = 146.7$ ppm).⁴¹ Similar results were also found in the simulation of the ^{117}Sn spectra for compound **11**.

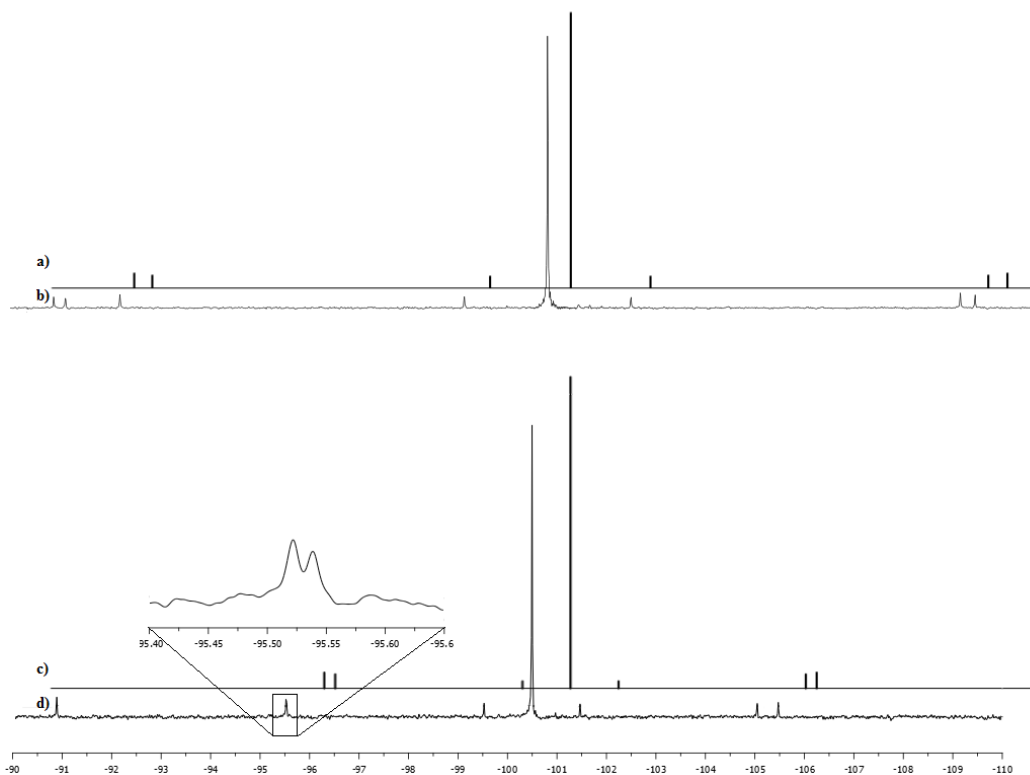


Figure 3.5: a) Calculated and b) Experimental ^{119}Sn and c) Calculated and d) Experimental ^{117}Sn NMR spectra of the SnMe_2 resonance for compound **11**. Calculated spectra shifted -1 ppm.

3.2.2 Electrochemistry

Further evidence for the [3.3]ferrocenophane structure of **11** was sought by employing cyclic voltammetry. An important metric of the communication between bridged ferrocenes is the degree to which they respond to oxidation/reduction as independent (insulated, single wave) or dependent (delocalized, two or more waves) metallocenes. The difference in the ΔE for

model systems (**6a-c**, **12a**) containing a single bridging element or singly bridged polymers (**8a-c**, **8e**) is heteroatom dependent.⁸⁶

Table 3.2: Half-potentials for bridged bisferrocenes and selected ferrocene polymers.

Compound	Bridge	${}^1E_{1/2}, {}^2E_{1/2}$, [V]	ΔE , [V]	d (Fe \cdots Fe), [Å]	Ref
4	-Me ₂ SnMe ₂ Sn-	-0.2, 0.16	0.18	9.63*	†
6a	-(<i>n</i> -Bu) ₂ Sn-	0.11, 0.31	0.20	5.50	50,133(a)
6b	-(<i>t</i> -Bu) ₂ Sn-	-0.06, 0.21	0.27	5.474(1)	116(b)
6c	-(Mes) ₂ Sn-	0.01, 0.27	0.28	5.248(1)	116(b)
8a	-(<i>n</i> -Bu) ₂ Sn-	-0.60, 0.18	0.24	-	86(b)
8b	-(<i>t</i> -Bu) ₂ Sn-	0.00, 0.24	0.24	-	116(b)
8c	-(Mes) ₂ Sn-	-0.07, 0.14	0.21	-	116(b)
11	-Me ₂ Sn(<i>n</i> -Bu) ₂ SnMe ₂ Sn-	0.01, 0.23	0.22	8.49*	† ^(c)
12a	-Me ₂ Si-	0.00, 0.15	0.15	6.83*	95 (d)
12b	-(Me ₂ Si) ₂ -	-0.02, 0.09	0.11	8.84, 8.80*	95 (d)
12c	-(Me ₂ Si) ₃ -	-0.04, 0.04	0.08	10.2*	95 (d)
12d	-(Me ₂ Si) ₆ -	0.58	0	16.9*	95(d)
13	-Me ₂ Sn-	n/a	n/a	6.12*	105
14	-N=C=N-	0.09, 0.29	0.20	7.64*	134(e)

All values normalized to Fc/Fc⁺ couple. Conditions: (a) DCM/0.1M [N(*n*-Bu)₄][BF₄], (b) DCM/0.1M [N(*n*-Bu)₄][PF₆], (c) MeCN/0.1M [N(*n*-Bu)₄][BF₄], (d) DCM/0.1M [NEt₄][ClO₄], (e) DMF/0.1M [N(*n*-Bu)₄][ClO₄]. *Calculated using Gaussian 9 (see below). † This work.

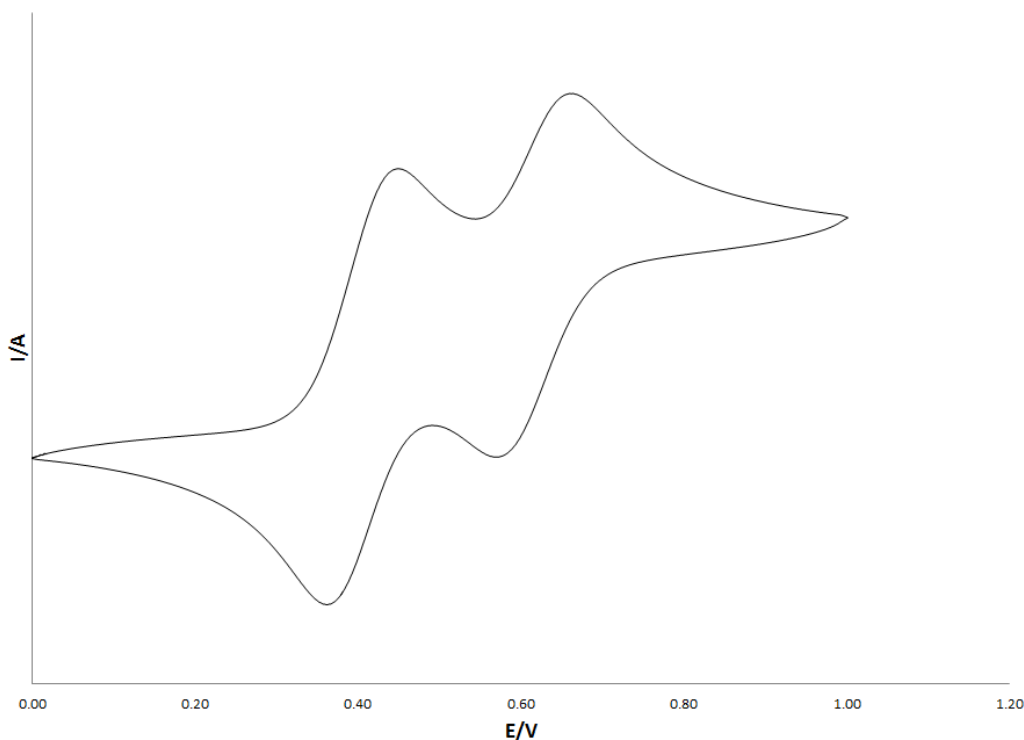


Figure 3.6: Cyclic voltammetry of **11** at 100 mV/s in a MeCN solution containing 0.1M [N(*n*-Bu)₄][BF₄] as supporting electrolyte.

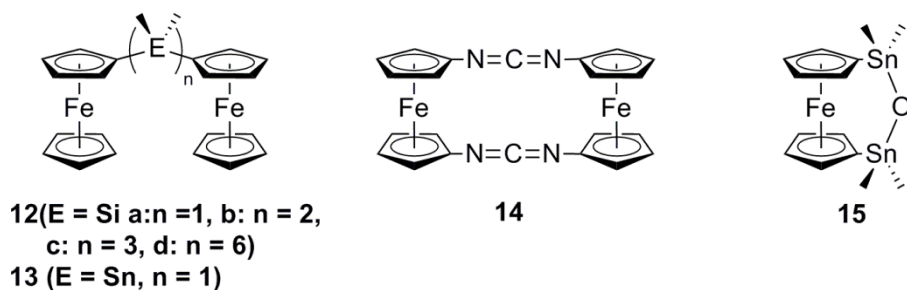


Figure 3.7: Structure of compound **12a-d**, **13**, **14**, and **15**.

This effect is smaller when compared to non-bridged polymetalloenes or metallocenes linked by conjugated vinyl or acetylene spacers that are assumed to communicate exclusively along a π orbital backbone. Ferrocene units bridged by a later Group 14 (Si, Ge, Sn) dialkyl or diaryl unit are believed to communicate both through the σ -bonded bridge and through direct Fe \cdots Fe interactions.¹³⁰ Model ferrocenes and polyferrocenes bridged by two or more spacers show substantially less interaction between metal centers, with ethylene bridges being essentially fully insulating.⁸⁶ Previous work by Pannell, who prepared a series of bisferrocenes with mono-

di-, tri-, and hexa(dimethylsilane) bridges (**12a-d**), reported a lower level of communication between metal centers as the bridge length increased (Table 2).⁹⁵ Beyond three bridging (dimethylsilylene) units, only a single reversible wave is observed by cyclic voltammetry. [1.1]Ferrocenophanes (**6b**, **6c**) show a similar degree of electronic communication ($\Delta E \approx 0.25\text{V}$) compared to singly bridged bisferrocenes. In the case of the [3.3]ferrocenophane **11**, cyclic voltammetry (Figure 3) in MeCN reveals two oxidation/reduction events at $^1E_{1/2}$ of 0.01V, and $^2E_{1/2}$ of 0.23V. The ΔE of 0.22V for **11** indicates a considerable degree of communication between ferrocene units and is within the same range as known tin-containing [1.1]ferrocenophanes (**6a-c**)^{116,133} and mono-tin-bridged ferrocenyl polymers (**8a-c**, **8e**)^{86,116,133} or the fully π -conjugated [3.3]bisferrocene **14**.^{134,135} The partial oxidation of **11** likely leads to a Class II mixed valence compound according to the Robin-Day classification.¹³⁶ In the case of **11**, this would suggest that electronic communication between ferrocene units is facilitated through both the π conjugation of the ferrocene ring system and the σ conjugation of the stannyl bridge.

3.2.3 DFT modelling and UV-Vis spectroscopy

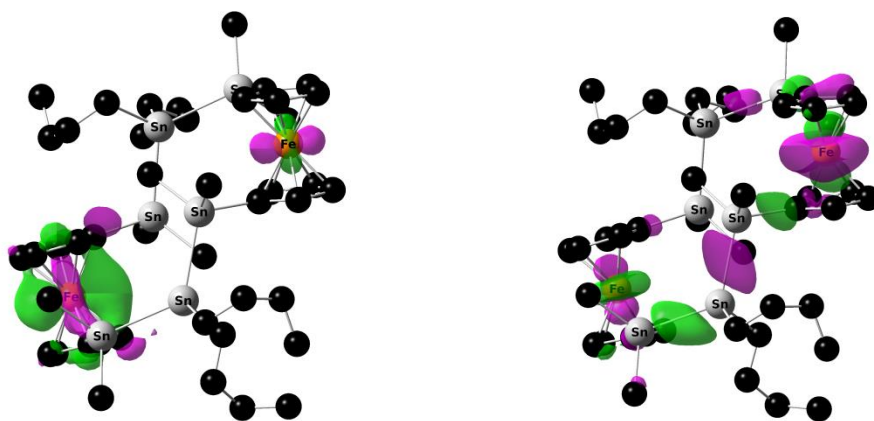


Figure 3.8: Molecular Orbital Diagrams of the HOMO Orbital of compound **11** (left) and the SOMO Orbital of its radical monocation (right).

Computational modeling was performed on compounds **11** and **9b** as well as several other similar structured compounds (**5a**, **12a-d**, **13**). Gaussian 9 was used for DFT and TD-DFT calculations and confirmed by zero point energy calculations. The LSDA method with the SDD basis set was used to calculate and optimize electronic and bonding structures. The electronics of **11** (Figure 4a) was then compared to its experimental λ_{max} value. The calculations from TD-DFT describe two minor energy transitions (HOMO/LUMO+1, HOMO-1/LUMO+1) and one major energy transition (HOMO-2/LUMO). The Fe•••Fe distance of known ferrocenyl silanes, stannanes, and ferrocenophanes were calculated and compared to those of calculated **11** and **9b**. The HOMO-2/LUMO gap energy experimentally established by UV-Vis spectroscopy for compound **11** was 2.72eV (calculated for $\lambda_{\text{max}} = 455.1$ nm in Et₂O). The calculated HOMO/LUMO energy gap for **11** was found to be 2.93eV using LSDA/SDD (7% difference from experimental). Calculated energies are often larger than actual values, which agree with similar calculations Gao *et al.*¹³⁷ performed with Pt compounds.

TD-DFT was used to simulate UV-Visible spectra and was compared to experimental spectra (Figure 3.8). The simulated spectra for compound **11** was in a higher agreement with the experimental spectra than the simulated for **9b**. DFT calculations were also performed on a singularly oxidized species of **11** (Figure 4b). Communication is predicted between the ferrocene centers along the tin bridge in the SOMO and lower energy orbitals (Figure 4). These conduction orbitals were approximately 1eV lower than the SOMO which was centered on one of the ferrocene units, consistent with the experimental electrochemistry undertaken in solution.

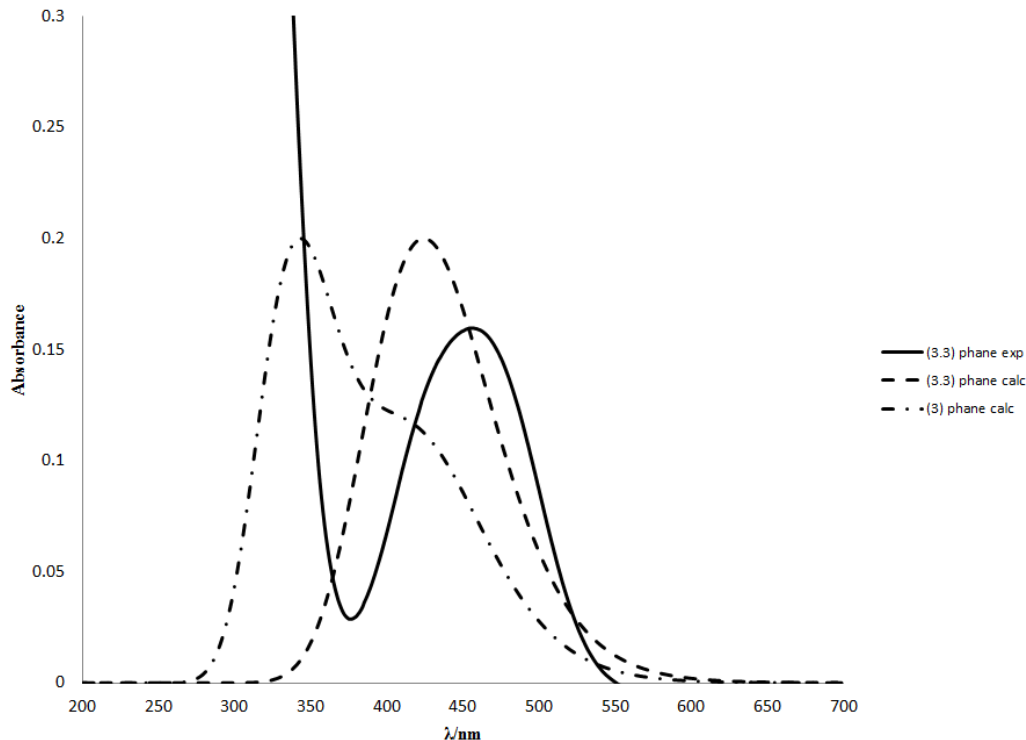


Figure 3.9: Comparison of calculated UV-Visible spectra for compounds **9b** and **11** with the UV-Vis spectrum of **11** in Et₂O.

3.2.4 Mass spectrometry

DART-TOF* mass spectrometry was also performed on compound **11**. The DART mass spectrum shown in Figure 5 was obtained at 300°C and provides direct evidence for the presence of compound **11** with a cluster of peaks centered at m/z 1428.9, which corresponds to a protonated molecular cation of formula [C₄₄H₇₆Fe₂Sn₆+H]. The peak within the cluster found at 1433.86 was calculated at m/z 1433.8621. Several other peaks are observed in the DART-MS spectrum and indicate that [3.3]ferrocenophane is both thermally labile and reactive under the conditions of the DART ionization. The DART ionization process produces singly-charged ions via gas-phase proton transfer and is akin to the classical mechanism of chemical ionization

* Direct Analysis in Real Time – Time Of Flight

(CI).¹³⁸ The analyte molecule must first be vaporized in the heated DART stream and so the ionization efficiency is related directly to the volatility of the analyte species. Higher molecular weight products will therefore generally require higher temperatures to promote efficient ionization; however, in the case of reactive or thermally labile compounds, the higher temperature may also contribute to extensive degradation.

In addition to the parent ion species $[M+H]^+$, several of the most abundant peaks in the DART-MS spectrum have been identified which support the assignment of compound **11**. These include: loss of $-Bu_2Sn$ (m/z 1196.8), loss of $-Me_2SnSnBu_2$ (m/z 1044.8), scission of compound **11** into two halves* ($\approx m/z$ 713.9) and other assignable ferrocenophanes that include oxygen atoms in their structures (Table 3). When the sample was left in the heated DART stream for an extended period of time (e.g. 10-20s), the intensity of the peak at m/z 1428.9 decreased and a strong peak was observed centered at m/z 498.9. This likely corresponds to the known oxygen containing [3]ferrocenophane **15** (Figure 3.7).

To provide further certainty towards the identity of **11**, DART-TOF mass spectra were measured at several temperatures (100°-300°C) and the results are listed in Appendix S3. Unsurprisingly, the signal for the protonated **11** is not observed at low temperatures (100°C), however, decomposition products of **11** as well as new species that include oxygen were detected. As the temperature was further increased from 200°C to 300°C, a distinguishable protonated molecular species appeared (m/z 1428.9), as well as peaks associated with larger fragmentation products including the loss of a single $Sn(n-Bu_2)$ unit at m/z 1196.8 and a new peak at m/z 1212.8 that corresponds to the addition of oxygen to this latter species.

* Compound **11** is divided into two halves differing only by either a proton or an electron.

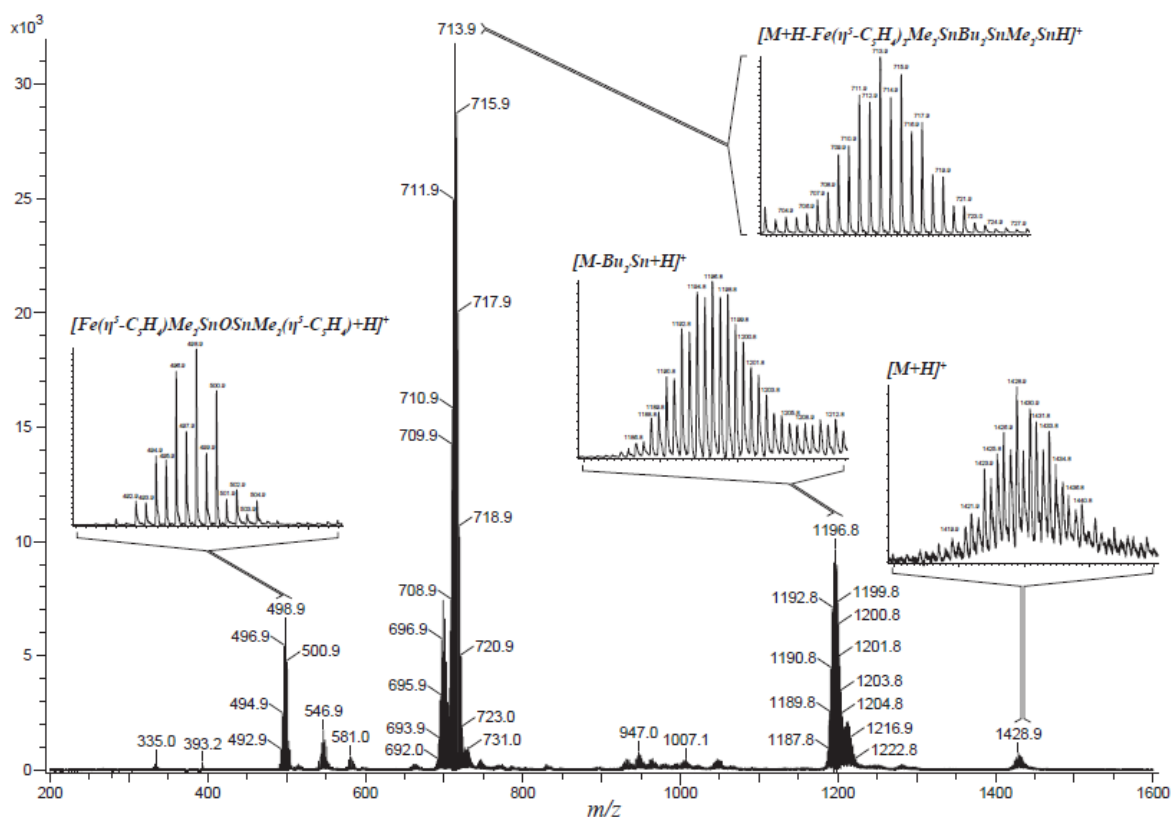


Figure 3.10: DART-TOF MS spectrum of **11** at 300°C.

Due to the structural symmetry of the products **11** and **9b**, the possibility for dimerization of **9b** to form **11** during the ionization process was also considered. In this case the protonated molecule [M+H]⁺ of **9b** was expected at *m/z* 714.9 but was found to be absent from the DART-MS spectrum. Rather, the peak observed at *m/z* 713.9 is a decomposition product of the [M+H]⁺ ion of **11**. DART-TOF-MS was also performed at different skimmer potentials ranging from 20V-80V with a constant temperature of 200°C (Table 2). Application of a higher skimmer voltage in the interface region of the mass spectrometer effectively increases the energy of collisions and prevents dimerization. As the skimmer potential was raised, the peaks at *m/z* 1428.9, as well as peaks larger than *m/z* 713.9 were found in relatively higher abundance. At a

skimmer potential of 80V, the m/z 1428.9 was still detected and provides good evidence that this is not a dimer of **9b**, but is in fact the molecular charged species derived from **11**.

Table 3.3: DART-TOF-MS relative abundance of mass fragments @200°C and 300°C.

m/z	Fragment	RA (%)	
		200°C	300°C
1428.9	$[M+H]^+$	0.8	2.3
1212.8	$[M+OH]^+ - [Bu_2Sn]$	30	6.5
1196.8	$[M+H]^+ - [Bu_2Sn]$	44	30.3
1046.8	$[M]^+ - [Me_2SnSnBu_2]$	7.7	-
996.8	$[M+H]^+ + O_2 - [(Bu_2Sn)_2]$	32	-
713.9	$[M]^+ - [Fe(\eta^5-C_5H_4)Me_2SnBu_2SnMe_2Sn(\eta^5-C_5H_4)]$	67	100
698.9	$[M]^+ - [Fe(\eta^5-C_5H_4)SnMe_2SnBu_2SnMe_2(\eta^5-C_5H_4)]$	7.4	24.4
546.9	$[M]^+ - [(\eta^5-C_5H_4)Fe(\eta^5-C_5H_4)SnMe_2SnBu_2SnMe_2(\eta^5-C_5H_4)Fe(\eta^5-C_5H_4)]$	-	5.5
498.9	$[M+OH]^+ - [(\eta^5-C_5H_4)Fe(\eta^5-C_5H_4)SnMe_2SnBu_2SnMe_2(\eta^5-C_5H_4)Fe(\eta^5-C_5H_4) + Bu_2Sn]$	100	19.4

M = Compound **11**

3.3 Conclusion

A new higher yielding catalytic route to the previously known distanna-bridged [2]ferrocenophane, **5a**, was identified. Species of this type will be used for future polymerization investigations in the preparation of polyferrocenes with two tin bridges. The first tristanna-bridged [3.3]ferrocenophane **11** was also synthesised in good yield through a reaction of 1,1'-bis(dimethylstannyl)ferrocene **3** and di-*n*-butylbis(diethylamino)stannane **10a**. An in-house Sn NMR simulation program was used effectively to model the complex Sn NMR spectrum of compound **11** and was found to be in good agreement with the experimental values. MS characterization provides strong evidence to support the assignment of [3.3]ferrocenophane **11**. Finally, characterization of the electrical properties of **11** revealed exceptionally strong communication between ferrocene centers through the tristannana-bridge that is within the same magnitude as a single tin-bridged [1.1]ferrocenophane compound, which was also supported by DFT modelling.

4.0 Experimental

4.1 Equipment and procedures

Most solvents (THF, Et₂O, hexanes) were dispensed from an MBraun MB-SPS solvent system to remove trace water and oxygen. DMF was distilled over activated molecular sieves to remove trace water. All reagents were purchased from Sigma-Aldrich with the exception of tin chlorides which were purchased from both Strem and Sigma-Aldrich. All reagents were used as received. Standard Schlenk techniques were used with all air sensitive compounds. (η^5 -C₅H₄Li)Fe•TMEDA was synthesized according to literature procedure.¹³⁹ Di-*n*-butylbis(diethylamino)stannane **10a** was prepared according to a reported procedure.³³ Elemental Analysis was performed by Atlantic Microlab, Inc. of Norcross Georgia.

4.1.2 Nuclear magnetic resonance

¹H NMR (400 MHz), ¹³C NMR (100.6 MHz) and ¹¹⁹Sn NMR (79.5 MHz) spectra were recorded on a Bruker Avance 400 MHz NMR spectrometer with a BBFO 5-mm direct probe. A ¹H pulse width of 30° was used, acquiring a spectral window of 8223 Hz (20 ppm) using a relaxation delay of 1s, acquisition time 3.98s, 32k points (16 scans). The ¹H 90° pulse width was 10.4 μs. A ¹³C pulse width of 30° was used, acquiring a spectral window of 24038 Hz (239 ppm) using a relaxation delay of 2s, acquisition time 1.36s, 32k points (4096 scans). The ¹³C 90° pulse width was 8.7 μs. A ¹¹⁹Sn pulse width of 30° was used, 8.75 μs, acquiring a spectral window of 100000 Hz (670 ppm) using a relaxation delay of 1s, acquisition time 0.33s, 32k points (15360 scans) with inverse gated proton decoupling. ¹¹⁷Sn NMR (249.29 MHz) spectra were recorded on an Agilent DD2 700 MHz NMR spectrometer. For ¹¹⁷Sn NMR, a pulse width of 30° was used, 4.03 μs, acquiring a spectral window of 62500 Hz (250.7 ppm) using 256k points with inverse

gated proton decoupling. ^1H and ^{13}C were referenced internally to the deuterated solvent resonances, while $^{117,119}\text{Sn}$ was referenced to external tetramethylstannane. All J coupling values are reported as absolute values.

4.1.3 ^{119}Sn NMR simulator

A statistical analysis model (see Appendix 4) was developed to identify all ^{119}Sn - ^{119}Sn and ^{117}Sn - ^{117}Sn coupling patterns that arise from the ^{117}Sn or ^{119}Sn NMR spectra of compound **11**. As well, this simulator was used with values given for 2,2-dibutyl-1,1,3,3-tetramethyltristannanediyl-[3]-ferrocenophane **9b** as a method of control. Integration for these peaks were calculated by first building a matrix of matrices representing all possible permutations of isotopes. Each smaller matrix was then assigned a probability (intensity) and spectra. All identical coupling patterns were summed and normalized to the largest singlet. Chemical shift assignments were estimated from the chemical shift difference of the two largest resonances, with smaller coupling resonances centered on each peak. Several peaks generated by the simulation are not observed in the actual spectra as they integrate for less than 0.2% strength of the largest signal and are below the signal to noise cut-off.

4.1.4 Cyclic voltammetry

Experiments were performed under inert atmosphere conditions ($\text{N}_2(g)$) through the use of Schlenk conditions. Prior to analysis, samples were degassed for 5 min. Samples of compound **4** and **11** for electrochemistry were prepared at 1×10^{-5} M in DCM and MeCN respectively. $[\text{N}(n\text{-Bu})_4][\text{BF}_4]$ was used as a supporting electrode in ≈ 0.1 M concentration. Electrochemistry for compound **4** and **11** were performed on a MetroOhm FRA2 $\mu\text{AUTOLAB}$ type II and type III

respectively, Potentiostat/Galvanostat with a glassy carbon working electrode, Pt counter electrode, and a Ag/AgCl Reference Electrode between 0.1-1.0V potentials.

4.1.5 Density functional theory calculations

Gaussian 9 Inc. revC1 was used for all Density Functional Theory (DFT) and Time Dependent (TD-DFT) calculations using the LSDA method with the SDD basis set to determine electronic and bonding structures for **4a**, **4b**, **9a**, and **11**. Zero point energy (ZPE) calculations found no imaginary frequencies and therefore confirmed that all structures were in a local minimum (see Appendix 5).

4.1.6 UV-Visible spectroscopy

UV-Vis was carried out on a Perkin Elymer Lambda 20 UV-VIS Spectrophotometer. Original samples were collected in the range of 300-800 nm with consecutive data runs collected at 30 s intervals for 100 spectra. All samples were prepared in C₆H₆ at a concentration $\approx 10^{-3}$ M.

4.1.7 Gel permeation chromatography

Gel Permeation Chromatography (GPC) was performed on a Visocotek GPCmax VE2001 with a TDA302 triple detector system. Chromatograph was collected at 1.0 mL/min using a (need info) column. Sample was prepared at 10mg/mL in dry THF. DMF oligomers were run with the UV absorbing agent benzotriazole-5-carboxylic acid.

4.1.8 Mass spectrometry

Time-of-flight mass spectrometry analyses were performed using a JMS-T1000LC mass spectrometer (JEOL Inc., Peabody, MA) equipped with a Direct Analysis in Real Time (DART) ionization source (DART-SVP, Ionsense Inc., Saugus, MA). The DART source was operated

with He gas and the temperature was adjusted in the range 100-400°C. Isotopic distributions for the observed ionic species were calculated using the Mass Center utility (JEOL) and were in good agreement with the measured mass spectra.

4.2 Preparation of 1,1'-bis(trimethyl stannyl) ferrocene **1a**

Exactly 5.71 g (17.7 mmol) of (η^5 -C₅H₄Li)Fe•TMEDA was added to a 500 mL Schlenk flask in an N₂(g) atmosphere. To this flask 150 mL of dry hexanes was added. 7.01 g (35.2mmol) of Me₃SnCl was added to a separate 50 mL Schlenk flask, which was then diluted with 50 mL of dry hexanes. Both flasks were cooled to 0°C under N₂(g). The Me₃SnCl solution was added slowly to the Fe(η^5 -C₅H₄Li) •TMEDA solution. The reaction was allowed to stir for 12 h under an inert environment. LiCl was filtered off, and the resulting oil purified at 130°C *in vacuo* to remove TMEDA and byproducts. The NMR (¹H, ¹¹⁹Sn) chemical shifts were similar to reported values.¹⁰⁶ Yield 81%, 7.34 g (dark red oil). ¹H-NMR (400.130 MHz, CDCl₃, δ): 4.272 (m, 4H, Cp), 4.033 (m, 4H, Cp), 0.277 (s, ²J_{Me-Sn} = 54.3 Hz, 18H, CH₃) ppm. ¹¹⁹Sn-NMR (149.211 MHz, CDCl₃, δ): -5.56 ppm.

4.3 Preparation of 1,1'-bis(dimethyl stannyl) ferrocene **3a**

Exactly 7.22 g (14.1 mmol) of **1a** was added to a 250 mL Schlenk flask, followed by 6.20 g (28.2 mmol) of Me₂SnCl₂. The reaction was placed under static vacuum then heated to 140°C. After 3 h the flask was allowed to cool to room temperature and dynamic vacuum was applied to remove Me₃SnCl. The intermediate, **2a**, was reacted further without purification and identified only by ¹¹⁹Sn NMR spectroscopy (δ = 126.8 ppm, CDCl₃), in good agreement with reported literature values.¹⁰⁶

Approximately 150 mL of Et₂O was added to the previous reaction mixture. 58 mL (58 mmol) of LiAlH₄ (1 M in Et₂O) was added to a separate 1000 mL Schlenk flask and diluted with an additional 50 mL of Et₂O. Both flasks were then cooled to 0°C, and the solution of **2a** was added drop wise to the LiAlH₄ solution over a period of 1h. The reaction was allowed to warm to room temperature. After 5 h the reaction was quenched with degassed water. The product was extracted with Et₂O, and dried over MgSO₄ and finally the Et₂O removed *in vacuo*. The resulting oil was distilled at 90°C (1×10⁻³ mmHg) and stored under N₂(g) at -33°C. The chemical shifts are similar to those previously reported by Herberhold and Wrackmeyer.¹⁰⁶ Yield 82%, 5.59 g (dark orange oil). ¹H-NMR (400.130 MHz, C₆D₆, δ): 5.468 (septet, ³J_{SnH-Me} = 2.3 Hz, 2H, SnH) 4.245 (m, 4H, Cp), 4.013 (m, 4H, Cp), 0.274 (d, ²J_{Me-Sn} = 59.0 Hz, ³J_{Me-SnH} = 2.3 Hz, 12H, CH₃) ppm. ¹³C-NMR (100.613 MHz, C₆D₆, δ): 74.88 (Cp), 71.24 (Cp), 68.31 (*ipso*-Cp), -11.07 (¹J_{Me-Sn} = 369.7 Hz, CH₃) ppm. ¹¹⁹Sn-NMR (149.211 MHz, C₆D₆, δ): -101.31 ppm.

4.4 Preparation of 1,1'-bis(tributyl stannyl) ferrocene **1b**

A 20.39 g (63 mmol) sample of (η⁵-C₅H₄Li)₂Fe•TMEDA was added to a 500 mL Schlenk flask in an N₂(g) atmosphere. To this flask 150 mL of hexanes was added followed by the slow addition of 37 mL (136 mmol) of (*n*-Bu)₃SnCl. The reaction was allowed to stir for 12 h under an N₂(g). LiCl was filtered off and the resulting oil purified *in vacuo* at 210°C to remove TMEDA and byproducts. Chemical shifts are similar to those previously reported by Dodo.¹⁰³ Yield 85%, 41.0 g (dark orange oil). ¹H NMR (400.130 MHz, CDCl₃, δ): 4.243 (m, 4H, Cp), 3.973 (m, 4H, Cp), 1.574 (tt, ³J = 7.8 Hz, ³J = 7.8 Hz, 12H, SnCH₂CH₂CH₂CH₃), 1.359 (tq, ³J = 7.3 Hz, ³J = 7.3 Hz, 12H, SnCH₂CH₂CH₂CH₃), 1.021 (t, ²J_{Sn-CH₂} = 26.6 Hz, 12H, ³J = 8.2 Hz, SnCH₂CH₂CH₂CH₃), 0.920 (t, ³J = 7.3 Hz, 18H, SnCH₂CH₂CH₂CH₃) ppm. ¹³C-NMR (100.613 MHz, C₆D₆, δ): 74.74 (²J_{119Sn-Cp} = 21.7 Hz, ²J_{117Sn-Cp} = 20.6 Hz, Cp), 71.16 (³J_{119Sn-Cp} = 17.6 Hz,

$^3J_{117\text{Sn-Cp}} = 17.0$ Hz, Cp), 68.95 (*ipso*-Cp), 29.75 ($^3J_{\text{Sn-CH}_2} = 9.9$ Hz, CH₂CH₂CH₂CH₃), 27.88 ($^2J_{119\text{Sn-CH}_2} = 28.5$ Hz, $^2J_{119\text{Sn-CH}_2} = 27.2$ Hz, CH₂CH₂CH₂CH₃), 14.00 (CH₂CH₂CH₂CH₃), 10.67 ($^1J_{\text{Sn-CH}_2} = 172.7$ Hz, $^1J_{\text{Sn-CH}_2} = 165.0$ Hz, CH₂CH₂CH₂CH₃) ppm. ¹¹⁹Sn NMR (149.211 MHz, CDCl₃, δ): -19.09 ppm.

4.5 Attempted preparation of 1,1'-bis(chlorodi(*n*-butyl) stannyl) ferrocene 2b through route 1

In an inert atmosphere, 2.65 g (5.5 mmol) of **1b** was added to a Schlenk flask. This was followed by 3.32 g (10.9 mmol) of (*n*-Bu)₂SnCl₂. The reaction was placed under static vacuum and heated to 150°C. The reaction was allowed to stir for 2 d. The reaction was monitored by ¹¹⁹Sn NMR spectroscopy and found to be impure. Purification through distillation was unsuccessful as a result no further analysis of these products was carried out.

4.6 Attempted preparation of 1,1'-bis(chlorodi(*n*-butyl) stannyl) ferrocene 2b through route 2

In an inert atmosphere, 2.0 g (6.2 mmol) of (η⁵-C₅H₄Li)₂Fe•TMEDA along with 200 mL of dry hexane was added to a Schlenk flask. In a separate Schlenk flask, 4.22 g (12.3 mmol) of (*n*-Bu)₂Sn(NEt₂)Cl was dissolved in 50 mL of dry hexanes. The (*n*-Bu)₂Sn(NEt₂)Cl solution was added to the slurry of (η⁵-C₅H₄Li)₂Fe•TMEDA and allowed to stir at RT overnight. The reaction mixture was filtered to remove LiCl, and solvent removed *in vacuo*. The crude product mixture was a sticky dark orange oil. All attempts to purify through distillation and column chromatography were unsuccessful.

4.7 Preparation of polybis(dimethyl stannyl) ferrocene 4 route 1

Exactly 1.008 g (2.1 mmol) of **3a** was added to a dry 50 mL Schlenk flask in a N₂ atmosphere. This was dissolved in 5 mL of DMF. To this solution 94 mg of a 2% solution of Karstedt's catalyst in xylenes (0.0049 mmol of active catalyst) was added. The reaction was stirred under dynamic nitrogen at ambient room temperature for 3 h. After the 3 h, 1 mL of MeOH was added to quench the reaction. Solvent was then removed under high vacuum. The sticky orange reaction mixture was dissolved in minimal THF and precipitated into \approx 400 mL of dry MeOH to remove oligomers, as well as other by-products.

For the main polymer **4**: ¹H NMR (400.130MHz, C₆D₆, δ): 4.342 (s, br, 4H, Cp), 4.276 (s, br, Cp end group), 4.150 (s, br, 4H, Cp), 4.079 (s, br, Cp end group), 0.594 (s, br, ²J_{Me-Sn} = 236.59 Hz, 4H, Me), 0.294 (s, br, ²J_{CH₃-Sn} = 57.74Hz, 4H, Me end group) ppm. ¹³C-NMR (100.613 MHz, C₆D₆, δ): 74.82 (Cp end group), 74.62 (Cp), 71.41 (Cp end group) 71.23 (Cp), 69.32 (*ipso*-Cp), -8.68 (CH₃) ppm. ¹¹⁹Sn-NMR (149.211 MHz C₆D₆, δ): -101.01 (end group), -104.39 (¹J_{119Sn-117Sn} = 5261.5 Hz) ppm. λ_{max} = 452.4 nm (ϵ = 115.98 L•mol⁻¹•cm⁻¹).

4.8 Preparation of polybis(dimethyl stannyl)ferrocene 4 route 2

Exactly 0.48g (0.99 mmol) of **3a** was added to a dry Schlenk flask in a N₂ atmosphere. This was dissolved in 3.1 mL of C₆H₆. To the solution 55 mg of a 2% solution of Karstedt's catalyst in xylenes (0.0028 mmol of active catalyst) was added drop wise. The reaction was heated to 70°C and allowed to stir for 3 d. The reaction mixture was then allowed to cool and solvent was removed *in vacuo*. Reaction mixture was dissolved in minimal tetrahydrofuran and precipitated into \approx 400 mL of MeOH to remove oligomers as well as by-products. See above for characterization.

4.9 Ring-opening polymerization of **5a** to form polybis(dimethyl stannyl) ferrocene **4**

To a Schlenk flask, 0.195 g (0.4 mmol) of **5b** was added under an inert atmosphere. To this, 0.016 g (0.0012 mmol) of Pd(PPh₃)₄ was added in 5 mL of C₆H₆. The reaction was heated to 60°C and allowed to stir for 3 d under dynamic N₂(g). The reaction was studied by ¹¹⁹Sn NMR spectroscopy and determined to be incomplete. The crude reaction mixture was dissolved in minimal THF and precipitated into MeOH. Only characterization that was possible was ¹¹⁹Sn NMR spectroscopy. ¹¹⁹Sn NMR (149.211, C₆D₆, δ): -11.627 (unknown), -104.73 (**4**).

4.10 Preparation of 1,1,2,2-tetramethyl-distannanediyl-[2]ferrocenophane **5a** from the reaction of **3** with Pd₂(dba)₃

A 1.0 g (2.07 mmol) sample of **3** was added to a 50 mL Schlenk flask. To the flask was added 10 mL of C₆H₆ and 0.081 g (0.09 mmol) of Pd₂(dba)₃. The mixture was then allowed to stir for 24 h at room temperature under N₂(g). C₆H₆ was removed *in vacuo*. The mixture was dissolved in hexane then filtered under N₂(g) to remove residual Pd₂(dba)₃. This data was in good agreement to data reported by Herberhold.⁴¹ Yield = 90%, 0.8973 g (orange solid). ¹H-NMR (400.130 MHz, C₆D₆, δ): 4.36 (m, *J* = 1.6 Hz, *J*_{Cp-Sn} = 4.8 Hz, 4H, Cp), 4.23 (m, *J* = 1.6 Hz, Cp), 0.41 (s, ²*J*_{Me-119Sn} = 50.1 Hz, ²*J*_{Me-117Sn} = 48.0 Hz, ³*J*_{Me-Sn} = 15.3 Hz, SnMe) ppm. ¹³C-NMR (100.613 MHz, C₆D₆, δ): 77.84 (²*J*_{119Sn-13C} = 49.9 Hz, ²*J*_{117Sn-13C} = 49.9 Hz, *ipso*-Cp), 74.58 (²*J*_{119/117Sn-13C} = 44.9 Hz, C2, C5), 69.34 (³*J*_{119/117Sn-13C} = 32.7 Hz, ⁴*J*_{119/117Sn-13C} = 4.8 Hz, C3, C4), -8.43 (¹*J*_{119Sn-13C} = 241.6 Hz, ¹*J*_{117Sn-13C} = 230.5 Hz, ²*J*_{119Sn-13C} = 91.0 Hz, ²*J*_{117Sn-13C} = 86.5 Hz, SnCH₃) ppm. ¹¹⁹Sn-NMR (149.211, C₆D₆, δ): -43.0 (s, *J*_{119Sn-117Sn} = 5261.5 Hz) ppm.

4.11 Attempted preparation of 5a with Pt(acac)₂

A 0.50 g (1.03 mmol) sample of **3a** was added to a 50 mL Schlenk flask. To the flask was added 5.0 mL of C₆H₆ and 0.012 g (0.031 mmol) of Pt(acac)₂. The mixture was then allowed to stir for 2 d at room temperature under N₂(g). The mixture was then filtered under N₂(g) to remove Pt(acac)₂, and the solvent reduced *in vacuo*. Analysis by ¹H and ¹¹⁹Sn NMR (C₆D₆) revealed only the presence of starting material **3a**.

4.12 Attempted preparation of 5a with ClRh(PPh₃)₃

A 0.50 g (2.07 mmol) sample of **3a** was added to a 50 mL Schlenk flask. To the flask was added 25 mL of DCM with 0.012 g (0.013 mmol) of ClRh(PPh₃)₃. The mixture was allowed to stir for 4 d at room temperature under N₂(g). The mixture was then filtered under N₂(g) to remove ClRh(PPh₃)₃, and the solvent reduced *in vacuo*. Analysis by ¹H and ¹¹⁹Sn NMR (C₆D₆) revealed only the presence of starting material **3a**.

4.13 Preparation of 1,1,14,14-tetra-n-butyl-2,2,13,13,15,15,26,26-octamethyl-1,2,13,14,15,26-hexastanna-[3.3]ferrocenophane **11** (low dilution)

A 2.0 g (4.1 mmol) sample of **3a** was added to a 3-neck round bottomed flask and diluted with 40 mL of Et₂O. A 1.56 g (4.2 mmol) of **10a** was added in a separate Schlenk flask and diluted with 30 mL of Et₂O. Both flasks were cooled to 0°C and the solution containing compound **10a** was added slowly (over a 30 min period) via double tip cannula to the flask containing **6**. The mixture was then heated to reflux for 2 h and then allowed to cool to RT. All

volatiles were then removed *in vacuo*. The crude product was run through a silica column in an N₂(g) atmosphere eluting with pure hexanes. Recovered Yield = 82%, 4.80 g (light orange oil) of **11**, 5%, 0.099 g (orange solid) of **5a**.

For **11**: ¹H-NMR (400.130 MHz, C₆D₆, δ): 4.294 (m, *J* = 1.6 Hz, ⁴*J*_{Cp-Sn} = 7.4 Hz, 8H, 3,4-H Cp), 4.058 (m, *J* = 1.6 Hz, ³*J*_{Cp-Sn} = 10.4 Hz, 8H, 2,5-H Cp), 1.717 (m, 8H, SnCH₂CH₂CH₂CH₃), 1.421 (m, 16H, SnCH₂CH₂CH₂CH₃), 0.953 (t, *J* = 7.3 Hz, 12H, CH₂CH₂CH₂CH₃), 0.532 (s, ²*J*_{119Sn-Me} = 47.9 Hz, ²*J*_{117Sn-Me} = 45.9 Hz, ³*J*_{SnBu-SnMe} = 11.7 Hz, 24H, SnCH₃) ppm. ¹³C-NMR (100.613 MHz, C₆D₆, δ): 75.70 (²*J*_{119Sn-13C} = 48.5 Hz, ²*J*_{117Sn-13C} = 46.5 Hz, ³*J*_{119/117Sn-13C} = 9.8 Hz, C2, C5), 71.04 (¹*J*_{119Sn-13C} = 34.5 Hz, ²*J*_{117Sn-13C} = 33.2 Hz, ³*J*_{119/117Sn-13C} = 4.4 Hz, C3, C4) 69.13 (¹*J*_{119/117Sn-13C} = 336 Hz, *ipso*-Cp), 32.92 (³*J*_{119Sn-13C} = 13.1 Hz, ³*J*_{117Sn-13C} = 17.1 Hz, SnCH₂CH₂CH₂CH₃), 27.67 (²*J*_{119Sn-13C} = 53.18 Hz, ²*J*_{117Sn-13C} = 51.0 Hz, ⁴*J*_{119Sn-13C} = 3.4 Hz, ⁴*J*_{117Sn-13C} = 1.9 Hz, SnCH₂CH₂CH₂CH₃), 13.94 (SnCH₂CH₂CH₂CH₃), 9.10 (¹*J*_{119Sn-13C} = 207.4 Hz, ¹*J*_{117Sn-13C} = 200.1 Hz, ²*J*_{119Sn-13C} = 29 Hz, ²*J*_{117Sn-13C} = 27 Hz, SnCH₂CH₂CH₂CH₃), -8.12 (¹*J*_{119Sn-13C} = 239.9 Hz, ¹*J*_{117Sn-13C} = 229.2 Hz, ²*J*_{119Sn-13C} = 36.9 Hz, ²*J*_{117Sn-13C} = 35.2 Hz, ³*J*_{119Sn117Sn-13C} = 16.3 Hz, SnCH₃) ppm. ¹¹⁹Sn-NMR (149.211 MHz, C₆D₆, δ): -100.44 (¹*J*_{119SnMe-119SnBu} = 2741.2 Hz, ¹*J*_{117SnMe-119SnBu} = 2437.2 Hz, ²*J*_{119SnMe-117SnMe} = 483.6 Hz, SnMe₂), -211.75 (¹*J*_{119SnBu-119SnMe} = 2638.5 Hz, ¹*J*_{119SnBu-117SnMe} = 2437.9 Hz, SnBu₂) ppm. ¹¹⁷Sn-NMR (249.472 MHz, C₆D₆, δ): -100.5 (¹*J*_{117SnMe-119SnBu} = 2480.7 Hz, ¹*J*_{117SnMe-117SnBu} = 2370.6 Hz, ²*J*_{117SnMe-117SnMe} = 483.7 Hz, SnMe₂), -211.84 (¹*J*_{117SnBu-119SnMe} = 2478.8 Hz, ¹*J*_{117SnBu-117SnMe} = 2372.2 Hz, SnBu₂) ppm. R_f = 0.5 (hexanes). HRMS (DART-TOF) calcd. for C₄₄H₇₆Fe₂Sn₆: 1433.8621; found 1433.8588. E.A.: Anal. Calcd C, 36.98; H, 5.36. Found: C, 36.94; H, 5.37.

4.14 Preparation of 1,1,14,14-tetra-*n*-butyl-2,2,13,13,15,15,26,26-octamethyl-1,2,13,14,15,26-hexastanna-[3.3]ferrocenophane **11** (high dilution)

The preceding reaction was run under identical conditions at higher dilution (0.20 g, 0.41 mmol of **3**, 10 mL of Et₂O, 0.16 g, 0.42 mmol of **10a**) resulting in similar yield of products **5a** and **11**. Recovered Yield = 64%, 0.375 g (light orange oil) of **11**, 7.5%, 0.015g (orange solid) of **5a**.

For **11**: ¹¹⁹Sn-NMR (149.211 MHz, C₆D₆, δ): -100.43 (¹J_{119SnMe-119SnBu} = 2741.2 Hz, ¹J_{117SnMe-119SnBu} = 2437.2 Hz, ²J_{119SnMe-117SnMe} = 483.6 Hz, *SnMe*₂), -211.79 (¹J_{119SnBu-119SnMe} = 2638.5 Hz, ¹J_{119SnBu-117SnMe} = 2437.9 Hz, *SnBu*₂) ppm.

For **5a**: ¹¹⁹Sn-NMR (149.211, C₆D₆, δ): -42.4 (s, *J*_{119Sn-117Sn} = 5261.5 Hz) ppm.

5.0 Conclusion

A novel polymer polybis(dimethyl stannyl)ferrocene, **4**, was synthesized through a dehydrogenative coupling condensation polymerization. The crude polymer was not fully purified, however it was characterized by ^1H , ^{13}C and ^{119}Sn NMR spectroscopy, as well as through cyclic voltammetry, gel permeation chromatography and UV-Visible spectroscopy. Additionally, model systems were studied through DFT calculations. This polymer is the first evidence of a dibridged polyferrocenyl distannane. The polymer was found to be of low to moderate molecular weight and maintained a degree of electronic communication that is similar to known monobridged polyferrocenyl stannanes. The presence of an intramolecularly coupled [2]ferrocenophane was also discovered as a byproduct of this polymerization.

The first tristanna-bridged [3.3]ferrocenophane, **11**, was discovered through an amine coupling of a tin amine **10a**, and 1,1'-bis(dimethyl stannyl) ferrocene **3a**. This [3.3]ferrocenophane was fully characterized through ^1H , ^{13}C and ^{119}Sn NMR and UV-Visible spectroscopies, mass spectrometry, and cyclic voltammetry. The [3.3]ferrocenophane was found to maintain strong interaction between connected ferrocenes despite the large distance between Fe centers of the connected ferrocenes.

Finally, a new and much improved synthesis of 1,1,2,2-tetramethyldistannanediyl-[2]ferrocenophane, **5a**, was found. This metal catalyzed intramolecular dehydrogenative coupling employed $\text{Pd}_2(\text{dba})_3$ as a catalyst with a yield of 90%. This was a significant improvement on work previously carried out by Herberhold and Wrackmeyer.⁴¹

Appendix

Appendix 1 ^1H , ^{13}C , ^{117}Sn , and ^{119}Sn NMR

Appendix 1.1: 1a

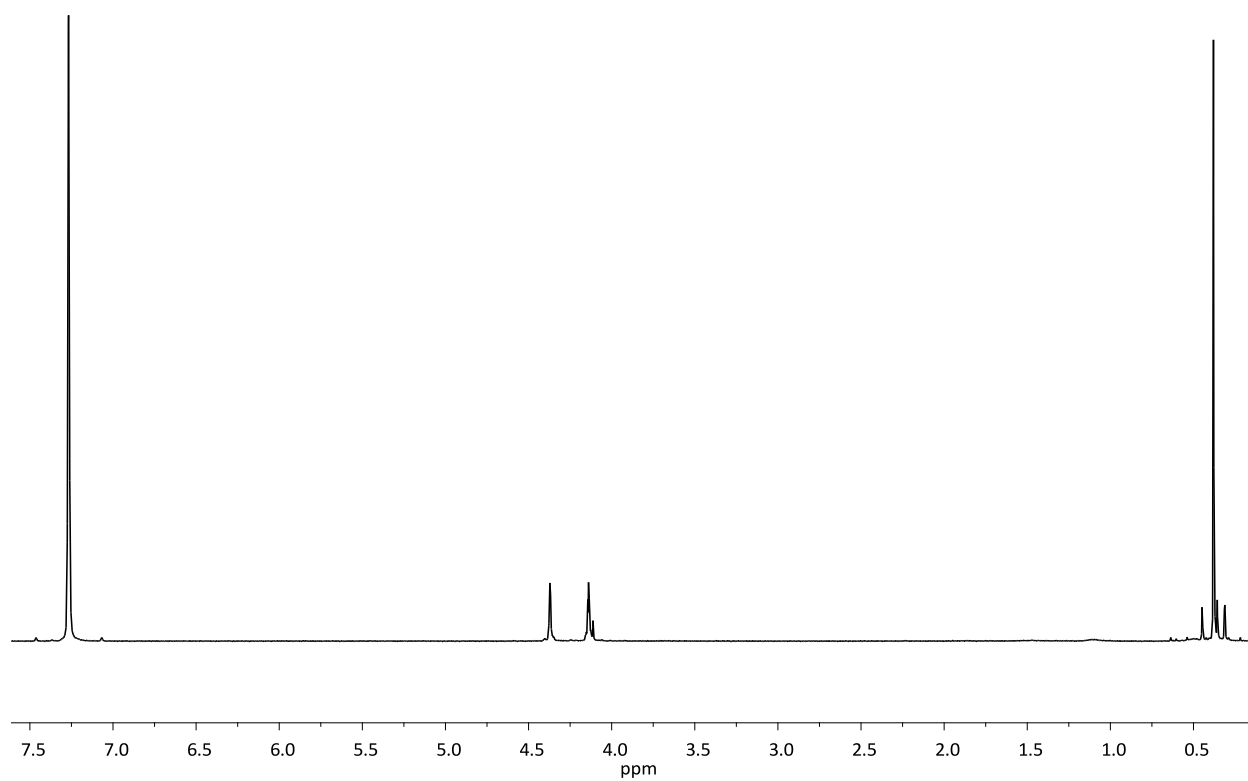


Figure A1.1: ^1H NMR (CDCl_3) of **1a**.

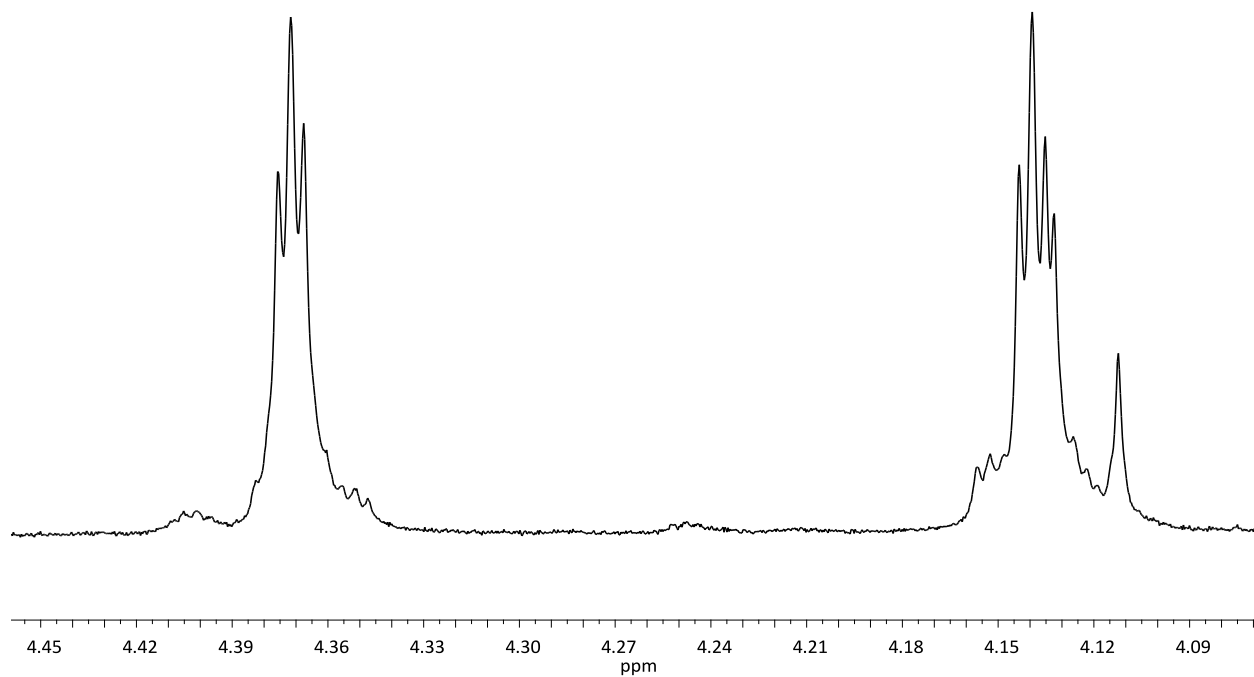


Figure A1.2: Cyclopentadiene region of ^1H NMR (CDCl_3) of **1a**.

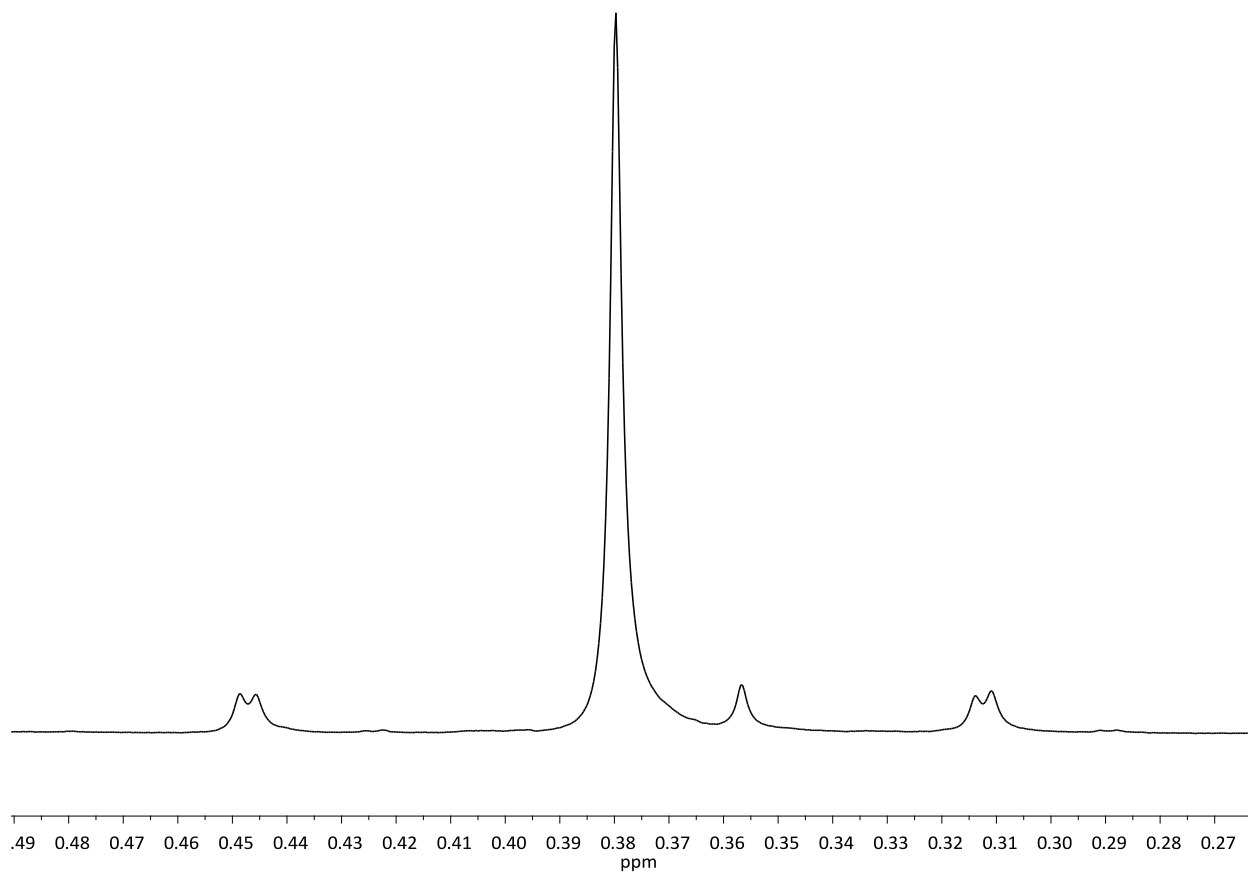


Figure A1.3: Methyl region of ^1H NMR (CDCl_3) of **1a**.

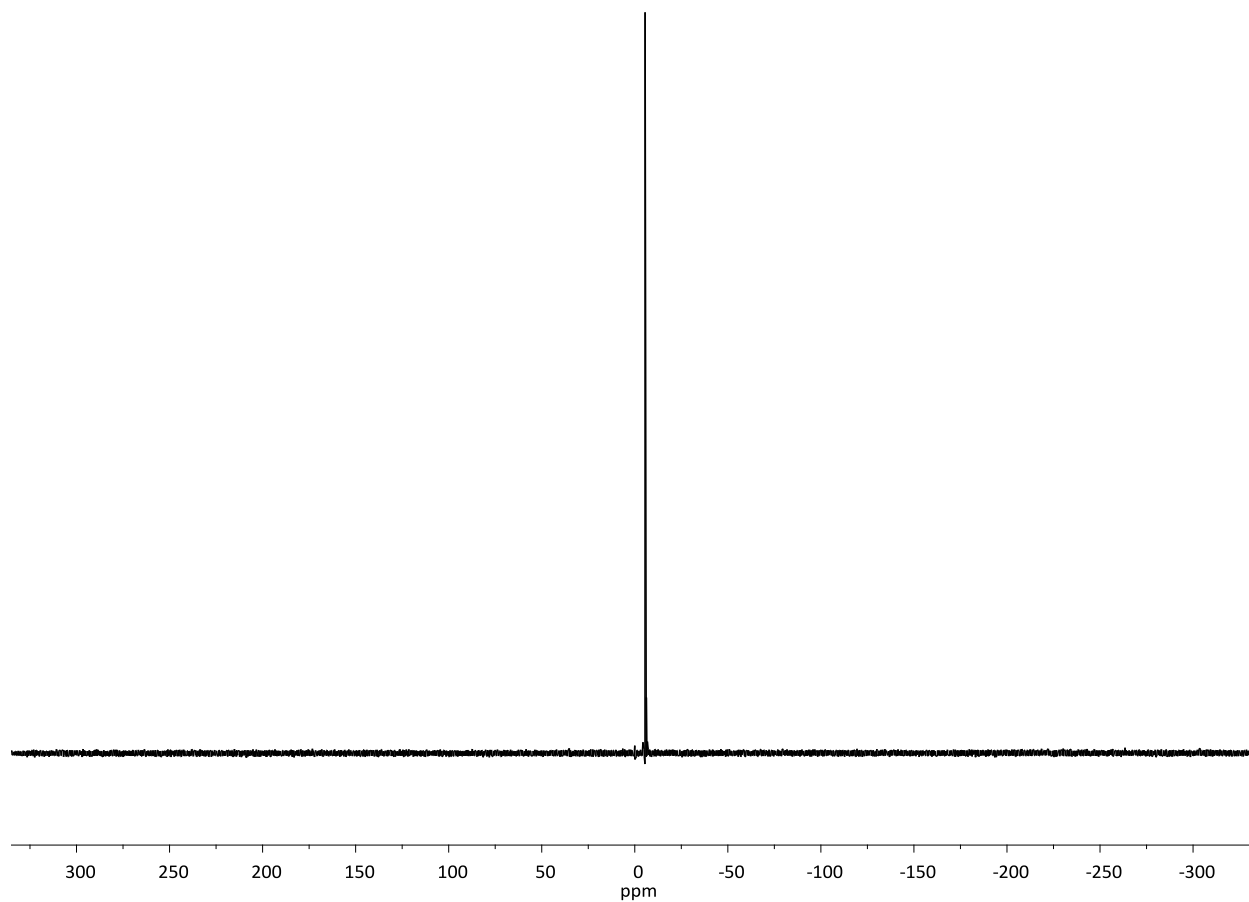


Figure A1.4: ^{119}Sn NMR (CDCl_3) of **1a**.

Appendix 1.2: 2a

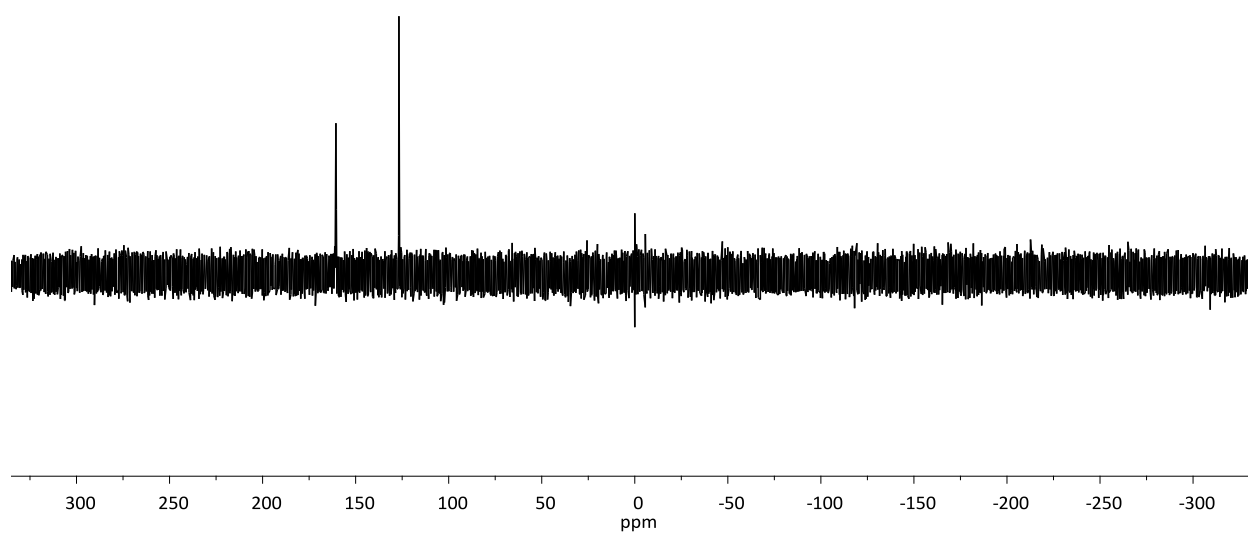


Figure A1.5: ^{119}Sn NMR (CDCl_3) of crude **2a**.

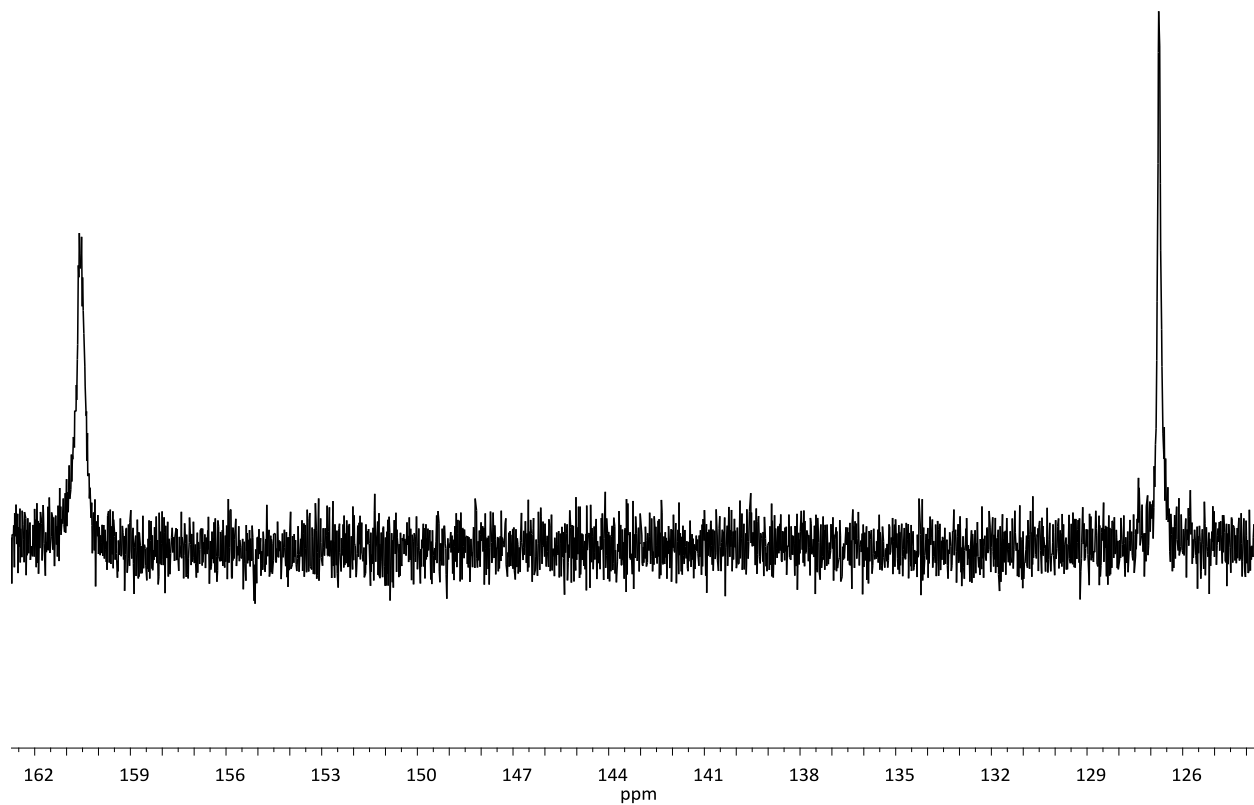


Figure A1.6: ^{119}Sn NMR (CDCl_3) Crude **2a**, signal at 126.8 ppm is **2a** and signal at 160 ppm is Me_3SnCl .

Appendix 1.3: 3a

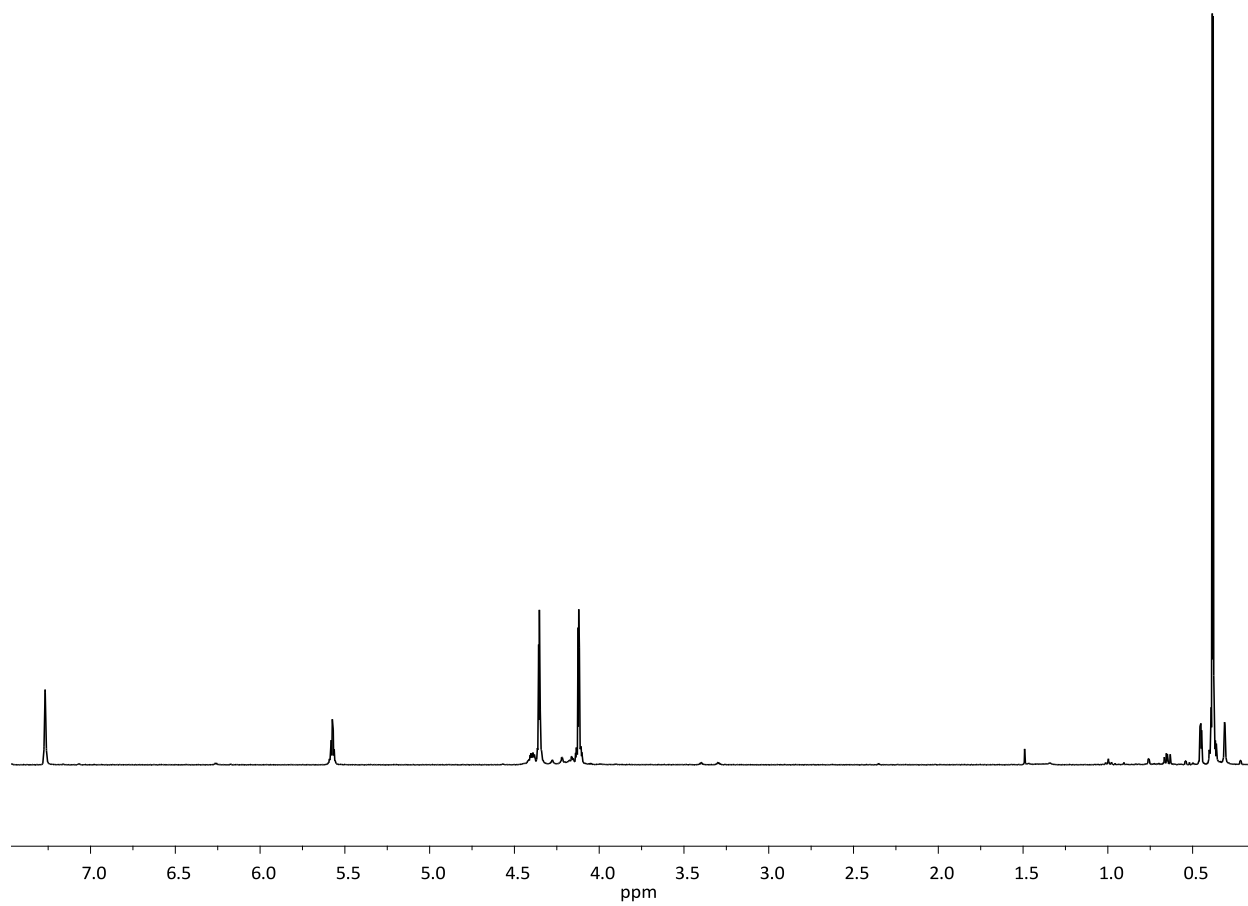


Figure A1.7: ^1H NMR (C_6D_6) of **3a**.

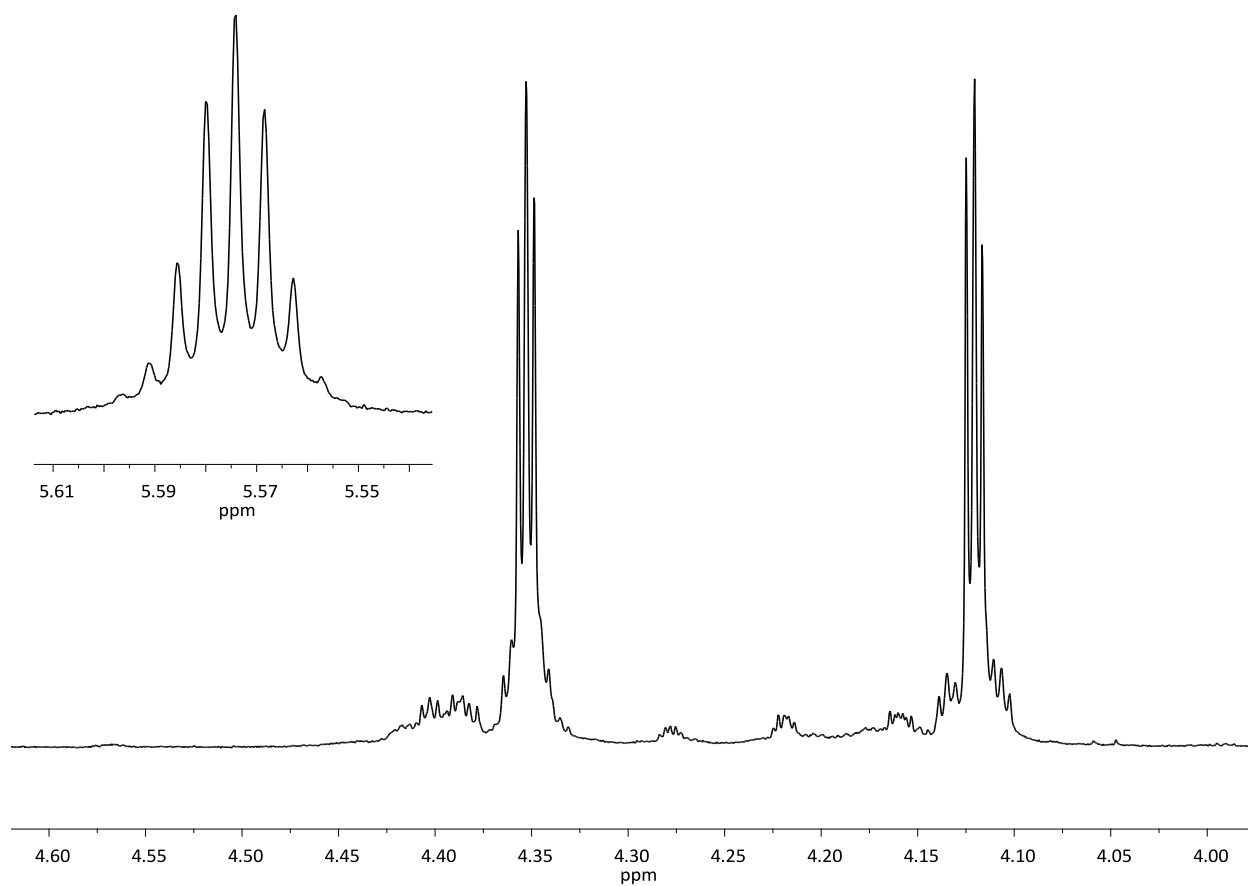


Figure A1.8: cyclopentadiene region ^1H NMR (C_6D_6) of **3a** with insert of hydride region.

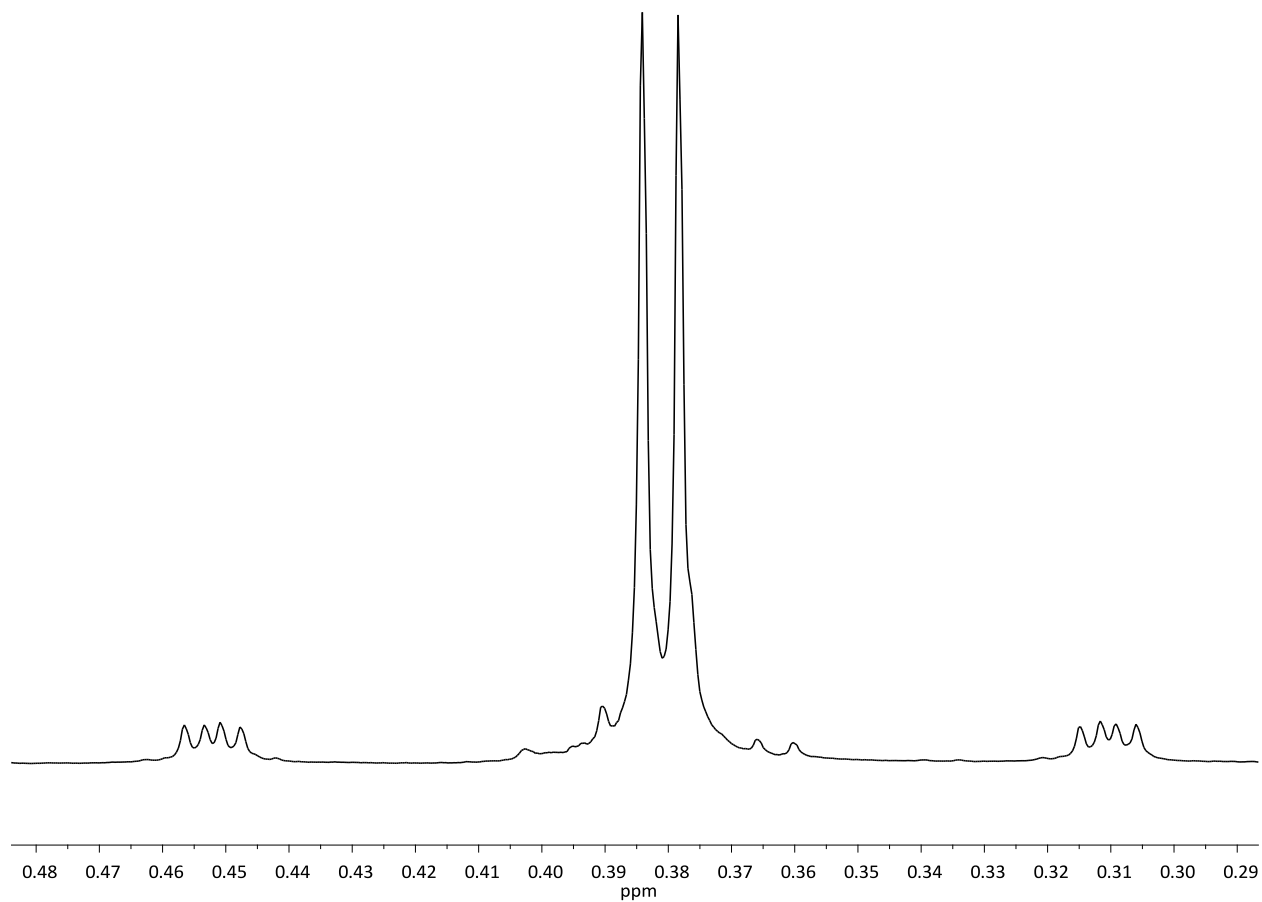


Figure A1.9: Methyl region ^1H NMR (C_6D_6) of **3a**.

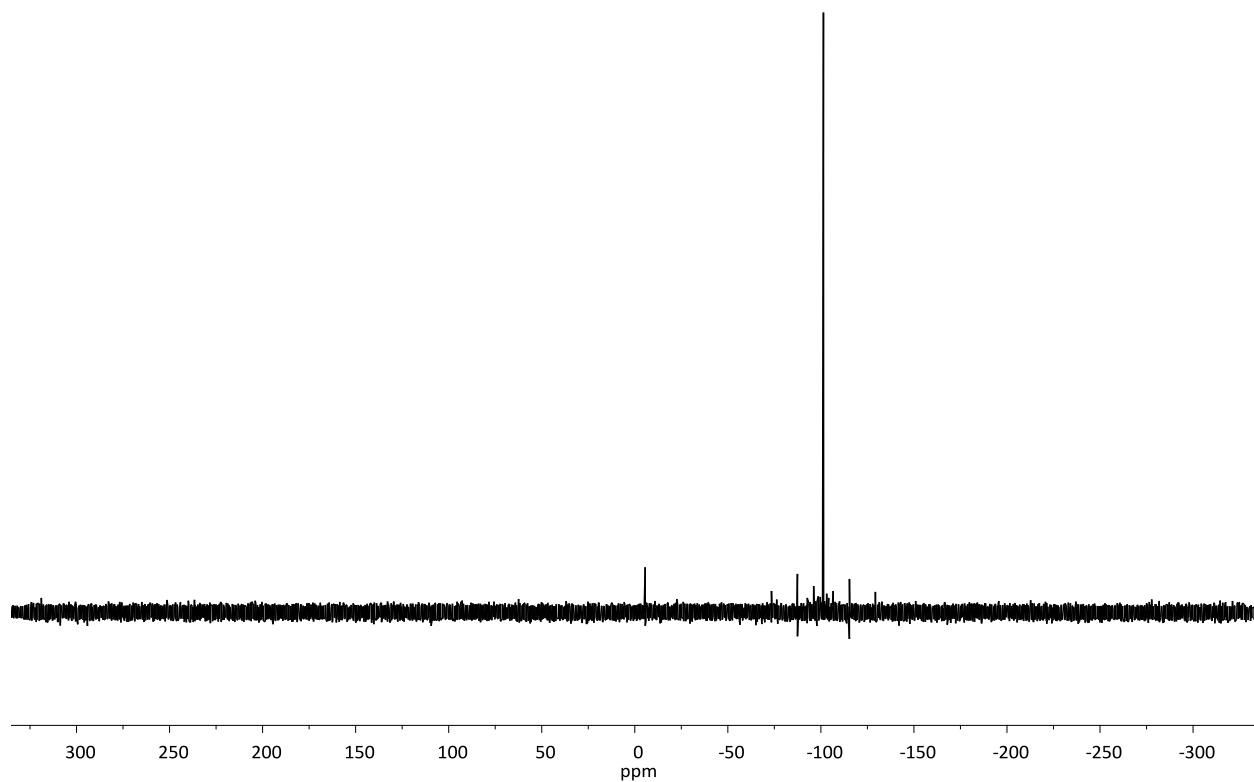


Figure A1.10: ^{119}Sn NMR (C_6D_6) of **3a**, the chemical shift found at -6 ppm is unreacted **1a**.

Appendix 1.4: 1b

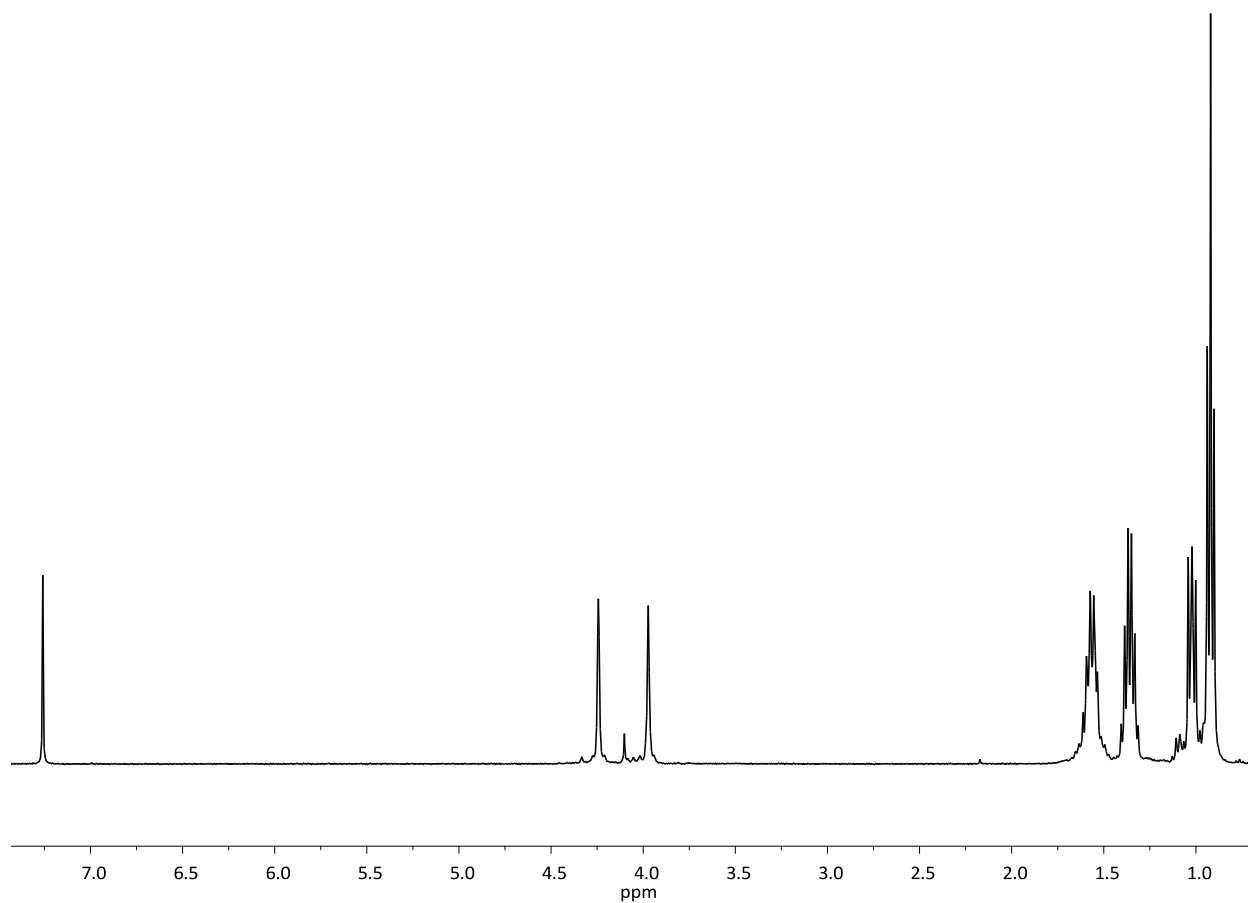


Figure A1.11: ^1H NMR (CDCl_3) of **1b**.

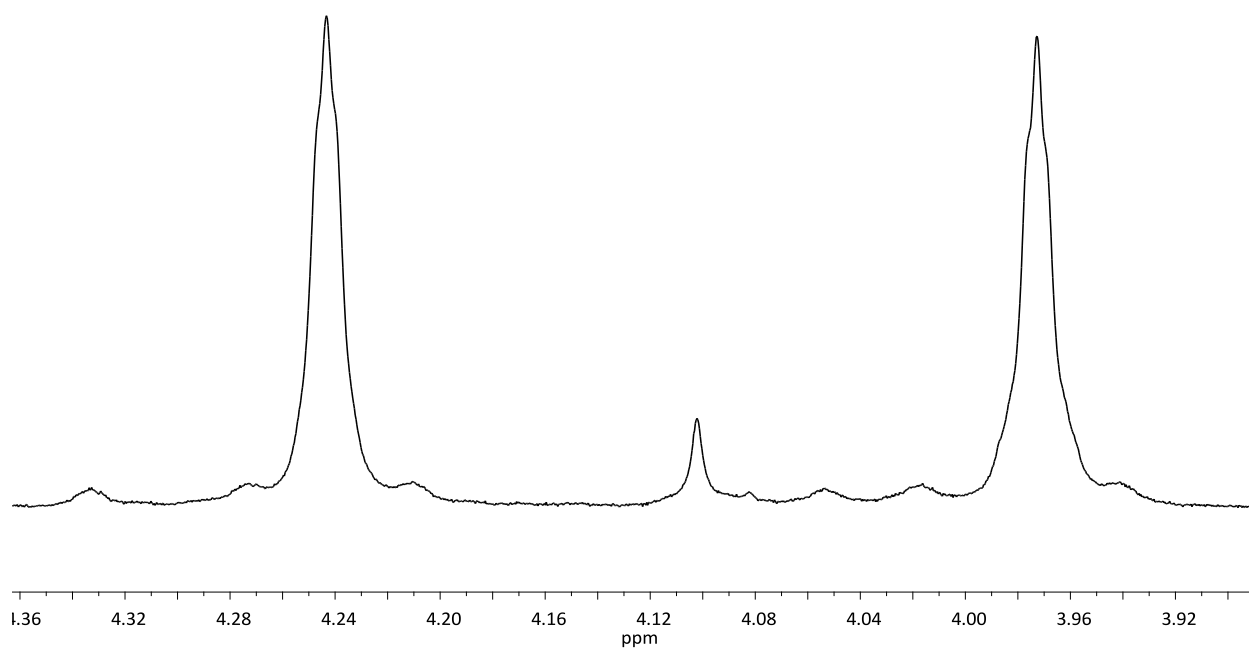


Figure A1.12: Cyclopentadiene region of ^1H NMR (CDCl_3) of **1b**.

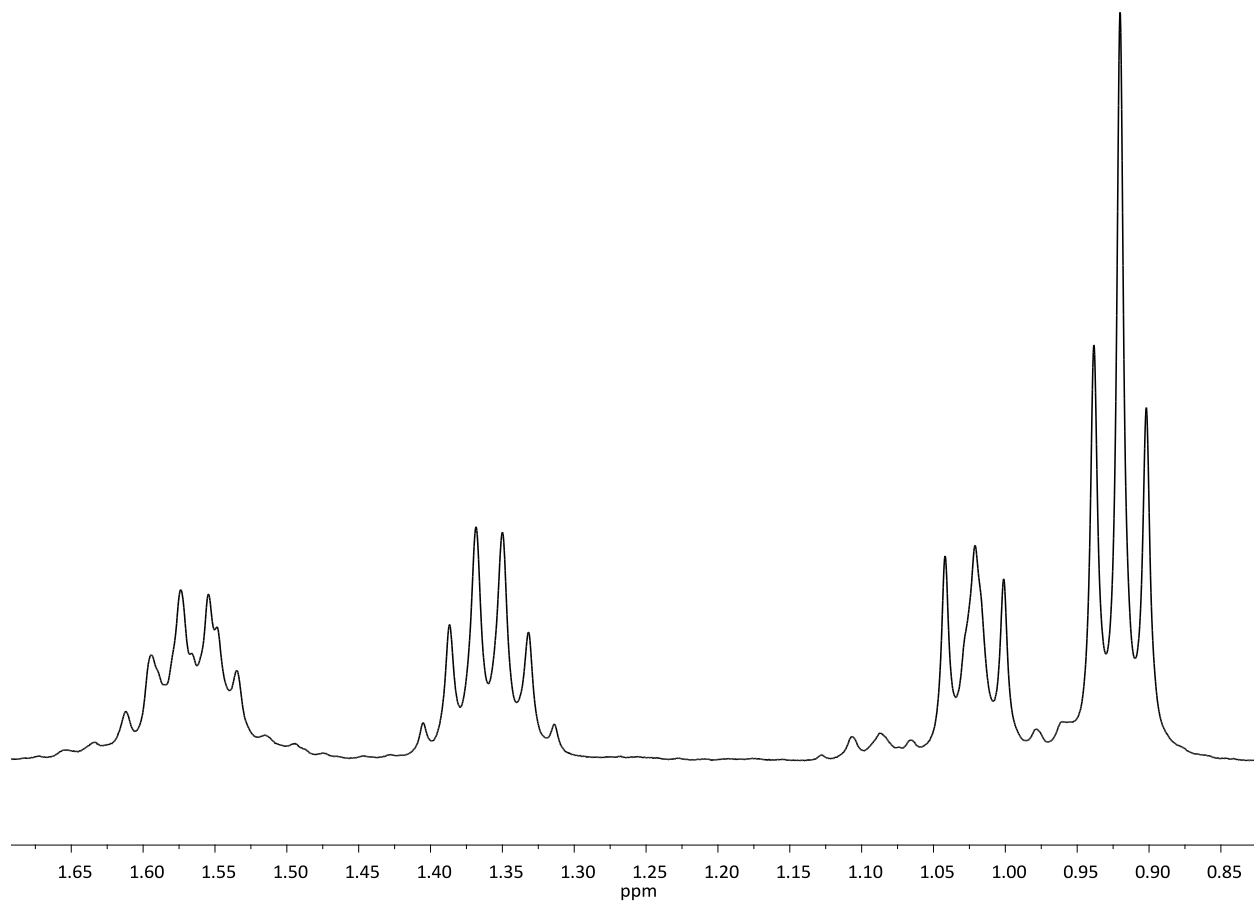


Figure A1.13: Methyl region of ^1H NMR (CDCl_3) of **1b**.

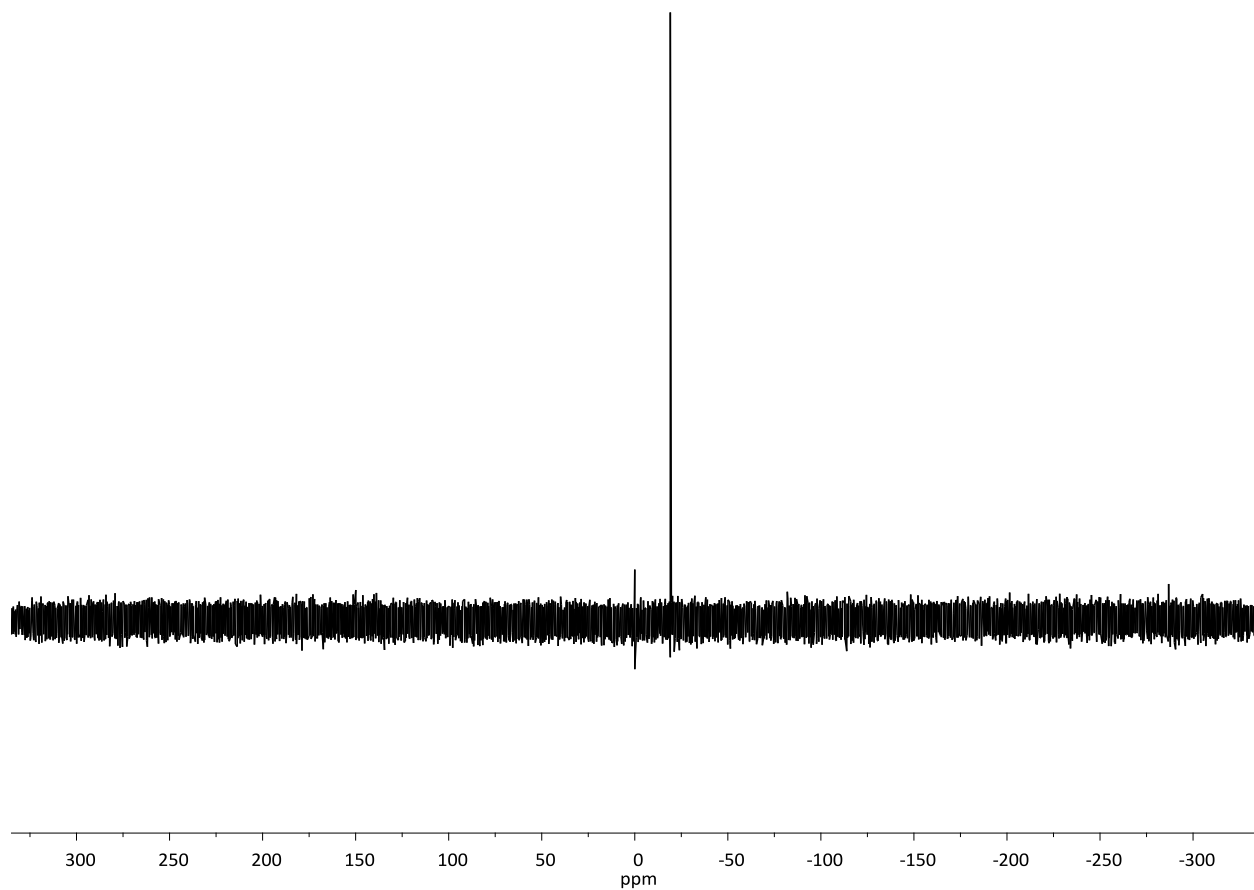


Figure A1.14: ^{119}Sn NMR (CDCl_3) of **1b**.

Appendix 1.5: 4 formed through Condensation polymerization.

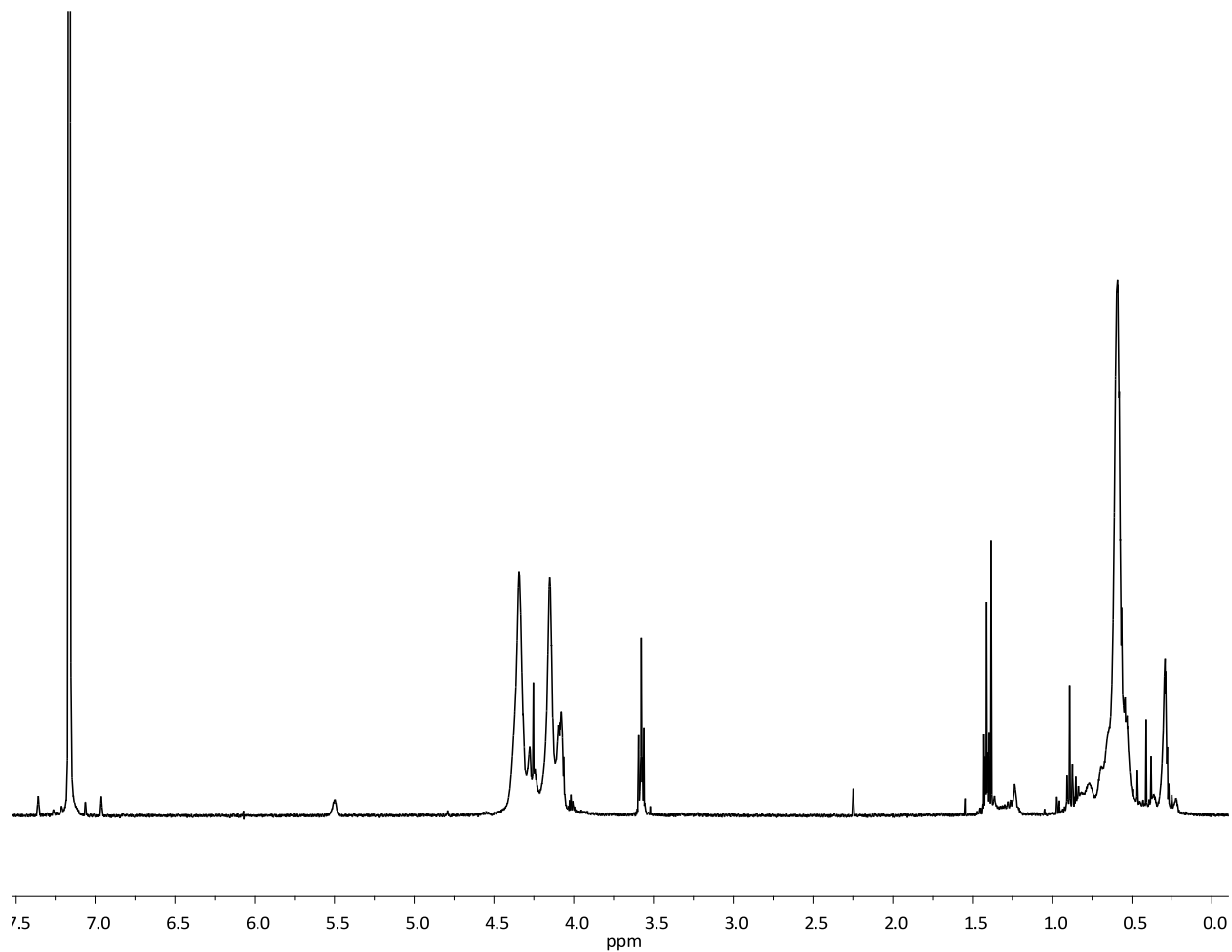


Figure A1.15: ^1H NMR (C_6D_6) of 4.

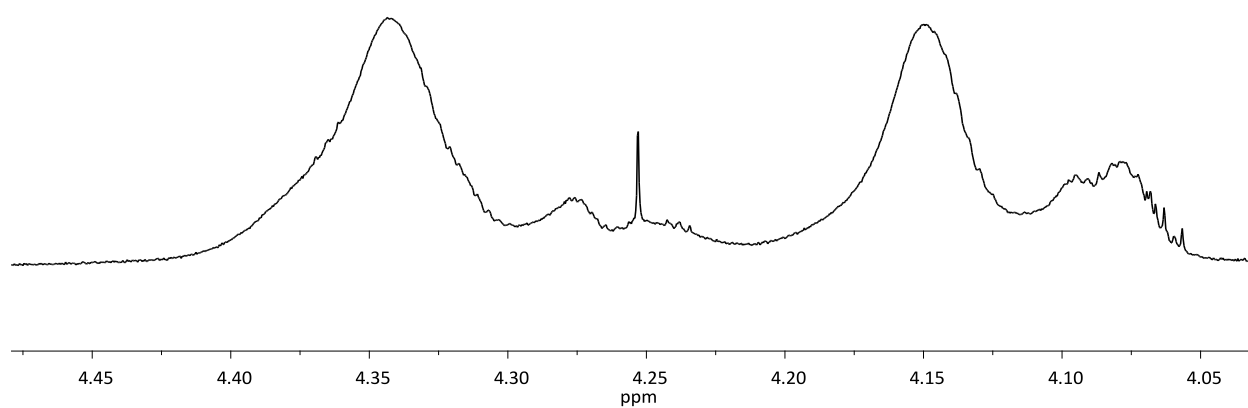


Figure A1.16: Cyclopentadiene region of ^1H NMR (C_6D_6) of **4**.

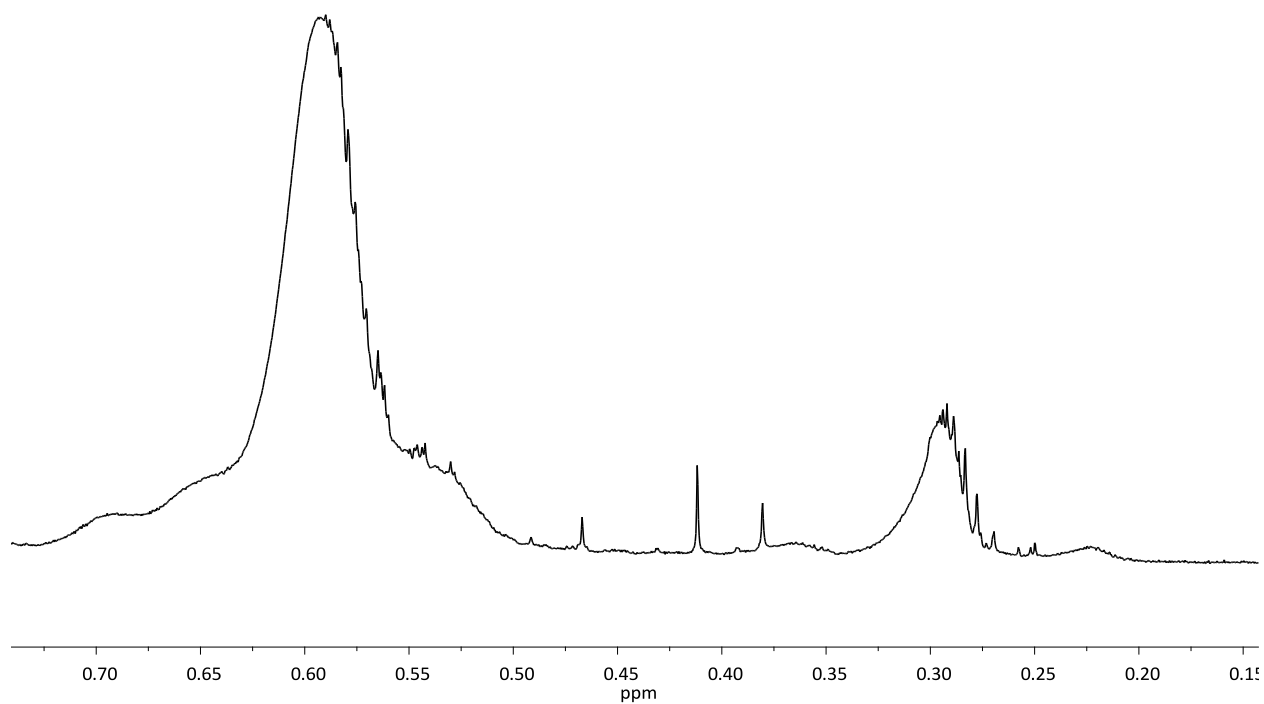


Figure A1.17: Methyl region of ^1H NMR (C_6D_6) of **4**.

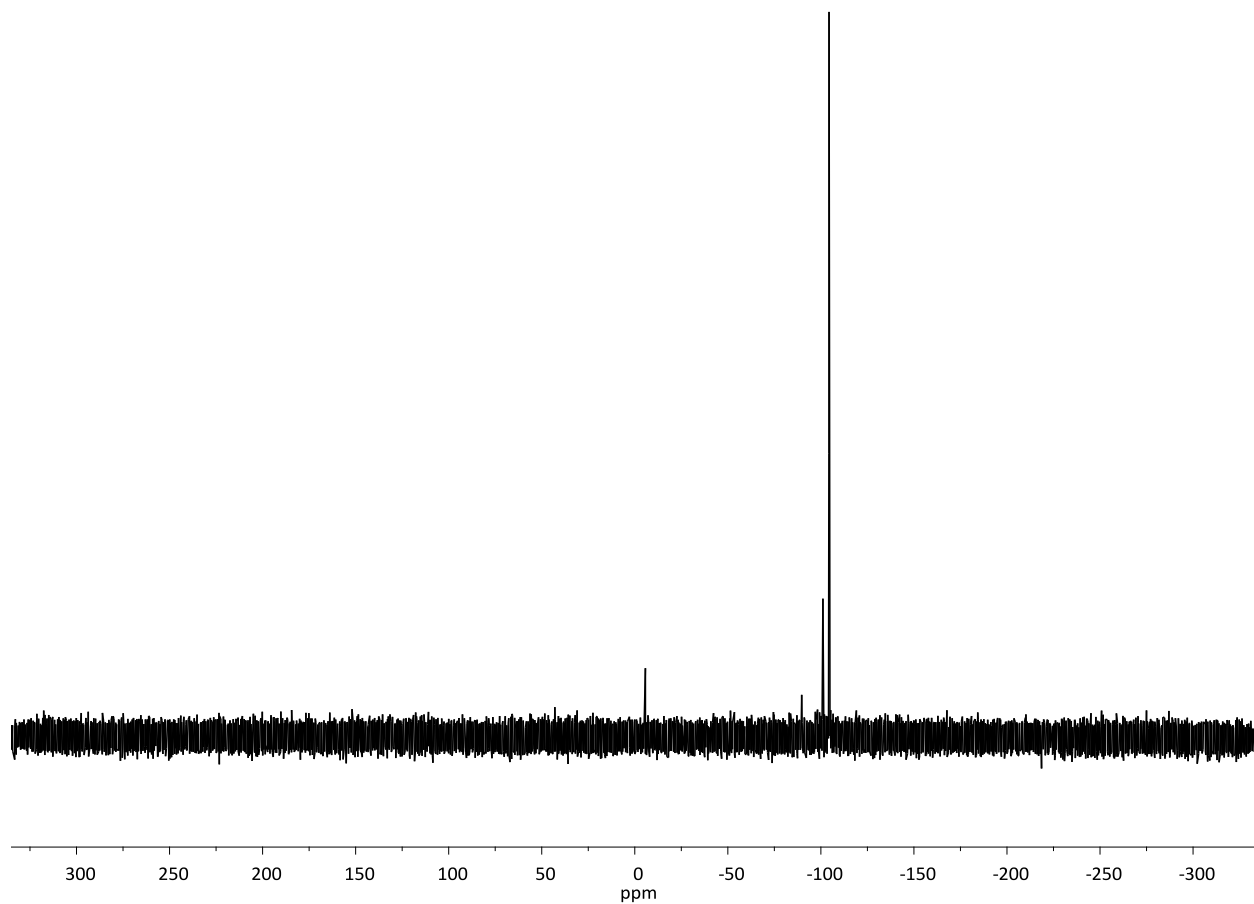


Figure A1.18: ^{119}Sn NMR (C_6D_6) of **4**.

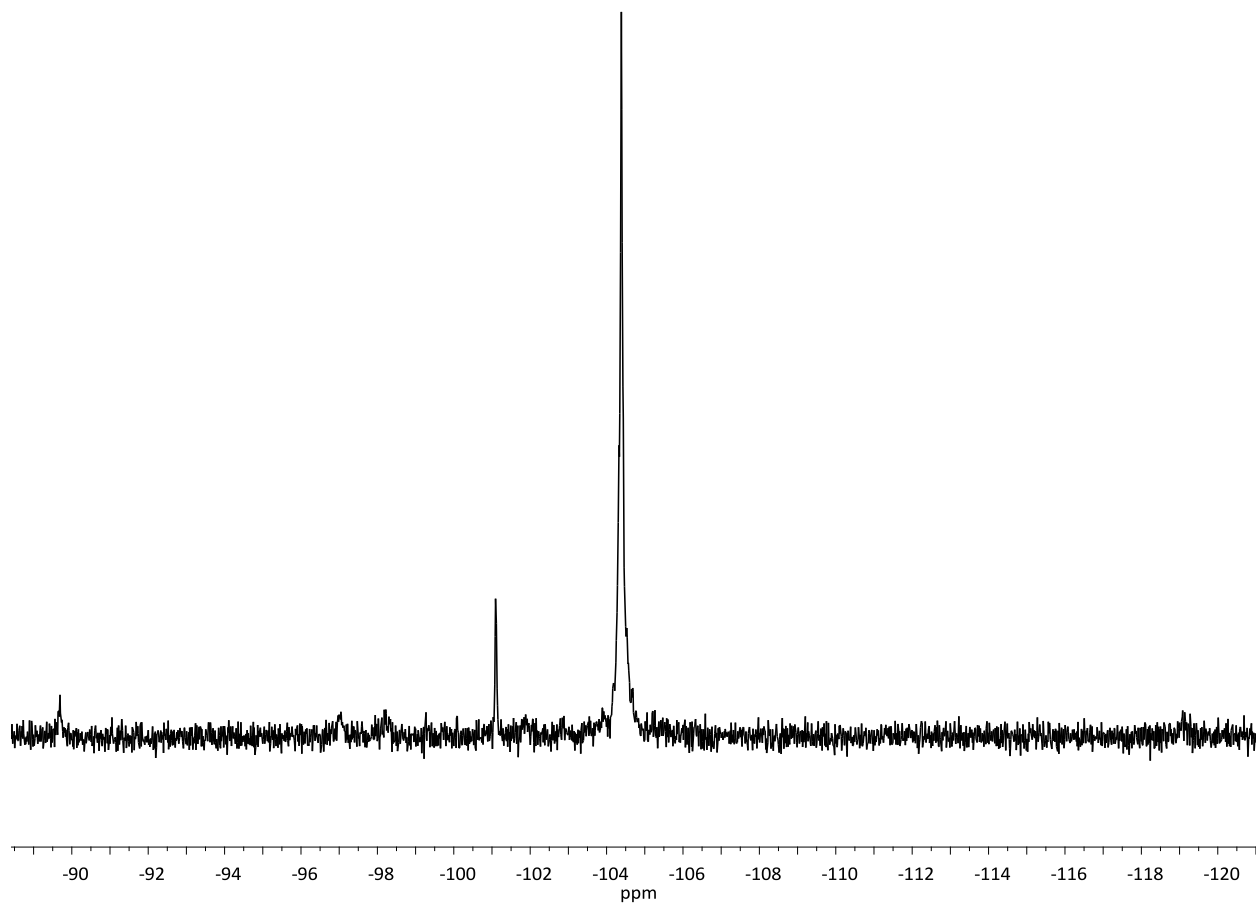


Figure A1.19: Polymer region of ^{119}Sn NMR (C_6D_6) of **4**.

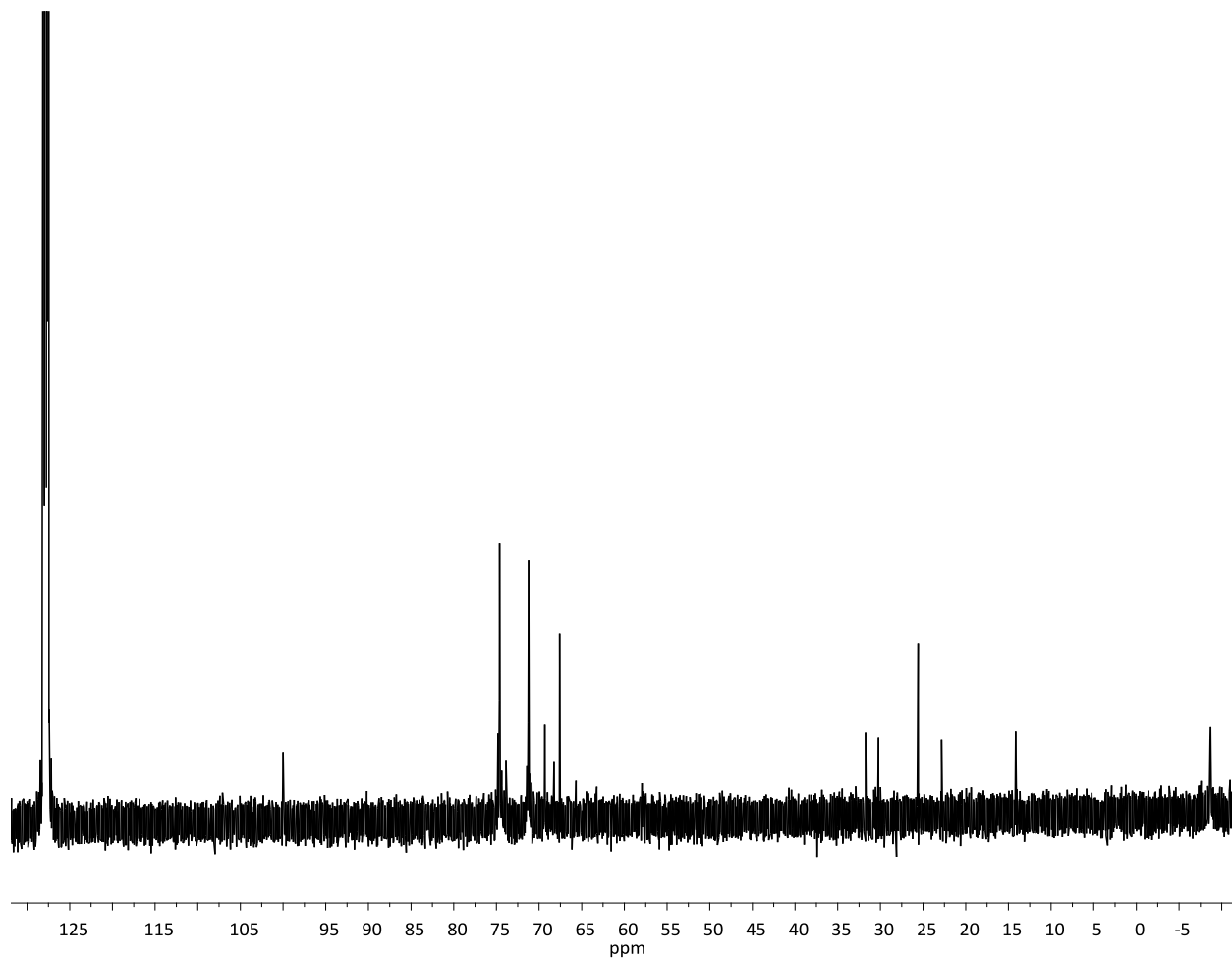


Figure A1.20: ^{13}C NMR (C_6D_6) of 4.

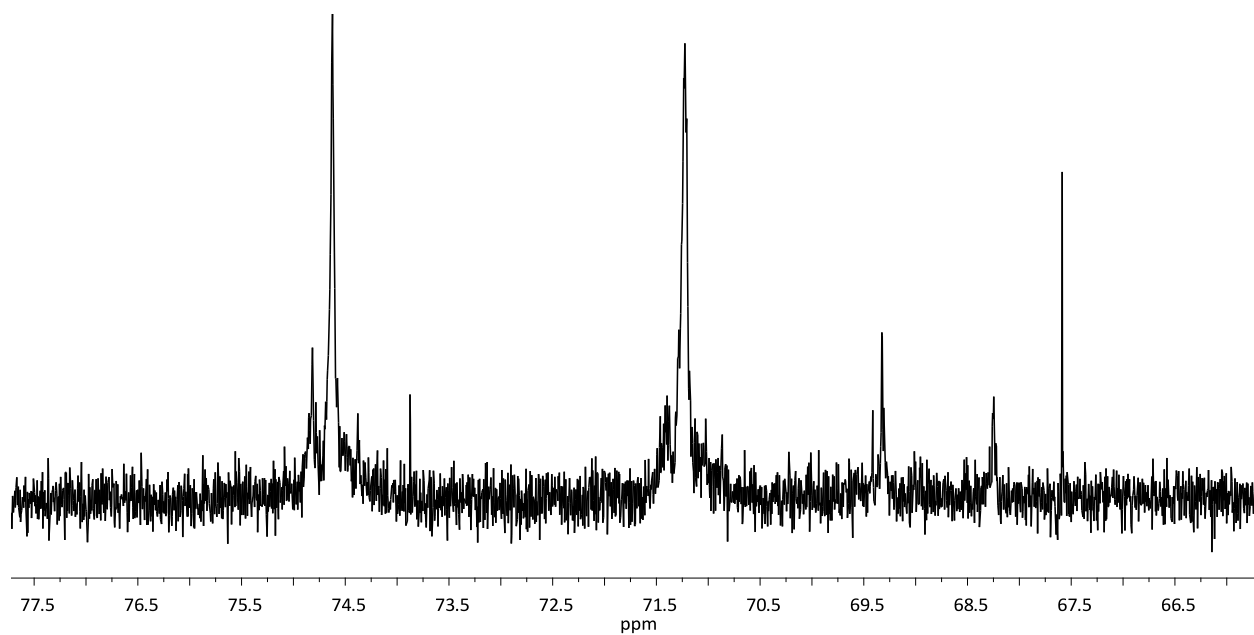


Figure A1.21: Cyclopentadiene region of ^{13}C NMR (C_6D_6) of **4**.

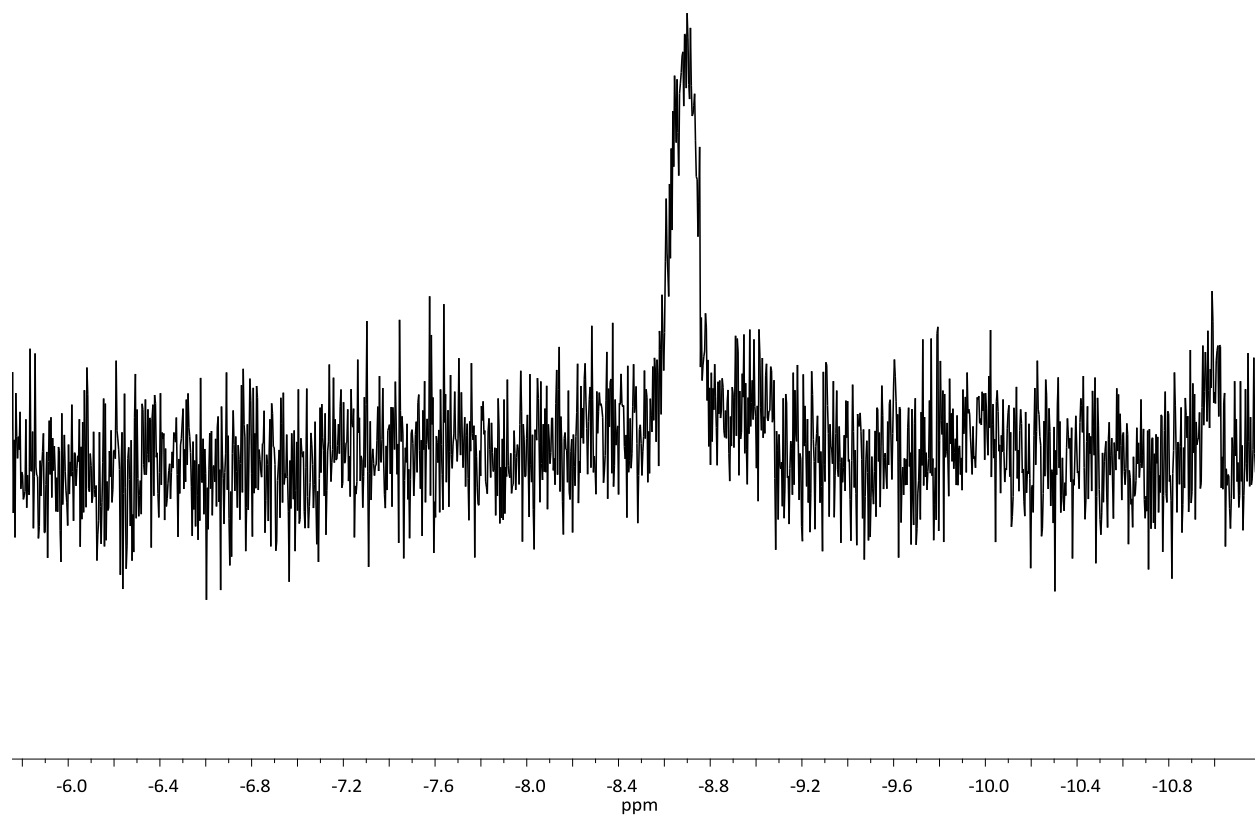


Figure A1.22: Methyl region of ^{13}C NMR (C_6D_6) of 4.

Appendix 1.6: 4 prepared through ROP

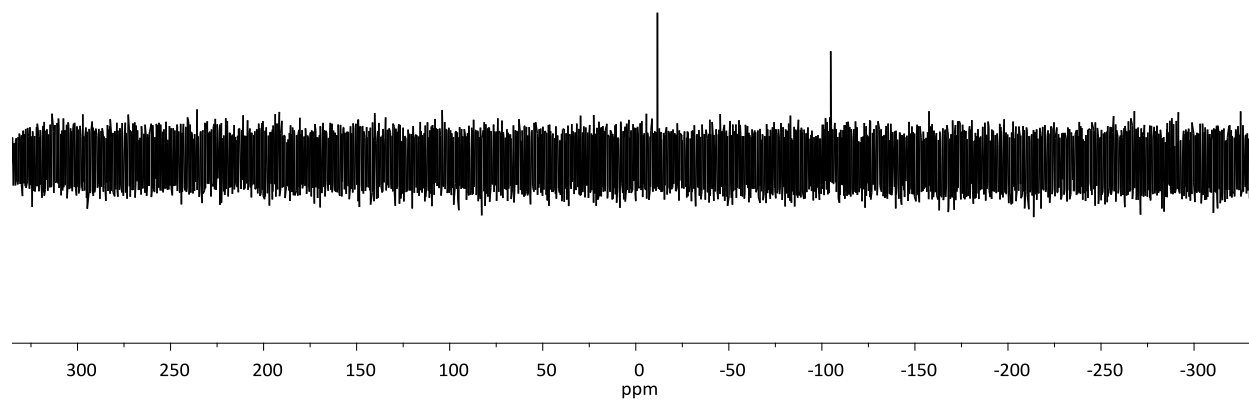


Figure A1.23: ^{119}Sn NMR (C_6D_6) of **4** prepared through ROP.

Appendix 1.7: 5a

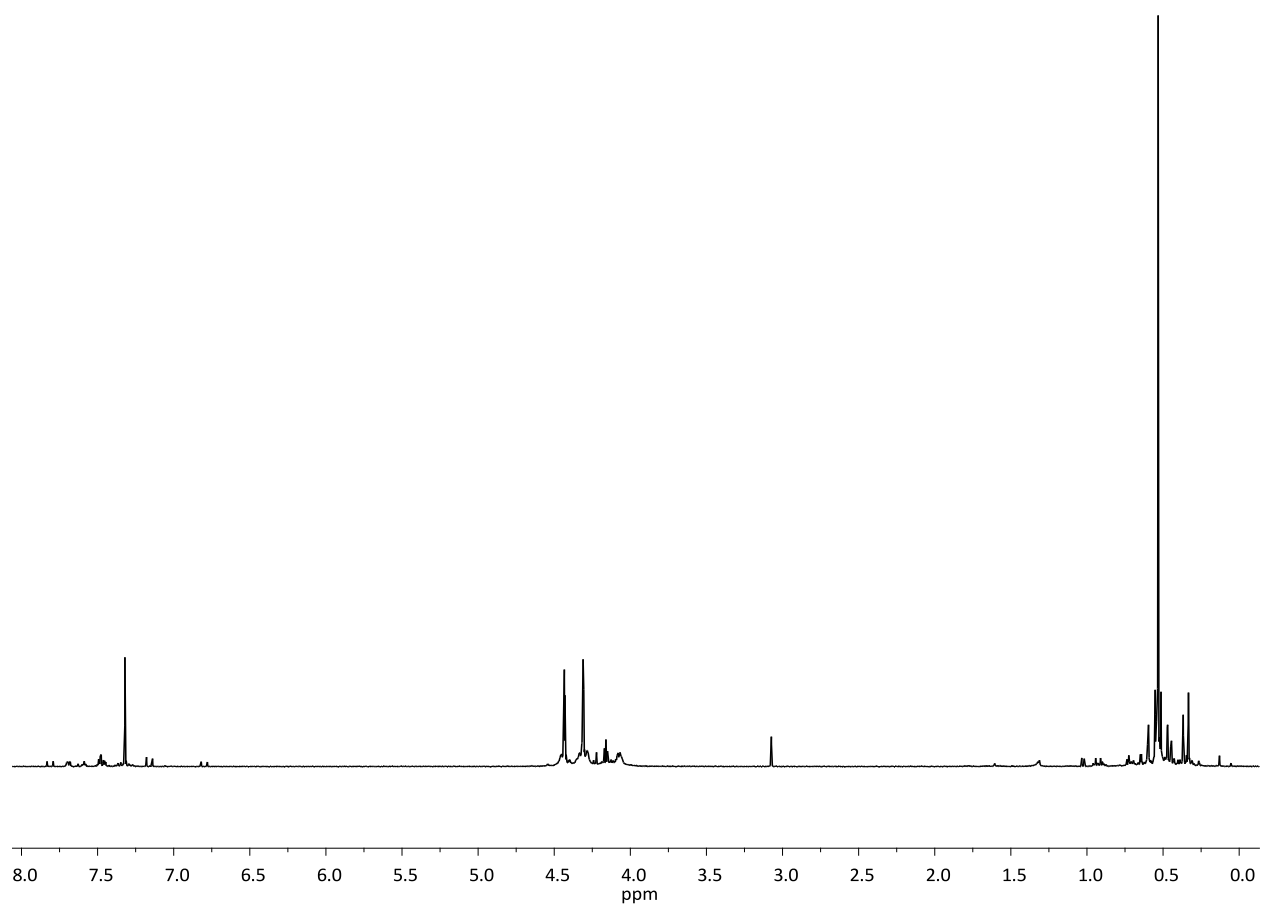


Figure A1.24: ^1H NMR (C_6D_6) of **5a**.

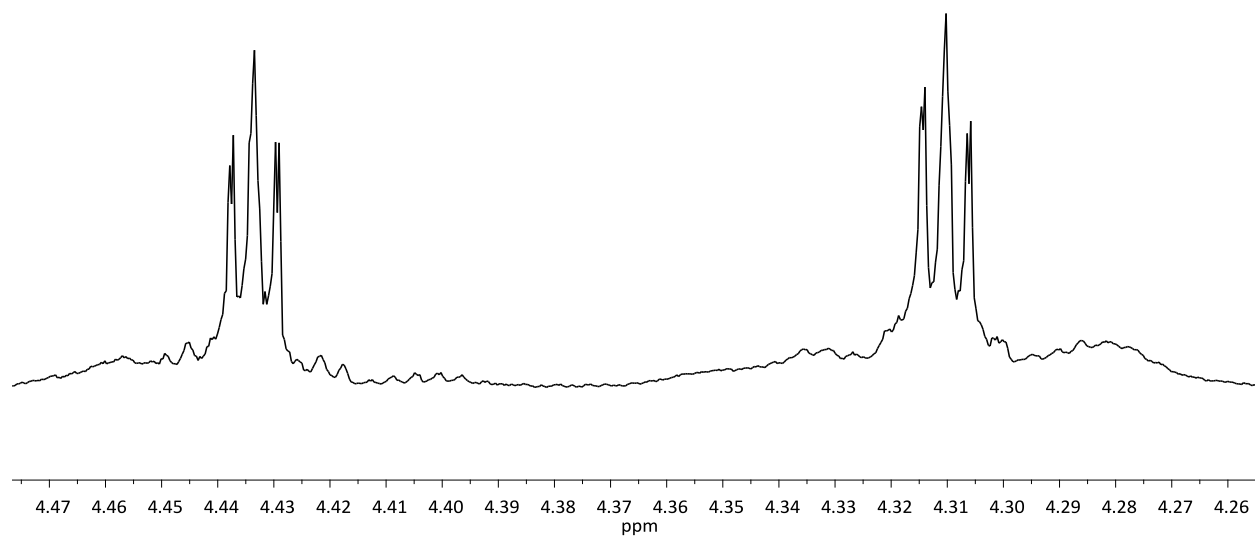


Figure A1.25: Cyclopentadiene region of ^1H NMR (C_6D_6) of **5a**.

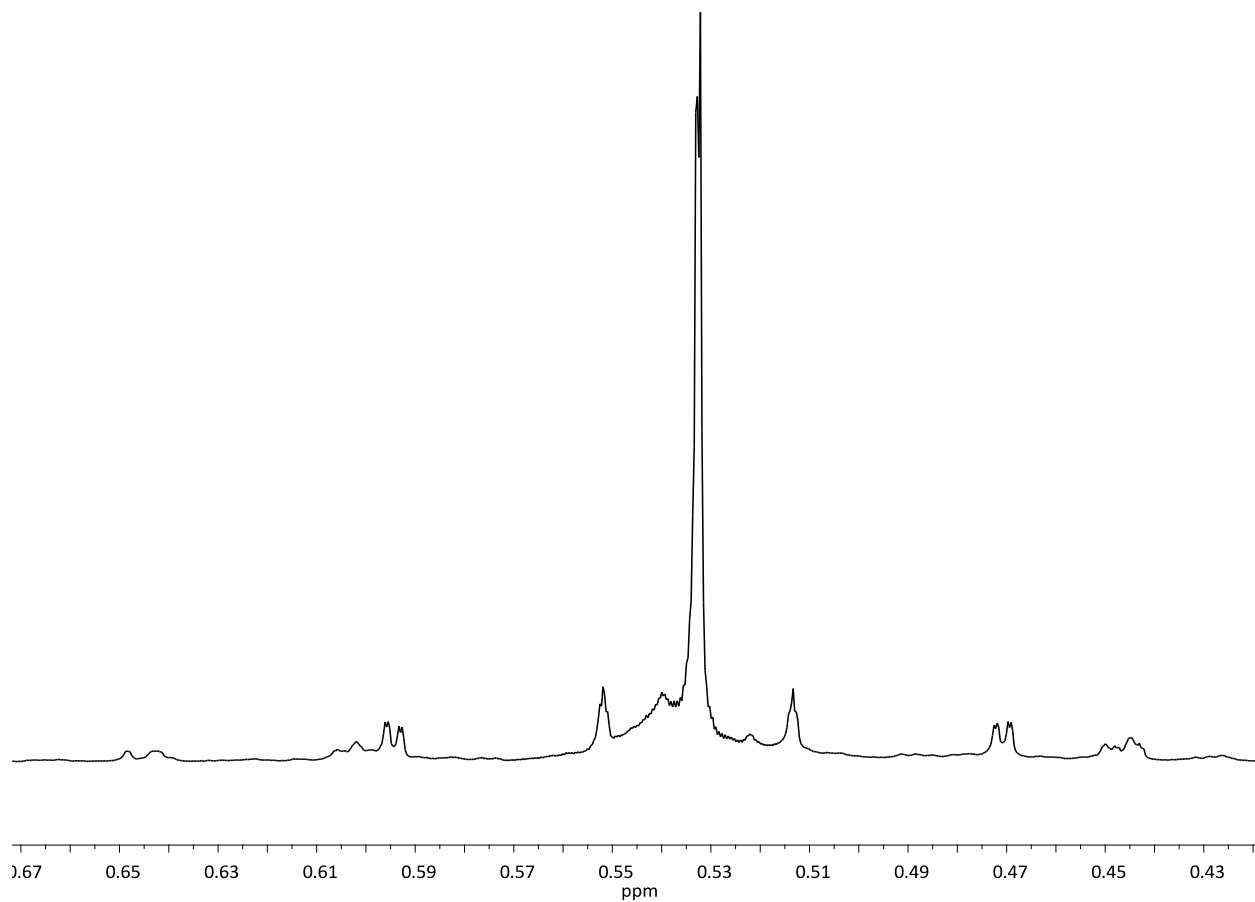


Figure A1.26: Methyl region of ^1H NMR (C_6D_6) of **5a**.

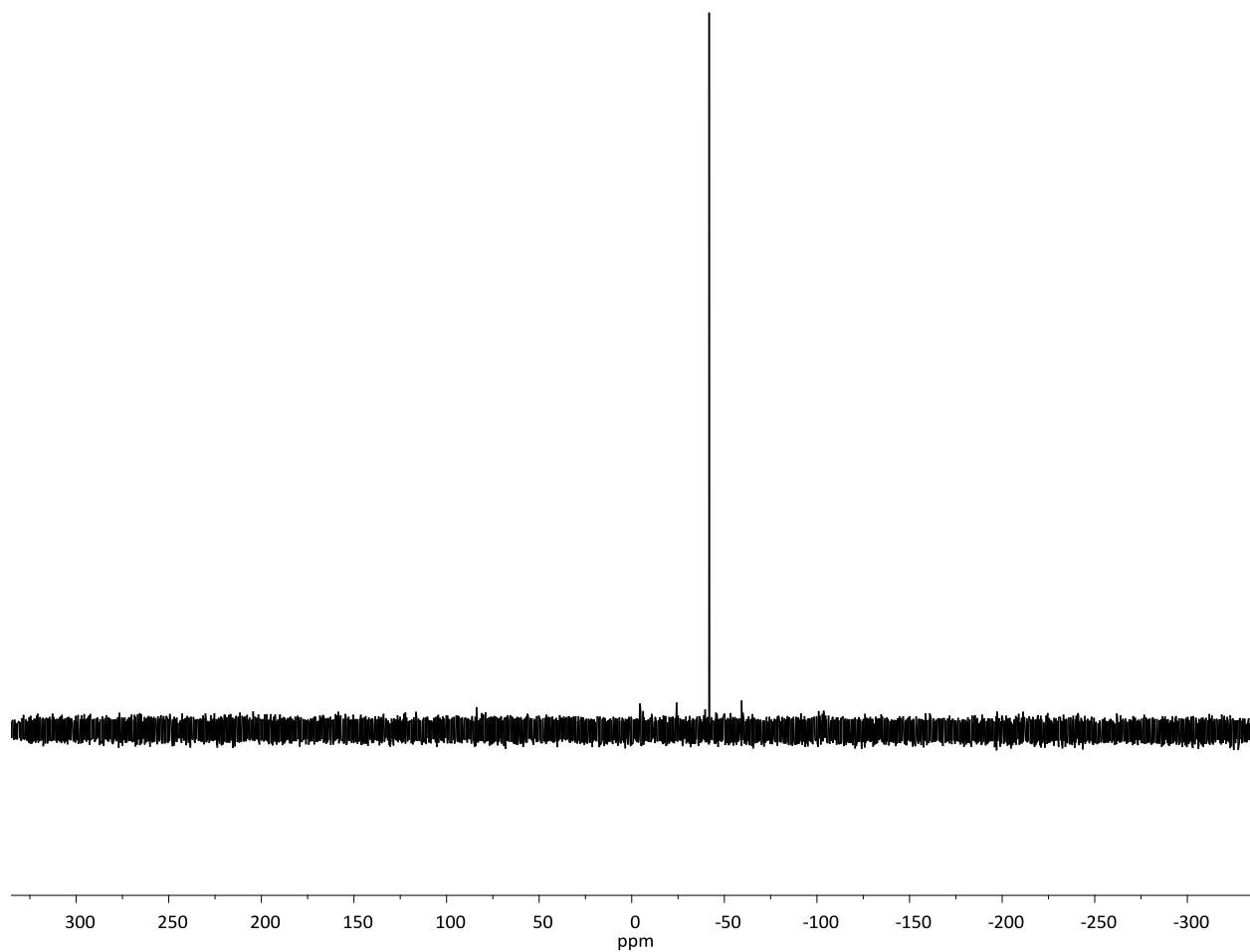


Figure A1.27: ^{119}Sn NMR (C_6D_6) of **5a**.

Appendix 1.8: 11

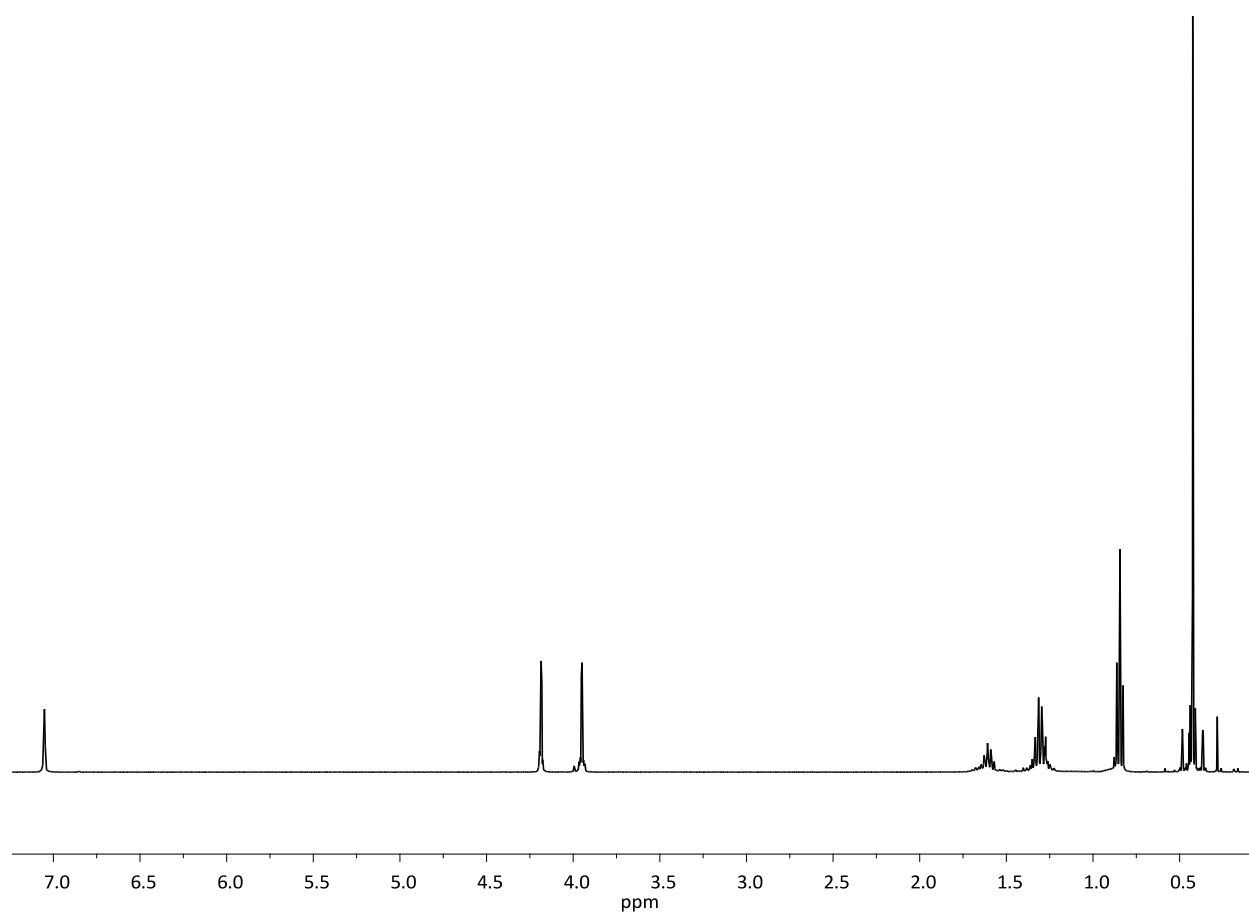


Figure A1.28: ^1H NMR (C_6D_6) of **11**.

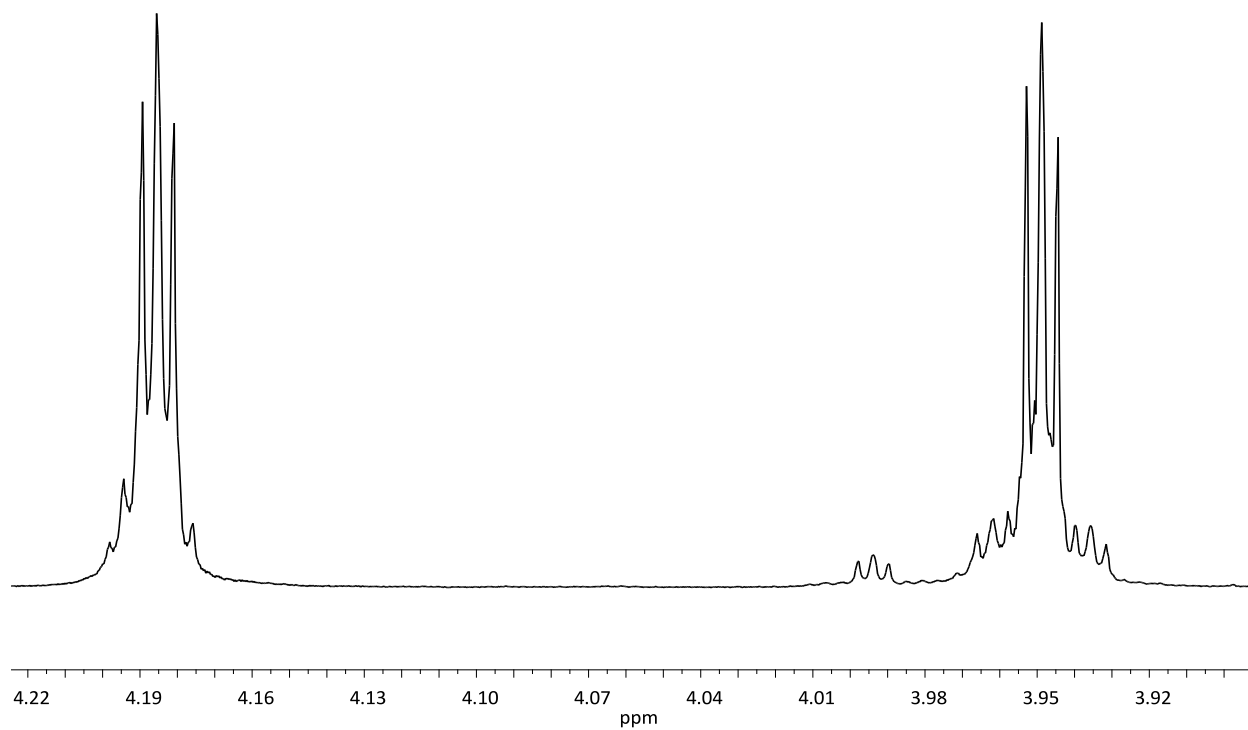


Figure A1.29: Cyclopentadiene region of ^1H NMR (C_6D_6) of **11**.

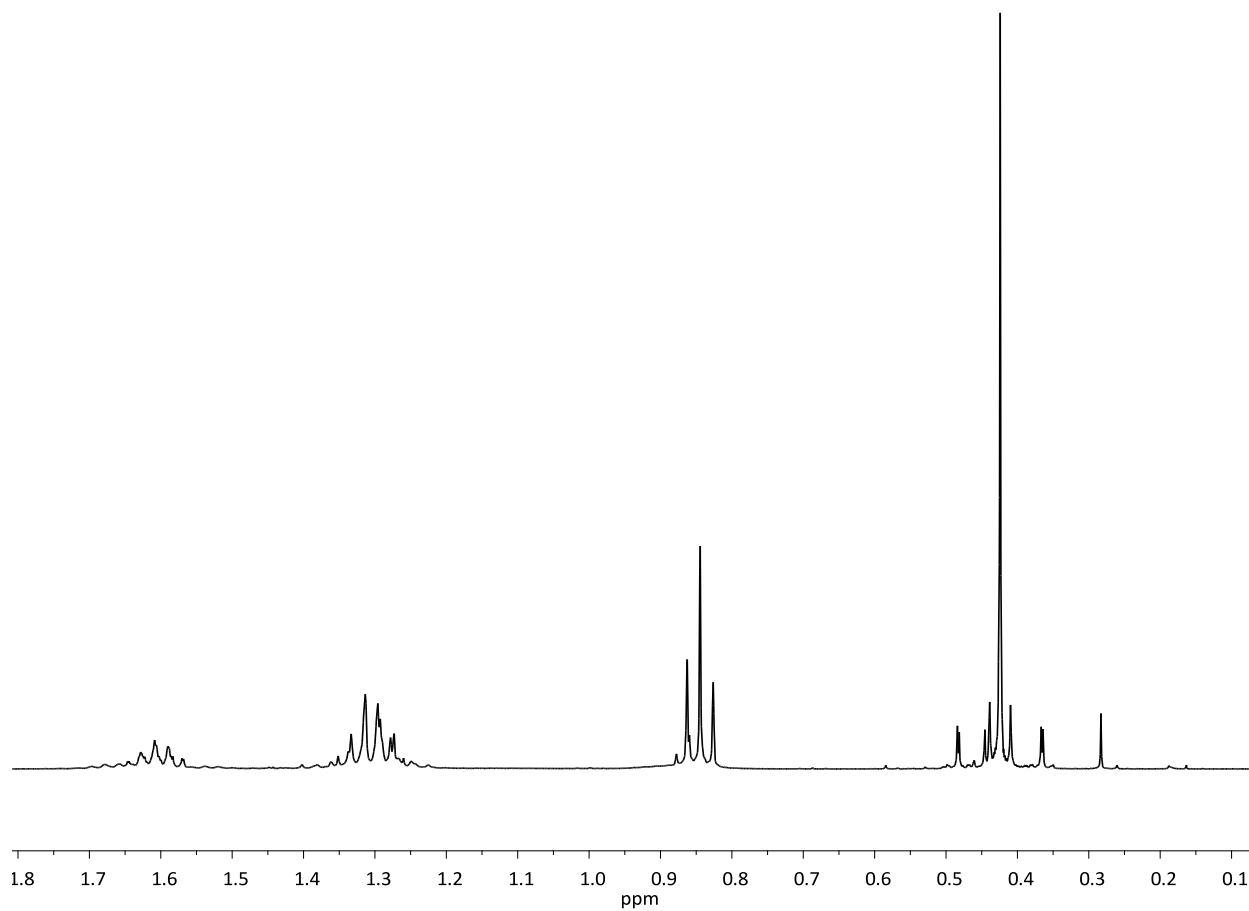


Figure A1.30: Methyl and *n*-butyl region of ^1H NMR (C_6D_6) of **11**.

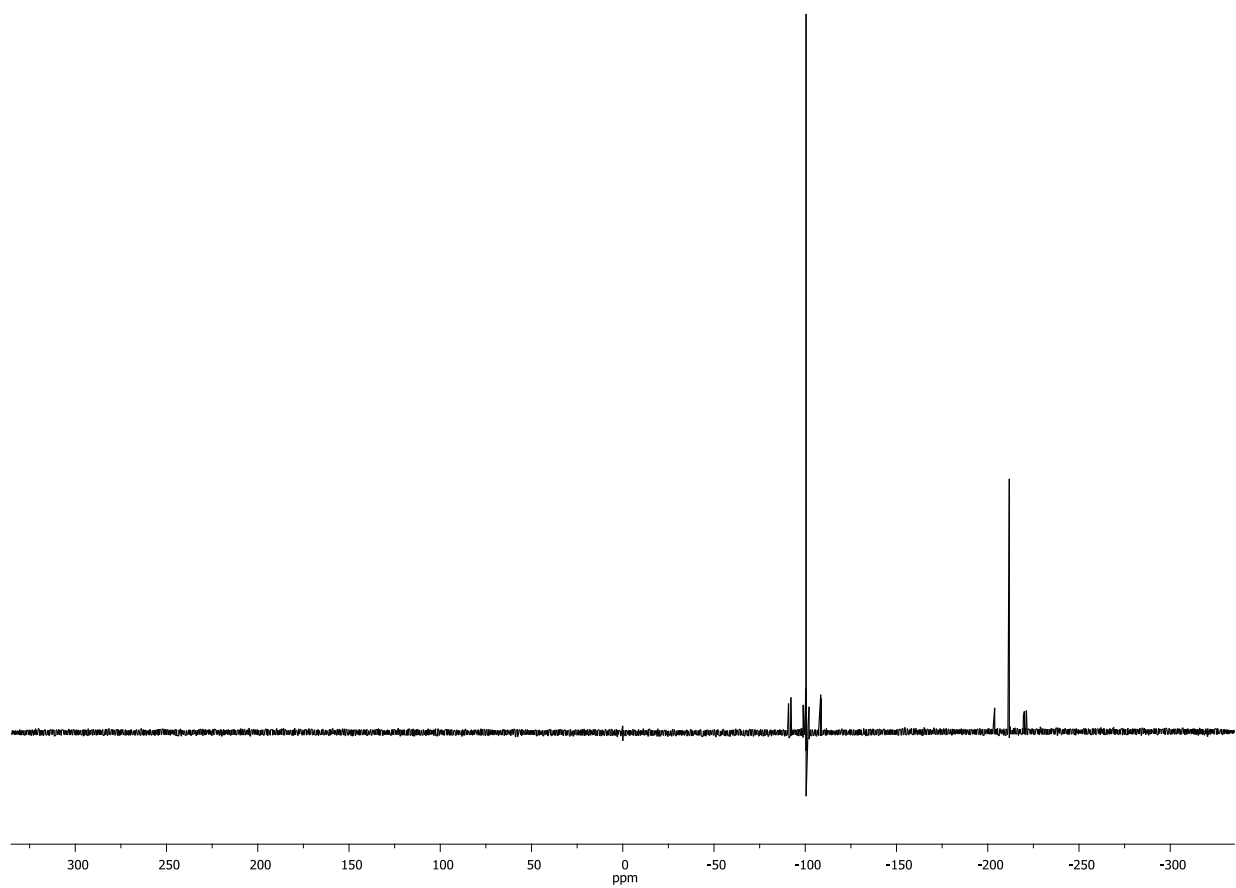


Figure A1.31: ^{119}Sn NMR of **11** (C_6D_6) of **11**.

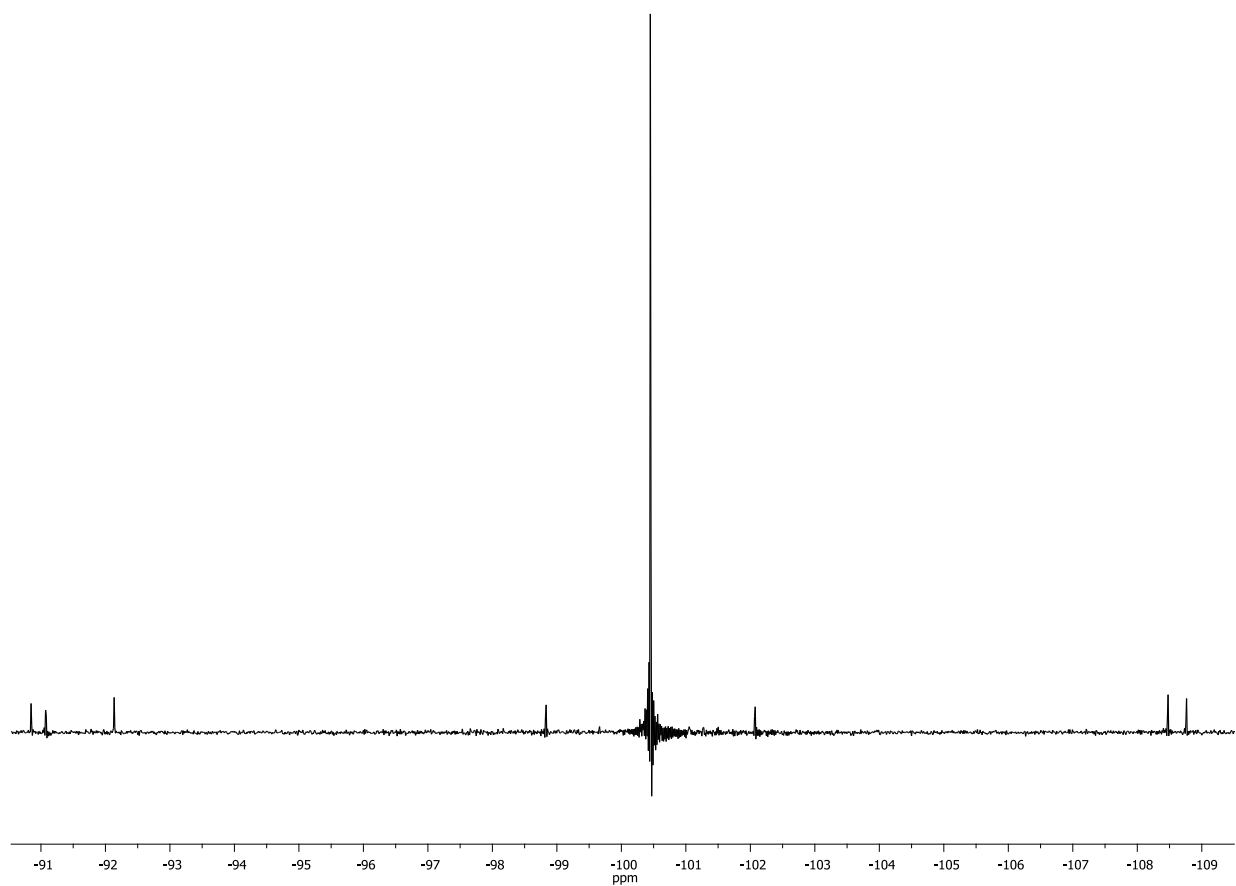


Figure A1.32: Dimethyl stannane region of ^{119}Sn NMR (C_6D_6) of **11**.

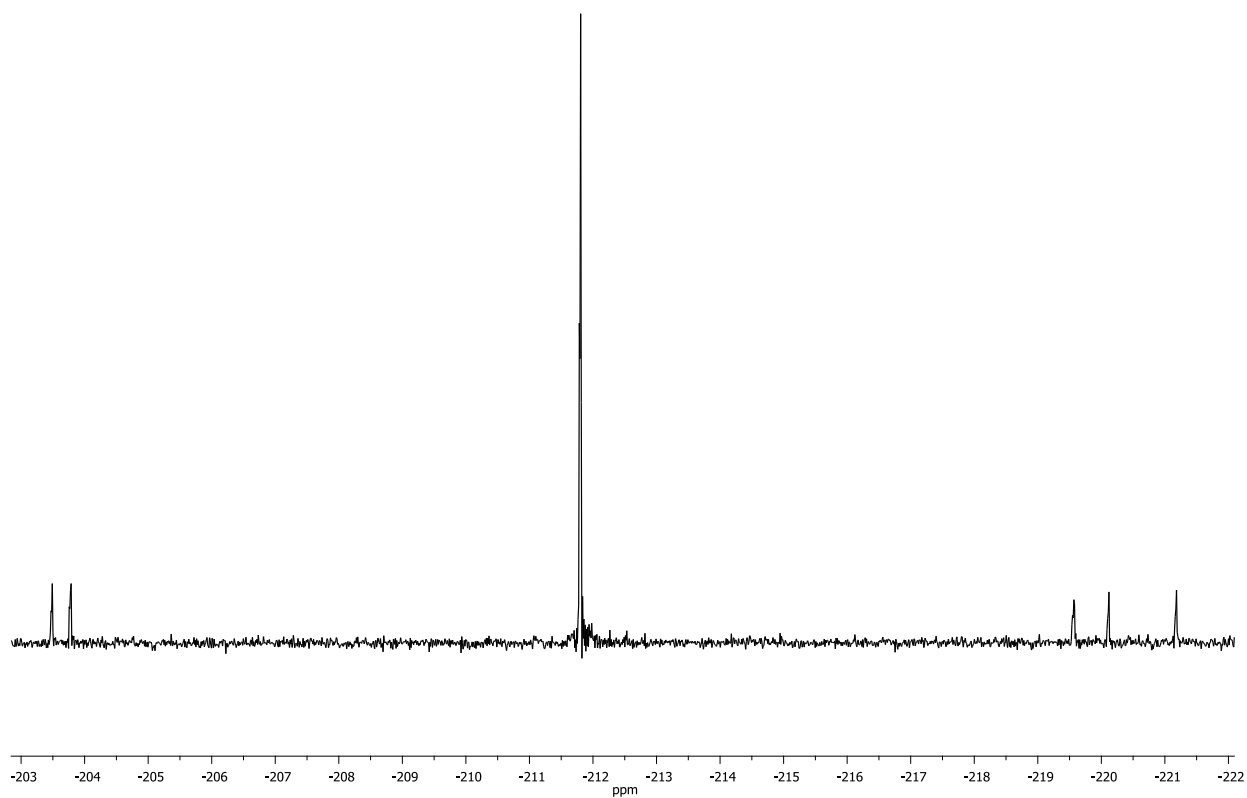


Figure A1.33: Di(*n*-butyl) stannane region of ^{119}Sn NMR (C_6D_6) of **11**.

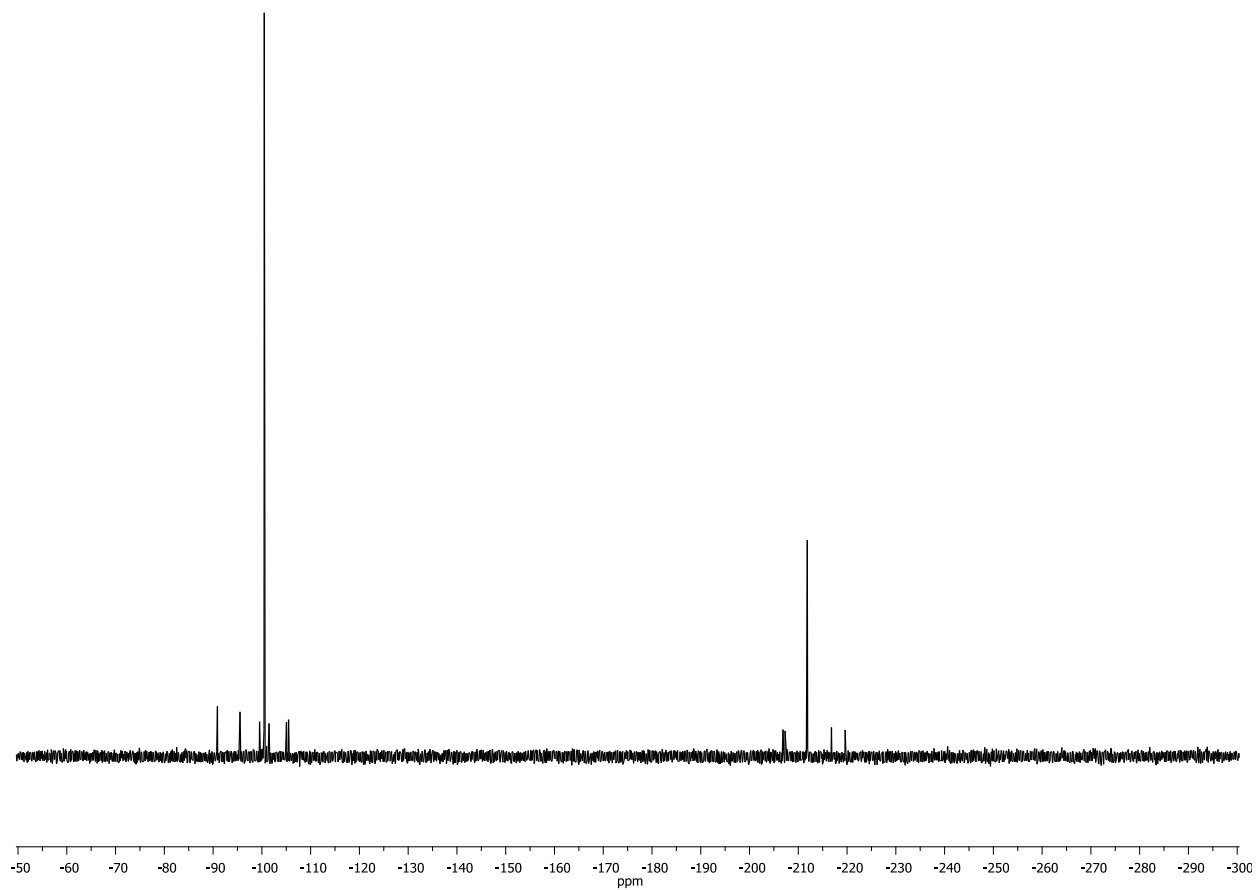


Figure A1.34: ^{117}Sn NMR (C_6D_6) of **11** run.

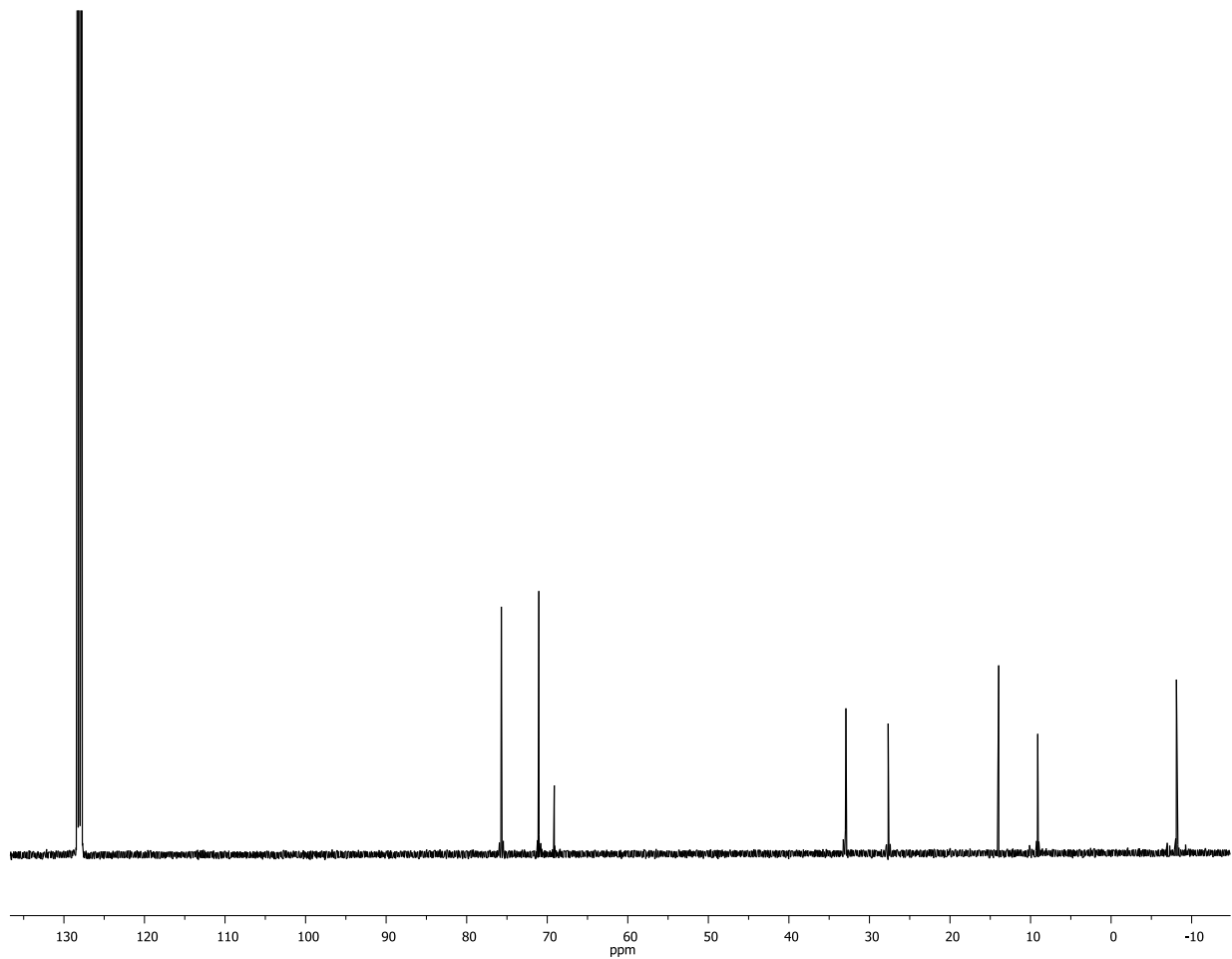


Figure A1.35: ^{13}C NMR (C_6D_6) of **11**.

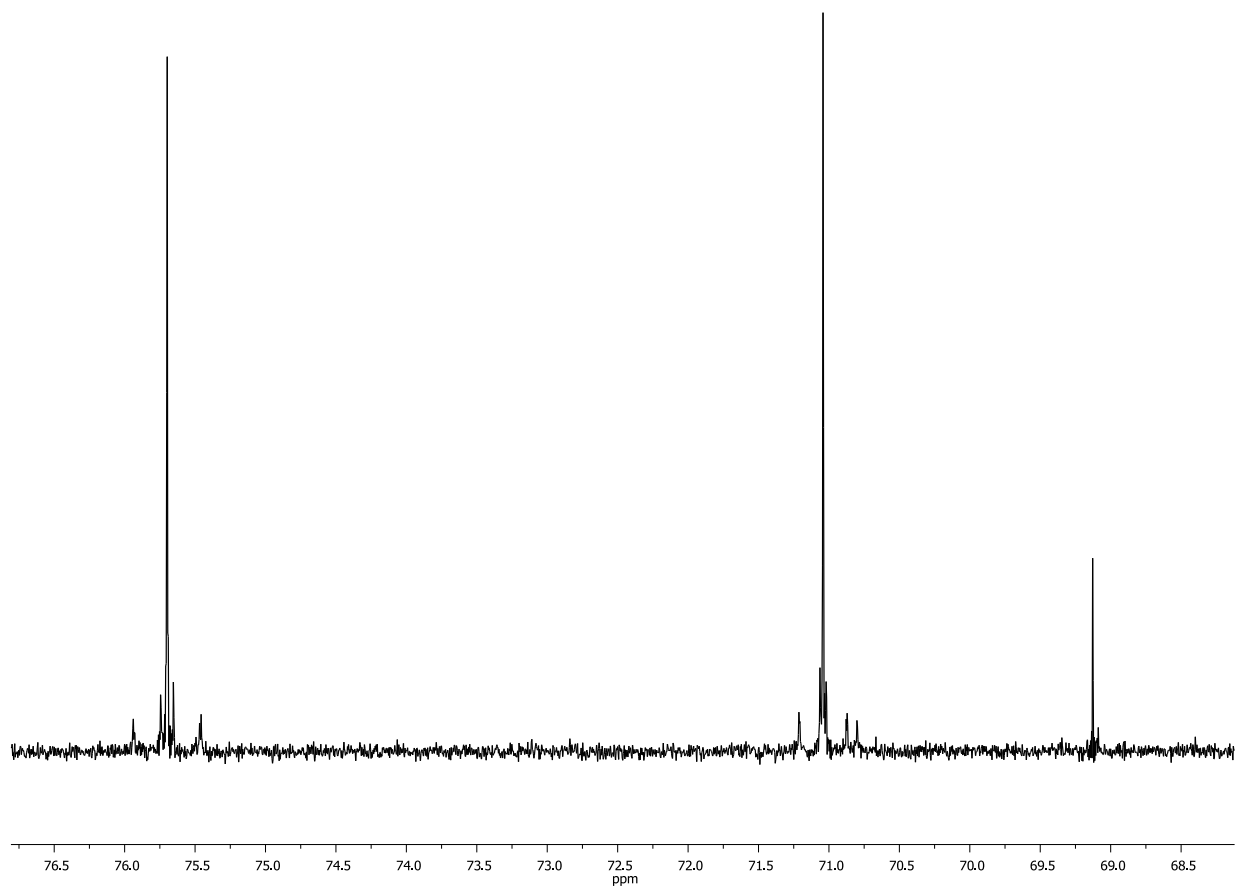


Figure A1.35: Cyclopentadiene region of ^{13}C NMR (C_6D_6) of **11**.

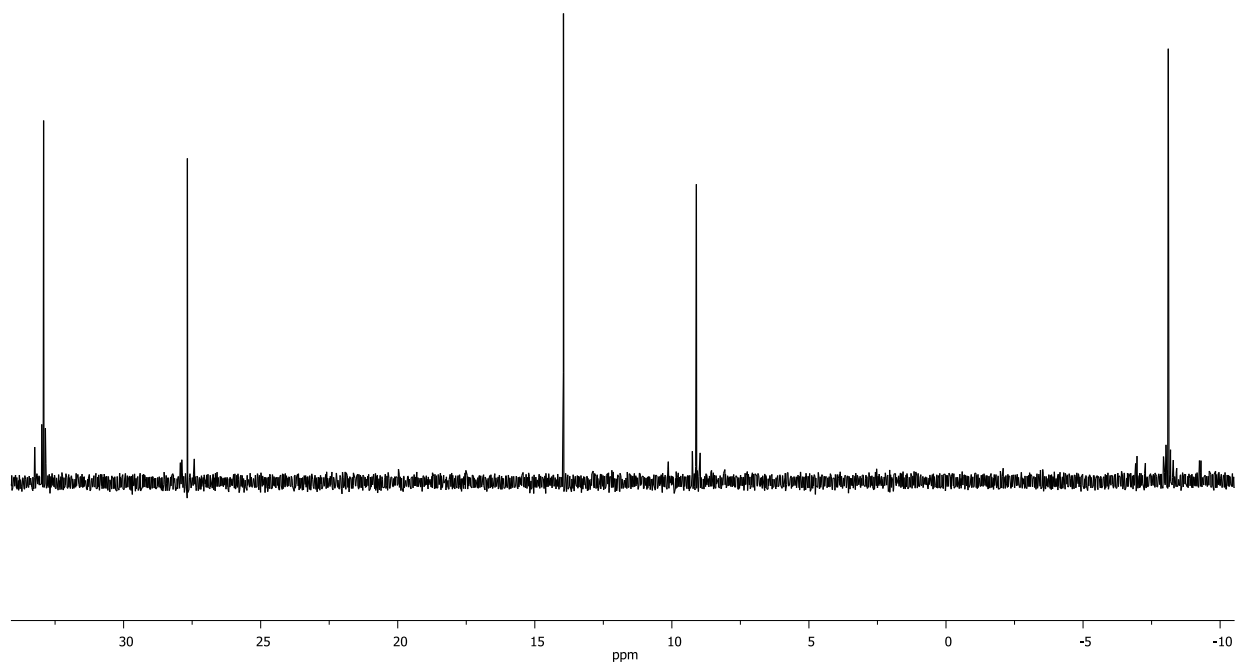


Figure A1.37: Methyl and *n*-butyl region of ^{13}C NMR (C_6D_6) of **11**.

Appendix 2: Mass spectrometry

Table A2.1: Relative abundance for DART-TOF of **11** at different temperatures (Figures A2.1-A2.3) and Skimmer Potentials (Figures A2.4-A2.6).

T/C	E/V	m/z	RA(%)	T/C	E/V	m/z	RA(%)
100	20	498.9	100	200	40	498.9	88.1
		698.9	N/A			698.9	95.6
		713.9	5.2			713.9	100
		1212.8	0.1			1212.8	11.1
		1428.9	N/A			1428.9	2.0
200	20	498.9	100	200	60	498.9	75.3
		698.9	36.7			698.9	1
		713.9	72.6			713.9	82.5
		1212.8	10.2			1212.8	3.1
		1428.9	1.0			1428.9	0.8
300	20	498.9	38.2	200	80	498.9	46.8
		698.9	1			698.9	100
		713.9	94.7			713.9	41.1
		1212.8	3.8			1212.8	0.5
		1428.9	3.1			1428.9	0.2
		1428.9	0.5				

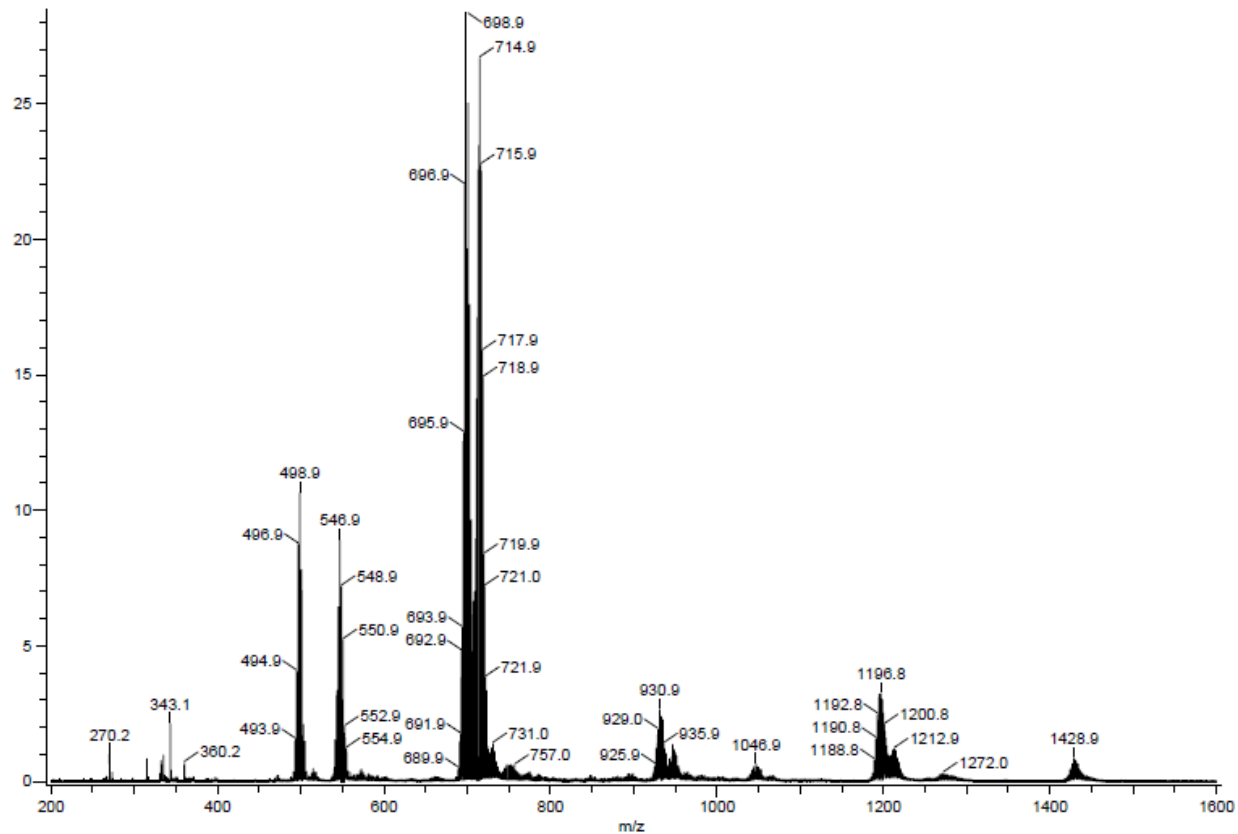


Figure S2.1: DART-TOF of 11 at 300°C, 20V

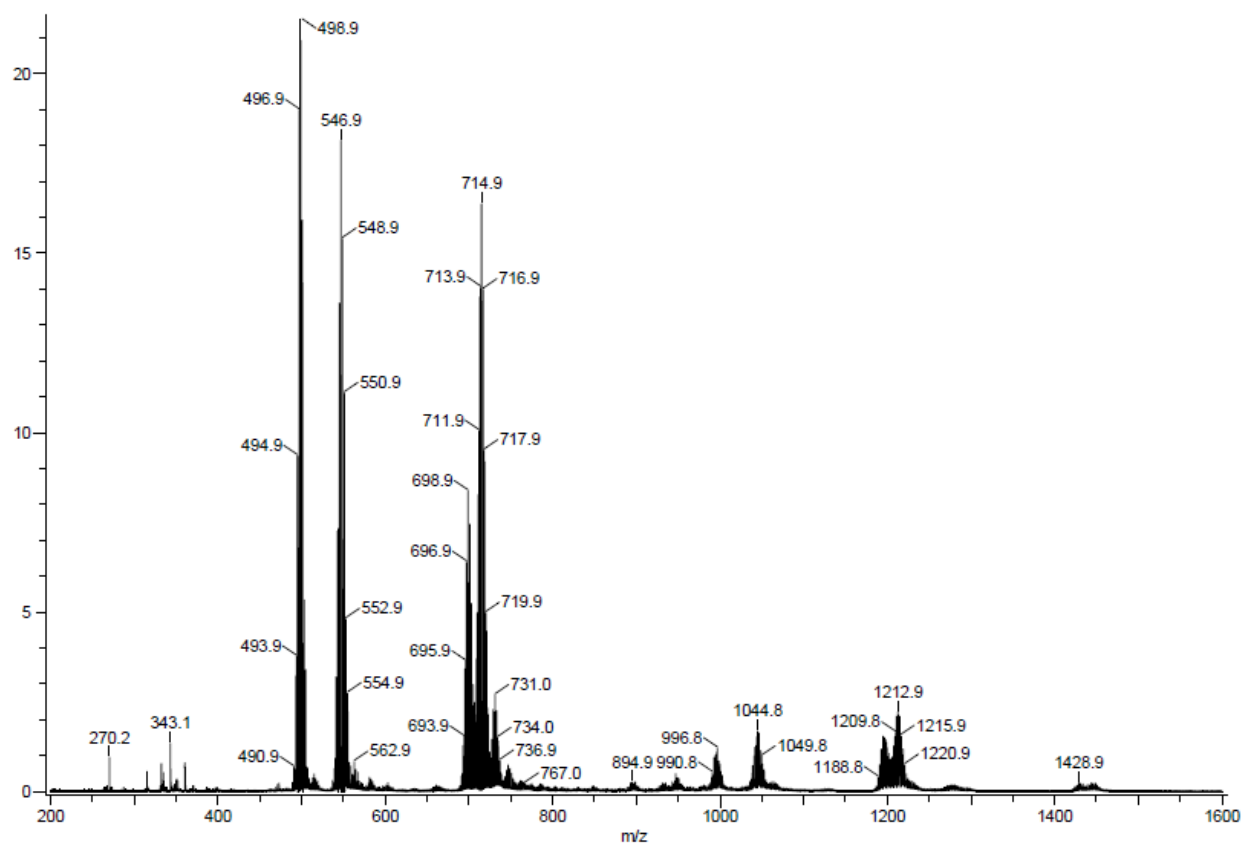


Figure A2.2: DART-MS-TOF of **11** at 200°C, 20V.

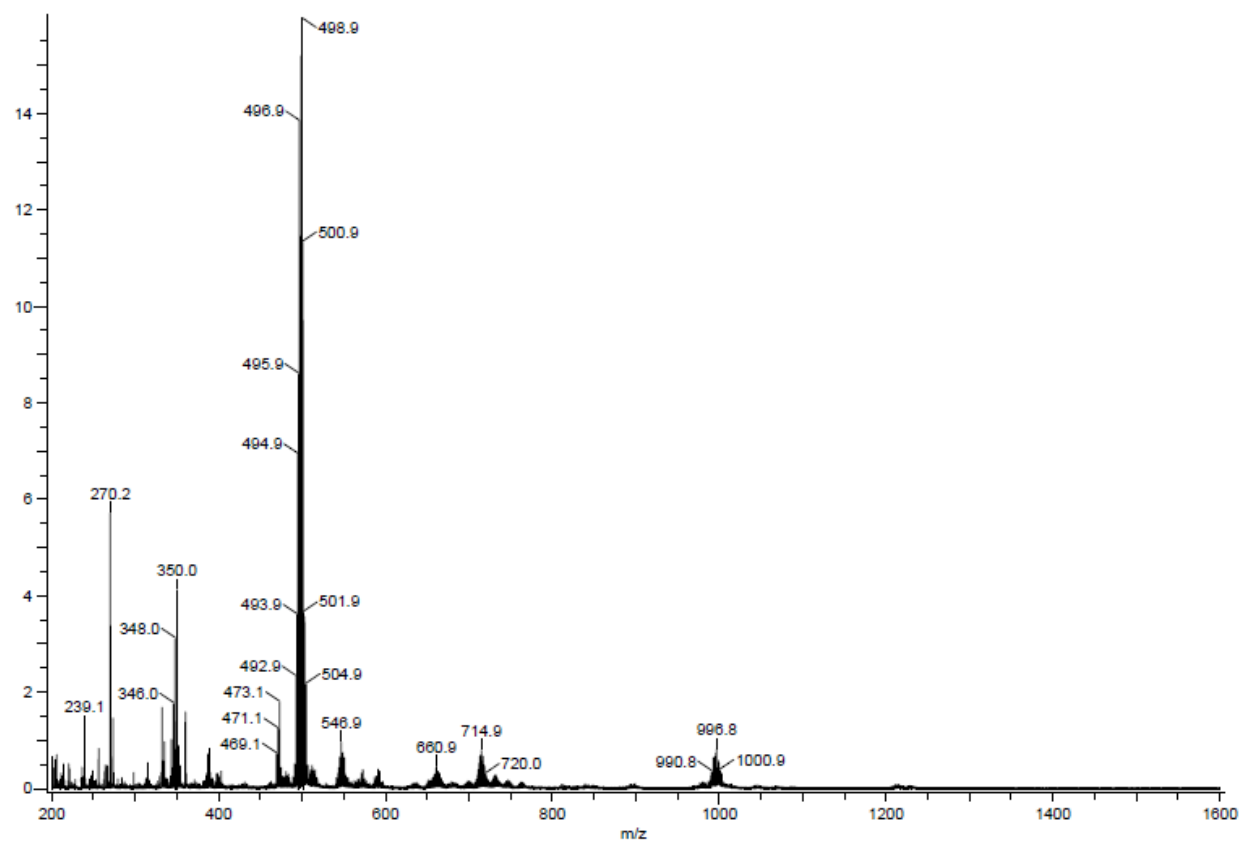


Figure A2.3: DART-MS-TOF of **11** at 100°C, 20V.

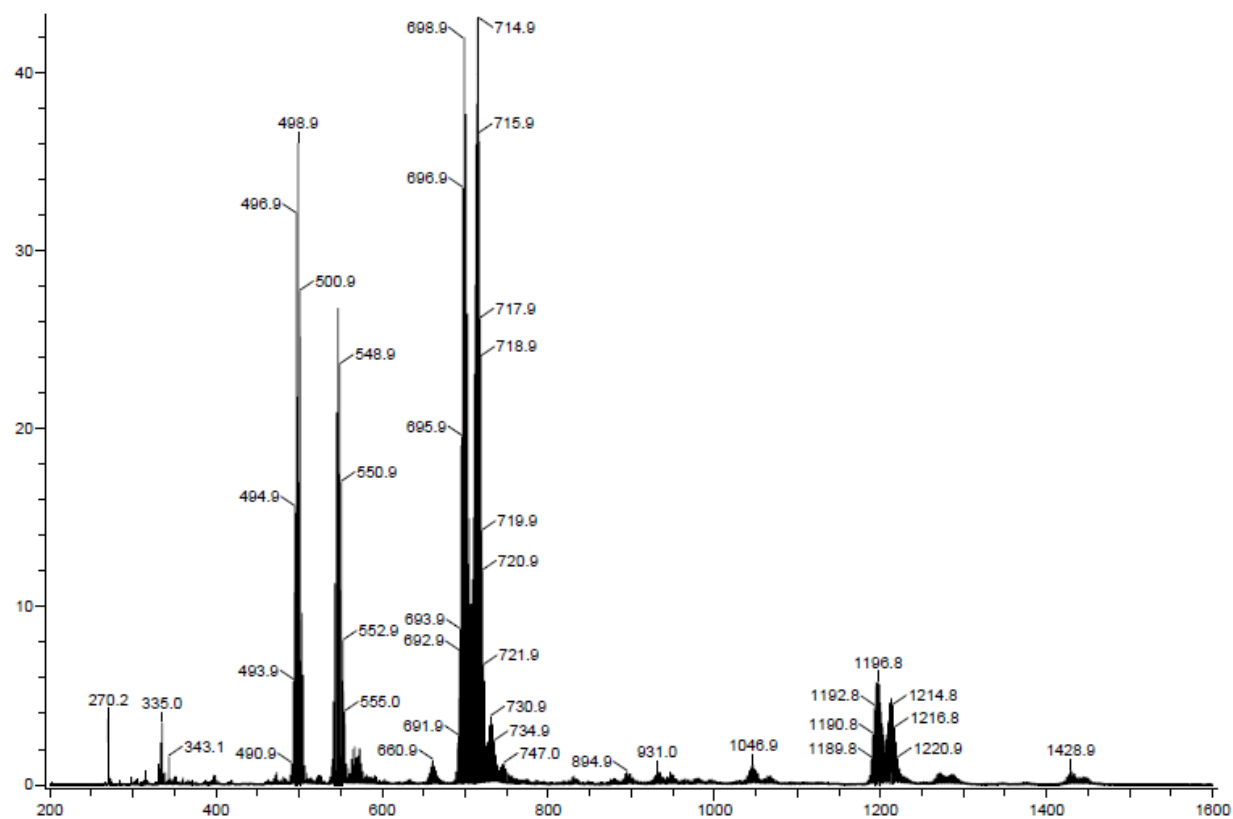


Figure A2.4: DART-MS-TOF of **11** at 200°C, 40V

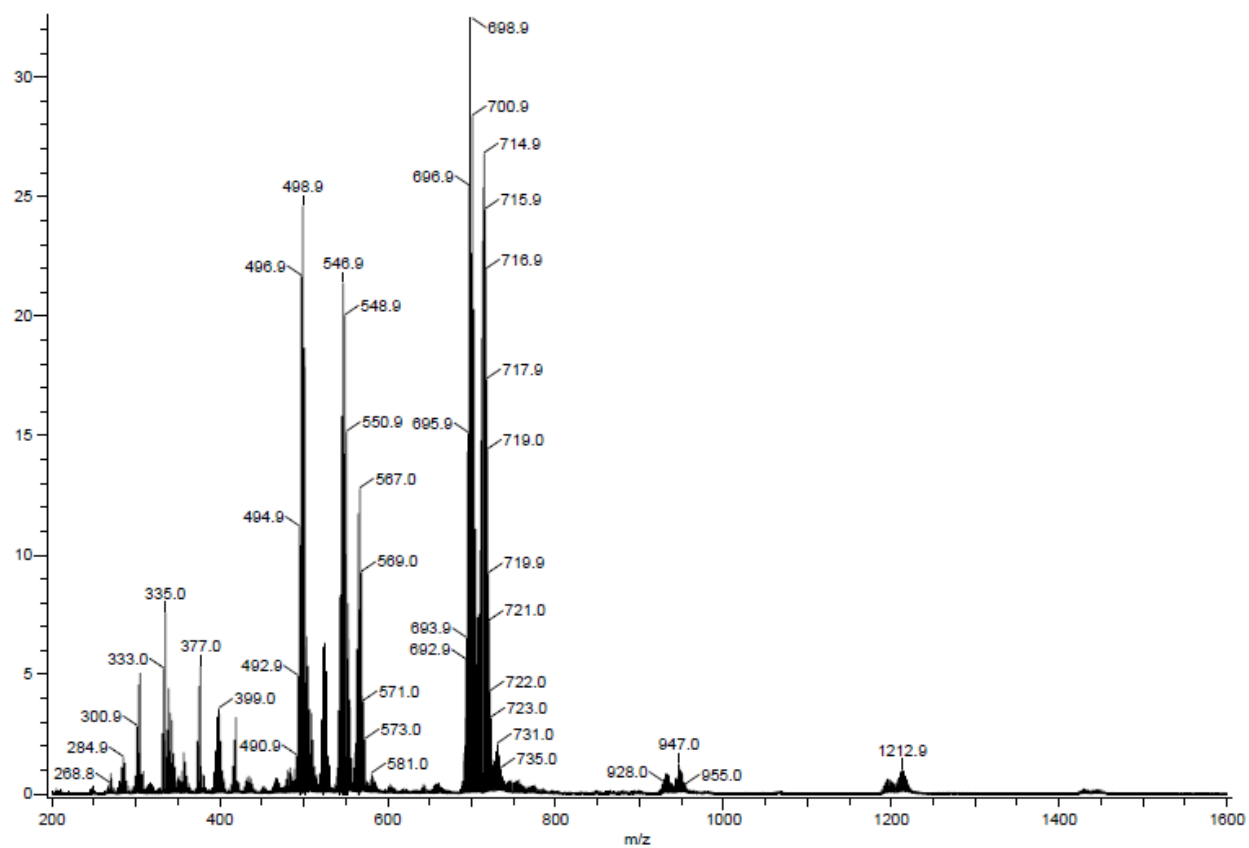


Figure A2.5: DART-MS-TOF of **11** at 200°C, 60V.

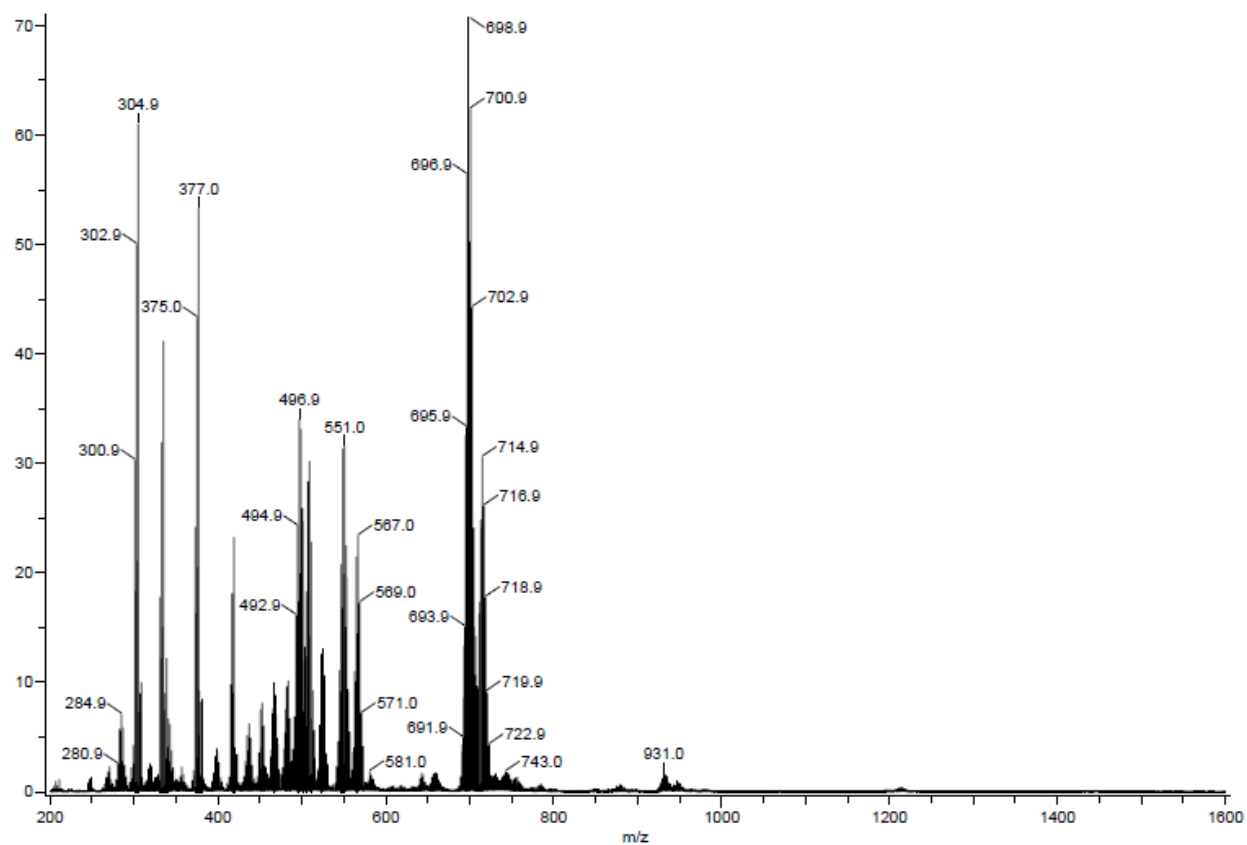


Figure A2.6: DART-MS-TOF of **11** at 200°C, 80V.

Appendix 3: Cyclic voltammetry

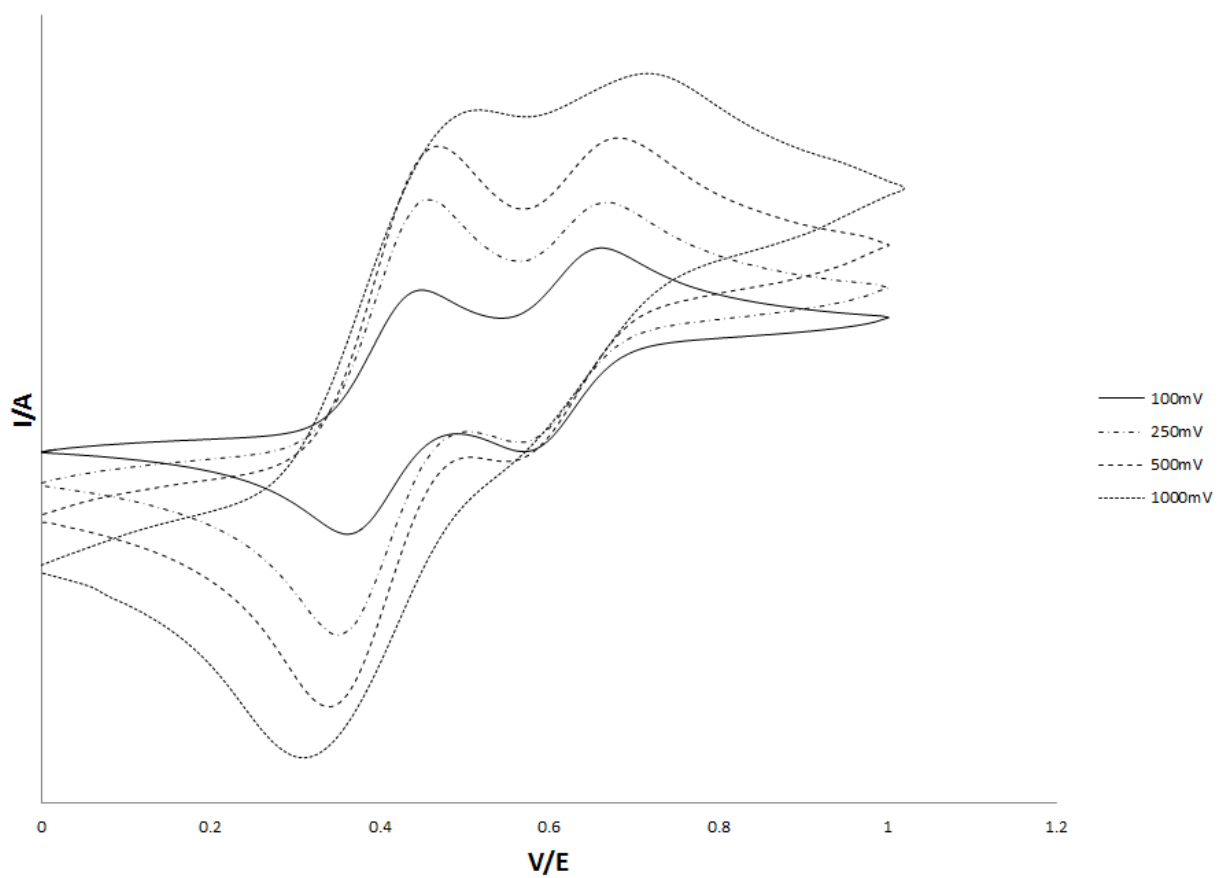


Figure A3.1: Cyclic Voltammetry of compound **11** at 100mV, 250mV, 500mV, and 1000mV scan speeds.

Appendix 4: Sn NMR simulator program for calculating isotopic intensities

Instructions: program must be run in python. Programed in python 2.7.

Copy and save this in a text file with the extension .py. in command line load to directory that the file is in and run command “python xxx.py” where xxx is the name of the file.

Values are input into lines 1319-1323

```
def coupling(a):
    b = -2.00208 / -2.09456
    e = a*b
    return e

def matrix(x,aa,bb):
    # builds matrix of possible combinations
    y = []
    # bb is the number of tins in the bridge aa is the number of
    bridges for straight chain a = 1
    if bb == 2:
        # matrix for 2 tins in the bridge
        if aa == 1:
            for a in x:
                for b in x:
                    y.append([[a,b]])
        if aa == 2:
            for a in x:
                for b in x:
                    for c in x:
                        for d in x:
                            y.append([[a,b],[c,d]])
        if aa == 3:
            for a in x:
                for b in x:
                    for c in x:
                        for d in x:
                            for e in x:
                                for f in x:
                                    y.append([[a,b],[c,d],[e,f]])
        if aa == 4:
            for a in x:
                for b in x:
                    for c in x:
```

```

        for d in x:
            for e in x:
                for f in x:
                    for g in x:
                        for h in x:
                            y.append([[a,b],[c,d],[e,f],[g,h]])
if bb == 3:
# matrix for 3 tins in the bridge
    if aa == 1:
        for a in x:
            for b in x:
                for c in x:
                    y.append([[a,b,c]])
    if aa == 2:
        for a in x:
            for b in x:
                for c in x:
                    for d in x:
                        for e in x:
                            for f in x:
                                y.append([[a,b,c],[d,e,f]])
    if aa == 3:
        for a in x:
            for b in x:
                for c in x:
                    for d in x:
                        for e in x:
                            for f in x:
                                for g in x:
                                    for h in x:
                                        for i in x:
                                            y.append([[a,b,c],[d,e,f],[g,h,i]])
    if aa == 4:
        for a in x:
            for b in x:
                for c in x:
                    for d in x:
                        for e in x:
                            for f in x:
                                for g in x:
                                    for h in x:
                                        for i in x:
                                            for j in x:
                                                for k in x:
                                                    for l in x:

y.append([[a,b,c],[d,e,f],[g,h,i],[j,k,l]])

```

```

return y

def probb(mat,aa,bb):
    # finds the product of the matrix
    mat2 = []
    jj = []
    if bb == 2:
        if aa == 1:
            for ii in mat:
                jj.append(ii)
                a = ii[0][0]
                b = ii[0][1]
                xx = a*b
                jj.append(xx)
                mat2.append(jj)
                jj = []
        if aa == 2:
            for ii in mat:
                jj.append(ii)
                a = ii[0][0]
                b = ii[0][1]
                c = ii[1][0]
                d = ii[1][1]
                xx = a*b*c*d
                jj.append(xx)
                mat2.append(jj)
                jj = []
        if aa == 3:
            for ii in mat:
                jj.append(ii)
                a = ii[0][0]
                b = ii[0][1]
                c = ii[1][0]
                d = ii[1][1]
                e = ii[2][0]
                f = ii[2][1]
                xx = a*b*c*d*e*f
                jj.append(xx)
                mat2.append(jj)
                jj = []
        if aa == 4:
            for ii in mat:
                jj.append(ii)
                a = ii[0][0]
                b = ii[0][1]
                c = ii[1][0]
                d = ii[1][1]

```

```

    e = ii[2][0]
    f = ii[2][1]
    g = ii[3][0]
    h = ii[3][1]
    xx = a*b*c*d*e*f*g*h
    jj.append(xx)
    mat2.append(jj)
    jj = []
if bb == 3:
    if aa == 1:
        for ii in mat:
            jj.append(ii)
            a = ii[0][0]
            b = ii[0][1]
            c = ii[0][2]
            xx = a*b*c
            jj.append(xx)
            mat2.append(jj)
            jj = []
    if aa == 2:
        for ii in mat:
            jj.append(ii)
            a = ii[0][0]
            b = ii[0][1]
            c = ii[0][2]
            d = ii[1][0]
            e = ii[1][1]
            f = ii[1][2]
            xx = a*b*c*d*e*f
            jj.append(xx)
            mat2.append(jj)
            jj = []
    if aa == 3:
        for ii in mat:
            jj.append(ii)
            a = ii[0][0]
            b = ii[0][1]
            c = ii[0][2]
            d = ii[1][0]
            e = ii[1][1]
            f = ii[1][2]
            g = ii[2][0]
            h = ii[2][1]
            i = ii[2][2]
            xx = a*b*c*d*e*f*g*h*i
            jj.append(xx)
            mat2.append(jj)

```

```

        jj = []
    if aa == 4:
        for ii in mat:
            jj.append(ii)
            a = ii[0][0]
            b = ii[0][1]
            c = ii[0][2]
            d = ii[1][0]
            e = ii[1][1]
            f = ii[1][2]
            g = ii[2][0]
            h = ii[2][1]
            i = ii[2][2]
            j = ii[3][0]
            k = ii[3][1]
            l = ii[3][2]
            xx = a*b*c*d*e*f*g*h*i*j*k*l
            jj.append(xx)
        mat2.append(jj)
        jj = []
    print mat2
    return mat2
def probadd(mat):
    a = 0
    for ii in mat:
        a = a + ii[-1]
    print a
    return a

def intigrat(mat,aa,bb,xx):
    # sums presence of active nucleus
    if bb == 2:
        if aa == 1:
            a = 0
            jj = []
            kk = []
            ll = []
            mat3 = []
            for ii in mat:
                jj.append(ii[0])
                if ii[0][0][0] == xx:
                    a = a + 1
                if ii[0][0][1] == xx:
                    a = a + 1
                jj.append(ii[1])
                kk.append(a)
                ll.append(kk)

```

```

        jj.append(l1)
        mat3.append(jj)
        jj = []
        kk = []
        ll = []
        a = 0
if aa == 2:
    a = 0
    b = 0
    jj = []
    kk = []
    ll = []
    mm = []
    mat3 = []
    for ii in mat:
        jj.append(ii[0])
        if ii[0][0][0] == xx:
            a = a + 1
        if ii[0][0][1] == xx:
            a = a + 1
        if ii[0][1][0] == xx:
            b = b + 1
        if ii[0][1][1] == xx:
            b = b + 1
        jj.append(ii[1])
        kk.append(a)
        ll.append(b)
        mm.append(kk)
        mm.append(ll)
        jj.append(mm)
        mat3.append(jj)
        jj = []
        kk = []
        ll = []
        mm = []
        a = 0
        b = 0
if aa == 3:
    a = 0
    b = 0
    c = 0
    jj = []
    kk = []
    ll = []
    mm = []
    nn = []
    mat3 = []

```

```

for ii in mat:
    jj.append(ii[0])
    if ii[0][0][0] == xx:
        a = a + 1
    if ii[0][0][1] == xx:
        a = a + 1
    if ii[0][1][0] == xx:
        b = b + 1
    if ii[0][1][1] == xx:
        b = b + 1
    if ii[0][2][0] == xx:
        c = c + 1
    if ii[0][2][1] == xx:
        c = c + 1
    jj.append(ii[1])
    kk.append(a)
    ll.append(b)
    mm.append(c)
    nn.append(kk)
    nn.append(ll)
    nn.append(mm)
    jj.append(nn)
    mat3.append(jj)
    jj = []
    kk = []
    ll = []
    mm = []
    nn = []
    a = 0
    b = 0
    c = 0
if aa == 4:
    a = 0
    b = 0
    c = 0
    d = 0
    jj = []
    kk = []
    ll = []
    mm = []
    nn = []
    oo = []
    mat3 = []
    for ii in mat:
        jj.append(ii[0])
        if ii[0][0][0] == xx:
            a = a + 1

```

```

    if ii[0][0][1] == xx:
        a = a + 1
    if ii[0][1][0] == xx:
        b = b + 1
    if ii[0][1][1] == xx:
        b = b + 1
    if ii[0][2][0] == xx:
        c = c + 1
    if ii[0][2][1] == xx:
        c = c + 1
    if ii[0][3][0] == xx:
        d = d + 1
    if ii[0][3][1] == xx:
        d = d + 1
    jj.append(ii[1])
    kk.append(a)
    ll.append(b)
    mm.append(c)
    nn.append(d)
    oo.append(kk)
    oo.append(ll)
    oo.append(mm)
    oo.append(nn)
    jj.append(oo)
    mat3.append(jj)
    jj = []
    kk = []
    ll = []
    mm = []
    nn = []
    oo = []
    a = 0
    b = 0
    c = 0
    d = 0
if bb == 3:
    if aa == 1:
        a = 0
        b = 0
        jj = []
        kk = []
        ll = []
        mat3 = []
        for ii in mat:
            jj.append(ii[0])
            if ii[0][0][0] == xx:
                a = a + 1

```

```

    if ii[0][0][2] == xx:
        a = a + 1
    if ii[0][0][1] == xx:
        b = b + 1
    jj.append(ii[1])
    kk.append(a)
    kk.append(b)
    ll.append(kk)
    jj.append(ll)
    mat3.append(jj)
    jj = []
    kk = []
    ll = []
    a = 0
    b = 0
if aa == 2:
    a = 0
    b = 0
    c = 0
    d = 0
    jj = []
    kk = []
    ll = []
    mm = []
    mat3 = []
    for ii in mat:
        jj.append(ii[0])
        if ii[0][0][0] == xx:
            a = a + 1
        if ii[0][0][2] == xx:
            a = a + 1
        if ii[0][1][0] == xx:
            b = b + 1
        if ii[0][1][2] == xx:
            b = b + 1
        if ii[0][0][1] == xx:
            c = c + 1
        if ii[0][1][1] == xx:
            d = d + 1
        jj.append(ii[1])
        kk.append(a)
        ll.append(b)
        kk.append(c)
        ll.append(d)
        mm.append(kk)
        mm.append(ll)
        jj.append(mm)

```

```

mat3.append(jj)
jj = []
kk = []
ll = []
mm = []
a = 0
b = 0
c = 0
d = 0
if aa == 3:
a = 0
b = 0
c = 0
d = 0
e = 0
f = 0
jj = []
kk = []
ll = []
mm = []
nn = []
mat3 = []
for ii in mat:
    jj.append(ii[0])
    if ii[0][0][0] == xx:
        a = a + 1
    if ii[0][0][2] == xx:
        a = a + 1
    if ii[0][1][0] == xx:
        b = b + 1
    if ii[0][1][2] == xx:
        b = b + 1
    if ii[0][2][0] == xx:
        c = c + 1
    if ii[0][2][2] == xx:
        c = c + 1
    if ii[0][0][1] == xx:
        d = d + 1
    if ii[0][1][1] == xx:
        e = e + 1
    if ii[0][2][1] == xx:
        f = f + 1
    jj.append(ii[1])
    kk.append(a)
    ll.append(b)
    mm.append(c)
    kk.append(d)

```

```

    ll.append(e)
    mm.append(f)
    nn.append(kk)
    nn.append(ll)
    nn.append(mm)
    jj.append(nn)
    mat3.append(jj)
    jj = []
    kk = []
    ll = []
    mm = []
    nn = []
    a = 0
    b = 0
    c = 0
    d = 0
    e = 0
    f = 0
if aa == 4:
    a = 0
    b = 0
    c = 0
    d = 0
    e = 0
    f = 0
    g = 0
    h = 0
    jj = []
    kk = []
    ll = []
    mm = []
    nn = []
    oo = []
    mat3 = []
    for ii in mat:
        jj.append(ii[0])
        if ii[0][0][0] == xx:
            a = a + 1
        if ii[0][0][2] == xx:
            a = a + 1
        if ii[0][1][0] == xx:
            b = b + 1
        if ii[0][1][2] == xx:
            b = b + 1
        if ii[0][2][0] == xx:
            c = c + 1
        if ii[0][2][2] == xx:

```

```

    c = c + 1
    if ii[0][3][0] == xx:
        d = d + 1
    if ii[0][3][2] == xx:
        d = d + 1
    if ii[0][0][1] == xx:
        e = e + 1
    if ii[0][1][1] == xx:
        f = f + 1
    if ii[0][2][1] == xx:
        g = g + 1
    if ii[0][3][1] == xx:
        h = h + 1
    jj.append(ii[1])
    kk.append(a)
    ll.append(b)
    mm.append(c)
    nn.append(d)
    kk.append(e)
    ll.append(f)
    mm.append(g)
    nn.append(h)
    oo.append(kk)
    oo.append(ll)
    oo.append(mm)
    oo.append(nn)
    jj.append(oo)
    mat3.append(jj)
    jj = []
    kk = []
    ll = []
    mm = []
    nn = []
    oo = []
    a = 0
    b = 0
    c = 0
    d = 0
    e = 0
    f = 0
    g = 0
    h = 0
return mat3

```

```

def spectra(mat,b,xx,yy,zz):
    k = []
    l = []

```

```

m = []
n = []

if b == 2:
    sig = ''
    kk = []
    ll = []
    mm = []
    mat4 = []
    for ii in mat:
        mm.append(ii[1])
        mm.append(ii[2])
        for jj in ii[0]:
            if jj[0] == xx and jj[1] == xx:
                sig = sig + 's'
            if jj[0] == xx and jj[1] == zz:
                sig = sig + 's'
            if jj[0] == zz and jj[1] == xx:
                sig = sig + 's'
            if jj[0] == xx and jj[1] == yy:
                sig = sig + 'd(a)'
            if jj[0] == yy and jj[1] == xx:
                sig = sig + 'd(a)'
            kk.append(sig)
            ll.append(kk)
            sig = ''
            up = ''
            kk = []
        mm.append(ll)
        mat4.append(mm)
        ll = []
        mm = []
if b == 3:
    down = ''
    up = ''
    kk = []
    ll = []
    mm = []
    mat4 = []
    for ii in mat:
        mm.append(ii[1])
        mm.append(ii[2])
        for jj in ii[0]:
            if jj[0] == xx and jj[1] != xx and jj[1] != yy and jj[2]
!= xx and jj[2] != yy:
                down = down + 's'

```

```

        if jj[2] == xx and jj[0] != xx and jj[0] != xx and jj[1]
!= xx and jj[1] != yy:
            down = down + 's'
            if jj[1] == xx and jj[0] != xx and jj[0] != yy and jj[2]
!= xx and jj[2] != yy:
                up = up + 's'
                if jj[0] == xx and jj[2] == xx and jj[1] != xx and jj[1]
!= yy:
                    down = down + 's'
                    if jj[0] == xx and jj[1] == xx and jj[2] != xx and jj[2]
!= yy:
                        down = down + 'd(a)'
                        up = up + 'd(a)'
                        if jj[2] == xx and jj[1] == xx and jj[0] != xx and jj[0]
!= yy:
                            down = down + 'd(a)'
                            up = up + 'd(a)'
                            if jj[0] == xx and jj[1] == xx and jj[2] == xx:
                                down = down + 'd(a)'
                                up = up + 't(a)'
                                if jj[0] == xx and jj[1] == yy and jj[2] != xx and jj[2]
!= yy:
                                    down = down + 'd(c)'
                                    if jj[2] == xx and jj[1] == yy and jj[0] != xx and jj[0]
!= yy:
                                        down = down + 'd(c)'
                                        if jj[0] == xx and jj[2] == yy and jj[1] != xx and jj[1]
!= yy:
                                            down = down + 'd(e)'
                                            if jj[2] == xx and jj[0] == yy and jj[1] != xx and jj[1]
!= yy:
                                                down = down + 'd(e)'
                                                if jj[0] == xx and jj[1] == yy and jj[2] == yy:
                                                    down = down + 'd(c)d(e)'
                                                if jj[2] == xx and jj[1] == yy and jj[0] == yy:
                                                    down = down + 'd(c)d(e)'
                                                if jj[1] == xx and jj[0] == yy and jj[2] != xx and jj[2]
!= yy:
                                                    up = up + 'd(c)'
                                                    if jj[1] == xx and jj[2] == yy and jj[0] != xx and jj[0]
!= yy:
                                                        up = up + 'd(c)'
                                                        if jj[1] == xx and jj[0] == yy and jj[2] == yy:
                                                            up = up + 't(c)'
                                                        if jj[0] == xx and jj[1] == yy and jj[2] == xx:
                                                            down = down + 'd(c)'
                                                        if jj[0] == xx and jj[1] == xx and jj[2] == yy:

```

```

        down = down + 'd(a)d(e) '
        up = up + 'd(a)d(c) '
    if jj[0] == yy and jj[1] == xx and jj[2] == xx:
        down = down + 'd(a)d(e) '
        up = up + 'd(a)d(c) '
    kk.append(down)
    kk.append(up)
    ll.append(kk)
    down = ''
    up = ''
    kk = []
    mm.append(ll)
    mat4.append(mm)
    ll = []
    mm = []
return mat4

```

```

def sumation(mat,aa,bb,Z,C1,C2,C3):
    kk = []
    ll = []
    a = 0
    b = 0
    c = 0
    mat5 = []
    mat6 = []
    down_s = 0
    down_da = 0
    down_dc = 0
    down_de = 0
    down_dade = 0
    down_dcde = 0
    up_s = 0
    up_da = 0
    up_dc = 0
    up_ta = 0
    up_tc = 0
    up_dadc = 0
    if aa == 1:
        if bb == 2:
            for ii in mat:
                a = ii[0]
                if ii[2][0][0] == 's':
                    b = ii[1][0][0]
                    c = a*b
                    down_s = down_s + c
                if ii[2][0][0] == 'd(a)':
                    b = ii[1][0][0]

```

```

        c = a*b
        down_da = down_da + c
    a = 0
    b = 0
if bb == 3:
    for ii in mat:
        a = ii[0]
        if ii[2][0][0] == 's':
            b = ii[1][0][0]
            c = a*b
            down_s = down_s + c
        if ii[2][0][0] == 'd(a)':
            b = ii[1][0][0]
            c = a*b
            down_da = down_da + c
        if ii[2][0][0] == 'd(c)':
            b = ii[1][0][0]
            c = a*b
            down_dc = down_dc + c
        if ii[2][0][0] == 'd(e)':
            b = ii[1][0][0]
            c = a*b
            down_de = down_de + c
        if ii[2][0][0] == 'd(a)d(e)':
            b = ii[1][0][0]
            c = a*b
            down_dade = down_dade + c
        if ii[2][0][0] == 'd(c)d(e)':
            b = ii[1][0][0]
            c = a*b
            down_dcde = down_dcde + c
        if ii[2][0][1] == 's':
            b = ii[1][0][1]
            c = a*b
            up_s = up_s + c
        if ii[2][0][1] == 'd(a)':
            b = ii[1][0][1]
            c = a*b
            up_da = up_da + c
        if ii[2][0][1] == 'd(c)':
            b = ii[1][0][1]
            c = a*b
            up_dc = up_dc + c
        if ii[2][0][1] == 't(a)':
            b = ii[1][0][1]
            c = a*b
            up_ta = up_ta + c

```

```

    if ii[2][0][1] == 't(c)':
        b = ii[1][0][1]
        c = a*b
        up_tc = up_tc + c
    if ii[2][0][1] == 'd(a)d(c)':
        b = ii[1][0][1]
        c = a*b
        up_dadc = up_dadc + c
    m = 0
if aa == 2:
    if bb == 2:
        for ii in mat:
            a = ii[0]/2
            if ii[2][0][0] == 's':
                b = ii[1][0][0]
                c = a*b
                down_s = down_s + c
            if ii[2][0][0] == 'd(a)':
                b = ii[1][0][0]
                c = a*b
                down_da = down_da + c
            if ii[2][1][0] == 's':
                b = ii[1][1][0]
                c = a*b
                down_s = down_s + c
            if ii[2][1][0] == 'd(a)':
                b = ii[1][1][0]
                c = a*b
                down_da = down_da + c
            a = 0
            b = 0
    if bb == 3:
        for ii in mat:
            a = ii[0]/2
            if ii[2][0][0] == 's':
                b = ii[1][0][0]
                c = a*b
                down_s = down_s + c
            if ii[2][0][0] == 'd(a)':
                b = ii[1][0][0]
                c = a*b
                down_da = down_da + c
            if ii[2][0][0] == 'd(c)':
                b = ii[1][0][0]
                c = a*b
                down_dc = down_dc + c
            if ii[2][0][0] == 'd(e)':

```

```

    b = ii[1][0][0]
    c = a*b
    down_de = down_de + c
if ii[2][0][0] == 'd(a)d(e)':
    b = ii[1][0][0]
    c = a*b
    down_dade = down_dade + c
if ii[2][0][0] == 'd(c)d(e)':
    b = ii[1][0][0]
    c = a*b
    down_dcde = down_dcde + c
if ii[2][0][1] == 's':
    b = ii[1][0][1]
    c = a*b
    up_s = up_s + c
if ii[2][0][1] == 'd(a)':
    b = ii[1][0][1]
    c = a*b
    up_da = up_da + c
if ii[2][0][1] == 'd(c)':
    b = ii[1][0][1]
    c = a*b
    up_dc = up_dc + c
if ii[2][0][1] == 't(a)':
    b = ii[1][0][1]
    c = a*b
    up_ta = up_ta + c
if ii[2][0][1] == 't(c)':
    b = ii[1][0][1]
    c = a*b
    up_tc = up_tc + c
if ii[2][0][1] == 'd(a)d(c)':
    b = ii[1][0][1]
    c = a*b
    up_dadc = up_dadc + c
if ii[2][1][0] == 's':
    b = ii[1][1][0]
    c = a*b
    down_s = down_s + c
if ii[2][1][0] == 'd(a)':
    b = ii[1][1][0]
    c = a*b
    down_da = down_da + c
if ii[2][1][0] == 'd(c)':
    b = ii[1][1][0]
    c = a*b
    down_dc = down_dc + c

```

```

if ii[2][1][0] == 'd(e)':
    b = ii[1][1][0]
    c = a*b
    down_de = down_de + c
if ii[2][1][0] == 'd(a)d(e)':
    b = ii[1][1][0]
    c = a*b
    down_dade = down_dade + c
if ii[2][1][0] == 'd(c)d(e)':
    b = ii[1][1][0]
    c = a*b
    down_dcde = down_dcde + c
if ii[2][1][1] == 's':
    b = ii[1][1][1]
    c = a*b
    up_s = up_s + c
if ii[2][1][1] == 'd(a)':
    b = ii[1][1][1]
    c = a*b
    up_da = up_da + c
if ii[2][1][1] == 'd(c)':
    b = ii[1][1][1]
    c = a*b
    up_dc = up_dc + c
if ii[2][1][1] == 't(a)':
    b = ii[1][1][1]
    c = a*b
    up_ta = up_ta + c
if ii[2][1][1] == 't(c)':
    b = ii[1][1][1]
    c = a*b
    up_tc = up_tc + c
if ii[2][1][1] == 'd(a)d(c)':
    b = ii[1][1][1]
    c = a*b
    up_dadc = up_dadc + c
a = 0
b = 0
if aa == 3:
    if bb == 2:
        for ii in mat:
            a = ii[0]/3
            if ii[2][0][0] == 's':
                b = ii[1][0][0]
                c = a*b
                down_s = down_s + c
            if ii[2][0][0] == 'd(a)':

```

```

    b = ii[1][0][0]
    c = a*b
    down_da = down_da + c
if ii[2][1][0] == 's':
    b = ii[1][1][0]
    c = a*b
    down_s = down_s + c
if ii[2][1][0] == 'd(a)':
    b = ii[1][1][0]
    c = a*b
    down_da = down_da + c
if ii[2][2][0] == 's':
    b = ii[1][2][0]
    c = a*b
    down_s = down_s + c
if ii[2][2][0] == 'd(a)':
    b = ii[1][2][0]
    c = a*b
    down_da = down_da + c
a = 0
b = 0
if bb == 3:
for ii in mat:
    a = ii[0]/3
    if ii[2][0][0] == 's':
        b = ii[1][0][0]
        c = a*b
        down_s = down_s + c
    if ii[2][0][0] == 'd(a)':
        b = ii[1][0][0]
        c = a*b
        down_da = down_da + c
    if ii[2][0][0] == 'd(c)':
        b = ii[1][0][0]
        c = a*b
        down_dc = down_dc + c
    if ii[2][0][0] == 'd(e)':
        b = ii[1][0][0]
        c = a*b
        down_de = down_de + c
    if ii[2][0][0] == 'd(a)d(e)':
        b = ii[1][0][0]
        c = a*b
        down_dade = down_dade + c
    if ii[2][0][0] == 'd(c)d(e)':
        b = ii[1][0][0]
        c = a*b

```

```

    down_dcde = down_dcde + c
if ii[2][0][1] == 's':
    b = ii[1][0][1]
    c = a*b
    up_s = up_s + c
if ii[2][0][1] == 'd(a)':
    b = ii[1][0][1]
    c = a*b
    up_da = up_da + c
if ii[2][0][1] == 'd(c)':
    b = ii[1][0][1]
    c = a*b
    up_dc = up_dc + c
if ii[2][0][1] == 't(a)':
    b = ii[1][0][1]
    c = a*b
    up_ta = up_ta + c
if ii[2][0][1] == 't(c)':
    b = ii[1][0][1]
    c = a*b
    up_tc = up_tc + c
if ii[2][0][1] == 'd(a)d(c)':
    b = ii[1][0][1]
    c = a*b
    up_dadc = up_dadc + c
if ii[2][1][0] == 's':
    b = ii[1][1][0]
    c = a*b
    down_s = down_s + c
if ii[2][1][0] == 'd(a)':
    b = ii[1][1][0]
    c = a*b
    down_da = down_da + c
if ii[2][1][0] == 'd(c)':
    b = ii[1][1][0]
    c = a*b
    down_dc = down_dc + c
if ii[2][1][0] == 'd(e)':
    b = ii[1][1][0]
    c = a*b
    down_de = down_de + c
if ii[2][1][0] == 'd(a)d(e)':
    b = ii[1][1][0]
    c = a*b
    down_dade = down_dade + c
if ii[2][1][0] == 'd(c)d(e)':
    b = ii[1][1][0]

```

```

    c = a*b
    down_dcde = down_dcde + c
if ii[2][1][1] == 's':
    b = ii[1][1][1]
    c = a*b
    up_s = up_s + c
if ii[2][1][1] == 'd(a)':
    b = ii[1][1][1]
    c = a*b
    up_da = up_da + c
if ii[2][1][1] == 'd(c)':
    b = ii[1][1][1]
    c = a*b
    up_dc = up_dc + c
if ii[2][1][1] == 't(a)':
    b = ii[1][1][1]
    c = a*b
    up_ta = up_ta + c
if ii[2][1][1] == 't(c)':
    b = ii[1][1][1]
    c = a*b
    up_tc = up_tc + c
if ii[2][1][1] == 'd(a)d(c)':
    b = ii[1][1][1]
    c = a*b
    up_dadc = up_dadc + c
if ii[2][2][0] == 's':
    b = ii[1][2][0]
    c = a*b
    down_s = down_s + c
if ii[2][2][0] == 'd(a)':
    b = ii[1][2][0]
    c = a*b
    down_da = down_da + c
if ii[2][2][0] == 'd(c)':
    b = ii[1][2][0]
    c = a*b
    down_dc = down_dc + c
if ii[2][2][0] == 'd(e)':
    b = ii[1][2][0]
    c = a*b
    down_de = down_de + c
if ii[2][2][0] == 'd(a)d(e)':
    b = ii[1][2][0]
    c = a*b
    down_dade = down_dade + c
if ii[2][2][0] == 'd(c)d(e)':

```

```

    b = ii[1][2][0]
    c = a*b
    down_dcde = down_dcde + c
if ii[2][2][1] == 's':
    b = ii[1][2][1]
    c = a*b
    up_s = up_s + c
if ii[2][2][1] == 'd(a)':
    b = ii[1][2][1]
    c = a*b
    up_da = up_da + c
if ii[2][2][1] == 'd(c)':
    b = ii[1][2][1]
    c = a*b
    up_dc = up_dc + c
if ii[2][2][1] == 't(a)':
    b = ii[1][2][1]
    c = a*b
    up_ta = up_ta + c
if ii[2][2][1] == 't(c)':
    b = ii[1][2][1]
    c = a*b
    up_tc = up_tc + c
if ii[2][2][1] == 'd(a)d(c)':
    b = ii[1][2][1]
    c = a*b
    up_dadc = up_dadc + c
a = 0
b = 0
if aa == 4:
    if bb == 2:
        for ii in mat:
            a = ii[0]/4
            if ii[2][0][0] == 's':
                b = ii[1][0][0]
                c = a*b
                down_s = down_s + c
            if ii[2][0][0] == 'd(a)':
                b = ii[1][0][0]
                c = a*b
                down_da = down_da + c
            if ii[2][1][0] == 's':
                b = ii[1][1][0]
                c = a*b
                down_s = down_s + c
            if ii[2][1][0] == 'd(a)':
                b = ii[1][1][0]

```

```

    c = a*b
    down_da = down_da + c
if ii[2][2][0] == 's':
    b = ii[1][2][0]
    c = a*b
    down_s = down_s + c
if ii[2][2][0] == 'd(a)':
    b = ii[1][2][0]
    c = a*b
    down_da = down_da + c
if ii[2][3][0] == 's':
    b = ii[1][3][0]
    c = a*b
    down_s = down_s + c
if ii[2][3][0] == 'd(a)':
    b = ii[1][3][0]
    c = a*b
    down_da = down_da + c
a = 0
b = 0
if bb == 3:
    for ii in mat:
        a = ii[0]/4
        if ii[2][0][0] == 's':
            b = ii[1][0][0]
            c = a*b
            down_s = down_s + c
        if ii[2][0][0] == 'd(a)':
            b = ii[1][0][0]
            c = a*b
            down_da = down_da + c
        if ii[2][0][0] == 'd(c)':
            b = ii[1][0][0]
            c = a*b
            down_dc = down_dc + c
        if ii[2][0][0] == 'd(e)':
            b = ii[1][0][0]
            c = a*b
            down_de = down_de + c
        if ii[2][0][0] == 'd(a)d(e)':
            b = ii[1][0][0]
            c = a*b
            down_dade = down_dade + c
        if ii[2][0][0] == 'd(c)d(e)':
            b = ii[1][0][0]
            c = a*b
            down_dcde = down_dcde + c

```

```

if ii[2][0][1] == 's':
    b = ii[1][0][1]
    c = a*b
    up_s = up_s + c
if ii[2][0][1] == 'd(a)':
    b = ii[1][0][1]
    c = a*b
    up_da = up_da + c
if ii[2][0][1] == 'd(c)':
    b = ii[1][0][1]
    c = a*b
    up_dc = up_dc + c
if ii[2][0][1] == 't(a)':
    b = ii[1][0][1]
    c = a*b
    up_ta = up_ta + c
if ii[2][0][1] == 't(c)':
    b = ii[1][0][1]
    c = a*b
    up_tc = up_tc + c
if ii[2][0][1] == 'd(a)d(c)':
    b = ii[1][0][1]
    c = a*b
    up_dadc = up_dadc + c
if ii[2][1][0] == 's':
    b = ii[1][1][0]
    c = a*b
    down_s = down_s + c
if ii[2][1][0] == 'd(a)':
    b = ii[1][1][0]
    c = a*b
    down_da = down_da + c
if ii[2][1][0] == 'd(c)':
    b = ii[1][1][0]
    c = a*b
    down_dc = down_dc + c
if ii[2][1][0] == 'd(e)':
    b = ii[1][1][0]
    c = a*b
    down_de = down_de + c
if ii[2][1][0] == 'd(a)d(e)':
    b = ii[1][1][0]
    c = a*b
    down_dade = down_dade + c
if ii[2][1][0] == 'd(c)d(e)':
    b = ii[1][1][0]
    c = a*b

```

```

    down_dcde = down_dcde + c
if ii[2][1][1] == 's':
    b = ii[1][1][1]
    c = a*b
    up_s = up_s + c
if ii[2][1][1] == 'd(a)':
    b = ii[1][1][1]
    c = a*b
    up_da = up_da + c
if ii[2][1][1] == 'd(c)':
    b = ii[1][1][1]
    c = a*b
    up_dc = up_dc + c
if ii[2][1][1] == 't(a)':
    b = ii[1][1][1]
    c = a*b
    up_ta = up_ta + c
if ii[2][1][1] == 't(c)':
    b = ii[1][1][1]
    c = a*b
    up_tc = up_tc + c
if ii[2][1][1] == 'd(a)d(c)':
    b = ii[1][1][1]
    c = a*b
    up_dadc = up_dadc + c
if ii[2][2][0] == 's':
    b = ii[1][2][0]
    c = a*b
    down_s = down_s + c
if ii[2][2][0] == 'd(a)':
    b = ii[1][2][0]
    c = a*b
    down_da = down_da + c
if ii[2][2][0] == 'd(c)':
    b = ii[1][2][0]
    c = a*b
    down_dc = down_dc + c
if ii[2][2][0] == 'd(e)':
    b = ii[1][2][0]
    c = a*b
    down_de = down_de + c
if ii[2][2][0] == 'd(a)d(e)':
    b = ii[1][2][0]
    c = a*b
    down_dade = down_dade + c
if ii[2][2][0] == 'd(c)d(e)':
    b = ii[1][2][0]

```

```

    c = a*b
    down_dcde = down_dcde + c
if ii[2][2][1] == 's':
    b = ii[1][2][1]
    c = a*b
    up_s = up_s + c
if ii[2][2][1] == 'd(a)':
    b = ii[1][2][1]
    c = a*b
    up_da = up_da + c
if ii[2][2][1] == 'd(c)':
    b = ii[1][2][1]
    c = a*b
    up_dc = up_dc + c
if ii[2][2][1] == 't(a)':
    b = ii[1][2][1]
    c = a*b
    up_ta = up_ta + c
if ii[2][2][1] == 't(c)':
    b = ii[1][2][1]
    c = a*b
    up_tc = up_tc + c
if ii[2][2][1] == 'd(a)d(c)':
    b = ii[1][2][1]
    c = a*b
    up_dadc = up_dadc + c
if ii[2][3][0] == 's':
    b = ii[1][3][0]
    c = a*b
    down_s = down_s + c
if ii[2][3][0] == 'd(a)':
    b = ii[1][3][0]
    c = a*b
    down_da = down_da + c
if ii[2][3][0] == 'd(c)':
    b = ii[1][3][0]
    c = a*b
    down_dc = down_dc + c
if ii[2][3][0] == 'd(e)':
    b = ii[1][3][0]
    c = a*b
    down_de = down_de + c
if ii[2][3][0] == 'd(a)d(e)':
    b = ii[1][3][0]
    c = a*b
    down_dade = down_dade + c
if ii[2][3][0] == 'd(c)d(e)':

```

```

    b = ii[1][3][0]
    c = a*b
    down_dcde = down_dcde + c
if ii[2][3][1] == 's':
    b = ii[1][3][1]
    c = a*b
    up_s = up_s + c
if ii[2][3][1] == 'd(a)':
    b = ii[1][3][1]
    c = a*b
    up_da = up_da + c
if ii[2][3][1] == 'd(c)':
    b = ii[1][3][1]
    c = a*b
    up_dc = up_dc + c
if ii[2][3][1] == 't(a)':
    b = ii[1][3][1]
    c = a*b
    up_ta = up_ta + c
if ii[2][3][1] == 't(c)':
    b = ii[1][3][1]
    c = a*b
    up_tc = up_tc + c
if ii[2][3][1] == 'd(a)d(c)':
    b = ii[1][3][1]
    c = a*b
    up_dadc = up_dadc + c
a = 0
b = 0
down_s1 = down_s
down_s1 = down_s / down_s
down_da = down_da / down_s
down_dc = down_dc / down_s
down_de = down_de / down_s
down_dade = down_dade / down_s
down_dcde = down_dcde / down_s
up_s = up_s / down_s
up_da = up_da / down_s
up_dc = up_dc / down_s
up_ta = up_ta / down_s
up_tc = up_tc / down_s
up_dadc = up_dadc / down_s
down_s1 = down_s1
down_da = down_da / 2
down_dc = down_dc / 2
down_de = down_de / 2
down_dade = down_dade / 4

```

```

down_dcde = down_dcde / 4
a = up_ta / 2
b = up_tc / 2
up_s = up_s + a + b
up_da = up_da / 2
up_dc = up_dc / 2
up_ta = up_ta / 4
up_tc = up_tc / 4
up_dadc = up_dadc / 4
print 'Spectrum for ', Z, 'Sn NMR'
print 'down s = ', down_s1
print 'down d(a) = ', down_da
print 'down d(c) = ', down_dc
print 'down d(e) = ', down_de
print 'down d(a)d(e) = ', down_dade
print 'down d(c)d(e) = ', down_dcde
print 'up s = ', up_s
print 'up d(a) = ', up_da
print 'up d(c) = ', up_dc
print 'up t(a) = ', up_ta
print 'up t(c) = ', up_tc
print 'up d(a)d(c) = ', up_dadc
print 'a = ', C1
if bb == 3:
    print 'c = ', C2
    print 'e = ', C3

def main():
    #next 5 values must be changed in code inorder to calculate
    spectrum
    X = 2 #number of bridges 1 - 4. must change in the code
    Y = 2 #number of tins in bridge 2 - 3. must change in the code
    Z = 117 #nucleus. must change in the code
    C1 = 3223.9 #largest experimental coupling constant
    C3 = 537.2 #smallest coupling constant
    if Z == 119:
        #119Sn values
        Q = 0.0859 #119 abundance
        P = 0.0768 #119 abundance
        R = 0.8373 #Other Sn abundance
    if Z == 117:
        #117Sn values
        Q = 0.0768 #117 abundance
        P = 0.0859 #119 abundance
        R = 0.8373 #Other Sn abundance
    if X > 4:
        print 'ring size to large'

```

```
if Y > 3:
    print 'to many tin molecules'
if Y == 1:
    print 'no coupling pattern'
if Y <= 4 and Y > 1 and X <= 4:
    C2 = coupling(C1)
    MAT = matrix([Q,P,R],X,Y)
    MAT = prob(MAT,X,Y)
    A = probadd(MAT)
    MAT = intigrat(MAT,X,Y,Q)
    MAT = spectra(MAT,Y,Q,P,R)
    MAT = sumation(MAT,X,Y,Z,C1,C2,C3)

if __name__ == '__main__':
    main()
```

Appendix 5: DFT .mol2 files for optimized structures

Table A5.1: Total Energies LSDA/SDD

Compound	Optimized Energy (a.u.)	Zero Point Energy (a.u.)
4a	-1182.25541824	-1182.25541822
4b	-1855.62932036	-1855.62932036
5a	-673.35512007	-673.35512007
9b	-990.74034313	-990.74034314
11	-1981.51367409	-1981.51367410
11 (mono cation)	-1981.28185554	-1981.28185530
12a	-1384.62175373	-1384.62175372
12b	-1752.64314207	-1752.64314207
12c	-2120.66623312	-2120.66623312
12d	-2755.45948976	-2755.45948975
13	-1099.41100877	-1099.41100877
14	-1308.91976962	-1308.91976962

A5.1: Compound 4a .mol2

```
# Title Card Required
# Created by GaussView 5.0.9
#
```

```
#
#
```

```
@<TRIPOS>MOLECULE
Molecule Name
58 77
SMALL
NO_CHARGES
```

```
@<TRIPOS>ATOM
1 Fe1 -4.8216 0.3181 0.1092 Fe
2 H2 -5.0818 -1.2813 -2.1905 H
3 C3 -5.4053 -1.1446 -1.1568 C
4 C4 -6.5330 -0.3587 -0.7195 C
```

5	H5	-3.8956	-2.3538	0.0224	H
6	H6	-7.2090	0.2068	-1.3627	H
7	C7	-6.5958	-0.4314	0.7193	C
8	H8	-7.3284	0.0684	1.3549	H
9	C9	-5.5071	-1.2618	1.1711	C
10	H10	-5.2738	-1.5054	2.2095	H
11	C11	-4.7754	-1.7064	0.0116	C
12	H12	-3.3229	1.3616	-2.0145	H
13	C13	-3.5870	1.4991	-0.9631	C
14	C14	-2.8793	0.9267	0.1650	C
15	H15	-5.4509	2.7790	-1.0863	H
16	C16	-3.6026	1.3328	1.3540	C
17	H17	-3.3516	1.0494	2.3791	H
18	C18	-4.7293	2.1442	0.9621	C
19	H19	-5.4683	2.5853	1.6331	H
20	C20	-4.7195	2.2471	-0.4756	C
21	Fe21	4.7843	-0.3433	-0.2067	Fe
22	H22	3.1163	-0.9477	-2.3758	H
23	C23	3.4361	-1.2736	-1.3829	C
24	C24	2.8215	-0.8851	-0.1288	C
25	H25	5.2287	-2.5770	-1.8471	H
26	C26	3.5945	-1.5177	0.9217	C
27	H27	3.4195	-1.4074	1.9947	H
28	C28	4.6576	-2.2870	0.3233	C
29	H29	5.4138	-2.8643	0.8579	H
30	C30	4.5596	-2.1354	-1.1067	C
31	H31	5.1266	1.5408	-2.2750	H
32	C32	5.4359	1.2498	-1.2692	C
33	C33	6.5268	0.3660	-0.9403	C
34	H34	3.9635	2.3463	0.0500	H
35	H35	7.1821	-0.1369	-1.6532	H
36	C36	6.5839	0.2436	0.4953	C
37	H37	7.2903	-0.3677	1.0590	H
38	C38	5.5278	1.0515	1.0538	C
39	H39	5.2984	1.1622	2.1156	H
40	C40	4.8216	1.6759	-0.0367	C
41	Sn41	-1.2996	-0.5114	0.0702	Sn
42	Sn42	1.3119	0.6092	0.1430	Sn
43	C43	-1.6914	-1.8460	1.7415	C
44	H44	-2.7246	-1.6541	2.0875	H
45	H45	-0.9898	-1.6753	2.5755	H
46	H46	-1.6061	-2.8992	1.4191	H
47	C47	-1.5995	-1.5563	-1.8108	C
48	H48	-1.2775	-0.9302	-2.6616	H
49	H49	-2.6756	-1.7842	-1.9228	H
50	H50	-1.0216	-2.4971	-1.8271	H
51	C51	1.6475	2.0180	-1.4802	C
52	H52	0.8490	1.9679	-2.2397	H
53	H53	2.6167	1.7632	-1.9488	H
54	H54	1.6956	3.0499	-1.0878	H
55	C55	1.8044	1.5272	2.0475	C
56	H56	1.3393	2.5246	2.1346	H

57	H57	2.9046	1.6274	2.1007	H
58	H58	1.4612	0.9019	2.8902	H

@<TRIPOS>BOND

1 1 3 1
2 1 4 1
3 1 7 1
4 1 9 1
5 1 11 1
6 1 13 1
7 1 14 1
8 1 16 1
9 1 18 1
10 1 20 1
11 2 3 1
12 3 4 Ar
13 3 11 Ar
14 4 6 1
15 4 7 Ar
16 5 11 1
17 7 8 1
18 7 9 Ar
19 9 10 1
20 9 11 Ar
21 12 13 1
22 13 14 1
23 13 20 Ar
24 14 16 1
25 14 41 1
26 15 20 1
27 16 17 1
28 16 18 Ar
29 18 19 1
30 18 20 Ar
31 21 23 1
32 21 24 1
33 21 26 1
34 21 28 1
35 21 30 1
36 21 32 1
37 21 33 1
38 21 36 1
39 21 38 1
40 21 40 1
41 22 23 1
42 23 24 1
43 23 30 Ar
44 24 26 1
45 24 42 1
46 25 30 1
47 26 27 1
48 26 28 Ar
49 28 29 1

```
50 28 30 Ar
51 31 32 1
52 32 33 Ar
53 32 40 Ar
54 33 35 1
55 33 36 Ar
56 34 40 1
57 36 37 1
58 36 38 Ar
59 38 39 1
60 38 40 Ar
61 41 42 1
62 41 43 1
63 41 47 1
64 42 51 1
65 42 55 1
66 43 44 1
67 43 45 1
68 43 46 1
69 47 48 1
70 47 49 1
71 47 50 1
72 51 52 1
73 51 53 1
74 51 54 1
75 55 56 1
76 55 57 1
77 55 58 1
```

A5.2: Compound 4b .mol2

```
# DFT LSDA SDD no symm
# Created by GaussView 5.0.9
#
```

```
#
#
```

```
@<TRIPOS>MOLECULE
Molecule Name
95 124
SMALL
NO_CHARGES
```

```
@<TRIPOS>ATOM
1 Fe1      -4.6891      -0.0859      0.0987 Fe
2 H2       -4.7963      -2.2721     -1.6762 H
3 C3       -5.1797      -1.8599     -0.7409 C
4 C4       -6.3403      -1.0160     -0.5988 C
```

5	H5	-3.7182	-2.6473	0.7931	H
6	H6	-6.9873	-0.6734	-1.4079	H
7	C7	-6.4837	-0.6874	0.7980	C
8	H8	-7.2570	-0.0507	1.2305	H
9	C9	-5.4115	-1.3286	1.5191	C
10	H10	-5.2336	-1.2647	2.5945	H
11	C11	-4.6098	-2.0569	0.5682	C
12	H12	-2.9569	0.3332	-2.0672	H
13	C13	-3.3440	0.7642	-1.1406	C
14	C14	-2.7705	0.5821	0.1782	C
15	H15	-5.1810	1.8824	-1.8485	H
16	C16	-3.6261	1.3009	1.1021	C
17	H17	-3.4952	1.3453	2.1861	H
18	C18	-4.7020	1.9148	0.3631	C
19	H19	-5.5145	2.5095	0.7840	H
20	C20	-4.5270	1.5817	-1.0283	C
21	Fe21	4.2589	0.5054	-1.7161	Fe
22	H22	1.7908	0.6888	-3.0285	H
23	C23	2.4843	0.0040	-2.5341	C
24	C24	2.4934	-0.3125	-1.1197	C
25	H25	3.8167	-0.6620	-4.2407	H
26	C26	3.6020	-1.2233	-0.9088	C
27	H27	3.9106	-1.6340	0.0567	H
28	C28	4.2521	-1.4691	-2.1717	C
29	H29	5.1219	-2.1098	-2.3370	H
30	C30	3.5634	-0.7035	-3.1794	C
31	H31	5.7666	1.7761	-3.7077	H
32	C32	5.5260	1.7738	-2.6417	C
33	C33	6.2262	1.0199	-1.6210	C
34	H34	3.7267	3.1459	-2.5397	H
35	C35	5.5440	1.2884	-0.3699	C
36	H36	5.8003	0.8517	0.5993	H
37	C37	4.4540	2.1982	-0.6175	C
38	H38	3.7536	2.5861	0.1262	H
39	C39	4.4387	2.4957	-2.0274	C
40	Sn40	-1.1648	-0.7317	0.6983	Sn
41	Sn41	1.3259	0.6120	0.4154	Sn
42	C42	-1.6226	-1.4062	2.7108	C
43	H43	-2.7093	-1.6045	2.7681	H
44	H44	-1.3597	-0.6348	3.4554	H
45	H45	-1.0698	-2.3315	2.9497	H
46	C46	-1.2991	-2.3823	-0.7085	C
47	H47	-2.2579	-2.2933	-1.2533	H
48	H48	-1.2756	-3.3501	-0.1758	H
49	H49	-0.4624	-2.3540	-1.4280	H
50	C50	1.0007	2.6594	-0.2389	C
51	H51	1.3059	3.3720	0.5487	H
52	H52	-0.0634	2.8306	-0.4777	H
53	H53	1.6151	2.8356	-1.1417	H
54	C54	2.6127	0.5599	2.1644	C
55	H55	2.6192	-0.4470	2.6173	H
56	H56	2.2786	1.2882	2.9238	H

57	H57	3.6400	0.8145	1.8418	H
58	Sn58	7.7412	-0.4563	-1.9403	Sn
59	Sn59	10.3472	0.6793	-1.8847	Sn
60	C60	11.4854	0.1395	-3.6153	C
61	Fe61	13.3618	0.8847	-3.8649	Fe
62	C62	11.6015	0.8964	-4.8463	C
63	C63	12.4742	-0.9182	-3.6874	C
64	C64	13.1805	-0.8151	-4.9406	C
65	C65	12.6393	0.3107	-5.6598	C
66	C66	14.8077	2.2203	-4.3125	C
67	C67	15.3493	1.1013	-3.5817	C
68	C68	14.6579	1.0173	-2.3187	C
69	C69	13.6933	2.0871	-2.2675	C
70	C70	13.7822	2.8282	-3.5007	C
71	H71	11.0191	1.7838	-5.1055	H
72	H72	12.6693	-1.6588	-2.9080	H
73	H73	13.9925	-1.4621	-5.2767	H
74	H74	12.9688	0.6675	-6.6371	H
75	H75	15.1086	2.5396	-5.3115	H
76	H76	14.8310	0.2705	-1.5412	H
77	H77	13.0022	2.2936	-1.4468	H
78	H78	13.1726	3.6914	-3.7750	H
79	H79	16.1324	0.4265	-3.9305	H
80	C80	10.2737	2.8518	-1.9264	C
81	H81	10.6620	3.2677	-0.9789	H
82	H82	10.9155	3.1963	-2.7591	H
83	H83	9.2434	3.2175	-2.0758	H
84	C84	11.5533	0.0026	-0.2075	C
85	H85	12.6055	-0.0414	-0.5463	H
86	H86	11.4724	0.7095	0.6374	H
87	H87	11.2422	-0.9984	0.1374	H
88	C88	7.3213	-1.3075	-3.8961	C
89	H89	6.3273	-0.9492	-4.2230	H
90	H90	8.0854	-1.0023	-4.6318	H
91	H91	7.3071	-2.4110	-3.8412	H
92	C92	7.4147	-1.9342	-0.3815	C
93	H93	6.3239	-2.0406	-0.2301	H
94	H94	7.8386	-2.9109	-0.6742	H
95	H95	7.8796	-1.6162	0.5681	H

@<TRIPOS>BOND

1 1 3 1
2 1 4 1
3 1 7 1
4 1 9 1
5 1 11 1
6 1 13 1
7 1 14 1
8 1 16 1
9 1 18 1
10 1 20 1
11 2 3 1
12 3 4 Ar

13 3 11 Ar
14 4 6 1
15 4 7 Ar
16 5 11 1
17 7 8 1
18 7 9 Ar
19 9 10 1
20 9 11 Ar
21 12 13 1
22 13 14 1
23 13 20 Ar
24 14 16 1
25 14 40 1
26 15 20 1
27 16 17 1
28 16 18 Ar
29 18 19 1
30 18 20 Ar
31 21 23 1
32 21 24 1
33 21 26 1
34 21 28 1
35 21 30 1
36 21 32 1
37 21 33 1
38 21 35 1
39 21 37 1
40 21 39 1
41 22 23 1
42 23 24 1
43 23 30 Ar
44 24 26 1
45 24 41 1
46 25 30 1
47 26 27 1
48 26 28 Ar
49 28 29 1
50 28 30 Ar
51 31 32 1
52 32 33 1
53 32 39 Ar
54 33 35 1
55 33 58 1
56 34 39 1
57 35 36 1
58 35 37 Ar
59 37 38 1
60 37 39 Ar
61 40 41 1
62 40 42 1
63 40 46 1
64 41 50 1

65 41 54 1
66 42 43 1
67 42 44 1
68 42 45 1
69 46 47 1
70 46 48 1
71 46 49 1
72 50 51 1
73 50 52 1
74 50 53 1
75 54 55 1
76 54 56 1
77 54 57 1
78 58 59 1
79 58 88 1
80 58 92 1
81 59 60 1
82 59 80 1
83 59 84 1
84 60 61 1
85 60 62 1
86 60 63 1
87 61 62 1
88 61 63 1
89 61 64 1
90 61 65 1
91 61 66 1
92 61 67 1
93 61 68 1
94 61 69 1
95 61 70 1
96 62 65 Ar
97 62 71 1
98 63 64 Ar
99 63 72 1
100 64 65 Ar
101 64 73 1
102 65 74 1
103 66 67 Ar
104 66 70 Ar
105 66 75 1
106 67 68 Ar
107 67 79 1
108 68 69 Ar
109 68 76 1
110 69 70 Ar
111 69 77 1
112 70 78 1
113 80 81 1
114 80 82 1
115 80 83 1
116 84 85 1

117 84 86 1
118 84 87 1
119 88 89 1
120 88 90 1
121 88 91 1
122 92 93 1
123 92 94 1
124 92 95 1

A5.3: Compound 5a .mol2

DFT SDD LSDA no symm
Created by GaussView 5.0.9
#

#

@<TRIPOS>MOLECULE
Molecule Name
37 45
SMALL
NO_CHARGES

@<TRIPOS>ATOM

1	Fe1	0.0026	0.0200	-0.0066	Fe
2	C2	-1.6263	1.0081	-0.7527	C
3	C3	-1.6165	0.9996	0.6967	C
4	H4	-1.5873	-0.7338	-2.2049	H
5	C5	-1.5983	-0.3676	1.1587	C
6	H6	-1.5788	-0.6953	2.1995	H
7	C7	-1.5882	-1.2233	-0.0006	C
8	H8	-1.5605	-2.3142	0.0055	H
9	C9	-1.6006	-0.3793	-1.1713	C
10	H10	1.5733	1.9212	1.3424	H
11	C11	1.5966	1.0296	0.7108	C
12	C12	1.6311	1.0200	-0.7380	C
13	H13	1.5559	-0.6468	2.2342	H
14	C14	1.6301	-0.3728	-1.1392	C
15	H15	1.6386	-0.7392	-2.1688	H
16	C16	1.6086	-1.2024	0.0414	C
17	H17	1.5945	-2.2934	0.0610	H
18	C18	1.5885	-0.3321	1.1898	C
19	H19	-1.6150	1.8840	1.3388	H
20	Sn20	1.4191	2.7151	-2.0516	Sn
21	Sn21	-1.4162	2.7422	-2.0142	Sn
22	C22	-2.3644	2.3182	-3.9198	C
23	H23	-3.4414	2.1292	-3.7643	H

24	H24	-2.2449	3.1722	-4.6090	H
25	H25	-1.9089	1.4250	-4.3827	H
26	C26	-2.4280	4.3969	-1.0435	C
27	H27	-2.3274	5.3208	-1.6388	H
28	H28	-3.5002	4.1528	-0.9383	H
29	H29	-2.0036	4.5736	-0.0397	H
30	C30	2.2848	2.1551	-3.9614	C
31	H31	2.0799	2.9242	-4.7260	H
32	H32	3.3775	2.0363	-3.8536	H
33	H33	1.8548	1.1959	-4.3009	H
34	C34	2.5026	4.3928	-1.2066	C
35	H35	3.5669	4.1181	-1.0969	H
36	H36	2.4258	5.2759	-1.8641	H
37	H37	2.0985	4.6536	-0.2129	H

@<TRIPOS>BOND

1 1 3 1
2 1 5 1
3 1 7 1
4 1 9 1
5 1 11 1
6 1 14 1
7 1 16 1
8 1 18 1
9 2 3 1
10 2 9 1
11 2 21 1
12 3 5 Ar
13 3 19 1
14 4 9 1
15 5 6 1
16 5 7 Ar
17 7 8 1
18 7 9 Ar
19 10 11 1
20 11 12 1
21 11 18 Ar
22 12 14 1
23 12 20 1
24 13 18 1
25 14 15 1
26 14 16 Ar
27 16 17 1
28 16 18 Ar
29 20 21 1
30 20 30 1
31 20 34 1
32 21 22 1
33 21 26 1
34 22 23 1
35 22 24 1
36 22 25 1
37 26 27 1

38 26 28 1
39 26 29 1
40 30 31 1
41 30 32 1
42 30 33 1
43 34 35 1
44 34 36 1
45 34 37 1

A5.4: Compound 9b .mol2

DFT SDD LSDA no symm
Created by GaussView 5.0.9
#

#

@<TRIPOS>MOLECULE
Molecule Name
64 72
SMALL
NO_CHARGES

@<TRIPOS>ATOM
1 Fe1 1.9364 -0.6648 0.1928 Fe
2 C2 -0.0600 -0.1421 0.4050 C
3 C3 0.6011 -0.3303 1.6809 C
4 H4 -0.2501 -1.5710 -1.3448 H
5 C5 1.1357 -1.6683 1.7406 C
6 H6 1.6897 -2.1050 2.5736 H
7 C7 0.8328 -2.3186 0.4901 C
8 H8 1.1185 -3.3337 0.2084 H
9 C9 0.1132 -1.3767 -0.3317 C
10 H10 3.6718 1.2516 1.3311 H
11 C11 3.5501 0.5174 0.5307 C
12 C12 3.0337 0.7979 -0.7931 C
13 H13 4.3019 -1.3919 1.4901 H
14 C14 3.0244 -0.4649 -1.5039 C
15 H15 2.6716 -0.6178 -2.5279 H
16 C16 3.5647 -1.4911 -0.6474 C
17 H17 3.6850 -2.5457 -0.9018 H
18 C18 3.8899 -0.8812 0.6177 C
19 H19 0.6758 0.4202 2.4718 H
20 Sn20 2.5784 2.7477 -1.5789 Sn
21 Sn21 -1.2296 1.5612 -0.1711 Sn
22 Sn22 -0.0260 2.3599 -2.6001 Sn
23 C23 4.0890 3.2167 -3.0739 C
24 H24 4.0453 4.2870 -3.3426 H
25 H25 5.0927 2.9826 -2.6769 H

26	H26	3.9115	2.6137	-3.9841	H
27	C27	2.7675	4.0922	0.1137	C
28	H28	3.7570	3.9550	0.5868	H
29	H29	2.6688	5.1436	-0.2073	H
30	H30	1.9800	3.8742	0.8583	H
31	C31	0.3012	0.5863	-3.8651	C
32	H32	-0.6090	0.4385	-4.4818	H
33	H33	0.3898	-0.2834	-3.1818	H
34	C34	-0.9749	3.8650	-3.8755	C
35	H35	-0.1647	4.3190	-4.4800	H
36	H36	-1.4236	4.6683	-3.2596	H
37	C37	-3.3176	0.9612	-0.1749	C
38	H38	-3.5841	0.5671	0.8219	H
39	H39	-3.9670	1.8223	-0.4097	H
40	H40	-3.4832	0.1706	-0.9272	H
41	C41	-0.9022	3.0061	1.4191	C
42	H42	-1.1834	4.0256	1.1041	H
43	H43	-1.5041	2.7256	2.3022	H
44	H44	0.1672	3.0038	1.7016	H
45	C45	1.5376	0.7220	-4.7531	C
46	H46	2.4602	0.7090	-4.1291	H
47	H47	1.6210	-0.1574	-5.4297	H
48	C48	-2.0261	3.2210	-4.7768	C
49	H49	-2.8378	2.7904	-4.1541	H
50	H50	-1.5747	2.3668	-5.3290	H
51	C51	1.5620	1.9879	-5.6021	C
52	H52	0.5968	2.0890	-6.1443	H
53	H53	1.6271	2.8719	-4.9279	H
54	C54	2.7255	2.0101	-6.5813	C
55	H55	2.6704	1.1547	-7.2810	H
56	H56	2.7474	2.9384	-7.1800	H
57	H57	3.6923	1.9343	-6.0448	H
58	C58	-2.6212	4.1915	-5.7981	C
59	H59	-3.4570	3.6944	-6.3306	H
60	H60	-3.0604	5.0581	-5.2624	H
61	C61	-1.5916	4.6775	-6.8105	C
62	H62	-2.0457	5.3316	-7.5764	H
63	H63	-0.7824	5.2506	-6.3201	H
64	H64	-1.1223	3.8195	-7.3314	H

@<TRIPOS>BOND

1 1 3 1
2 1 5 1
3 1 7 1
4 1 9 1
5 1 11 1
6 1 14 1
7 1 16 1
8 1 18 1
9 2 3 1
10 2 9 1
11 2 21 1
12 3 5 Ar

13 3 19 1
14 4 9 1
15 5 6 1
16 5 7 Ar
17 7 8 1
18 7 9 Ar
19 10 11 1
20 11 12 1
21 11 18 Ar
22 12 14 1
23 12 20 1
24 13 18 1
25 14 15 1
26 14 16 Ar
27 16 17 1
28 16 18 Ar
29 20 22 1
30 20 23 1
31 20 27 1
32 21 22 1
33 21 37 1
34 21 41 1
35 22 31 1
36 22 34 1
37 23 24 1
38 23 25 1
39 23 26 1
40 27 28 1
41 27 29 1
42 27 30 1
43 31 32 1
44 31 33 1
45 31 45 1
46 34 35 1
47 34 36 1
48 34 48 1
49 37 38 1
50 37 39 1
51 37 40 1
52 41 42 1
53 41 43 1
54 41 44 1
55 45 46 1
56 45 47 1
57 45 51 1
58 48 49 1
59 48 50 1
60 48 58 1
61 51 52 1
62 51 53 1
63 51 54 1
64 54 55 1

65 54 56 1
66 54 57 1
67 58 59 1
68 58 60 1
69 58 61 1
70 61 62 1
71 61 63 1
72 61 64 1

A5.5: Compound 11 .mol2

DFT LSDA SDD no symm
Created by GaussView 5.0.9
#

#

@<TRIPOS>MOLECULE
Molecule Name
128 148
SMALL
NO_CHARGES

@<TRIPOS>ATOM
1 Fe1 -0.8838 4.4140 -0.0890 Fe
2 Fe2 0.9627 -4.1478 0.1484 Fe
3 H3 -1.7439 -4.8351 -0.1805 H
4 C4 -1.0182 -4.3653 0.4890 C
5 C5 -0.6648 -2.9591 0.4830 C
6 H6 -0.2777 -6.1101 1.7254 H
7 C7 0.3459 -2.7893 1.5083 C
8 H8 0.8528 -1.8511 1.7551 H
9 C9 0.5990 -4.0653 2.1331 C
10 H10 1.3282 -4.2579 2.9227 H
11 C11 -0.2472 -5.0428 1.4988 C
12 H12 0.5922 -4.6138 -2.6097 H
13 C13 1.3255 -4.5613 -1.8020 C
14 C14 1.7360 -5.6532 -0.9566 C
15 H15 1.9568 -2.3869 -1.8219 H
16 H16 1.3619 -6.6776 -1.0023 H
17 C17 2.7065 -5.1437 -0.0199 C
18 H18 3.1819 -5.7255 0.7736 H
19 C19 2.9150 -3.7323 -0.2760 C
20 C20 2.0500 -3.3863 -1.3856 C
21 C21 -2.7179 4.1341 0.7532 C
22 C22 -2.6177 5.4223 0.0917 C
23 H23 -1.4482 3.2747 2.4225 H

24	H24	-3.2463	5.7638	-0.7348	H
25	C25	-1.5323	6.1699	0.6745	C
26	H26	-1.2061	7.1681	0.3772	H
27	C27	-0.9393	5.3532	1.7025	C
28	H28	-0.0816	5.6201	2.3238	H
29	C29	-1.6672	4.1085	1.7504	C
30	H30	-1.5479	4.0977	-2.7937	H
31	C31	-0.7596	3.9611	-2.0509	C
32	C32	-0.5586	2.7874	-1.2363	C
33	H33	0.3529	5.9310	-2.1035	H
34	H34	-1.1747	1.8832	-1.2577	H
35	C35	0.5697	3.0125	-0.3558	C
36	C36	1.0550	4.3491	-0.6455	C
37	H37	1.8870	4.8461	-0.1386	H
38	C38	0.2428	4.9293	-1.6844	C
39	Sn39	4.1117	-2.3914	0.8931	Sn
40	Sn40	3.5627	0.2814	0.1066	Sn
41	Sn41	1.4208	1.8120	1.2022	Sn
42	Sn42	-4.0715	2.6153	0.0759	Sn
43	Sn43	-3.5806	-0.1097	0.7026	Sn
44	Sn44	-1.6606	-1.5773	-0.8256	Sn
45	C45	2.1197	3.3004	2.6220	C
46	H46	1.2477	3.6763	3.1897	H
47	H47	2.5784	4.1460	2.0767	H
48	H48	2.8594	2.8819	3.3259	H
49	C49	-0.1075	0.6524	2.2140	C
50	H50	-0.6065	-0.0666	1.5370	H
51	H51	-0.8743	1.3443	2.6091	H
52	H52	0.3304	0.0899	3.0589	H
53	C53	3.4164	0.1520	-2.0799	C
54	H54	2.4305	-0.2645	-2.3686	H
55	H55	3.4502	1.1900	-2.4679	H
56	C56	5.3970	1.4326	0.5037	C
57	H57	6.1354	1.1079	-0.2585	H
58	H58	5.7948	1.1218	1.4891	H
59	C59	6.2064	-2.7908	0.4632	C
60	H60	6.4116	-2.5781	-0.6013	H
61	H61	6.4408	-3.8507	0.6684	H
62	H62	6.8552	-2.1507	1.0867	H
63	C63	3.7491	-2.8439	2.9867	C
64	H64	2.7352	-2.5140	3.2755	H
65	H65	4.4903	-2.3277	3.6216	H
66	H66	3.8321	-3.9339	3.1531	H
67	C67	-0.2052	-0.4956	-2.0150	C
68	H68	-0.6980	0.1936	-2.7235	H
69	H69	0.3755	-1.2414	-2.5895	H
70	H70	0.4855	0.0951	-1.3842	H
71	C71	-2.7322	-2.9061	-2.1736	C
72	H72	-2.9741	-2.3874	-3.1184	H
73	H73	-3.6729	-3.2642	-1.7159	H
74	H74	-2.0817	-3.7733	-2.3967	H
75	C75	-5.4534	-1.0132	-0.0154	C

76	H76	-6.2909	-0.6675	0.6266	H
77	H77	-5.3605	-2.1093	0.1332	H
78	C78	-3.3546	-0.5341	2.8461	C
79	H79	-4.3639	-0.4207	3.2911	H
80	H80	-2.7090	0.2519	3.2825	H
81	C81	-4.1124	2.8785	-2.0838	C
82	H82	-5.0264	2.4260	-2.5084	H
83	H83	-3.2290	2.4010	-2.5452	H
84	H84	-4.0979	3.9591	-2.3206	H
85	C85	-6.0770	3.0424	0.8041	C
86	H86	-6.7626	2.2345	0.4891	H
87	H87	-6.4325	4.0010	0.3858	H
88	H88	-6.0829	3.1073	1.9059	H
89	C89	4.5489	-0.6944	-2.6554	C
90	H90	4.4636	-1.7368	-2.2757	H
91	H91	5.5332	-0.3139	-2.2964	H
92	C92	5.1842	2.9455	0.4563	C
93	H93	6.1552	3.4622	0.6256	H
94	H94	4.5219	3.2520	1.2934	H
95	C95	4.5663	-0.7220	-4.1853	C
96	H96	3.5892	-1.1073	-4.5447	H
97	H97	5.3335	-1.4448	-4.5291	H
98	C98	4.5952	3.4504	-0.8598	C
99	H99	3.5738	3.0283	-0.9998	H
100	H100	4.4577	4.5499	-0.8020	H
101	C101	4.8394	0.6432	-4.8033	C
102	H102	4.8748	0.5904	-5.9064	H
103	H103	5.8084	1.0485	-4.4511	H
104	H104	4.0564	1.3749	-4.5282	H
105	C105	5.4598	3.1061	-2.0639	C
106	H106	5.0345	3.5052	-3.0033	H
107	H107	5.5576	2.0103	-2.1901	H
108	H108	6.4793	3.5215	-1.9461	H
109	C109	-5.7236	-0.6750	-1.4786	C
110	H110	-4.8286	-0.9185	-2.0958	H
111	H111	-5.8761	0.4217	-1.5857	H
112	C112	-2.7762	-1.9202	3.1235	C
113	H113	-2.7557	-2.0924	4.2227	H
114	H114	-1.7216	-1.9652	2.7819	H
115	C115	-6.9267	-1.4157	-2.0654	C
116	H116	-7.1379	-1.0274	-3.0821	H
117	H117	-7.8229	-1.1934	-1.4499	H
118	C118	-3.5462	-3.0681	2.4755	C
119	H119	-3.4585	-2.9883	1.3673	H
120	H120	-3.0465	-4.0236	2.7329	H
121	C121	-6.7094	-2.9223	-2.1334	C
122	H122	-7.5684	-3.4402	-2.5965	H
123	H123	-6.5661	-3.3535	-1.1245	H
124	H124	-5.8065	-3.1600	-2.7305	H
125	C125	-5.0130	-3.1073	2.8766	C
126	H126	-5.5295	-3.9899	2.4566	H
127	H127	-5.5514	-2.2079	2.5204	H

128 H128 -5.1172 -3.1460 3.9783 H

@<TRIPOS>BOND

1 1 21 1
2 1 22 1
3 1 25 1
4 1 27 1
5 1 29 1
6 1 31 1
7 1 32 1
8 1 35 1
9 1 36 1
10 1 38 1
11 2 4 1
12 2 5 1
13 2 7 1
14 2 9 1
15 2 11 1
16 2 13 1
17 2 14 1
18 2 17 1
19 2 19 1
20 2 20 1
21 3 4 1
22 4 5 1
23 4 11 Ar
24 5 7 1
25 5 44 1
26 6 11 1
27 7 8 1
28 7 9 Ar
29 9 10 1
30 9 11 Ar
31 12 13 1
32 13 14 Ar
33 13 20 Ar
34 14 16 1
35 14 17 Ar
36 15 20 1
37 17 18 1
38 17 19 1
39 19 20 1
40 19 39 1
41 21 22 1
42 21 29 1
43 21 42 1
44 22 24 1
45 22 25 Ar
46 23 29 1
47 25 26 1
48 25 27 Ar
49 27 28 1
50 27 29 Ar

51 30 31 1
52 31 32 Ar
53 31 38 Ar
54 32 34 1
55 32 35 1
56 33 38 1
57 35 36 1
58 35 41 1
59 36 37 1
60 36 38 Ar
61 39 40 1
62 39 59 1
63 39 63 1
64 40 41 1
65 40 53 1
66 40 56 1
67 41 45 1
68 41 49 1
69 42 43 1
70 42 81 1
71 42 85 1
72 43 44 1
73 43 75 1
74 43 78 1
75 44 67 1
76 44 71 1
77 45 46 1
78 45 47 1
79 45 48 1
80 49 50 1
81 49 51 1
82 49 52 1
83 53 54 1
84 53 55 1
85 53 89 1
86 56 57 1
87 56 58 1
88 56 92 1
89 59 60 1
90 59 61 1
91 59 62 1
92 63 64 1
93 63 65 1
94 63 66 1
95 67 68 1
96 67 69 1
97 67 70 1
98 71 72 1
99 71 73 1
100 71 74 1
101 75 76 1
102 75 77 1

103 75 109 1
104 78 79 1
105 78 80 1
106 78 112 1
107 81 82 1
108 81 83 1
109 81 84 1
110 85 86 1
111 85 87 1
112 85 88 1
113 89 90 1
114 89 91 1
115 89 95 1
116 92 93 1
117 92 94 1
118 92 98 1
119 95 96 1
120 95 97 1
121 95 101 1
122 98 99 1
123 98 100 1
124 98 105 1
125 101 102 1
126 101 103 1
127 101 104 1
128 105 106 1
129 105 107 1
130 105 108 1
131 109 110 1
132 109 111 1
133 109 115 1
134 112 113 1
135 112 114 1
136 112 118 1
137 115 116 1
138 115 117 1
139 115 121 1
140 118 119 1
141 118 120 1
142 118 125 1
143 121 122 1
144 121 123 1
145 121 124 1
146 125 126 1
147 125 127 1
148 125 128 1

A5.6: Compound 11 (mono cation) .mol2

DFT LSDA SDD no symm

Created by GaussView 5.0.9

#

#

#

@<TRIPOS>MOLECULE

Molecule Name

128 140

SMALL

NO_CHARGES

@<TRIPOS>ATOM

1	Fe1	0.6348	4.4754	0.0809	Fe
2	Fe2	-0.6206	-4.2079	0.0398	Fe
3	H3	2.1334	-4.7770	0.4409	H
4	C4	1.4069	-4.3742	-0.2698	C
5	C5	1.0114	-2.9892	-0.3620	C
6	H6	0.7373	-6.2201	-1.3870	H
7	C7	0.0038	-2.9182	-1.3987	C
8	H8	-0.5210	-2.0113	-1.7115	H
9	C9	-0.2044	-4.2386	-1.9409	C
10	H10	-0.9087	-4.5047	-2.7313	H
11	C11	0.6682	-5.1418	-1.2341	C
12	H12	-0.3334	-4.5638	2.8311	H
13	C13	-1.0416	-4.5640	2.0005	C
14	C14	-1.3828	-5.6958	1.1770	C
15	H15	-1.7727	-2.4238	1.9376	H
16	H16	-0.9755	-6.7041	1.2670	H
17	C17	-2.3534	-5.2509	0.2066	C
18	H18	-2.7872	-5.8733	-0.5797	H
19	C19	-2.6376	-3.8484	0.4236	C
20	C20	-1.8181	-3.4422	1.5380	C
21	C21	2.5358	4.2585	-0.7181	C
22	C22	2.3530	5.5341	-0.0524	C
23	H23	1.3685	3.3616	-2.4298	H
24	H24	2.9356	5.8946	0.7990	H
25	C25	1.2626	6.2447	-0.6740	C
26	H26	0.8930	7.2325	-0.3946	H
27	C27	0.7471	5.4111	-1.7291	C
28	H28	-0.0864	5.6516	-2.3921	H
29	C29	1.5326	4.2046	-1.7532	C
30	H30	1.2553	4.2036	2.7965	H
31	C31	0.4807	4.0362	2.0457	C
32	C32	0.3112	2.8470	1.2468	C
33	H33	-0.6873	5.9752	2.0622	H
34	H34	0.9561	1.9638	1.2717	H
35	C35	-0.8208	3.0293	0.3659	C
36	C36	-1.3378	4.3528	0.6294	C
37	H37	-2.1764	4.8217	0.1078	H
38	C38	-0.5464	4.9712	1.6588	C

39	Sn39	-3.9149	-2.6020	-0.7920	Sn
40	Sn40	-3.6062	0.1028	0.0219	Sn
41	Sn41	-1.6040	1.7498	-1.1817	Sn
42	Sn42	3.9710	2.8060	-0.0205	Sn
43	Sn43	3.6704	0.0796	-0.7629	Sn
44	Sn44	1.8883	-1.4595	0.8818	Sn
45	C45	-2.3715	3.1694	-2.6277	C
46	H46	-1.5218	3.5967	-3.1926	H
47	H47	-2.8985	3.9876	-2.1035	H
48	H48	-3.0707	2.6974	-3.3386	H
49	C49	0.0497	0.6742	-2.0852	C
50	H50	0.6599	0.1563	-1.3189	H
51	H51	0.7015	1.3895	-2.6209	H
52	H52	-0.3160	-0.0694	-2.8166	H
53	C53	-3.3994	0.0067	2.1996	C
54	H54	-2.3689	-0.2794	2.4927	H
55	H55	-3.5652	1.0368	2.5747	H
56	C56	-5.5103	1.1164	-0.3913	C
57	H57	-6.2140	0.7873	0.4005	H
58	H58	-5.9052	0.7368	-1.3530	H
59	C59	-5.9552	-3.1800	-0.3319	C
60	H60	-6.1646	-2.9819	0.7344	H
61	H61	-6.0994	-4.2567	-0.5311	H
62	H62	-6.6675	-2.6041	-0.9480	H
63	C63	-3.4401	-3.1139	-2.8432	C
64	H64	-2.4378	-2.7395	-3.1182	H
65	H65	-4.1837	-2.6776	-3.5322	H
66	H66	-3.4581	-4.2134	-2.9601	H
67	C67	0.2931	-0.4905	1.9935	C
68	H68	0.6819	0.3144	2.6417	H
69	H69	-0.1713	-1.2581	2.6407	H
70	H70	-0.4773	-0.0657	1.3221	H
71	C71	3.0586	-2.6175	2.2914	C
72	H72	3.3447	-1.9945	3.1571	H
73	H73	3.9815	-3.0025	1.8205	H
74	H74	2.4532	-3.4696	2.6543	H
75	C75	5.5850	-0.7458	-0.0921	C
76	H76	6.3848	-0.4064	-0.7827	H
77	H77	5.5187	-1.8487	-0.1963	H
78	C78	3.3536	-0.2918	-2.8996	C
79	H79	4.3430	-0.1446	-3.3774	H
80	H80	2.6757	0.4898	-3.2925	H
81	C81	3.9052	3.0275	2.1382	C
82	H82	4.7588	2.4957	2.5952	H
83	H83	2.9681	2.6119	2.5514	H
84	H84	3.9705	4.0985	2.4066	H
85	C85	5.9281	3.4362	-0.7134	C
86	H86	6.6935	2.7121	-0.3812	H
87	H87	6.1690	4.4284	-0.2922	H
88	H88	5.9508	3.5008	-1.8147	H
89	C89	-4.4260	-0.9637	2.7830	C
90	H90	-4.1835	-2.0022	2.4657	H

91	H91	-5.4392	-0.7445	2.3733	H
92	C92	-5.3835	2.6389	-0.4151	C
93	H93	-6.3865	3.0858	-0.5878	H
94	H94	-4.7584	2.9464	-1.2799	H
95	C95	-4.5042	-0.9094	4.3100	C
96	H96	-3.4946	-1.0999	4.7299	H
97	H97	-5.1528	-1.7321	4.6708	H
98	C98	-4.8074	3.2360	0.8676	C
99	H99	-3.7605	2.8790	1.0129	H
100	H100	-4.7370	4.3376	0.7566	H
101	C101	-5.0380	0.4198	4.8279	C
102	H102	-5.1167	0.4235	5.9293	H
103	H103	-6.0461	0.6243	4.4175	H
104	H104	-4.3847	1.2651	4.5393	H
105	C105	-5.6367	2.9039	2.0997	C
106	H106	-5.2291	3.3777	3.0113	H
107	H107	-5.6746	1.8132	2.2876	H
108	H108	-6.6786	3.2551	1.9746	H
109	C109	5.9111	-0.3434	1.3440	C
110	H110	5.0538	-0.5830	2.0142	H
111	H111	6.0466	0.7597	1.4017	H
112	C112	2.8034	-1.6858	-3.1901	C
113	H113	2.7552	-1.8313	-4.2913	H
114	H114	1.7597	-1.7634	-2.8208	H
115	C115	7.1589	-1.0359	1.8949	C
116	H116	7.4171	-0.5979	2.8794	H
117	H117	8.0161	-0.8245	1.2236	H
118	C118	3.6250	-2.8254	-2.5932	C
119	H119	3.5718	-2.7766	-1.4804	H
120	H120	3.1498	-3.7900	-2.8634	H
121	C121	6.9787	-2.5412	2.0426	C
122	H122	7.8784	-3.0177	2.4700	H
123	H123	6.7835	-3.0256	1.0670	H
124	H124	6.1265	-2.7708	2.7128	H
125	C125	5.0798	-2.8117	-3.0372	C
126	H126	5.6315	-3.6910	-2.6590	H
127	H127	5.6078	-1.9097	-2.6717	H
128	H128	5.1547	-2.8182	-4.1413	H

@<TRIPOS>BOND

1	1	22	1
2	1	25	1
3	1	27	1
4	1	31	1
5	1	32	1
6	1	38	1
7	2	7	1
8	2	9	1
9	2	11	1
10	2	13	1
11	2	14	1
12	2	17	1
13	3	4	1

14 4 5 Ar
15 4 11 Ar
16 5 7 Ar
17 5 44 1
18 6 11 1
19 7 8 1
20 7 9 Ar
21 9 10 1
22 9 11 Ar
23 12 13 1
24 13 14 Ar
25 13 20 Ar
26 14 16 1
27 14 17 Ar
28 15 20 1
29 17 18 1
30 17 19 Ar
31 19 20 Ar
32 19 39 1
33 21 22 1
34 21 29 Ar
35 21 42 1
36 22 24 1
37 22 25 Ar
38 23 29 1
39 25 26 1
40 25 27 Ar
41 27 28 1
42 27 29 Ar
43 30 31 1
44 31 32 Ar
45 31 38 Ar
46 32 34 1
47 32 35 Ar
48 33 38 1
49 35 36 Ar
50 35 41 1
51 36 37 1
52 36 38 Ar
53 39 40 1
54 39 59 1
55 39 63 1
56 40 41 1
57 40 53 1
58 40 56 1
59 41 45 1
60 41 49 1
61 42 43 1
62 42 81 1
63 42 85 1
64 43 44 1
65 43 75 1

66 43 78 1
67 44 67 1
68 44 71 1
69 45 46 1
70 45 47 1
71 45 48 1
72 49 50 1
73 49 51 1
74 49 52 1
75 53 54 1
76 53 55 1
77 53 89 1
78 56 57 1
79 56 58 1
80 56 92 1
81 59 60 1
82 59 61 1
83 59 62 1
84 63 64 1
85 63 65 1
86 63 66 1
87 67 68 1
88 67 69 1
89 67 70 1
90 71 72 1
91 71 73 1
92 71 74 1
93 75 76 1
94 75 77 1
95 75 109 1
96 78 79 1
97 78 80 1
98 78 112 1
99 81 82 1
100 81 83 1
101 81 84 1
102 85 86 1
103 85 87 1
104 85 88 1
105 89 90 1
106 89 91 1
107 89 95 1
108 92 93 1
109 92 94 1
110 92 98 1
111 95 96 1
112 95 97 1
113 95 101 1
114 98 99 1
115 98 100 1
116 98 105 1
117 101 102 1

118 101 103 1
119 101 104 1
120 105 106 1
121 105 107 1
122 105 108 1
123 109 110 1
124 109 111 1
125 109 115 1
126 112 113 1
127 112 114 1
128 112 118 1
129 115 116 1
130 115 117 1
131 115 121 1
132 118 119 1
133 118 120 1
134 118 125 1
135 121 122 1
136 121 123 1
137 121 124 1
138 125 126 1
139 125 127 1
140 125 128 1

A5.7: Compound 12a .mol2

```
# DFT SDD LSDA no symm  
# Created by GaussView 5.0.9  
#
```

```
#  
#
```

```
@<TRIPOS>MOLECULE  
Molecule Name  
49 68  
SMALL  
NO_CHARGES
```

```
@<TRIPOS>ATOM  
1 Fe1      0.0161      3.2449      1.0844 Fe  
2 H2       1.7864      2.5197      3.1397 H  
3 C3       1.6461      3.1675      2.2723 C  
4 C4       1.0623      4.4864      2.2842 C  
5 H5       2.4440      1.9151      0.5619 H  
6 H6       0.6830      5.0119      3.1619 H  
7 C7       1.0424      4.9775      0.9284 C  
8 H8       0.6472      5.9406      0.6013 H  
9 C9       1.6138      3.9623      0.0782 C
```

10	H10	1.7321	4.0250	-1.0051	H
11	C11	1.9902	2.8460	0.9096	C
12	H12	-1.0913	1.3066	2.7648	H
13	C13	-1.2717	1.9157	1.8757	C
14	C14	-0.9235	1.5425	0.5206	C
15	H15	-2.1893	3.7970	2.7352	H
16	C16	-1.2990	2.6559	-0.3240	C
17	H17	-1.1551	2.7080	-1.4059	H
18	C18	-1.8650	3.6956	0.4977	C
19	H19	-2.2251	4.6653	0.1501	H
20	C20	-1.8483	3.2358	1.8637	C
21	Fe21	-0.5149	-3.1910	-1.1277	Fe
22	H22	-1.3061	-1.0750	-2.7875	H
23	C23	-1.5691	-1.6596	-1.9026	C
24	C24	-1.1608	-1.3625	-0.5463	C
25	H25	-2.7918	-3.3515	-2.7749	H
26	C26	-1.7122	-2.4078	0.2893	C
27	H27	-1.5694	-2.4970	1.3689	H
28	C28	-2.4442	-3.3314	-0.5384	C
29	H29	-2.9568	-4.2328	-0.1986	H
30	C30	-2.3555	-2.8669	-1.8999	C
31	H31	2.1103	-2.2170	-0.8104	H
32	C32	1.5026	-3.0928	-1.0492	C
33	C33	1.0584	-3.4726	-2.3667	C
34	H34	1.1400	-4.0424	0.9727	H
35	H35	1.2685	-2.9355	-3.2933	H
36	C36	0.2779	-4.6783	-2.2429	C
37	H37	-0.2129	-5.2113	-3.0587	H
38	C38	0.2377	-5.0420	-0.8478	C
39	H39	-0.2875	-5.8992	-0.4239	H
40	C40	0.9942	-4.0605	-0.1091	C
41	C41	1.1601	0.4138	-1.4129	C
42	H42	2.2080	0.1510	-1.1720	H
43	H43	1.1270	1.4969	-1.6342	H
44	H44	0.8767	-0.1514	-2.3202	H
45	C45	0.8964	-0.6274	1.5519	C
46	H46	1.5532	0.1611	1.9639	H
47	H47	1.5056	-1.5197	1.3184	H
48	H48	0.1723	-0.9109	2.3397	H
49	Si49	-0.0033	-0.0057	0.0176	Si

@<TRIPOS>BOND

1	1	3	1
2	1	4	1
3	1	7	1
4	1	9	1
5	1	11	1
6	1	13	1
7	1	14	1
8	1	16	1
9	1	18	1
10	1	20	1
11	2	3	1

12 3 4 Ar
13 3 11 Ar
14 4 6 1
15 4 7 Ar
16 5 11 1
17 7 8 1
18 7 9 Ar
19 9 10 1
20 9 11 Ar
21 12 13 1
22 13 14 1
23 13 20 Ar
24 14 16 Ar
25 14 49 1
26 15 20 1
27 16 17 1
28 16 18 Ar
29 18 19 1
30 18 20 Ar
31 21 23 1
32 21 24 1
33 21 26 1
34 21 28 1
35 21 30 1
36 21 32 1
37 21 33 1
38 21 36 1
39 21 38 1
40 21 40 1
41 22 23 1
42 23 24 Ar
43 23 30 Ar
44 24 26 Ar
45 24 49 1
46 25 30 1
47 26 27 1
48 26 28 Ar
49 28 29 1
50 28 30 Ar
51 31 32 1
52 32 33 Ar
53 32 40 Ar
54 33 35 1
55 33 36 Ar
56 34 40 1
57 36 37 1
58 36 38 Ar
59 38 39 1
60 38 40 Ar
61 41 42 1
62 41 43 1
63 41 44 1

```
64 41 49 1
65 45 46 1
66 45 47 1
67 45 48 1
68 45 49 1
```

A5.8: Compound 12b .mol2

```
# DFT LSDA SDD no symm
# Created by GaussView 5.0.9
#
```

```
#
#
```

```
@<TRIPOS>MOLECULE
Molecule Name
58 77
SMALL
NO_CHARGES
```

```
@<TRIPOS>ATOM
1 Fe1      -4.4169      0.2917      0.1398 Fe
2 H2       -4.7375     -1.1122     -2.2703 H
3 C3       -5.0496     -1.0529     -1.2262 C
4 C4       -6.1558     -0.2826     -0.7130 C
5 H5       -3.5429     -2.3688     -0.1676 H
6 H6       -6.8294      0.3430     -1.3008 H
7 C7       -6.2006     -0.4642      0.7167 C
8 H8       -6.9147     -0.0011      1.3996 H
9 C9       -5.1228     -1.3478      1.0878 C
10 H10     -4.8755     -1.6698      2.1009 H
11 C11     -4.4150     -1.7137     -0.1133 C
12 H12     -2.8880      1.4247     -1.9144 H
13 C13     -3.1454      1.4989     -0.8549 C
14 C14     -2.4578      0.8200      0.2235 C
15 H15     -4.9569      2.8552     -0.8748 H
16 C16     -3.1564      1.1697      1.4434 C
17 H17     -2.9068      0.8006      2.4411 H
18 C18     -4.2520      2.0490      1.1195 C
19 H19     -4.9700      2.4691      1.8256 H
20 C20     -4.2450      2.2533     -0.3078 C
21 Fe21      4.3475     -0.4021     -0.1803 Fe
22 H22      2.5813     -0.8626     -2.3032 H
23 C23      2.8700     -1.1902     -1.3012 C
24 C24      2.3387     -0.6587     -0.0627 C
25 H25      4.4554     -2.7507     -1.7190 H
26 C26      3.0251     -1.3483      1.0099 C
27 H27      2.8750     -1.1655      2.0767 H
```

28	C28	3.9631	-2.2837	0.4404	C
29	H29	4.6389	-2.9359	0.9961	H
30	C30	3.8664	-2.1856	-0.9948	C
31	H31	4.8169	1.3908	-2.2939	H
32	C32	5.1407	1.0822	-1.2983	C
33	C33	6.1295	0.0752	-1.0017	C
34	H34	3.8797	2.3712	0.0698	H
35	H35	6.6870	-0.5117	-1.7334	H
36	C36	6.2363	-0.0360	0.4320	C
37	H37	6.8884	-0.7222	0.9747	H
38	C38	5.3137	0.9027	1.0219	C
39	H39	5.1448	1.0520	2.0897	H
40	C40	4.6403	1.5958	-0.0478	C
41	C41	-1.1117	-1.5821	1.5277	C
42	H42	-2.0927	-2.0918	1.5720	H
43	H43	-0.9681	-1.0390	2.4810	H
44	H44	-0.3157	-2.3455	1.4506	H
45	C45	-1.1408	-1.2696	-1.6002	C
46	H46	-1.1646	-0.5330	-2.4260	H
47	H47	-2.0502	-1.8947	-1.6780	H
48	H48	-0.2533	-1.9140	-1.7461	H
49	C49	1.2040	1.8230	-1.4116	C
50	H50	0.9851	1.2521	-2.3341	H
51	H51	2.2269	2.2348	-1.5019	H
52	H52	0.4866	2.6619	-1.3546	H
53	C53	1.3466	1.6138	1.7255	C
54	H54	0.6022	2.4186	1.8653	H
55	H55	2.3590	2.0597	1.7553	H
56	H56	1.2574	0.9178	2.5809	H
57	Si57	1.0628	0.6991	0.0991	Si
58	Si58	-1.0383	-0.3864	0.0678	Si

@<TRIPOS>BOND

1	1	3	1
2	1	4	1
3	1	7	1
4	1	9	1
5	1	11	1
6	1	13	1
7	1	14	1
8	1	16	1
9	1	18	1
10	1	20	1
11	2	3	1
12	3	4	Ar
13	3	11	Ar
14	4	6	1
15	4	7	Ar
16	5	11	1
17	7	8	1
18	7	9	Ar
19	9	10	1
20	9	11	Ar

21 12 13 1
22 13 14 1
23 13 20 Ar
24 14 16 1
25 14 58 1
26 15 20 1
27 16 17 1
28 16 18 Ar
29 18 19 1
30 18 20 Ar
31 21 23 1
32 21 24 1
33 21 26 1
34 21 28 1
35 21 30 1
36 21 32 1
37 21 33 1
38 21 36 1
39 21 38 1
40 21 40 1
41 22 23 1
42 23 24 1
43 23 30 Ar
44 24 26 1
45 24 57 1
46 25 30 1
47 26 27 1
48 26 28 Ar
49 28 29 1
50 28 30 Ar
51 31 32 1
52 32 33 Ar
53 32 40 Ar
54 33 35 1
55 33 36 Ar
56 34 40 1
57 36 37 1
58 36 38 Ar
59 38 39 1
60 38 40 Ar
61 41 42 1
62 41 43 1
63 41 44 1
64 41 58 1
65 45 46 1
66 45 47 1
67 45 48 1
68 45 58 1
69 49 50 1
70 49 51 1
71 49 52 1
72 49 57 1

73 53 54 1
74 53 55 1
75 53 56 1
76 53 57 1
77 57 58 1

A5.9: Compound 12c .mol2

DFT LSDA SDD no symm
Created by GaussView 5.0.9
#

#

@<TRIPOS>MOLECULE
Molecule Name
67 86
SMALL
NO_CHARGES

@<TRIPOS>ATOM
1 Fe1 -2.9735 0.7818 -0.3594 Fe
2 H2 -3.1315 -1.5042 -1.9812 H
3 C3 -3.5089 -1.0299 -1.0737 C
4 C4 -4.6502 -0.1523 -0.9857 C
5 H5 -2.0563 -1.7367 0.5115 H
6 H6 -5.2916 0.1505 -1.8147 H
7 C7 -4.7805 0.2734 0.3859 C
8 H8 -5.5388 0.9540 0.7762 H
9 C9 -3.7200 -0.3405 1.1462 C
10 H10 -3.5347 -0.2058 2.2132 H
11 C11 -2.9367 -1.1480 0.2444 C
12 H12 -1.3298 1.0103 -2.6124 H
13 C13 -1.6551 1.5101 -1.6967 C
14 C14 -1.0319 1.3660 -0.3973 C
15 H15 -3.4735 2.6725 -2.3795 H
16 C16 -1.8091 2.1683 0.5245 C
17 H17 -1.6194 2.2598 1.5968 H
18 C18 -2.8914 2.7921 -0.1957 C
19 H19 -3.6576 3.4418 0.2306 H
20 C20 -2.7947 2.3845 -1.5750 C
21 Fe21 7.7153 1.3785 0.3066 Fe
22 H22 6.0401 3.1790 1.6425 H
23 C23 6.3694 2.8343 0.6594 C
24 C24 5.7637 1.7577 -0.0969 C
25 H25 8.1626 4.1507 0.2422 H
26 C26 6.5393 1.6197 -1.3121 C
27 H27 6.3614 0.8772 -2.0937 H

28	C28	7.6023	2.5935	-1.3019	C
29	H29	8.3615	2.7243	-2.0748	H
30	C30	7.4965	3.3479	-0.0779	C
31	H31	7.9379	1.1060	3.0956	H
32	C32	8.2936	0.7355	2.1326	C
33	C33	9.4168	1.2494	1.3885	C
34	H34	6.8399	-0.9330	1.6603	H
35	H35	10.0610	2.0772	1.6891	H
36	C36	9.5257	0.4928	0.1658	C
37	H37	10.2675	0.6461	-0.6195	H
38	C38	8.4692	-0.4890	0.1536	C
39	H39	8.2711	-1.2088	-0.6424	H
40	C40	7.7108	-0.3406	1.3707	C
41	C41	0.3694	-0.1889	1.8246	C
42	H42	-0.5878	-0.7064	2.0290	H
43	H43	0.4290	0.6951	2.4872	H
44	H44	1.1988	-0.8694	2.0941	H
45	C45	0.5343	-1.1508	-1.1584	C
46	H46	0.5887	-0.8047	-2.2081	H
47	H47	-0.3677	-1.7825	-1.0524	H
48	H48	1.4284	-1.7729	-0.9642	H
49	C49	4.2196	0.6815	2.3106	C
50	H50	4.1278	1.7100	2.7088	H
51	H51	5.1305	0.2266	2.7441	H
52	H52	3.3383	0.1088	2.6568	H
53	C53	4.4892	-1.0165	-0.3117	C
54	H54	3.7071	-1.6957	0.0778	H
55	H55	5.4804	-1.4431	-0.0657	H
56	H56	4.3930	-0.9891	-1.4135	H
57	C57	2.4627	1.9627	-2.2770	C
58	H58	3.3325	2.5974	-2.5308	H
59	H59	1.5487	2.4497	-2.6671	H
60	H60	2.5833	0.9929	-2.7954	H
61	C61	2.0566	3.3784	0.4726	C
62	H62	2.8467	4.1038	0.2023	H
63	H63	2.0654	3.2560	1.5722	H
64	H64	1.0762	3.8040	0.1849	H
65	Si65	0.4702	0.3314	0.0107	Si
66	Si66	2.3342	1.7182	-0.4012	Si
67	Si67	4.3021	0.7164	0.4230	Si

@<TRIPOS>BOND

1 1 3 1
2 1 4 1
3 1 7 1
4 1 9 1
5 1 11 1
6 1 13 1
7 1 14 1
8 1 16 1
9 1 18 1
10 1 20 1
11 2 3 1

12 3 4 Ar
13 3 11 Ar
14 4 6 1
15 4 7 Ar
16 5 11 1
17 7 8 1
18 7 9 Ar
19 9 10 1
20 9 11 Ar
21 12 13 1
22 13 14 1
23 13 20 Ar
24 14 16 1
25 14 65 1
26 15 20 1
27 16 17 1
28 16 18 Ar
29 18 19 1
30 18 20 Ar
31 21 23 1
32 21 24 1
33 21 26 1
34 21 28 1
35 21 30 1
36 21 32 1
37 21 33 1
38 21 36 1
39 21 38 1
40 21 40 1
41 22 23 1
42 23 24 1
43 23 30 Ar
44 24 26 1
45 24 67 1
46 25 30 1
47 26 27 1
48 26 28 Ar
49 28 29 1
50 28 30 Ar
51 31 32 1
52 32 33 Ar
53 32 40 Ar
54 33 35 1
55 33 36 Ar
56 34 40 1
57 36 37 1
58 36 38 Ar
59 38 39 1
60 38 40 Ar
61 41 42 1
62 41 43 1
63 41 44 1

64 41 65 1
65 45 46 1
66 45 47 1
67 45 48 1
68 45 65 1
69 49 50 1
70 49 51 1
71 49 52 1
72 49 67 1
73 53 54 1
74 53 55 1
75 53 56 1
76 53 67 1
77 57 58 1
78 57 59 1
79 57 60 1
80 57 66 1
81 61 62 1
82 61 63 1
83 61 64 1
84 61 66 1
85 65 66 1
86 66 67 1

A5.10: Compound 12d .mol2

```
# DFT LSDA SDD no symm  
# Created by GaussView 5.0.9  
#
```

```
#  
#
```

```
@<TRIPOS>MOLECULE  
Molecule Name  
58 77  
SMALL  
NO_CHARGES
```

```
@<TRIPOS>ATOM  
1 Fe1 -0.0485 0.0399 -0.0122 Fe  
2 H2 -1.7349 1.8729 -1.2924 H  
3 C3 -1.7028 1.0047 -0.6308 C  
4 C4 -1.6034 1.0414 0.8057 C  
5 C5 -1.5608 -0.3181 1.2822 C  
6 H6 -1.4694 -0.6320 2.3231 H  
7 C7 -1.6332 -1.1912 0.1385 C  
8 H8 -1.6025 -2.2825 0.1627 H
```

9	C9	-1.7205	-0.3797	-1.0589	C
10	H10	1.6234	1.9580	1.1818	H
11	C11	1.5972	1.0592	0.5638	C
12	C12	1.4932	1.0218	-0.8738	C
13	H13	1.7035	-0.6099	2.0874	H
14	H14	1.4248	1.8858	-1.5366	H
15	C15	1.4737	-0.3606	-1.2823	C
16	H16	1.3819	-0.7250	-2.3078	H
17	C17	1.5616	-1.1782	-0.0980	C
18	H18	1.5526	-2.2689	-0.0707	H
19	C19	1.6390	-0.3003	1.0433	C
20	H20	-1.5519	1.9403	1.4219	H
21	Si21	-1.7383	-0.9970	-2.8137	Si
22	H22	-1.0345	-0.0106	-3.7127	H
23	H23	-1.0140	-2.3176	-2.8985	H
24	Si24	-3.9299	-1.2981	-3.6160	Si
25	H25	-4.6609	-2.2841	-2.7411	H
26	H26	-4.6771	0.0094	-3.5461	H
27	Si27	-3.9862	-2.0759	-5.8276	Si
28	H28	-3.2700	-3.3986	-5.9210	H
29	H29	-3.2636	-1.1065	-6.7272	H
30	Si30	-6.1886	-2.3353	-6.5888	Si
31	H31	-6.9124	-3.3013	-5.6864	H
32	H32	-6.8998	-1.0099	-6.4904	H
33	Si33	-6.2747	-3.1065	-8.8020	Si
34	H34	-5.5922	-4.4480	-8.8787	H
35	H35	-5.5016	-2.1519	-9.6755	H
36	Si36	-8.4886	-3.2785	-9.5807	Si
37	H37	-9.2235	-4.2662	-8.7085	H
38	H38	-9.1423	-1.9277	-9.4211	H
39	C39	-8.5762	-3.8193	-11.3581	C
40	C40	-8.6320	-2.9567	-12.5212	C
41	C41	-8.6897	-5.1815	-11.8394	C
42	H42	-8.5928	-1.8656	-12.5031	H
43	C43	-8.7795	-3.7770	-13.6963	C
44	C44	-8.8157	-5.1544	-13.2740	C
45	H45	-8.7008	-6.0759	-11.2128	H
46	H46	-8.8676	-3.4163	-14.7222	H
47	H47	-8.9362	-6.0227	-13.9235	H
48	H48	-11.6291	-3.3390	-10.0321	H
49	C49	-11.7603	-3.6511	-11.0704	C
50	C50	-11.8170	-2.7785	-12.2166	C
51	C51	-11.8751	-5.0102	-11.5368	C
52	C52	-11.9707	-3.5989	-13.3925	C
53	H53	-11.7404	-1.6904	-12.1976	H
54	H54	-11.8515	-5.9054	-10.9136	H
55	C55	-12.0070	-4.9781	-12.9723	C
56	H56	-12.0336	-3.2403	-14.4210	H
57	H57	-12.1005	-5.8454	-13.6273	H
58	Fe58	-10.2893	-4.0903	-12.3871	Fe

@<TRIPOS>BOND

1 1 3 1

2 1 4 1
3 1 5 1
4 1 7 1
5 1 9 1
6 1 11 1
7 1 12 1
8 1 15 1
9 1 17 1
10 1 19 1
11 2 3 1
12 3 4 Ar
13 3 9 1
14 4 5 Ar
15 4 20 1
16 5 6 1
17 5 7 Ar
18 7 8 1
19 7 9 1
20 9 21 1
21 10 11 1
22 11 12 Ar
23 11 19 Ar
24 12 14 1
25 12 15 Ar
26 13 19 1
27 15 16 1
28 15 17 Ar
29 17 18 1
30 17 19 Ar
31 21 22 1
32 21 23 1
33 21 24 1
34 24 25 1
35 24 26 1
36 24 27 1
37 27 28 1
38 27 29 1
39 27 30 1
40 30 31 1
41 30 32 1
42 30 33 1
43 33 34 1
44 33 35 1
45 33 36 1
46 36 37 1
47 36 38 1
48 36 39 1
49 39 40 1
50 39 41 1
51 39 58 1
52 40 42 1
53 40 43 Ar

```
54 40 58 1
55 41 44 Ar
56 41 45 1
57 41 58 1
58 43 44 Ar
59 43 46 1
60 43 58 1
61 44 47 1
62 44 58 1
63 48 49 1
64 49 50 Ar
65 49 51 Ar
66 49 58 1
67 50 52 Ar
68 50 53 1
69 50 58 1
70 51 54 1
71 51 55 Ar
72 51 58 1
73 52 55 Ar
74 52 56 1
75 52 58 1
76 55 57 1
77 55 58 1
```

A5.11: Compound 13 .mol2

```
# DFT SDD LSDA no symm
# Created by GaussView 5.0.9
#
```

```
#
#
```

```
@<TRIPOS>MOLECULE
Molecule Name
49 68
SMALL
NO_CHARGES
```

```
@<TRIPOS>ATOM
1 Fe1      0.0167      3.3945      1.1120 Fe
2 H2       1.7440      2.4907      3.1352 H
3 C3       1.6582      3.1393      2.2616 C
4 C4       1.2344      4.5179      2.2645 C
5 H5       2.2712      1.7824      0.5537 H
6 H6       0.9452      5.0985      3.1419 H
7 C7       1.2377      4.9887      0.9012 C
```

8 H8	0.9506	5.9871	0.5678 H
9 C9	1.6635	3.9016	0.0552 C
10 H10	1.7627	3.9338	-1.0314 H
11 C11	1.9267	2.7608	0.8965 C
12 H12	-1.2887	1.6473	2.8642 H
13 C13	-1.4087	2.2519	1.9619 C
14 C14	-1.1517	1.8061	0.6071 C
15 H15	-2.0642	4.2517	2.7959 H
16 C16	-1.3956	2.9451	-0.2549 C
17 H17	-1.2717	2.9613	-1.3404 H
18 C18	-1.8043	4.0659	0.5555 C
19 H19	-2.0475	5.0663	0.1937 H
20 C20	-1.8130	3.6355	1.9310 C
21 Fe21	-0.5315	-3.3323	-1.1557 Fe
22 H22	-1.5730	-1.3162	-2.7948 H
23 C23	-1.7732	-1.9420	-1.9215 C
24 C24	-1.4384	-1.6128	-0.5499 C
25 H25	-2.7324	-3.7724	-2.8452 H
26 C26	-1.8467	-2.7458	0.2565 C
27 H27	-1.7135	-2.8395	1.3368 H
28 C28	-2.4291	-3.7468	-0.6029 C
29 H29	-2.8188	-4.7163	-0.2882 H
30 C30	-2.3837	-3.2479	-1.9541 C
31 H31	1.9435	-2.0982	-0.5813 H
32 C32	1.4553	-3.0031	-0.9506 C
33 C33	1.1161	-3.2790	-2.3244 C
34 H34	1.1343	-4.2177	0.9326 H
35 H35	1.2940	-2.6163	-3.1734 H
36 C36	0.4893	-4.5768	-2.3749 C
37 H37	0.1030	-5.0681	-3.2692 H
38 C38	0.4372	-5.0998	-1.0319 C
39 H39	0.0075	-6.0572	-0.7331 H
40 C40	1.0316	-4.1253	-0.1504 C
41 Sn41	-0.1750	-0.0109	0.0715 Sn
42 C42	1.1195	0.4238	-1.6086 C
43 H43	2.1783	0.2315	-1.3535 H
44 H44	1.0160	1.4852	-1.8992 H
45 H45	0.8433	-0.2254	-2.4598 H
46 C46	0.8834	-0.6896	1.8294 C
47 H47	1.8383	-0.1448	1.9466 H
48 H48	1.0887	-1.7724	1.7451 H
49 H49	0.2703	-0.5104	2.7316 H

@<TRIPOS>BOND

1 1 3 1
2 1 4 1
3 1 7 1
4 1 9 1
5 1 11 1
6 1 13 1
7 1 14 1
8 1 16 1
9 1 18 1

10 1 20 1
11 2 3 1
12 3 4 Ar
13 3 11 Ar
14 4 6 1
15 4 7 Ar
16 5 11 1
17 7 8 1
18 7 9 Ar
19 9 10 1
20 9 11 Ar
21 12 13 1
22 13 14 1
23 13 20 Ar
24 14 16 1
25 14 41 1
26 15 20 1
27 16 17 1
28 16 18 Ar
29 18 19 1
30 18 20 Ar
31 21 23 1
32 21 24 1
33 21 26 1
34 21 28 1
35 21 30 1
36 21 32 1
37 21 33 1
38 21 36 1
39 21 38 1
40 21 40 1
41 22 23 1
42 23 24 1
43 23 30 Ar
44 24 26 1
45 24 41 1
46 25 30 1
47 26 27 1
48 26 28 Ar
49 28 29 1
50 28 30 Ar
51 31 32 1
52 32 33 Ar
53 32 40 Ar
54 33 35 1
55 33 36 Ar
56 34 40 1
57 36 37 1
58 36 38 Ar
59 38 39 1
60 38 40 Ar
61 41 42 1

62 41 46 1
63 42 43 1
64 42 44 1
65 42 45 1
66 46 47 1
67 46 48 1
68 46 49 1

A5.11: Compound 13 .mol2

Title Card Required
Created by GaussView 4.1.2
#

#

@<TRIPOS>MOLECULE

Molecule Name

44 64

SMALL

NO_CHARGES

@<TRIPOS>ATOM

1	Fe1	3.8180	-0.0002	0.0006	Fe
2	H2	5.6667	1.6250	-1.3697	H
3	C3	4.7836	1.6177	-0.7291	C
4	C4	4.7824	1.6260	0.7130	C
5	H5	3.0658	1.5627	-2.2110	H
6	C6	3.4151	1.5952	1.1603	C
7	H7	3.0620	1.5879	2.1925	H
8	C8	2.5584	1.5894	-0.0098	C
9	C9	3.4171	1.5820	-1.1783	C
10	H10	5.6660	-1.6263	1.3704	H
11	C11	4.7827	-1.6185	0.7300	C
12	C12	4.7812	-1.6269	-0.7120	C
13	H13	3.0653	-1.5624	2.2124	H
14	H14	5.6632	-1.6422	-1.3540	H
15	C15	3.4138	-1.5953	-1.1590	C
16	H16	3.0603	-1.5879	-2.1911	H
17	C17	2.5573	-1.5889	0.0114	C
18	C18	3.4163	-1.5820	1.1796	C
19	H19	5.6645	1.6407	1.3548	H
20	N20	1.2101	-1.5918	0.0141	N
21	N21	1.2112	1.5930	-0.0118	N
22	C22	-0.0005	-1.5676	-0.0033	C
23	C23	0.0005	1.5675	-0.0040	C
24	N24	-1.2111	-1.5934	-0.0224	N
25	N25	-1.2103	1.5922	0.0020	N

26	C26	-2.5574	1.5891	0.0064	C
27	C27	-3.4191	1.5954	-1.1600	C
28	C28	-3.4112	1.5820	1.1786	C
29	Fe29	-3.8180	0.0001	0.0013	Fe
30	C30	-4.7845	1.6269	-0.7069	C
31	H31	-3.0704	1.5879	-2.1937	H
32	C32	-4.7796	1.6185	0.7352	C
33	H33	-3.0556	1.5624	2.2098	H
34	C34	-4.7861	-1.6174	-0.7254	C
35	C35	-4.7796	-1.6264	0.7167	C
36	C36	-3.4106	-1.5957	1.1589	C
37	C37	-3.4213	-1.5815	-1.1796	C
38	H38	-5.6693	1.6420	-1.3450	H
39	H39	-5.6601	1.6263	1.3794	H
40	H40	-5.6717	-1.6245	-1.3626	H
41	H41	-5.6595	-1.6415	1.3616	H
42	H42	-3.0537	-1.5889	2.1899	H
43	C43	-2.5583	-1.5894	-0.0145	C
44	H44	-3.0737	-1.5616	-2.2136	H

@<TRIPOS>BOND

1	1	3	1
2	1	4	1
3	1	6	1
4	1	8	1
5	1	9	1
6	1	11	1
7	1	12	1
8	1	15	1
9	1	17	1
10	1	18	1
11	2	3	1
12	3	4	Ar
13	3	9	Ar
14	4	6	Ar
15	4	19	1
16	5	9	1
17	6	7	1
18	6	8	1
19	8	9	1
20	8	21	Ar
21	10	11	1
22	11	12	Ar
23	11	18	Ar
24	12	14	1
25	12	15	Ar
26	13	18	1
27	15	16	1
28	15	17	1
29	17	18	1
30	17	20	Ar
31	20	22	2
32	21	23	2

33 22 24 2
34 23 25 2
35 24 43 Ar
36 25 26 Ar
37 26 27 1
38 26 28 1
39 26 29 1
40 27 29 1
41 27 30 Ar
42 27 31 1
43 28 29 1
44 28 32 Ar
45 28 33 1
46 29 30 1
47 29 32 1
48 29 34 1
49 29 35 1
50 29 36 1
51 29 37 1
52 29 43 1
53 30 32 Ar
54 30 38 1
55 32 39 1
56 34 35 Ar
57 34 37 Ar
58 34 40 1
59 35 36 Ar
60 35 41 1
61 36 42 1
62 36 43 1
63 37 43 1
64 37 44 1

References

- (1) Mark, J. E.; Allcock, H. R.; West, R. *Inorganic Polymers*; 2nd ed.; Oxford University Press: New York, USA, 2005.
- (2) Braunstein, P.; Morise, X. *Chem. Rev.* **2000**, *100*, 3541.
- (3) Trummer, M.; Choffat, F.; Smith, P.; Caseri, W. *Macromol. Rapid Commun.* **2012**, *33*, 448.
- (4) Zou, W. K.; Yang, N. L. *Polym. Prepr. (Am. Chem. Soc., Div. Polym. Chem.)* **1992**, *33*, 188.
- (5) Devylder, N.; Hill, M.; Molloy, K. C.; Price, G. J. *Chem. Commun. (Cambridge)* **1996**, 711.
- (6) Okano, M.; Matsumoto, N.; Arakawa, M.; Tsuruta, T.; Hamano, H. *Chem. Commun.* **1998**, 1799.
- (7) Okano, M.; Watanabe, K.; Totsuka, S. *Electrochemistry* **2003**, *71*, 257.
- (8) Imori, T.; Tilley, T. D. *J. Chem. Soc., Chem. Commun.* **1993**, 1607.
- (9) Imori, T.; Lu, V.; Cai, H.; Tilley, T. D. *J. Am. Chem. Soc.* **1995**, *117*, 9931.
- (10) Lu, V. Y.; Tilley, T. D. *Macromolecules* **2000**, *33*, 2403.
- (11) Neale, N. R.; Tilley, T. D. *J. Am. Chem. Soc.* **2002**, *124*, 3802.
- (12) Babcock, J. R.; Sita, L. R. *J. Am. Chem. Soc.* **1996**, *118*, 12481.
- (13) Trummer, M.; Solenthaler, D.; Smith, P.; Caseri, W. *Rsc Advances* **2011**, *1*, 823.
- (14) Choffat, F.; Smith, P.; Caseri, W. *J. Mater. Chem.* **2005**, *15*, 1789.
- (15) Trummer, M.; Choffat, F.; Raemi, M.; Smith, P.; Caseri, A. *Phosphorus, Sulfur Silicon Relat. Elem.* **2011**, *186*, 1330.
- (16) Choffat, F.; Kaser, S.; Wolfer, P.; Schmid, D.; Mezzenga, R.; Smith, P.; Caseri, W. *Macromolecules* **2007**, *40*, 7878.
- (17) Khan, A.; Gossage, R. A.; Foucher, D. A. *Can. J. Chem.* **2010**, *88*, 1046.
- (18) Elschenbroich, C.; Salzer, A. *Organometallics: A Concise Introduction*; 1st ed.; VCH Verlagsgesellschaft: Weinheim, Germany, 1989.
- (19) Holder, S. J.; Jones, R. G.; Benfield, R. E.; Went, M. J. *Polymer* **1996**, *37*, 3477.

- (20) Mustafa, A.; Achilleos, M.; Ruiz-Iban, J.; Davies, J.; Benfield, R. E.; Jones, R. G.; Grandjean, D.; Holder, S. J. *React. Funct. Polym.* **2006**, *66*, 123.
- (21) Thompson, S. M.; Schubert, U. *Inorg. Chim. Acta* **2003**, *350*, 329.
- (22) Thompson, S. M.; Schubert, U. *Inorg. Chim. Acta* **2004**, *357*, 1959.
- (23) Woo, H. G.; Park, J. M.; Song, S. J.; Yang, S. Y.; Kim, I. S.; Kim, W. G. *Bull. Korean Chem. Soc.* **1997**, *18*, 1291.
- (24) Woo, H. G.; Song, S. J.; Kim, B. H. *Bull. Korean Chem. Soc.* **1998**, *19*, 1161.
- (25) Schittelkopf, K.; Fischer, R. C.; Meyer, S.; Wilfling, P.; Uhlig, F. *Appl. Organomet. Chem.* **2010**, *24*, 897.
- (26) Drenth, W.; Noltes, J. G.; Bulten, E. J.; Creemers, H. M. J. C. *J. Organometal. Chem.* **1969**, *17*, 173.
- (27) Sita, L. R.; Terry, K. W.; Shibata, K. *J. Am. Chem. Soc.* **1995**, *117*, 8049.
- (28) Takeda, K.; Shiraishi, K. *Chem. Phys. Lett.* **1992**, *195*, 121.
- (29) Liao, L., Ryerson University, 2011.
- (30) Adams, S.; Draeger, M. *Main Group Met. Chem.* **1988**, *11*, 151.
- (31) de Haas, M. P.; Choffat, F.; Caseri, W.; Smith, P.; Warman, J. M. *Adv. Mater.* **2006**, *18*, 44.
- (32) Choffat, F.; Wolfer, P.; Smith, P.; Caseri, W. *Macromol. Mater. Eng.* **2010**, *295*, 210.
- (33) Osborne, A. G.; Whiteley, R. H. *J. Organomet. Chem.* **1975**, *101*, C27.
- (34) Shul'pin, G. B.; Rybinskaya, M. I. *Usp. Khim.* **1974**, *43*, 1524.
- (35) Braunschweig, H.; Dirk, R.; Muller, M.; Nguyen, P.; Resendes, R.; Gates, D. P.; Manners, I. *Angew. Chem. Int. Ed. Engl.* **1997**, *36*, 2338.
- (36) Lund, C. L.; Schachner, J. A.; Quail, J. W.; Muller, J. *Organometallics* **2006**, *25*, 5817.
- (37) Osborne, A. G.; Whiteley, R. H. *J. Organomet. Chem.* **1980**, *193*, 345.
- (38) Rulkens, R.; Lough, A. J.; Manners, I. *Angew. Chem. Int. Ed. Engl.* **1996**, *35*, 1805.
- (39) Seyferth, D.; Withers, H. P. *Organometallics* **1982**, *1*, 1275.

- (40) Broussier, R.; Darold, A.; Gautheron, B.; Dromzee, Y.; Jeannin, Y. *Inorg. Chem.* **1990**, *29*, 1817.
- (41) Herberhold, M.; Steffl, U.; Milius, W.; Wrackmeyer, B. *Angew. Chem. Int. Ed. Engl.* **1996**, *35*, 1803.
- (42) Bishop, J. J.; Davison, A.; Katcher, M. L.; Lichtenb.Dw; Merrill, R. E.; Smart, J. *C. J. Organomet. Chem.* **1971**, *27*, 241.
- (43) Kuz'mina, L. G.; Struchkov, Y. T.; Lemenovskii, D. A.; Urazovskii, I. F.; Nifant'ev, I. E.; Perevalova, E. G. *Koord. Khim.* **1983**, *9*, 1212.
- (44) Lesley, M. J. G.; Mock, U.; Norman, N. C.; Orpen, A. G.; Rice, C. R.; Starbuck, J. *J. Organomet. Chem.* **1999**, *582*, 116.
- (45) Althoff, A.; Jutzi, P.; Lenze, N.; Neumann, B.; Stammler, A.; Stammler, H. G. *Organometallics* **2003**, *22*, 2766.
- (46) Schachner, J. A.; Lund, C. L.; Burgess, I. J.; Quail, J. W.; Schatte, G.; Mueller, J. *Organometallics* **2008**, *27*, 4703.
- (47) Watts, W. E. *J. Am. Chem. Soc.* **1966**, *88*, 855.
- (48) Zechel, D. L.; Foucher, D. A.; Pudelski, J. K.; Yap, G. P. A.; Rheingold, A. L.; Manners, I. *J. Chem. Soc., Dalton Trans.* **1995**, 1893.
- (49) Reddy, N. P.; Hayashi, T.; Tanaka, M. *Chem. Commun.* **1996**, 1865.
- (50) Clearfield, A.; Simmons, C. J.; Withers, H. P.; Seyferth, D. *Inorg. Chim. Acta* **1983**, *75*, 139.
- (51) Mizuta, T.; Imamura, Y.; Miyoshi, K.; Yorimitsu, H.; Oshima, K. *Organometallics* **2005**, *24*, 990.
- (52) Spang, C.; Edelmann, F. T.; Noltemeyer, M.; Roesky, H. W. *Chem. Ber.* **1989**, *122*, 1247.
- (53) Mueller-Westerhoff, U. T. *Angew. Chem.* **1986**, *98*, 700.
- (54) Gausset, O.; Delpon-Lacaze, G.; Schurmann, M.; Jurkschat, K. *Acta Crystallogr., Sect. C: Cryst. Struct. Commun.* **1998**, *54*, 1425.
- (55) Altmann, R.; Gausset, O.; Horn, D.; Jurkschat, K.; Schurmann, M.; Fontani, M.; Zanello, P. *Organometallics* **2000**, *19*, 430.
- (56) Nguyen, P.; Gomez-Elipse, P.; Manners, I. *Chem. Rev.* **1999**, *99*, 1515.
- (57) Manners, I. *Science* **2001**, *294*, 1664.

157. (58) Abd-El-Aziz, A. S.; Manners, I. *J. Inorg. Organomet. Polym. Mater.* **2005**, *15*, 157.
- (59) Arimoto, F. S.; Haven, A. C. *J. Am. Chem. Soc.* **1955**, *77*, 6295.
- (60) Miles, D.; Ward, J.; Foucher, D. A. *Organometallics* **2010**, *29*, 1057.
360. (61) Korshak, V. V.; Sosin, S. L.; Alexeeva, V. P. *Dok Akad Nauk SSSR* **1960**, *132*, 360.
- (62) Rosenberg, H.; Neuse, E. W. *J. Organomet. Chem.* **1966**, *6*, 76.
- (63) Rausch, M. D. *J. Org. Chem.* **1963**, *28*, 3337.
- (64) Neuse, E. W.; Bednarik, L. *Macromolecules* **1979**, *12*, 187.
- (65) Yamamoto, T.; Sanechika, K.; Yamamoto, A.; Katada, M.; Motoyama, I.; Sano, H. *Inorg. Chim. Acta* **1983**, *73*, 75.
- (66) Hirao, T.; Kurashina, M.; Aramaki, K.; Nishihara, H. *J. Chem. Soc., Dalton Trans.* **1996**, 2929.
- (67) Roling, P. V.; Rausch, M. D. *J. Org. Chem.* **1972**, *37*, 729.
- (68) Park, P.; Lough, A. J.; Foucher, D. A. *Macromolecules* **2002**, *35*, 3810.
- (69) Miles, D.; Ward, J.; Foucher, D. A. *Macromolecules* **2009**, *42*, 9199.
- (70) Itazaki, M.; Ueda, K.; Nakazawa, H. *Angew. Chem., Int. Ed.* **2009**, *48*, 3313.
- (71) Pittman, C. U.; Patterson, W. J.; McManus, S. P. *J. Polym. Sci., Part A: Polym. Chem.* **1971**, *9*, 3187.
- (72) Patterson, W. J.; McManus, S. P.; Pittman, C. U. *J. Polym. Sci., Part A: Polym. Chem.* **1974**, *12*, 837.
- (73) Brandt, P. F.; Rauchfuss, T. B. *J. Am. Chem. Soc.* **1992**, *114*, 1926.
- (74) Foucher, D. A.; Tang, B. Z.; Manners, I. *J. Am. Chem. Soc.* **1992**, *114*, 6246.
- (75) Ni, Y. Z.; Rulkens, R.; Pudelski, J. K.; Manners, I. *Macromol. Rapid Commun.* **1995**, *16*, 637.
2263. (76) Reddy, N. P.; Yamashita, H.; Tanaka, M. *J. Chem. Soc., Chem. Commun.* **1995**, 2263.
- (77) Ni, Y. Z.; Rulkens, R.; Manners, I. *J. Am. Chem. Soc.* **1996**, *118*, 4102.

- (78) Tanabe, M.; Vandermeulen, G. W. M.; Chan, W. Y.; Cyr, P. W.; Vanderark, L.; Rider, D. A.; Manners, I. *Nat. Mater.* **2006**, *5*, 467.
- (79) Chan, W. Y.; Lough, A. J.; Manners, I. *Chem.--Eur. J.* **2007**, *13*, 8867.
- (80) Chan, W. Y.; Lough, A. J.; Manners, I. *Organometallics* **2007**, *26*, 1217.
- (81) Tanabe, M.; Manners, I. *J. Am. Chem. Soc.* **2004**, *126*, 11434.
- (82) Jakle, F.; Berenbaum, A.; Lough, A. J.; Manners, I. *Chem.--Eur. J.* **2000**, *6*, 2762.
- (83) Schachner, J. A.; Tockner, S.; Lund, C. L.; Quail, J. W.; Rehahn, M.; Mueller, J. *Organometallics* **2007**, *26*, 4658.
- (84) Bagh, B.; Gilroy, J. B.; Staubitz, A.; Mueller, J. *J. Am. Chem. Soc.* **2010**, *132*, 1794.
- (85) Foucher, D. A.; Manners, I. *Makromol. Chem., Rapid Commun.* **1993**, *14*, 63.
- (86) Foucher, D. A.; Honeyman, C. H.; Nelson, J. M.; Tang, B. Z.; Manners, I. *Angew. Chem. Int. Ed. Engl.* **1993**, *32*, 1709.
- (87) Rulkens, R.; Gates, D. P.; Balaishis, D.; Pudelski, J. K.; McIntosh, D. F.; Lough, A. J.; Manners, I. *J. Am. Chem. Soc.* **1997**, *119*, 10976.
- (88) Foucher, D. A.; Ziembinski, R.; Tang, B. Z.; Macdonald, P. M.; Massey, J.; Jaeger, C. R.; Vancso, G. J.; Manners, I. *Macromolecules* **1993**, *26*, 2878.
- (89) Zechel, D. L.; Hultsch, K. C.; Rulkens, R.; Balaishis, D.; Ni, Y. Z.; Pudelski, J. K.; Lough, A. J.; Manners, I. *Organometallics* **1996**, *15*, 1972.
- (90) Bourke, S. C.; Jakle, F.; Vejzovic, E.; Lam, K. C.; Rheingold, A. L.; Lough, A. J.; Manners, I. *Chem.--Eur. J.* **2003**, *9*, 3042.
- (91) Braunschweig, H.; Adams, C. J.; Kupfer, T.; Manners, I.; Richardson, R. M.; Whittell, G. R. *Angew. Chem., Int. Ed.* **2008**, *47*, 3826.
- (92) Buretea, M. A.; Tilley, T. D. *Organometallics* **1997**, *16*, 1507.
- (93) Nelson, J. M.; Rengel, H.; Manners, I. *J. Am. Chem. Soc.* **1993**, *115*, 7035.
- (94) Mochida, K.; Shibayama, N.; Goto, M. *Chem. Lett.* **1998**, 339.
- (95) Dementev, V. V.; Cervanteslee, F.; Parkanyi, L.; Sharma, H.; Pannell, K. H.; Nguyen, M. T.; Diaz, A. *Organometallics* **1993**, *12*, 1983.
- (96) Paquet, C.; Cyr, P. W.; Kumacheva, E.; Manners, I. *Chem. Mater.* **2004**, *16*, 5205.
- (97) Paquet, C.; Cyr, P. W.; Kumacheva, E.; Manners, I. *Chem. Commun.* **2004**, 234.

- (98) Benkeser, R. A.; Goggin, D.; Schroll, G. *J. Am. Chem. Soc.* **1954**, *76*, 4025.
- (99) Rausch, M.; Vogel, M.; Rosenberg, H. *J. Org. Chem.* **1957**, *22*, 900.
- (100) Seyferth, D.; Hofmann, H. P.; Helling, J. F.; Burton, R. *Inorg. Chem.* **1962**, *1*, 227.
- (101) Pellegrini, J. P., Jr.; Spilners, I. J.; Gulf Research and Development Co. . 1967, p 4 pp.
- (102) Rosenberg, H.; United States Dept. of the Air Force . 1969, p 5 pp.
- (103) Dodo, T.; Suzuki, H.; Takiguchi, T. *Bull. Chem. Soc. Jpn.* **1970**, *43*, 288.
- (104) Kohler, F. H.; Geike, W. A.; Hertkorn, N. *J. Organomet. Chem.* **1987**, *334*, 359.
- (105) Kabouche, Z.; Dinh, N. H. *J. Organomet. Chem.* **1989**, *375*, 191.
- (106) Herberhold, M.; Milius, W.; Steffl, U.; Vitzithum, K.; Wrackmeyer, B.; Herber, R. H.; Fontani, M.; Zanello, P. *Eur. J. Inorg. Chem.* **1999**, 145.
- (107) Lenze, N.; Neumann, B.; Salmon, A.; Stammler, A.; Stammler, H. G.; Jutzi, P. *J. Organomet. Chem.* **2001**, *619*, 74.
- (108) Wu, Y. J.; Ding, L.; Zhou, Z. X.; Du, C. X.; Wang, W. L. *J. Organomet. Chem.* **1998**, *564*, 233.
- (109) Poehlker, C.; Schellenberg, I.; Poettgen, R.; Dehnen, S. *Chem. Commun.* **2010**, *46*, 2605.
- (110) Wright, M. E. *Organometallics* **1990**, *9*, 853.
- (111) Liu, C. M.; Lou, S. J.; Liang, Y. M. *Synth. Commun.* **1998**, *28*, 2271.
- (112) Guillaneux, D.; Kagan, H. B. *J. Org. Chem.* **1995**, *60*, 2502.
- (113) Butler, I. R.; Wilkes, S. B.; McDonald, S. J.; Hobson, L. J.; Taralp, A.; Wilde, C. *P. Polyhedron* **1993**, *12*, 129.
- (114) Zhang, W. B.; Yoneda, Y.; Kida, T.; Nakatsuji, Y.; Ikeda, I. *Tetrahedron: Asymmetry* **1998**, *9*, 3371.
- (115) Wright, M. E.; Sigman, M. S. *Macromolecules* **1992**, *25*, 6055.
- (116) Jakle, F.; Rulkens, R.; Zech, G.; Foucher, D. A.; Lough, A. J.; Manners, I. *Chem.-Eur. J.* **1998**, *4*, 2117.
- (117) Herberhold, M.; Steffl, U.; Wrackmeyer, B. *Z. Naturforsch., B: Chem. Sci.* **1999**, *54*, 57.

- (118) Herberhold, M.; Steffl, U.; Milius, W.; Wrackmeyer, B. *J. Organomet. Chem.* **1997**, *533*, 109.
- (119) Herberhold, M.; Steffl, U.; Milius, W.; Wrackmeyer, B. *Chem.--Eur. J.* **1998**, *4*, 1027.
- (120) Herberhold, M.; Steffl, U.; Milius, W.; Wrackmeyer, B. *Z. Anorg. Allg. Chem.* **1998**, *624*, 386.
- (121) Berenbaum, A.; Jakle, F.; Lough, A. J.; Manners, I. *Organometallics* **2002**, *21*, 2359.
- (122) Sharma, H. K.; Cervantes-Lee, F.; Mahmoud, J. S.; Pannell, K. H. *Organometallics* **1999**, *18*, 399.
- (123) Vogel, U.; Lough, A. J.; Manners, I. *Angew. Chem., Int. Ed.* **2004**, *43*, 3321.
- (124) Kuate, A. C. T.; Daniliuc, C. G.; Jones, P. G.; Tamm, M. *Eur. J. Inorg. Chem.* **2012**, 1727.
- (125) Jakle, F.; Rulkens, R.; Zech, G.; Massey, J. A.; Manners, I. *J. Am. Chem. Soc.* **2000**, *122*, 4231.
- (126) Baumgartner, T.; Jakle, F.; Rulkens, R.; Zech, G.; Lough, A. J.; Manners, I. *J. Am. Chem. Soc.* **2002**, *124*, 10062.
- (127) Bagh, B.; Breit, N. C.; Dey, S.; Gilroy, J. B.; Schatte, G.; Harms, K.; Mueller, J. *Chem.--Eur. J.* **2012**, *18*, 9722.
- (128) Petersen, R.; Foucher, D. A.; Tang, B. Z.; Lough, A.; Raju, N. P.; Greedan, J. E.; Manners, I. *Chem. Mater.* **1995**, *7*, 2045.
- (129) Bagh, B.; Breit, N. C.; Harms, K.; Schatte, G.; Burgess, I. J.; Braunschweig, H.; Mueller, J. *Inorg. Chem.* **2012**, *51*, 11155.
- (130) Chan, W. Y.; Lough, A. J.; Manners, I. *Angew. Chem., Int. Ed.* **2007**, *46*, 9069.
- (131) Bera, H.; Braunschweig, H.; Oechsner, A.; Seeler, F.; Sigritz, R. *J. Organomet. Chem.* **2010**, *695*, 2609.
- (132) Sato, M.; Anano, H. *J. Organomet. Chem.* **1998**, *555*, 167.
- (133) Dong, T. Y.; Hwang, M. Y.; Wen, Y. S.; Hwang, W. S. *J. Organomet. Chem.* **1990**, *391*, 377.
- (134) Tarraga, A.; Oton, F.; Espinosa, A.; Velasco, M. D.; Molina, P.; Evans, D. J. *Chem. Commun.* **2004**, 458.

- (135) Oton, F.; Espinosa, A.; Tarraga, A.; de Arellano, C. R.; Molina, P. *Chem.--Eur. J.* **2007**, *13*, 5742.
- (136) Robin, M. B.; Day, P. *Advan. Inorg. Chem. Radiochem.* **1967**, *10*, 247.
- (137) Gao, H.; Wei, X.; Liu, X.; Yan, T. *J. Phys. Chem. B* **2010**, *114*, 4056.
- (138) Cody, R. B.; Laramie, J. A.; Durst, H. D. *Anal. Chem.* **2005**, *77*, 2297.
- (139) Rausch, M. D.; Ciappene, D. *J. Organomet. Chem.* **1967**, *10*, 127.